

DISSERTATION

PHYSIOLOGICALLY-BASED

PHARMACOKINETIC/PHARMACODYNAMIC (PBPK/PD) MODELING OF

3,3',4,4',5-PENTACHLOROBIPHENYL (PCB126)

Submitted by

Manupat Lohitnavy

Department of Environmental and Radiological Health Sciences

In partial fulfillment of the requirements

For the Degree of Doctor of Philosophy

Colorado State University

Fort Collins, Colorado

Spring, 2008

UMI Number: 3321295

INFORMATION TO USERS

The quality of this reproduction is dependent upon the quality of the copy submitted. Broken or indistinct print, colored or poor quality illustrations and photographs, print bleed-through, substandard margins, and improper alignment can adversely affect reproduction.

In the unlikely event that the author did not send a complete manuscript and there are missing pages, these will be noted. Also, if unauthorized copyright material had to be removed, a note will indicate the deletion.

UMI[®]

UMI Microform 3321295

Copyright 2008 by ProQuest LLC.

All rights reserved. This microform edition is protected against unauthorized copying under Title 17, United States Code.

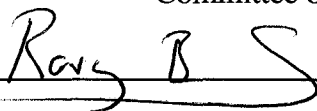
ProQuest LLC
789 E. Eisenhower Parkway
PO Box 1346
Ann Arbor, MI 48106-1346

COLORADO STATE UNIVERISTY

December 14, 2007

WE HEREBY RECOMMEND THAT THE DISSERTATION PREPARED UNDER OUR SUPERVISION BY MANUPAT LOHITNAVY ENTITLED PHYSIOLOGICALLY-BASED PHARMACOKINETIC/PHARMACODYNAMIC (PBPK/PD) MODELING OF 3,3',4,4',5-PENTACHLOROBIPHENYL (PCB126) BE ACCEPTED AS FULFILLING IN PART REQUIREMENTS FOR THE DEGREE OF DOCTOR OF PHILOSOPHY.

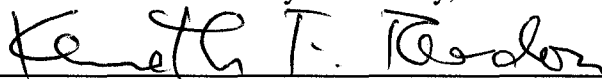
Committee on Graduate Work



Stephen A. Benjamin, Ph.D.



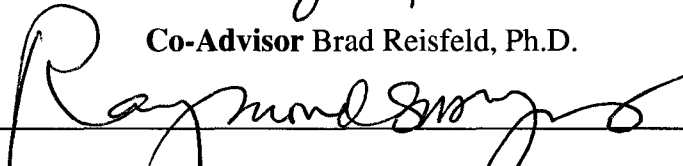
Rory B. Conolly, Ph.D.



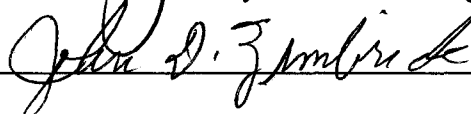
Kenneth F. Reardon, Ph.D.



Co-Advisor Brad Reisfeld, Ph.D.



Advisor Raymond S. H. Yang, Ph.D.



Department Head John D. Zimbrick, Ph.D.

ABSTRACT OF DISSERTATION
PHYSIOLOGICALLY-BASED
PHARMACOKINETIC/PHARMACODYNAMIC (PBPK/PD) MODELING OF
3,3',4,4',5-PENTACHLOROBIPHENYL (PCB126)

A central objective of this dissertation was to develop a physiologically-based pharmacokinetic/pharmacodynamic (PBPK/PD) model for 3,3',4,4',5-pentachlorobiphenyl (PCB126), a persistent environment carcinogen. Despite its high lipophilicity, PCB126 was primarily recovered from liver. In addition, PCB126 could achieve its steady state in the liver in a relatively short period of time. These results suggested that there might be a molecular mechanism responsible for hepatic protein binding and excretion of PCB126. In 2005, a three-dimensional quantitative structure-activity relationship (3D-QSAR) model of rat Mrp2, a versatile protein transporter, was developed by Hirono and colleagues in Japan. Using the 3D-QSAR model, PCB126 was predicted to be a Mrp2 substrate with a relatively high binding affinity (K_m) value.

With this novel information regarding the significant role of Mrp2 in PCB126 pharmacokinetics, we incorporated a Mrp2-mediated excretion process into our PCB126 PBPK model. Our model could successfully describe numerous tissue concentration-time courses in different dosing conditions from different laboratories. Our PBPK model, for the first time, revealed an important role of Mrp2 in PCB126 disposition. In addition, to establish a correlation between PCB126 pharmacokinetics and its pharmacodynamic (PD) endpoint (i.e. hepatocarcinogenic effect), we used a chosen internal dose surrogate [i.e. area under the curve of PCB126 in liver (AUC_{Liver})] to predict the PD effect of PCB126.

With this PBPK/PD model, correlation between the AUC_{Liver} and our liver glutathione-S-transferase placental form positive (GSTP⁺) foci development data was demonstrated.

Since PCB126 is a known carcinogen, we also investigated its hepatocarcinogenicity using our modified liver foci bioassay. From several *in silico* predictions, it was suggested that there are at least two populations of preneoplastic cells. These hypothetical cells (A and B cells) have different growth characteristics where B cells eventually gain growth advantages and progressively transform to malignancy. To prove the existence of A and B cells among liver GSTP⁺ foci, we conducted an experiment by exposing rats with PCB126, hexachlorobenzene (HCB) and their mixture up to 6 months. Liver foci positive or negative for GSTP⁺, transforming growth factor- α ⁺ (TGF α ⁺) and transforming growth factor- β Type 2 receptor⁻ (TGF β 2Rc⁻) were investigated. In rats treated with PCB126, time-dependent changes in all of three biomarkers were observed. Interestingly, when the GSTP⁺ foci were categorized into four phenotypic groups according to their TGF α and TGF β 2Rc expression, GSTP⁺ foci with TGF α expression and absence of TGF β 2Rc expression had significantly higher hepatocyte division rates than those of GSTP⁺ foci without TGF α expression and with TGF β 2Rc expression. These results provided the first experimental evidence suggesting that there are at least four different subpopulations among these liver GSTP⁺ foci.

PCB126 is an Mrp2 substrate with a relatively high K_m value compared to other Mrp2 substrates. We hypothesized that, when PCB126 and another Mrp2 substrate are concomitantly presenting in the body, PCB126 can interact with those Mrp2 substrate resulting in changes in its concentration-time courses. To prove this hypothesis, we conducted an *in vivo* pharmacokinetic interaction study. We exposed rats to multiple oral

doses of PCB126. Subsequently, we orally administered the rats with a single oral dose of methotrexate (MTX), a known Mrp2 substrate. The rats were sacrificed at specified time points and livers were harvested. Liver concentration levels of PCB126 and MTX were determined.

Firstly, to quantitatively describe pharmacokinetic interactions between these two Mrp2 substrates, a modified version of MTX PBPK model incorporated with hepatic Mrp2-mediated excretion process was developed. This PBPK model was modified from the Bischoff et al. MTX PBPK model developed in 1971. In a reconstructed MTX PBPK model, a first-order biliary MTX clearance was assumed. In our current MTX PBPK model, that biliary excretion was replaced by the Mrp2-mediated excretion process. The K_m value of MTX was a published value taken from the Hirono et al. (2005) paper. Our MTX PBPK model was able to describe a number of datasets obtained from several species in different experimental conditions.

Secondly, we hypothesized that the inhibition between PCB126 and MTX occurs at the hepatic Mrp2. Thus, we utilized this novel MTX PBPK model and our PCB126 PBPK/PD model by linking the two PBPK models together with a mathematical description of competitive inhibition processes between the two Mrp2 substrates. Computer simulation results from the extended PBPK model agreed well with our analytical data for both chemicals. These results not only supported the previous *in silico* predictions from the 3D-QSAR model that PCB126 is a Mrp2 substrate, but they also suggested that PCB126 can significantly affect pharmacokinetics and disposition of other Mrp2 substrates.

In summary, this research provided a better understanding in pharmacokinetics of PCB126 and its effects on liver foci formation. The prediction from the Hirono et al. 3D-QSAR model resulted in a successful development of the PCB126 PBPK model. The insight in pharmacokinetics of PCB126 and the roles of Mrp2 in PCB126 disposition led us to the development of the pharmacokinetic interaction model between PCB126 and MTX. The integrated PBPK model with the mathematical descriptions of the competitive inhibition processes provided us a computational tool for quantitative predictions of the interactions between the two Mrp2 substrates.

Manupat Lohitnavy

Department of Environmental and Radiological Health Sciences

Colorado State University

Fort Collins, CO 80523

Spring 2008

ACKNOWLEDGEMENTS

During the course of my Ph.D. study, I was indebted to many people. First and foremost, I would like to express my sincere gratitude and appreciation to Dr. Raymond S. H. Yang for serving as my academic advisor. With his valuable mentorship and financial supports, I had learned a great deal about science and, more importantly, found true values of being persistently persevering in my own belief.

I would like to thank the members of my graduate committee. Sincere thanks to Dr. Stephen Benjamin who gave me supports and advice on one of my scientific discoveries. With his expertise as a renowned pathologist, during our tough time in relocating our lab from our original place to a new establishment, he eagerly came over to look into stained tissue slides, shared his experiences to me, and gave me a huge encouragement. With that, I could hang on until this very last process of my Ph.D. study. Furthermore, I would like to thank Dr. Rory Conolly who supported me and gave me a chance to pursue Ph.D. in the US since I was in my home country Thailand. Sincere appreciation would like to be conveyed to Drs. Kenneth Reardon and Brad Reisfeld who served as my committee member and co-advisor, respectively.

There was one special individual who set a great and memorable example of being an exemplary scientist by lending a helping hand to a total stranger like me. This person was Dr. Shuichi Hirono of Kitasoto University, Tokyo, Japan. Without his kindness, I would not be able to finish my PBC126 PBPK model. From his selfless assistance to me, as far as my current and future expertise allows, I vow myself to help other fellow scientists without asking anything in return.

Another significant person who lent me a helping hand while I needed it most was Dr. Yasong Lu, my lab buddy. He was not only a major contributor involving in all experimentations in animals, but he was also a great helper in computer coding. He came to our lab to help me writing the codes even there was a blizzard until his very last day in Fort Collins. Although his contribution to my research work was very significant, but it is not going to be more important than our experience and friendship we have built and shared.

Also, I would like to express my sincere thankfulness to Mrs. Laura Chubb, Mrs. Elizabeth Eickman, Ms. Lisa Gerjevic, and, Ms. Corie Lane who actively assisted me in my experiments in animals and immunohistochemical staining. Special thanks would like to convey to Drs. Mike Lyons, Arthur Mayeno and Brad Reisifeld who generously helped my in computer coding and HPLC analysis.

My experiments always involved many people of the Quantitative and Computational Toxicology Group. They would not be successfully completed without help from members of the group. These great people included Mrs. Amanda Ashley, Mrs. Christine Battaglia, Dr. Carol Belfiore, Dr. Charley Dean, Dr. Jim Dennison, Dr. Ivan Dobrev, Dr. Sun Ku Lee, Dr. Ken Liao, Mrs. Linda Monum, Ms. Tracy Nichols, Dr. Jon “Todd” Painter, Dr. Damon Perez, Dr. Michaela Reddy, and, Ms. Caroline Yang, each of whom provided assistance and moral support. All technical assistance in animal cares was always excellently provided by Ms. Elisa French, Ms. Sheryl Carter, and Ms. Kim Olsen at the Painter Center at Colorado State University.

This research was supported by the NIOSH/CDC grant 1 RO1 OH07556. Tuitions & fees and my stipend were partially supported by Naresuan University, Phitsanulok,

Thailand, and the Royal Thai Government under the Royal Thai Scholarship Program. Without these financial supports, I would not be able to complete my study. Upon this regard, I would like to thank Dr. Mondhon Sanguansermisri, the President of Naresuan University, who gave me the chance of my lifetime at the first place.

Last but not least, I could not have anything without this very person, Mrs. Orrrat (Som) Lohitnavy. She is the only person who makes my life worthwhile and meaningful. All of joy and happiness in my life involve her, and is surrounded around and by her. She is the only reason why I do exist as a happy man.

DEDICATION

To my beloved wife, Omrat (Som) Lohitnavy, and my children, Norawish (Bai-Tong) & Thanath (Jack) Lohitnavy, for their unwavering support, relentless encouragement and unconditional love.

TABLE OF CONTENTS

	<u>Page</u>
Chapter 1	Literature review: A medium-term liver foci bioassay and multidrug-resistance-associated protein 2 (Mrp2) 1
Chapter 2	A possible role of multidrug-resistance-associated protein 2 (Mrp2) in hepatic excretion of PCB126, an environmental contaminant: PBPK/PD modeling 41
Chapter 3	Hepatic enzyme and receptor expression as biomarkers for carcinogenicity in rats exposed to PCB126, hexachlorobenzene, and, their mixture 87
Chapter 4	A novel physiologically-based pharmacokinetic model of methotrexate incorporating hepatic excretion via multidrug-resistance-associated protein 2 (Mrp2) in mice, rats, dogs, and humans 116
Chapter 5	Pharmacokinetic interactions at the level of multidrug-resistance-associated protein 2 (Mrp2) among methotrexate, 3,3',4,4',5-pentachlorobiphenyl (PCB126), and genipin in Rats: A physiologically-based pharmacokinetic model 147
Chapter 6	Overall summary and future directions 175
Appendix	Computer codes for PBPK models 197

CHAPTER 1

Literature Review:

A Medium-Term Liver Foci Bioassay and Multidrug-Resistance-Associated Protein 2 (Mrp2)

OUTLINE

1. Introduction
2. Medium-term liver bioassay as an experimental tool in chemical carcinogenesis
3. Development of liver GSTP⁺ foci and its implications in chemical carcinogenesis
4. 3,3',4,4',5-Pentachlorobiphenyl (PCB126)
5. Roles of protein transporters in the disposition of xenobiotics
6. Molecular structure and physiological function of Mrp2
7. Tissue distribution & cellular localization of Mrp2
8. Mode of action of Mrp2 in transporting its substrates
9. Regulations of Mrp2 expression
 - 9.1. *Dynamics of Mrp2: Retrieval and Recruitment*
 - 9.2. *Effects of Interactions between PCB126 and Genipin on Mrp2 Function*
 - 9.3. *Stimulants and Inhibitors of Mrp2*
10. Roles of Mrp2 in human diseases
11. Experimental models used to investigate the Mrp2-mediated transport
 - 11.1. *Animal Models for Studying Mrp2*
 - 11.1.1. *Eisai hyperbilirubinemic rats (EHBR)*
 - 11.1.2. *Groninger Yellow/transporter deficient rat (TR)*
 - 11.1.3. *Mrp2 gene knockout mice (Mrp2^{-/-} mice)*

11.2. In Vitro Models for Studying Mrp2

11.2.1. Canalicular membrane vesicle system

11.2.2. Sandwich-cultured hepatocyte system

11.3. In Silico Models of Mrp2

12. Methotrexate (MTX)

13. A possible connection between physiologically-based pharmacokinetic modeling and the three-dimensional quantitative structure-activity (3D-QSAR) model

1. INTRODUCTION

A central objective of this dissertation was to develop a physiologically-based pharmacokinetic/pharmacodynamic (PBPK/PD) model for 3,3',4',4',5-pentachlorobiphenyl (PCB126), a persistent environment carcinogen. To assess hepatocarcinogenicity of PCB126, a medium-term liver foci bioassay was utilized (Ito *et al.* 2003; Ogiso *et al.* 1990; Shirai 1997). Pharmacokinetically, despite its high lipophilicity, PCB126 was primarily recovered from liver (Chu 1994; Dean *et al.* 2002; Lohitnavy *et al.* 2004). In addition, PCB126 achieved its steady state in the liver with a relatively short period of time (Lohitnavy *et al.* 2004). These results suggested that there might be a molecular mechanism responsible for hepatic protein binding and biliary excretion of PCB126. More recently a three-dimensional quantitative structure-activity relationship (3D-QSAR) model of rat Mrp2, a versatile protein transporter, was developed (Hirono *et al.* 2005). Using the 3D-QSAR model, PCB126 was predicted to be a Mrp2 substrate with a relatively high binding affinity (K_m) value. Since it is likely that Mrp2 plays a pivotal role in PCB126 pharmacokinetics, biology, functions and roles of

Mrp2 in xenobiotic disposition are extensively discussed in this review. In addition, with the emerging new information regarding Mrp2 roles in PCB126 pharmacokinetics, it is feasible to incorporate the biochemical characteristics between PCB126 and Mrp2 into a PBPK model of PCB126 and other Mrp2 substrates, including a clinically important antineoplastic drug, methotrexate (MTX). Thus, this review also provides a brief background about the Mrp2 roles in MTX pharmacokinetics and possible pharmacokinetic interactions between PCB126 and MTX at the level of hepatic Mrp2.

2. MEDIUM-TERM LIVER BIOASSAY AS AN EXPERIMENTAL TOOL IN CHEMICAL CARCINOGENESIS

In the last century, knowledge in chemical carcinogenesis has been accumulated using *in vitro*, *in vivo* and *in silico* approaches. Many of the experimental models are proven to be useful in studying processes in chemical carcinogenesis (Shirai 1997; Solt and Farber 1976). Initiation-promotion models, involving a single dose administration of an initiator, followed by repeated administration of a promoter to animals, can reveal the capability of chemicals to cause cancer. Ito's medium-term liver bioassay is one of the most extensively studied protocols (Ito *et al.* 2003; Shirai 1997). Based on development of glutathione-S-transferase placental form positive (GSTP⁺) foci as a pre-neoplastic marker, this experimental model has shown excellent capability in predicting liver carcinogenicity in rats (Ogiso *et al.* 1990; Shirai 1997).

3. DEVELOPMENT OF LIVER GSTP⁺ FOCI AND ITS IMPLICATIONS IN CHEMICAL CARCINOGENESIS

Expression of GSTP in the liver is currently considered a reliable phenotypic marker used for identification of cancer initiation in analysis of the Ito's medium-term liver bioassay (Ito *et al.* 2003). In this particular model, to generate initiated cells, diethylnitrosamine (DEN), a potent initiator, is intraperitoneally administered to male F344 rats on day 0 (Fig. 1.1). From day 14, a promoter is orally administered to the animals until the sacrifice date at 8 weeks. To accelerate liver cell division, two-thirds partial hepatectomy is performed on day 21. At the sacrifice date, whole livers are removed; tissues are fixed, embedded in paraffin, and sectioned. Liver sections are stained for GSTP⁺ foci, which are used as the experimental endpoint.

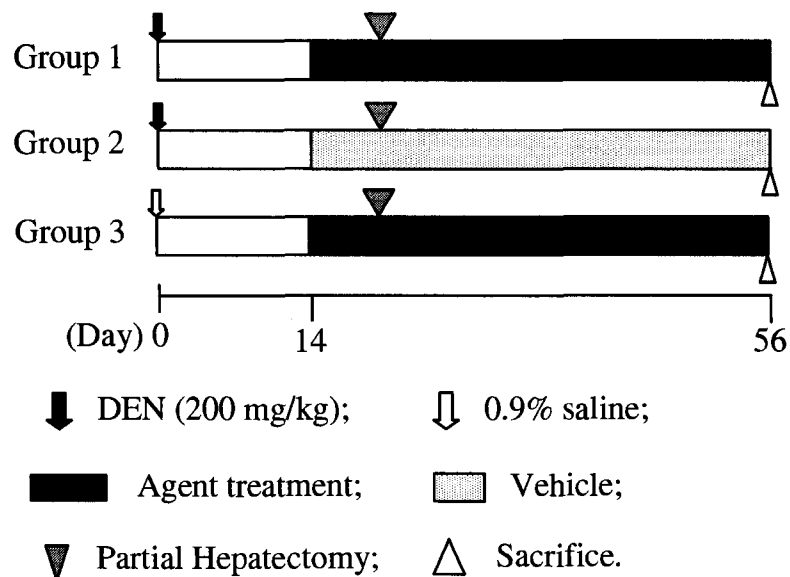


Fig. 1.1. Experimental protocol of the Ito's medium-term initiation-promotion liver foci bioassay (Ito *et al.* 2003; Shirai 1997).

Utilizing expression of GSTP as an indication of carcinogenic potential, 97% of mutagenic hepatocarcinogens, 88% of non-mutagenic hepatocarcinogens, and 23% of carcinogens not specific for hepatic tissue have been correctly identified (Ito *et al.* 2003). Currently GSTP correlates well with carcinogenic potential and is an early phenotypic marker of the onset of cancer (Dragan *et al.* 1994). Hepatocytes expressing GSTP represent the population of initiated cells (Dragan *et al.* 1993). Promotion is characterized by development of focal areas of proliferating cells. These foci represent clonal expansion of initiated cells, which grow continuously with increased rates of DNA synthesis compared to surrounding cells. Within a modified Ito's medium-term bioassay, initiation, marked by formation of GSTP⁺ cells, as well as promotion, are both analyzed to determine carcinogenic potential.

4. 3,3',4',4,5-PENTACHLOROBIPHENYL (PCB126)

Polychlorinated biphenyls (PCBs) are halogenated aromatic hydrocarbons that had been widely used in industry. Because of their persistence as environmental pollutants, they were discontinued from any usage since 1970's. However, a significant amount of PCBs is still detectable in foods, human and animal tissues, and in the environment (CDC 2005; Safe *et al.* 1985; Safe 1994). PCB126 (Fig. 1.2) is the most toxic congener of all PCBs with demonstrated carcinogenic effects. Using certain *in vivo* carcinogenicity tests, PCB126 could induce cancers in liver, lung and mouth in rats (Dean *et al.* 2002; Lohitnavy *et al.* 2004; NTP 2006). Since PCB126 is a coplanar PCB, it is capable of binding with aryl hydrocarbon receptor (AhR) and elicits biological effects which include the induction of cytochrome P4501A1 and 1A2 (CYP1A1, 1A2), thymic involution, wasting syndrome (Safe 1994).

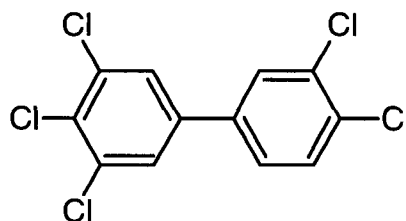


Fig. 1.2. Chemical structure of 3,3',4,4',5'-Pentachlorobiphenyl (PCB126)

Despite its high lipophilicity, the levels of PCB126 in the liver are much higher than those observed in adipose tissue (Chu 1994; Dean *et al.* 2002; Lohitnavy *et al.* 2004). This is similar to chlordecone and 2, 3, 7, 8-tetrachlorodibenzo-*p*-dioxin (TCDD) (Abraham *et al.* 1988; Belfiore *et al.* 2007), but at a much higher rate. These results suggested that protein binding is responsible for high levels of PCB126 in the liver. From a different perspective, while PCB126 is known to be persistent in the environment (Safe 1994), in our laboratory earlier results demonstrated that PCB126 could attain its steady state fairly rapidly (Lohitnavy *et al.* 2004). An initial pharmacokinetic estimation of half life for this chemical turned out to be around 3 days (unpublished data). These results suggested that there was a relatively high hepatic clearance of PCB126. Therefore, we further considered the possible involvement of transporter protein(s), specifically multidrug-resistance-associated protein 2 (Mrp2).

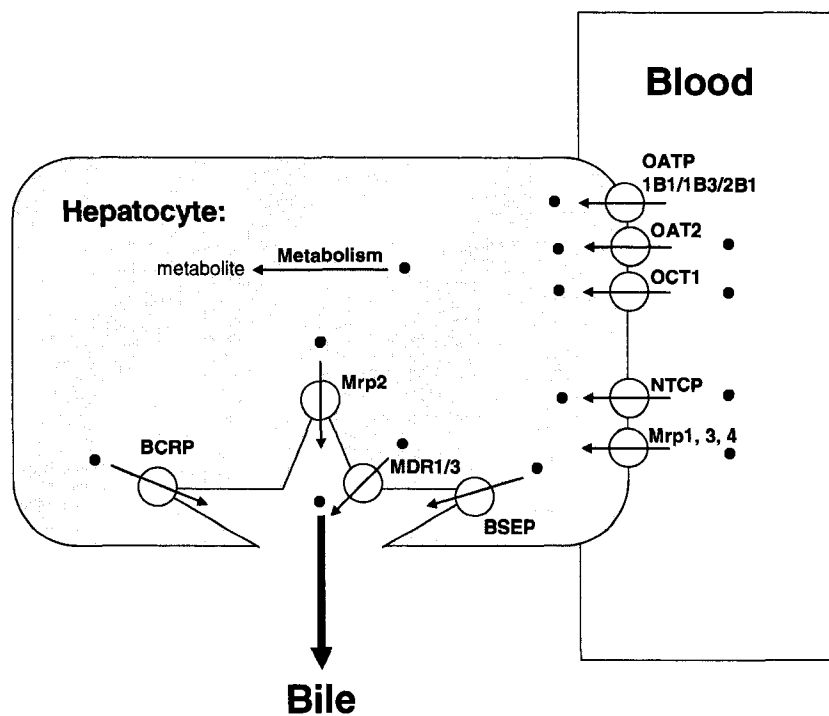
5. ROLES OF PROTEIN TRANSPORTERS IN TRANSPORTS OF XENOBIOTICS

The disposition of xenobiotics from the liver consists of the following processes; 1) hepatic uptake; 2) metabolism, and/or; 3) biliary excretion. Thus, transport of these chemicals from blood into hepatocytes and out of hepatocytes into the bile also plays an

important role in hepatic disposition of xenobiotics. These processes are depicted in Fig. 1.3. Hepatic transporter proteins regulate both influx and efflux of chemicals from blood into liver cells and out of the hepatocytes into bile. Transporters responsible for transporting chemicals from blood into liver cells are organic anion transporting peptides (OATP_s), Na⁺-dependent taurocholic cotransporting polypeptide (NTCP), organic cation transporters (OCT_s), and multidrug-resistance-associated proteins (Mrps; Mrp1, Mrp3 and Mrp4). In addition, hepatocytes also play a significant role in bile formation and biliary excretion. Protein transporters involving in these biliary excretion processes include breast cancer related protein (BCRP), multidrug resistance proteins (MDRs), bile acid export pump, and Mrp2.

6. MOLECULAR STRUCTURE AND PHYSIOLOGICAL FUNCTION OF MRP2

The roles of Mrps are significant in hepatic transport of chemicals in both directions, from blood into the liver and out of the liver into bile. Thus, we would like to provide basic information regarding the biology of this particular group of the transporter proteins. The Mrp family of ATP-binding cassette (ABC) transporters consists of nine transporter proteins, eight of which have now been determined to function as efflux pumps for a diverse range of lipophilic substrates. Based on their structures, Mrps can be classified as to whether or not they have a third (*N*-terminal) membrane spanning domain (MSD) (Fig. 1.4 and 1.5) (Kruh *et al.* 2007). If they have the third MSD, these proteins include Mrp1, Mrp2, Mrp3, Mrp6, and Mrp7 (Fig. 1.4) (Kruh *et al.* 2007). If the transporter proteins do not possess the third MSD, these members of Mrp family include Mrp4, Mrp5, Mrp8 and Mrp9 (Fig. 1.5) (Kruh *et al.* 2007).



OATPs: Organic anion transporting polypeptides
 NTCP: Na⁺-dependent taurocholic cotransporting polypeptide
 BCRP: Breast cancer related protein

MDR: Multidrug resistance-protein
 Mrp: Multidrug resistant associated protein
 BSEP: Bile acid export pump

Fig. 1.3. Protein transporters involving in transport of chemical across liver cell membrane in and out of hepatocytes (see text). Black dots represent chemicals in blood, hepatocytes and bile [adapted from Shitara et al (2006)].

Multidrug-resistance-associated protein 2 (Mrp2; previously known as ABCC2) is the second member of the subfamily of Mrp efflux pumps to be cloned from rat and human tissues. Mrp2 consists of 1,545 amino acids (Jedlitschky *et al.* 2006). Mrp2 can transport a broad range of substrates including a variety of endogenous substrates, many drugs, natural toxins and toxicants. Important Mrp2 substrates are listed in Table 1.1. Using mutant strains of rats, the physiological functions of Mrp2 were recognized long before its cloning by studies on the hepatobiliary elimination of organic anions in normal and

transport-deficient mutant rats (Jedlitschky *et al.* 2006; Nies and Keppler 2007). The loss of ATP-dependent transport across the hepatocyte canalicular membrane was identified in these mutant rats using inside-out membrane vesicles and various glutathione (GSH) *S*-conjugates as substrates (Nies and Keppler 2007).

The *Mrp2* gene was firstly cloned as a fragmented cDNA from rat livers (Cole *et al.* 1992). In addition, Mrp2 expression and its related proteins was found in 5 other mammalian species including human, rhesus monkey, rabbit, mouse, and, dog. It also has been discovered in other 3 vertebrates and 1 non-vertebrate species including the chicken, zebrafish and little skate, and, *Caenorhabditis elegans*, respectively (Nies and Keppler 2007). The conservation of this transporter protein among these species from a simple organism like *C. elegans* to a much more complex species like humans suggested significant roles of Mrp2 during their evolutionary processes.

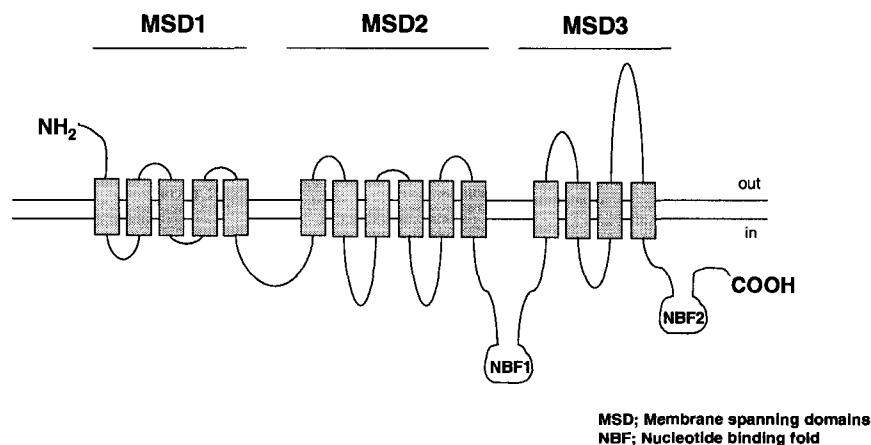


Fig. 1.4. Schematic structure of Mrp1, Mrp2, Mrp3, Mrp6, and Mrp7 [adapted from Kruh *et al.* (2007)]. These transporter proteins possess 3 membrane spanning domains (MSD_s; MSD1, MSD2 and MSD3) and 2 intracellular nucleotide binding folds (NBF_s; NBF1 and NBF2).

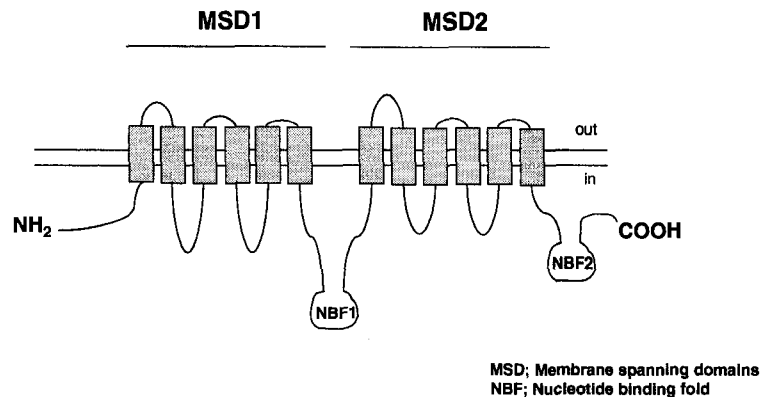


Fig. 1.5. Schematic structure of Mrp4, Mrp5, Mrp8, and Mrp9 [adapted from Kruh et al (2007)]. These transporter proteins possess 2 membrane spanning domains (MSD_s; MSD1 and MSD2) and 2 intracellular nucleotide binding folds (NBF_s; NBF1 and NBF2).

7. TISSUE DISTRIBUTION & CELLULAR LOCALIZATION OF MRP2

Mrp2 can be found primarily at canalicular membrane of hepatocytes (Konig *et al.* 1999). In addition, Mrp2 expression can also be observed in some other organs including kidney (Schaub *et al.* 1999; Schaub *et al.* 1997), proximal duodenum and distal ileum (Dietrich *et al.* 2003; Ito *et al.* 1997; Mottino *et al.* 2000; Paulusma *et al.* 1996). Mrp2 in these organs localizes in apical membranes of the cells in GI tract and kidney, suggesting its roles of the transporter protein in excreting its substrates into GI lumens and into urine, respectively (Konig *et al.* 1999). Furthermore, a small amount of Mrp2 expression can also be found in epithelial cells of gall bladder (Rost *et al.* 2001) and brain capillary epithelial cells (Dombrowski *et al.* 2001). In all of these organs, specific localization was observed. Interestingly, Mrp2 expression was also observed in placenta on the apical membrane of syncytiotrophoblasts (Meyer zu Schwabedissen *et al.* 2005; St-Pierre *et al.* 2000), these results suggested a role of Mrp2 in protecting fetuses from chemical exposures (Jedlitschky *et al.* 2006).

Table 1.1. Summary of Important Mrp2 Substrates.

Class of Mrp2 Substrates	Mrp2 Substrates
<i>Endogenous Substrates:</i>	Bilirubin glucuronides Conjugated bile sales Gluthathione Leukotriene C ₄ , D ₄ , E ₄ Steroids (17 β -glucuronosyl estradiol)
<i>Exogenous Substrates:</i>	
1) Drugs	
• Antineoplastic agents	Camptothecin Cisplatin Doxorubicin Etoposide Irinotecan Methotrexate Mitoxantrone Vincristine Vinblastine
• Anti-HIV drugs	Cidonavir Indinaivir Nelfinavir Ritonavir Saquinavir
• Antibiotics	Azithromycin Ampicillin Cefodizime Ceftriaxone Grepafloxacin
• Others	Conjugates of a variety of drugs (e.g. acetaminophen, indomethacin, phenobarbital, sulfapyrazone) Olmesartan Pravastatin Temocaprilate

Table 1.1. (continued). Summary of Important Mrp2 Substrates.

Class of Mrp2 Substrates	Mrp2 Substrates
<i>Exogenous Substrates:</i>	
2) Toxins and Toxicants	2-Amino-1-methyl-6-phenylimidazole- [4,5,b]-pyridine 4-(Methylnitrosamino)-1-(3-pyridyl)-1- butanol (NNAL) Heavy metal complexes (arsenic glutathione, Sb, Zn, Cu, Mn, Cd) NNAL- <i>O</i> -glucuronide α -naphylisothiocyanate Ochratoxin A <i>S</i> -glutathionyl-2,4-dinitrobenzene <i>S</i> -glutathionyl ethacrynic acid
<i>Exogenous Substrates:</i>	
3) Dyes	5-(6)-Carboxy-2',7'-dichlorofluorescein (CDF) Fluo-3 Sulfobromophthalein

8. MODE OF ACTION OF MRP2 IN TRANSPORTING ITS SUBSTRATES

Mrp2 can transport certain neutral or cationic compounds in a cotransport fashion with reduced GSH (Jedlitschky *et al.* 2006). For example, Mrp2 transports vincristine, a lipophilic neutral compound, and GSH simultaneously across the cell membrane by hydrolyzing 1 molecule of ATP to ADP (Fig. 1.6). For amphiphilic anions such as 4-(methylnitrosamino)-1-(3-pyridyl)-1-butanol (NNAL)-*O*-glucuronide and leukotriene C₄, Mrp2 can transport compounds in this group across the membrane directly by hydrolyzing an ATP molecule to ADP (Jedlitschky *et al.* 2006).

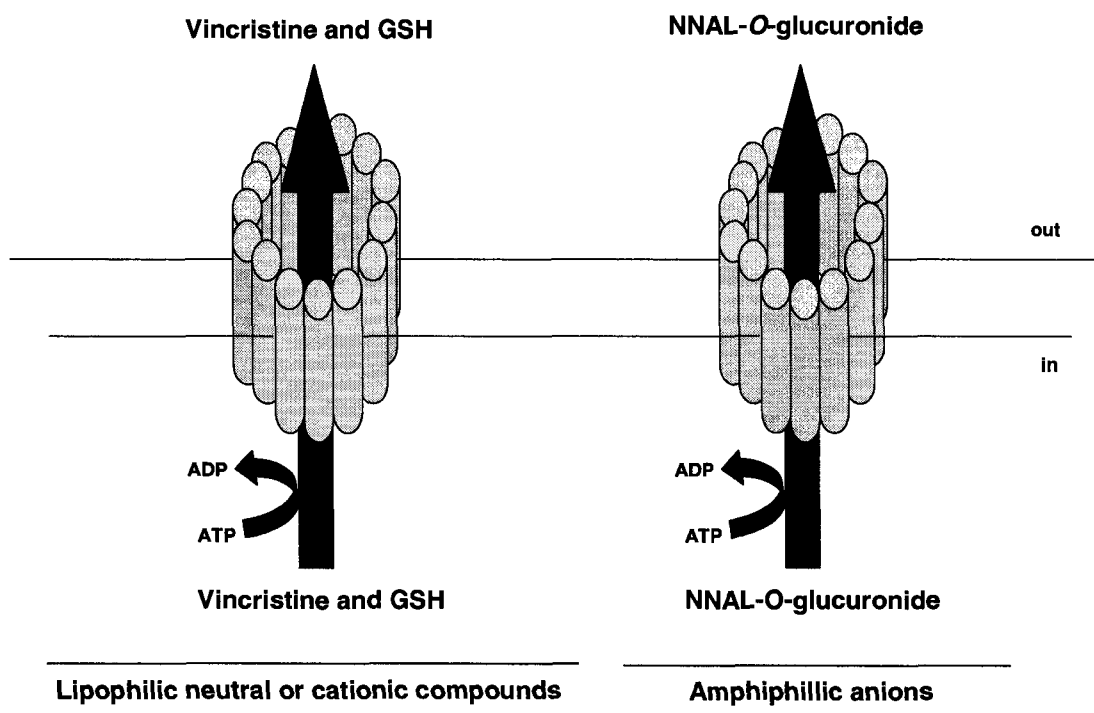


Fig. 1.6. Models of substrate transport by Mrp2 [adapted from Jedlitschky *et al.* (2007)]. Vincristine and vinblastine, lipophilic neutral compounds, can be transported across cell membrane with the presence of GSH and ATP (a co-transport mechanism). 4-(Methylnitrosamino)-1-(3-pyridyl)-1-butanol (NNAL)-*O*-glucuronide and leukotriene C₄ are examples of amphiphilic anions.

9. REGULATIONS OF MRP2 EXPRESSION

Regulation of Mrp2 function occurs at three levels; transcription level, translation level, and, endocytic retrieval from the cell membrane (Jedlitschky *et al.* 2006). At the transcription level, the promoter region of Mrp2 gene was cloned and characterized. In the promoter, there are several binding sites where certain transcriptional factors (i.e. AP1, SP1 and hepatocyte nuclear binding factor 1 and 3) can bind and increase the transcription process of mRNA Mrp2 synthesis (Jedlitschky *et al.* 2006). In rat hepatocyte culture, many chemicals including dexamethasone, 2-acetylaminofluorene, cisplatin, cycloheximide, phenobarbital, clotrimazole, and pregnenolone demonstrated an induction effect by increasing Mrp2 mRNA and the protein (Jedlitschky *et al.* 2006). In mice, exposure to PCB126 or 2,3,7,8-tetrachlorodibenzo-*p*-dioxin (TCDD) could increase Mrp2 expression levels in liver (Maher *et al.* 2005). In rats treated with ethinylestradiol, Mrp2 levels were decreased while there was no change in Mrp2 mRNA (Trauner *et al.* 1997). In the rhesus monkey, rifampicin could induce Mrp2 expression only in females, whereas tamoxifen could induce Mrp in both males and females. These results suggested that gender might play a role in Mrp2 expression (Kauffmann *et al.* 1998).

9.1. Dynamics of Mrp2: Retrieval and Recruitment

After completing its protein synthesis processes, Mrp2 molecules are either stored in intracellular vesicles or presented at cell membrane. Constant movement of the transporter protein between its storage site and the cell membrane is a key in Mrp2 regulation and its function. The function of Mrp2 is tightly controlled by the dynamics between the retrieval of the protein from cell membrane back to the storage vesicles and the recruitment of the protein from its intracellular pool to cell membrane (Kipp and

Arias 2000). Exposure to some chemicals and/or toxins can affect the presence of Mrp2 at its functional site. As a result, this may lead to changes in the Mrp2 functions. Some natural compounds such as phalloidin, a potent hepatotoxin, and genipin, an intestinal metabolite of geniposide, caused an increased recruitment of Mrp2 to the apical membrane of the liver, resulting in increased bile flow (Rost *et al.* 1999; Shoda *et al.* 2004). On the contrary, 17 β -glucuronosyl estradiol caused an inhibition of bile flow and retrieval of Mrp2 from canalicular membrane in rats (Mottino *et al.* 2002).

9.2. Effects of Interactions between PCB126 and Genipin on Mrp2 Function

In mice, exposure to PCB126 or TCDD could significantly increase hepatic Mrp2 expression levels (Maher *et al.* 2005). From these results, it can be inferred that PCB126 could induce hepatic Mrp2 expression via an aromatic hydrocarbon receptor (AhR)-dependent mechanism. Mechanistically, PCB126 also exerts their toxicological effects via binding to AhR similar to those of TCDD (Safe *et al.* 1985). The binding between AhR and its ligands results in diverse toxicological effects including over expression of hepatic cytochrome P450 1A1 and 1A2 (CYP1A and CYP1A2) (Chubb *et al.* 2004; NTP 2006). One of the prominent consequences of the overt induction in these CYP1A1 and CYP1A2 is a marked increase in oxidative stress (Jin *et al.* 2001). The resulting oxidative stress can affect the hepatic Mrp2 expression at the canalicular membrane (Ji *et al.* 2004; Sekine *et al.* 2006).

When hepatocytes were treated with ethacrynic acid, oxidative stress ensued (Ji *et al.* 2004; Sekine *et al.* 2006). Subsequently, the resulting increase in oxidative stress could perturb the intracellular Ca²⁺ homeostasis by enhancing Ca²⁺ efflux from endoplasmic reticulum, the intracellular storage pool of Ca²⁺. Thus, intracellular Ca²⁺

levels were elevated: this could lead to a series of enzyme activations [i.e. nitric oxide synthase (NOS), GC (cGMP producing enzyme), and, protein kinase C (PKC)] (Sekine *et al.* 2006). A net result of the activations of these regulatory enzymes was a reduction in membrane translocation of Mrp2 (Sekine *et al.* 2006).

As mentioned earlier, genipin can accelerate biliary excretion of Mrp2 substrates by enhancing the Mrp2 translocation process (Shoda *et al.* 2004). It was hypothesized that genipin could enhance the transport of Mrp2 from within its intracellular storage vesicles to its functional site, the canalicular membrane (Shoda *et al.* 2004). The complex interrelationship among PCB126, genipin, and Mrp2 expression/translocation are summarized in Fig. 1.7.

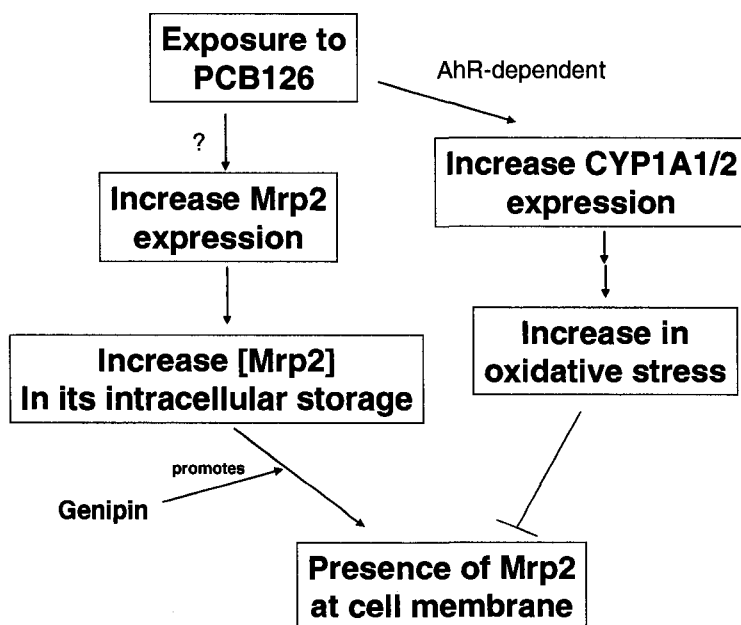


Fig. 1.7. Effect of 3,3',4,4',5-pentachlorobiphenyl (PCB126) and genipin on the regulation of Mrp2 expression and presence of Mrp2 at canalicular membrane in livers.

9.3. Stimulants and Inhibitors of Mrp2

Some drugs, chemicals from food, plants and beverages can function as stimulants or inhibitors of Mrp2. (Jedlitschky *et al.* 2006). A list of stimulants and inhibitors of Mrp2 are shown in Table 1.2.

Table 1.2. Stimulants and inhibitors of Mrp2.

<i>Stimulants:</i>	<i>Inhibitors:</i>
<ul style="list-style-type: none">• Bile salts• Gentamicin• Glutathione• Indomethacin• Sulfanitran• Ursodeoxycholic acid	<ul style="list-style-type: none">• α, β-unsaturated carbonyl compounds• Azithromycin• Benzoylated taxinine K• Curcumin• Cyclosporin A• Flavonoids• Furosemide• Grape fruit juice• Glibenclamid• Lonafarnib• Phenobarbital• PK-104P• Probenecid• Progestrins (norgestimate, progesterone)• Orange juice

10. ROLES OF MRP2 IN HUMAN DISEASES

In humans, mutations in the *Mrp2* gene can result in the autosomal recessive Dubin-Johnson syndrome (DJS). Several mutations leading to DJS have been identified (Keppler and König 2000). The DJS is characterized by a chronic, predominantly conjugated, non-hemolytic hyperbilirubinemia, caused by the hepatobiliary transport system of non-bile salt organic anions across the canalicular membrane (Elferink and Groen 2002). In addition, liver histology is normal except for the lysosomal accumulation of a black pigment which is considered to be the most prominent characteristics of DJS. Evidences from human cell lines suggested that, in humans with DJS, expression of Mrp3 expression levels was markedly induced (Stockel *et al.* 2000). This finding was also supported by some evidence from animal models lacking of Mrp2 expression (Kiuchi *et al.* 1998; Soroka *et al.* 2001).

11. EXPERIMENTAL MODELS USED TO INVESTIGATE THE MRP2-MEDIATED TRANSPORT

11.1. Animal Models for Studying Mrp2

To study Mrp2-mediated transport and effects of Mrp2 on xenobiotic dispositions, several animal models were developed. These include Eisai hyperbilirubinemic rats (EHBR), Groninger Yellow/transporter deficient rats (TR⁻), and, *mrp2* gene knockout mice (*mrp2*^{-/-} mice). All of these models featured a congenital absence in Mrp2 expression. Thus, all of these animal models can be used as a pivotal experimental tool in investigating Mrp2-mediated transport both *in vitro* and *in vivo*

studies. Characteristics of all of these important animal models of Mrp2 are summarized as follows:

11.1.1. Eisai hyperbilirubinemic rats (EHBR)

These mutant rats were firstly introduced by a group of researchers from Eisai Co., Ltd., Gifu, Japan (Hosokawa *et al.* 1992). EHBR is a mutant strain of inbred Sprague Dawley rats with autosomal recessive hyperbilirubinuria (Hosokawa *et al.* 1992). The absence of Mrp2 expression was the result of a one-nucleotide substitution resulting in a stop codon (Ito *et al.* 1997). However, induction of Mrp3 was observed (Hirohashi *et al.* 1998): this resulting Mrp3 induction might be a compensatory response to the lacking of Mrp2 expression. Noticeably, plasma bilirubin concentration levels in EHBR were significantly higher than that of the controls (Hosokawa *et al.* 1992). When administered with tetrabromosulfophthalein (BSP), plasma BSP clearance was significantly delayed in the EHBR. Plasma BSP elimination kinetics suggested that the pathophysiologic defect was not a result of impairment in either hepatic uptake or storage, but rather in secretion into bile (Hosokawa *et al.* 1992). Histopathology of the liver demonstrated brown pigment in the hepatocytes that appeared to be lipofuscin. The electron microscopic features of the hepatic pigment resembled those of the Dubin-Johnson syndrome (Hosokawa *et al.* 1992).

With these favorable characteristics, EHBR was the most widely used strain of the mutant rats lacking expression of Mrp2 available in the literature. In particular, EHBR was extensively utilized in numerous pharmacokinetic studies both *in vitro* and *in vivo*, leading to insights in roles of protein transporters in xenobiotic dispositions (Akita *et al.* 2001; Ito *et al.* 2004; Johnson *et al.* 2002; Johnson and Klaassen 2002; Kouzuki *et*

al. 2000; Naba *et al.* 2004; Prueksaritanont *et al.* 2003; Sathirakul *et al.* 1993; Sugie *et al.* 2004). Many pharmacokinetics of drugs such as benzylpenicillin (Ito *et al.* 2004), cefodizime (Sathirakul *et al.* 1993), indomethacin (Kouzuki *et al.* 2000), *L*-methotrexate (Naba *et al.* 2004) were examined using EHBR. These pharmacokinetic studies revealed the significant roles of Mrp2 in pharmacokinetics of these xenobiotics.

11.1.2. Groninger Yellow/transporter deficient rat (TR⁻)

TR⁻ is a mutant strain of inbred albino Wistar rats (Jansen *et al.* 1985). The absence of Mrp2 expression in this particular strain of rats was a result of a single nucleotide deletion leading to a frameshift mutation and a stop codon (Paulusma *et al.* 1996). This mutant strain of rats was characterized by autosomal recessive conjugated hyperbilirubinemia. Transport of conjugated bilirubin and BSP from liver to bile is severely impaired whereas uptake of organic anions from plasma to liver appears to be normal (Jansen *et al.* 1985). Serum bilirubin and bile acid levels in these mutant rats were significantly elevated, while liver marker enzyme activities and liver morphology were normal when compared to the controls (Jansen *et al.* 1985). The elevated serum levels of bilirubin and bile acid was a result of reduced bile flow. An impaired secretion of organic anions from the liver was suggested (Jansen *et al.* 1985).

Several *in vitro* and *in vivo* pharmacokinetic studies were performed using TR⁻ (de Waart *et al.* 2006; Gavrilova *et al.* 2007; Guminski *et al.* 2006; Hoffmaster *et al.* 2004; Leslie *et al.* 2007; Madejczyk *et al.* 2007; Maier-Salamon *et al.* 2007; Newton *et al.* 2005; Takada *et al.* 2004; Zamek-Gliszczyński *et al.* 2006a). For instance, disposition of a tobacco carcinogen 4-(methylnitrosamino)-1-(3-pyridyl)-1-butanone (NNK), its carcinogenic metabolite 4-(methylnitrosamino)-1-(3-pyridyl)-1-butanol (NNAL), and, its

non-carcinogenic glucuronidated metabolite NNAL-*O*-glucuronide were examined using TR⁻ (Leslie *et al.* 2007). The results from this study revealed a significant role of Mrp2 in the biliary excretion of NNAL-*O*-glucuronide (Leslie *et al.* 2007).

11.1.3. *Mrp2* gene knockout mice (*Mrp2*^{-/-} mice)

Recently, a strain of mice lacking Mrp2 expression was introduced (Chu *et al.* 2006). Inactivation of *Mrp2* gene was performed by a deletion of nucleotides 1886 to 1897 of the coding sequence of the *Mrp2* gene. As a result, the primary physiological functions of Mrp2 protein in these knockout mice were absent, these were demonstrated by: 1) increased levels of bilirubin and bilirubin glucuronides in serum and urine; 2) reduction in biliary excretion of bilirubin glucuronides, and; 3) reduction of total glutathione, and in the biliary excretion of dibromosulfophthalein (DBSP), an Mrp2 substrate (Chu *et al.* 2006). To identify possible compensatory mechanisms in *Mrp2*^{-/-} mice, unlike in *Mrp2* mutant rats, no induction of Mrp3 was detected (Chu *et al.* 2006). However, Mrp4 mRNA and protein in liver and kidney were increased approximately 6- and 2-fold, respectively. Phenotypic analysis of major cytochrome P450-mediated activities in liver microsomes did not show differences between wild-type and *Mrp2*^{-/-} mice (Chu *et al.* 2006).

In comparison with EHBR and TR⁻ rats, there were limited numbers of studies using the knockout mice, *Mrp2*^{-/-}, to explore the roles of Mrp2 in pharmacokinetics and disposition of xenobiotics as *Mrp2*^{-/-} mice were only introduced in 2006. (Nezasa *et al.* 2006; Tian *et al.* 2007; Vlaming *et al.* 2006; Zamek-Gliszczyński *et al.* 2006b).

11.2. *In Vitro* Models for Studying Mrp2

To study Mrp2-mediated transport, several *in vitro* systems had been developed (Ghibellini *et al.* 2006; Inoue *et al.* 1984; Inoue *et al.* 1983; Meier *et al.* 1984). The most commonly utilized *in vitro* systems for investigating Mrp2-mediated transports were canalicular membrane vesicles (CMV) and sandwich-cultured hepatocyte system from liver harvested from EHBR, TR⁻, Mrp2^{-/-} mice, and their controls. These hepatocytes can be further utilized in these *in vitro* systems:

11.2.1. Canalicular membrane vesicle system

Canalicular membrane vesicles (CMV) were among the first experimental system used in examining hepatic transporter proteins (Inoue *et al.* 1984; Inoue *et al.* 1983; Meier *et al.* 1984).

Using this *in vitro* system along with the available animal models (i.e. EHBR and mrp2^{-/-} mice), important kinetic/biochemical parameters including binding affinity values (K_m) of Mrp2 substrates could be calculated (Niinuma *et al.* 1997). In addition, using this experimental system, many of Mrp2 substrates were characterized. For examples, bile salts (Akita *et al.* 2001), dibromosulfophthalein (Chu *et al.* 2006), grepafloxacin (Hirono *et al.* 2005), 6-hydroxy-5,7-dimethyl-2-methylamino-4-(3-pyridylmethyl) benzothiazole-glucuronide (Niinuma *et al.* 1997), *L*-methotrexate (Hirono *et al.* 2005), leukotriene C₄ (Hirono *et al.* 2005; Keppler *et al.* 1997), PKI166 (Takada *et al.* 2004), pravastatin (Yamazaki *et al.* 1997), olmesartan (Yamada *et al.* 2007), *S*-(2,4-dinitrophenyl)-glutathione (Niinuma *et al.* 1997), and, temocaprilate (Hirono *et al.* 2005) were among drugs and chemicals identified as Mrp2 substrates using the CMV system.

11.2.2. Sandwich-cultured hepatocyte system

Although the CMV system is capable of providing important biochemical parameters related to the Mrp2-mediated transport in liver. However, the fact that CMV is a cell free fraction containing the functional transporter protein, not the whole living cells. Thus, a cell culture system consisting of living hepatocytes was developed (Liu *et al.* 1999). Hepatocytes from humans or animals can be used in this particular system (Ghibellini *et al.* 2006). Since the hepatocytes in this experimental system still retain metabolic capabilities and they can be maintained in culture environments up to 5 days (Liu *et al.* 1999), allowing for the study of drug interactions involving mechanisms. This hepatocyte culture system can serve as an *in vitro* tool to investigate hepatobiliary transport mechanisms.

11.3. *In Silico* Models of Mrp2

Up to present, there are three *in silico* models related to Mrp2 (Hirono *et al.* 2005; Lai *et al.* 2007; Ng *et al.* 2005). Lai and colleagues developed a three-dimensional quantitative structure-activity relationship (3D-QSAR) model to identify a selective Mrp2 inhibitor for therapeutic purposes (Lai *et al.* 2007), while Ng *et al.* used a 3D-QSAR approach to characterize structural requirements and molecular features for an Mrp2-mediated methotrexate (MTX) excretion process for further developments of antineoplastic MTX analogues (Ng *et al.* 2005). To identify overall structural features of Mrp2 substrates and to predict binding affinity values (K_m) of Mrp2 substrates, Hirono *et al.* developed a 3D-QSAR model of rat Mrp2 (Hirono *et al.* 2005). Because of its broader applications, the Hirono *et al.* 3D-QSAR model is more useful in the pharmacokinetics/toxicokinetics studies of Mrp2 substrates. Thus, in this review, we shall focus primarily on the third 3D-QSAR model developed by Hirono *et al.* (2005).

The third 3D-QSAR model for rat Mrp2 was developed using ligand-based drug design techniques (Hirono *et al.* 2005). In that paper, the authors used the 3D-QSAR modeling and computational chemistry approach to examine 18 Mrp2 substrates (16 used in a training set and 2 used in a test set). These chemicals included leukotriene C₄, *p*-nitrophenyl glucuronide, SN-38 glucuronide (lactone form), SN38-glucuronide (carboxylate form), E3040 glucuronide, leukotriene D₄, *N*-acetyl leukotriene E₄, *S*-grepafloxacin-glucuronide, *R*-grepafloxacin-glucuronide, *L*-methotrexate, 2, 4-dinitrophenyl-*S*-glutathione, BQ-123, SN-38 (carboxylate form), temocaprilate, 5-methyltetrahydrofolate, CPT-11 (carboxylate form), BQ-485, and MX-68. Binding affinity values (K_m) of Mrp2 to all of the 18 chemicals were determined experimentally using the CMV technique (see details above), and, then compared to predicted K_m values obtained from the 3D-QSAR model.

When compared to experimental measurements, their predicted values of $\log(1/K_m)$ from this 3D-QSAR were within 2% of the determined values for 16 chemicals in their training set (Hirono *et al.* 2005). The largest difference of 13% was seen between predicted and experimental values in one of the two chemicals in their test set. Using a number of molecular indices (i.e. steric field, electrostatic field and C log P), and computational chemistry, this 3D-QSAR model is capable of assessing the feasibility of Mrp2 binding, as well as estimating binding affinity (K_m), of chemicals. Using the 3D pharmacophore and comparative molecular-field analysis (CoMFA) map, a ligand binding region of Mrp2 was estimated (Fig. 1.8). From the structural analysis, an Mrp2 substrate must possess 2 hydrophobic regions with some required structural dimensions (Fig. 1.8). For example, any molecule similar to the required pharmacophore of SN-38

glucuronide (carboxylate form) has a potential to be an Mrp2 substrate (Fig. 1.9). Using a superposition technique, a candidate molecule [e.g. 3,3',4,4',5-pentachlorobiphenyl (PCB126)] can be tested whether or not it can be an Mrp2 substrate (Fig. 1.10). From this superposition study, PCB126 was identified as an Mrp2 substrate, and the binding affinity (K_m) between Mrp2 and PCB126 was calculated demonstrating a relatively high binding affinity.

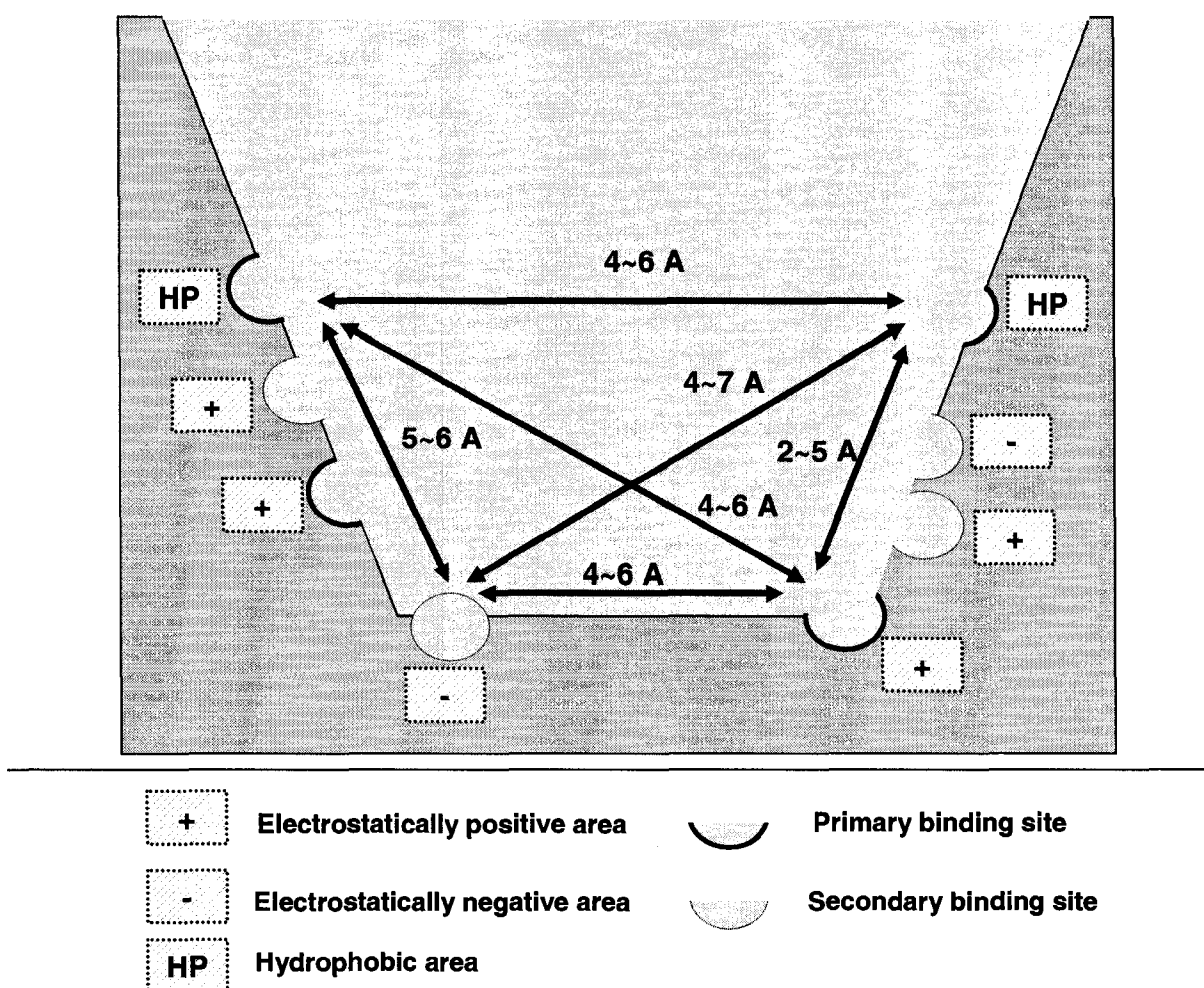


Fig. 1.8. Ligand binding region of Mrp2 using the 3D pharmacophore and CoMFA contour map (adapted from Hirono et al, 2005).

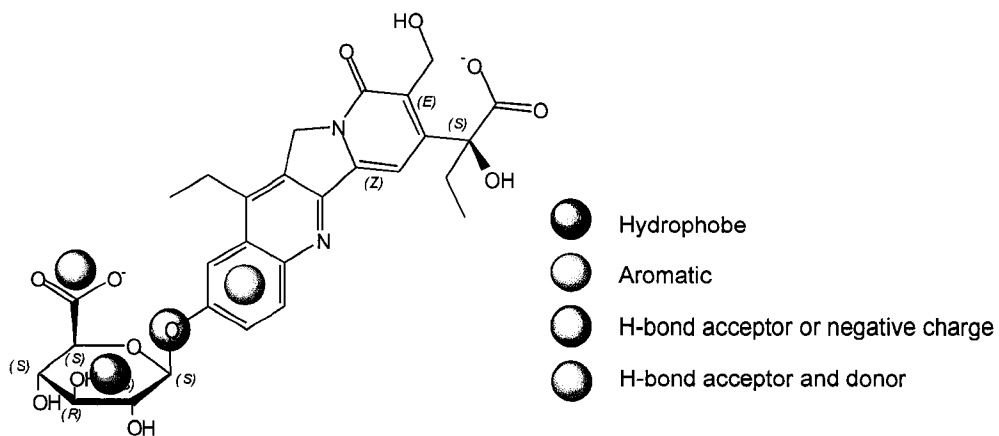


Fig. 1.9. A Pharmacophore of SN-38 glucuronide (carboxylate form) consisting of two H-bond acceptors (red), one aromatic group (light gray) and one hydrophobic group (dark gray). This figure of SN-38 glucuronide (carboxylate form) was kindly supplied by Dr. Shuichi Hirono.

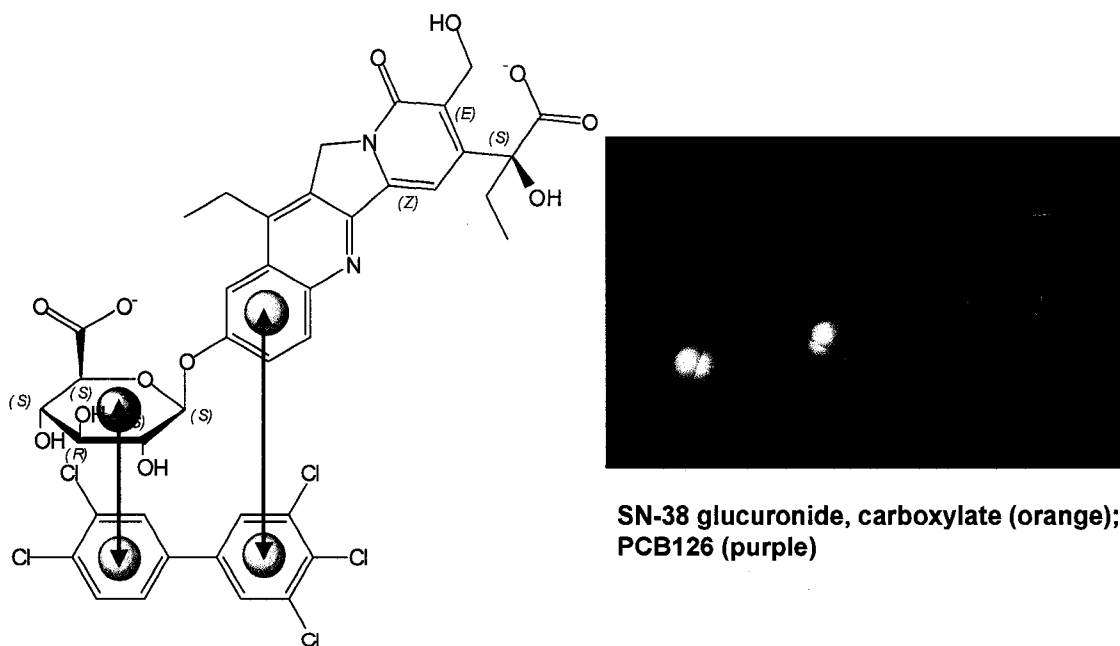


Fig 1.10. An example of structural superposition between SN-38 glucuronide (carboxylate form; a reference molecule, orange) and 3,3',4,4',5-pentachlorobiphenyl (PCB126; a candidate molecule, purple). This figure of PCB126 superposition was kindly supplied by Dr. Shuichi Hirono.

12. METHOTREXATE (MTX)

Methotrexate (MTX; Fig. 1.11) is a dihydrofolate reductase (DHFR) inhibitor which has been widely used in cancer treatments and rheumatoid arthritis (Treon and Chabner 1996; Walker and Ranatunga 2006). MTX exerts its pharmacological effects via an irreversible binding to DHFR resulting in its cytotoxic effects. In 1971, Bischoff *et al.* reported a physiologically-based pharmacokinetic (PBPK) model of MTX (Bischoff *et al.* 1971). A schematic diagram of this model is depicted in Fig. 1.12. This model is one of the earliest PBPK models published in the literature. This PBPK model was able to describe a variety of dose levels of MTX in several species, including mice, rats, dogs and humans. The model structure consisted of plasma, liver, kidney, muscle, gut lumen, and gut tissue compartments. In this model, entero-hepatic recirculation behavior of MTX was also mathematically incorporated. In the liver sub-compartment, MTX is excreted into bile using biliary secretion with a first order kinetic process. Subsequently, MTX is secreted into the gut lumen and reabsorbed completing its entero-hepatic recirculation.

In 2001, multidrug-resistance-associated protein 2 (Mrp2), a transporter protein, was identified as a molecular entity responsible for the biliary excretion of MTX (Han *et al.* 2001). A mutation at Trp1254 of *Mrp2* gene resulted in a loss of MTX transport activity in a cell culture system (Ito *et al.* 2001). Recently a three-dimensional quantitative structure-activity relationship (3D-QSAR) model of Mrp2 was developed (see above) (Hirono *et al.* 2005). In this paper, the authors reported a binding affinity (K_m) value of MTX to Mrp2 using a computational chemistry technique. With this newly available scientific information, we were able to employ this information regarding

biochemical characteristics of MTX at the molecular excretion site, and then incorporate this information into the existing PBPK model of MTX to describe available datasets obtained from different pharmacokinetic studies from several species with different dosing scenarios and experimental conditions (see Chapter 4).

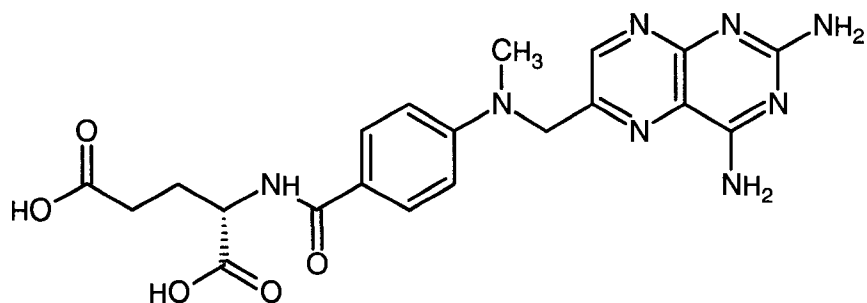


Fig. 1.11. A chemical structure of *L*-methotrexate (MTX)

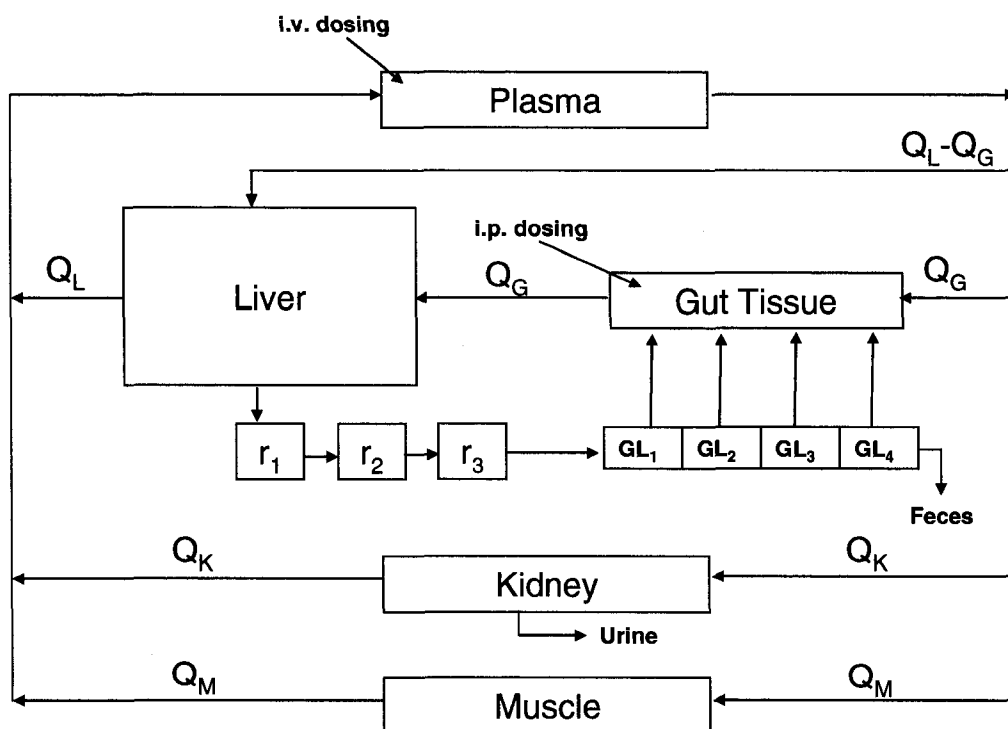


Fig. 1.12. A schematic diagram of the physiologically-based pharmacokinetic (PBPK) model of methotrexate [adapted from Bischoff et al. (1971)].

13. A POSSIBLE CONNECTION BETWEEN PHYSIOLOGICALLY-BASED PHARMACOKINETIC MODELING AND THE 3D-QSAR MODEL

As discussed earlier, Mrp2 has a very important role in biliary excretion of diverse groups of drugs and chemicals. Hirono and coworkers has recently developed a powerful *in silico* tool in predicting the structure-activity correlation of Mrp2 substrates (Hirono *et al.* 2005). Thus, there is a strong potential to incorporate this new scientific information into a mathematical model to describe concentration-time courses of Mrp2 substrates. Physiologically-based pharmacokinetics (PBPK) is a mathematical modeling approach with a high capability to simulate any biological and/or biochemical processes (Andersen 1995; Belfiore *et al.* 2007; Bischoff *et al.* 1971; Haddad *et al.* 2001; Lu *et al.* 2006; Ramsey and Andersen 1984). The Hirono *et al.* 3D-QSAR modeling technique to predict K_m values of the Mrp2 substrates in conjunction with the PBPK modeling technique should be a practical approach to facilitate better understandings of pharmacokinetics and dispositions of the Mrp2 substrates.

Since the key parameters (i.e. K_m) related to the Mrp2-mediated excretion process of a candidate for Mrp2 substrate and Mrp2 substrates (e.g. PCB126 and MTX) were available, thus incorporation of the available information into their PBPK models is feasible. Schematic diagrams of PBPK models of PCB126 and MTX with incorporations of the liver Mrp2-mediated excretion process are illustrated in Fig. 1.13 and 1.14, respectively. Hypothetically, PCB126 and MTX could be simultaneously presenting in the body. A schematic diagram of the interactions between PCB126 and MTX is illustrated in Fig. 1.15. In this case, a competitive inhibition between the two Mrp2 substrates at the hepatic Mrp2 excretion site is possible (Fig. 1.15). The competitive

inhibition process can be mathematically described and incorporated into the model. This pharmacokinetic interaction might result in changes in pharmacokinetics of PCB126 and/or MTX.

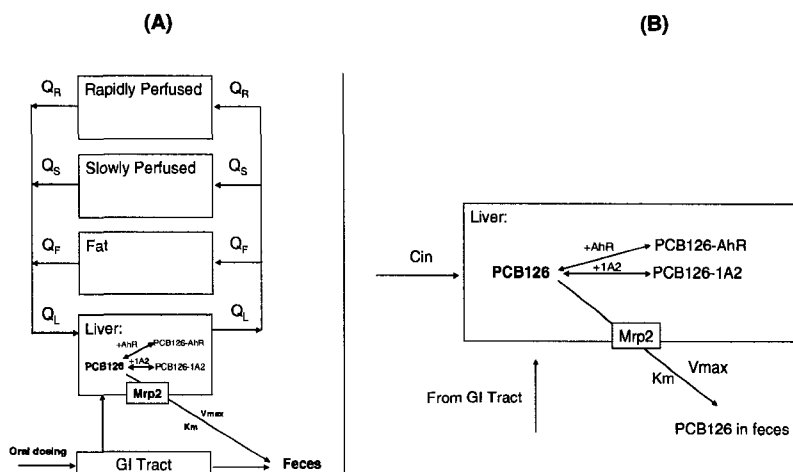


Fig. 1.13. A schematic diagram of a PBPK model structure of 3,3',4,4',5-pentachlorobiphenyl (PCB126) (A) and liver subcompartment consisting of binding between PCB126 and AhR, CYP1A2, and excretion via hepatic MRP2 (B). The calculation of the binding affinity (K_m) value can be obtained from the 3D-QSAR model earlier developed by Hirono et al., and be incorporated into the PBPK model.

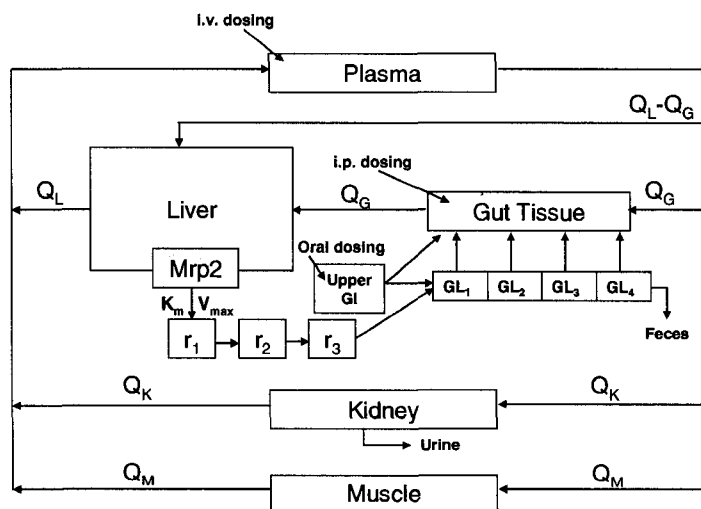


Fig. 1.14. A schematic diagram of a PBPK model of methotrexate (MTX). An MRP2-mediated biliary excretion process was incorporated. The calculation of the binding affinity (K_m) value can be obtained from the 3D-QSAR model earlier developed by Hirono et al, and utilized in the PBPK model.

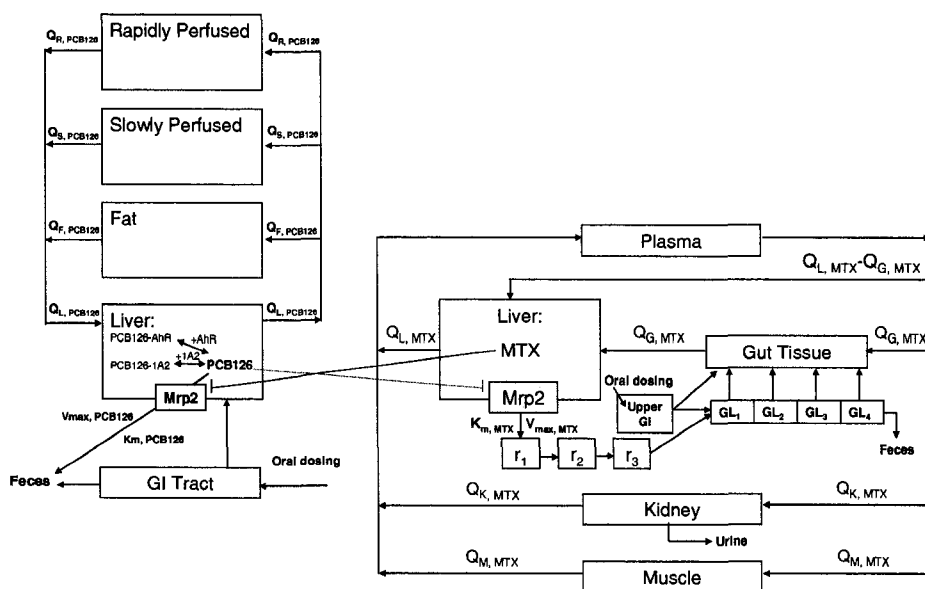


Fig. 1.15. A schematic diagram of possible pharmacokinetic interactions between PCB126 and methotrexate (MTX) at liver Mrp2. Competitive inhibitions between these two Mrp2 substrates may occur at the hepatic Mrp2. The symbols (\perp) represent competitive inhibition processes, resulting from the co-existence of MTX and PCB126.

In summary, this review introduced the biology of Mrp2, its tissue distribution & cellular localization, its physiological functions, its substrates, its mechanism of transporting the substrates, its regulations of expression, and, its role in human diseases. In addition, to study Mrp2, several experimental models were developed by various investigators: these include several kinds of animal models, some experimental *in vitro* techniques, and, *in silico* 3D-QSAR techniques. With all of these available experimental tools, scientists in the field are able to objectively investigate Mrp2 and its roles in dispositions of its endogenous substrates and various categories of xenobiotics including therapeutic agents and toxicants. In addition, the available *in silico* 3D-QSAR models of Mrp2 (Hirono *et al.* 2005) and the PBPK modeling technique, when utilized together, may provide a new and powerful quantitative tool in predicting pharmacokinetics of individual Mrp2 substrates and pharmacokinetic interactions between Mrp2 substrates.

REFERENCES

- Abraham, K., Krowke, R., and Neubert, D. (1988). Pharmacokinetics and biological activity of 2,3,7,8-tetrachlorodibenzo-p-dioxin. 1. Dose-dependent tissue distribution and induction of hepatic ethoxyresorufin O-deethylase in rats following a single injection. *Arch Toxicol* **62**, 359-68.
- Akita, H., Suzuki, H., Ito, K., Kinoshita, S., Sato, N., Takikawa, H., and Sugiyama, Y. (2001). Characterization of bile acid transport mediated by multidrug resistance associated protein 2 and bile salt export pump. *Biochim Biophys Acta* **1511**, 7-16.
- Andersen, M. E. (1995). Development of physiologically based pharmacokinetic and physiologically based pharmacodynamic models for applications in toxicology and risk assessment. *Toxicol Lett* **79**, 35-44.
- Belfiore, C. J., Yang, R. S., Chubb, L. S., Lohitnavy, M., Lohitnavy, O. S., and Andersen, M. E. (2007). Hepatic sequestration of chlordecone and hexafluoroacetone evaluated by pharmacokinetic modeling. *Toxicology* **234**, 59-72.
- Bischoff, K. B., Dedrick, R. L., Zaharko, D. S., and Longstreth, J. A. (1971). Methotrexate pharmacokinetics. *J Pharm Sci* **60**, 1128-33.
- CDC (2005). Third National Report on Human Exposure to Environmental Chemicals, pp. 186-7. National Center for Environmental Health, Atlanta.
- Chu, I., Villeneuve DC, Yagminas A, LeCavalier P, Poon R, Feeley M, Kennedy SW, Seegal RF, Hakansson H, Ahlborg UG, et al. (1994). Subchronic toxicity of 3,3',4,4',5-pentachlorobiphenyl in the rat. I. Clinical, biochemical, hematological, and histopathological changes. *Fundam Appl Toxicol.* **22**, 457-468.
- Chu, X. Y., Strauss, J. R., Mariano, M. A., Li, J., Newton, D. J., Cai, X., Wang, R. W., Yabut, J., Hartley, D. P., Evans, D. C., and Evers, R. (2006). Characterization of mice lacking the multidrug resistance protein MRP2 (ABCC2). *J Pharmacol Exp Ther* **317**, 579-89.
- Chubb, L. S., Andersen, M. E., Broccardo, C. J., Legare, M. E., Billings, R. E., Dean, C. E., and Hanneman, W. H. (2004). Regional induction of CYP1A1 in rat liver following treatment with mixtures of PCB 126 and PCB 153. *Toxicol Pathol* **32**, 467-73.
- Cole, S. P., Bhardwaj, G., Gerlach, J. H., Mackie, J. E., Grant, C. E., Almquist, K. C., Stewart, A. J., Kurz, E. U., Duncan, A. M., and Deeley, R. G. (1992). Overexpression of a transporter gene in a multidrug-resistant human lung cancer cell line. *Science* **258**, 1650-4.

- de Waart, D. R., Paulusma, C. C., Kunne, C., and Oude Elferink, R. P. (2006). Multidrug resistance associated protein 2 mediates transport of prostaglandin E2. *Liver Int* **26**, 362-8.
- Dean, C. E., Jr., Benjamin, S. A., Chubb, L. S., Tessari, J. D., and Keefe, T. J. (2002). Nonadditive hepatic tumor promoting effects by a mixture of two structurally different polychlorinated biphenyls in female rat livers. *Toxicol Sci* **66**, 54-61.
- Dietrich, C. G., Geier, A., and Oude Elferink, R. P. (2003). ABC of oral bioavailability: transporters as gatekeepers in the gut. *Gut* **52**, 1788-95.
- Dombrowski, S. M., Desai, S. Y., Marroni, M., Cucullo, L., Goodrich, K., Bingaman, W., Mayberg, M. R., Bengez, L., and Janigro, D. (2001). Overexpression of multiple drug resistance genes in endothelial cells from patients with refractory epilepsy. *Epilepsia* **42**, 1501-6.
- Dragan, Y. P., Hully, J. R., Nakamura, J., Mass, M. J., Swenberg, J. A., and Pitot, H. C. (1994). Biochemical events during initiation of rat hepatocarcinogenesis. *Carcinogenesis* **15**, 1451-8.
- Dragan, Y. P., Laufer, C., Koleske, A. J., Drinkwater, N., and Pitot, H. C. (1993). Quantitative comparison of initiation and mutation phenotypes in hepatocytes of the analbuminemic rat. *Jpn J Cancer Res* **84**, 175-83.
- Elferink, R. O., and Groen, A. K. (2002). Genetic defects in hepatobiliary transport. *Biochim Biophys Acta* **1586**, 129-45.
- Gavrilova, O., Geyer, J., and Petzinger, E. (2007). In vivo relevance of Mrp2-mediated biliary excretion of the Amanita mushroom toxin demethylphalloin. *Biochim Biophys Acta* (in press).
- Ghibellini, G., Leslie, E. M., and Brouwer, K. L. (2006). Methods to evaluate biliary excretion of drugs in humans: an updated review. *Mol Pharm* **3**, 198-211.
- Guminski, A. D., Balleine, R. L., Chiew, Y. E., Webster, L. R., Tapner, M., Farrell, G. C., Harnett, P. R., and Defazio, A. (2006). MRP2 (ABCC2) and cisplatin sensitivity in hepatocytes and human ovarian carcinoma. *Gynecol Oncol* **100**, 239-46.
- Haddad, S., Beliveau, M., Tardif, R., and Krishnan, K. (2001). A PBPK modeling-based approach to account for interactions in the health risk assessment of chemical mixtures. *Toxicol Sci* **63**, 125-31.
- Han, Y. H., Kato, Y., Haramura, M., Ohta, M., Matsuoka, H., and Sugiyama, Y. (2001). Physicochemical parameters responsible for the affinity of methotrexate analogs

- for rat canalicular multispecific organic anion transporter (cMOAT/MRP2). *Pharm Res* **18**, 579-86.
- Hirohashi, T., Suzuki, H., Ito, K., Ogawa, K., Kume, K., Shimizu, T., and Sugiyama, Y. (1998). Hepatic expression of multidrug resistance-associated protein-like proteins maintained in eisai hyperbilirubinemic rats. *Mol Pharmacol* **53**, 1068-75.
- Hirono, S., Nakagome, I., Imai, R., Maeda, K., Kusuhara, H., and Sugiyama, Y. (2005). Estimation of the three-dimensional pharmacophore of ligands for rat multidrug-resistance-associated protein 2 using ligand-based drug design techniques. *Pharm Res* **22**, 260-9.
- Hoffmaster, K. A., Zamek-Gliszczynski, M. J., Pollack, G. M., and Brouwer, K. L. (2004). Hepatobiliary disposition of the metabolically stable opioid peptide [D-Pen2, D-Pen5]-enkephalin (DPDPE): pharmacokinetic consequences of the interplay between multiple transport systems. *J Pharmacol Exp Ther* **311**, 1203-10.
- Hosokawa, S., Tagaya, O., Mikami, T., Nozaki, Y., Kawaguchi, A., Yamatsu, K., and Shamoto, M. (1992). A new rat mutant with chronic conjugated hyperbilirubinemia and renal glomerular lesions. *Lab Anim Sci* **42**, 27-34.
- Inoue, M., Kinne, R., Tran, T., and Arias, I. M. (1984). Taurocholate transport by rat liver canalicular membrane vesicles. Evidence for the presence of an Na⁺-independent transport system. *J Clin Invest* **73**, 659-63.
- Inoue, M., Kinne, R., Tran, T., Biempica, L., and Arias, I. M. (1983). Rat liver canalicular membrane vesicles. Isolation and topological characterization. *J Biol Chem* **258**, 5183-8.
- Ito, K., Koresawa, T., Nakano, K., and Horie, T. (2004). Mrp2 is involved in benzylpenicillin-induced choleresis. *Am J Physiol Gastrointest Liver Physiol* **287**, G42-9.
- Ito, K., Oleschuk, C. J., Westlake, C., Vasa, M. Z., Deeley, R. G., and Cole, S. P. (2001). Mutation of Trp1254 in the multispecific organic anion transporter, multidrug resistance protein 2 (MRP2) (ABCC2), alters substrate specificity and results in loss of methotrexate transport activity. *J Biol Chem* **276**, 38108-14.
- Ito, K., Suzuki, H., Hirohashi, T., Kume, K., Shimizu, T., and Sugiyama, Y. (1997). Molecular cloning of canalicular multispecific organic anion transporter defective in EHBR. *Am J Physiol* **272**, G16-22.
- Ito, N., Tamano, S., and Shirai, T. (2003). A medium-term rat liver bioassay for rapid in vivo detection of carcinogenic potential of chemicals. *Cancer Sci* **94**, 3-8.

- Jansen, P. L., Peters, W. H., and Lamers, W. H. (1985). Hereditary chronic conjugated hyperbilirubinemia in mutant rats caused by defective hepatic anion transport. *Hepatology* **5**, 573-9.
- Jedlitschky, G., Hoffmann, U., and Kroemer, H. K. (2006). Structure and function of the MRP2 (ABCC2) protein and its role in drug disposition. *Expert Opin Drug Metab Toxicol* **2**, 351-66.
- Ji, B., Ito, K., Sekine, S., Tajima, A., and Horie, T. (2004). Ethacrynic-acid-induced glutathione depletion and oxidative stress in normal and Mrp2-deficient rat liver. *Free Radic Biol Med* **37**, 1718-29.
- Jin, X., Kennedy, S. W., Di Muccio, T., and Moon, T. W. (2001). Role of oxidative stress and antioxidant defense in 3,3',4,4',5-pentachlorobiphenyl-induced toxicity and species-differential sensitivity in chicken and duck embryos. *Toxicol Appl Pharmacol* **172**, 241-8.
- Johnson, D. R., Habeebu, S. S., and Klaassen, C. D. (2002). Increase in bile flow and biliary excretion of glutathione-derived sulfhydryls in rats by drug-metabolizing enzyme inducers is mediated by multidrug resistance protein 2. *Toxicol Sci* **66**, 16-26.
- Johnson, D. R., and Klaassen, C. D. (2002). Role of rat multidrug resistance protein 2 in plasma and biliary disposition of dibromosulfophthalein after microsomal enzyme induction. *Toxicol Appl Pharmacol* **180**, 56-63.
- Kauffmann, H. M., Keppler, D., Gant, T. W., and Schrenk, D. (1998). Induction of hepatic mrp2 (cmrp/cmrat) gene expression in nonhuman primates treated with rifampicin or tamoxifen. *Arch Toxicol* **72**, 763-8.
- Keppler, D., and Konig, J. (2000). Hepatic secretion of conjugated drugs and endogenous substances. *Semin Liver Dis* **20**, 265-72.
- Keppler, D., Konig, J., and Buchler, M. (1997). The canalicular multidrug resistance protein, cMRP/MRP2, a novel conjugate export pump expressed in the apical membrane of hepatocytes. *Adv Enzyme Regul* **37**, 321-33.
- Kipp, H., and Arias, I. M. (2000). Intracellular trafficking and regulation of canalicular ATP-binding cassette transporters. *Semin Liver Dis* **20**, 339-51.
- Kiuchi, Y., Suzuki, H., Hirohashi, T., Tyson, C. A., and Sugiyama, Y. (1998). cDNA cloning and inducible expression of human multidrug resistance associated protein 3 (MRP3). *FEBS Lett* **433**, 149-52.
- Konig, J., Nies, A. T., Cui, Y., Leier, I., and Keppler, D. (1999). Conjugate export pumps of the multidrug resistance protein (MRP) family: localization, substrate

- specificity, and MRP2-mediated drug resistance. *Biochim Biophys Acta* **1461**, 377-94.
- Kouzuki, H., Suzuki, H., and Sugiyama, Y. (2000). Pharmacokinetic study of the hepatobiliary transport of indomethacin. *Pharm Res* **17**, 432-8.
- Kruh, G. D., Belinsky, M. G., Gallo, J. M., and Lee, K. (2007). Physiological and pharmacological functions of Mrp2, Mrp3 and Mrp4 as determined from recent studies on gene-disrupted mice. *Cancer Metastasis Rev* **26**, 5-14.
- Lai, Y., Xing, L., Poda, G. I., and Hu, Y. (2007). Structure-activity relationships for interaction with multidrug resistance protein 2 (ABCC2/MRP2): the role of torsion angle for a series of biphenyl-substituted heterocycles. *Drug Metab Dispos* **35**, 937-45.
- Leslie, E. M., Ghibellini, G., Nezasa, K. I., and Brouwer, K. L. (2007). Biotransformation and transport of the tobacco-specific carcinogen 4-(methylnitrosamino)-1-(3-pyridyl)-1-butanone (NNK) in bile duct-cannulated wild-type and Mrp2/Abcc2-deficient (TR-) Wistar rats. *Carcinogenesis* (in press).
- Liu, X., LeCluyse, E. L., Brouwer, K. R., Gan, L. S., Lemasters, J. J., Stieger, B., Meier, P. J., and Brouwer, K. L. (1999). Biliary excretion in primary rat hepatocytes cultured in a collagen-sandwich configuration. *Am J Physiol* **277**, G12-21.
- Lohitnavy, M., Chubb, L. S., Lohitnavy, O., Yang, C. C., Homberg, J., Campain, J. A., and Yang, R. S. (2004). Pharmacokinetic (PK)/Pharmacodynamic (PD) Relationship of PCB126 Under the Conditions of Modified Medium-Term Liver Bioassay. *Toxicologist* **78**, 271.
- Lu, Y., Lohitnavy, M., Reddy, M. B., Lohitnavy, O., Ashley, A., and Yang, R. S. (2006). An updated physiologically based pharmacokinetic model for hexachlorobenzene: incorporation of pathophysiological states following partial hepatectomy and hexachlorobenzene treatment. *Toxicol Sci* **91**, 29-41.
- Madejczyk, M. S., Aremu, D. A., Simmons-Willis, T. A., Clarkson, T. W., and Ballatori, N. (2007). Accelerated urinary excretion of methylmercury following administration of its antidote N-acetylcysteine requires Mrp2/Abcc2, the apical multidrug resistance-associated protein. *J Pharmacol Exp Ther* **322**, 378-84.
- Maher, J. M., Cheng, X., Slitt, A. L., Dieter, M. Z., and Klaassen, C. D. (2005). Induction of the multidrug resistance-associated protein family of transporters by chemical activators of receptor-mediated pathways in mouse liver. *Drug Metab Dispos* **33**, 956-62.
- Maier-Salamon, A., Hagenauer, B., Reznicek, G., Szekeres, T., Thalhammer, T., and Jager, W. (2007). Metabolism and disposition of resveratrol in the isolated

- perfused rat liver: Role of Mrp2 in the biliary excretion of glucuronides. *J Pharm Sci.* (in press)
- Meier, P. J., St Meier-Abt, A., Barrett, C., and Boyer, J. L. (1984). Mechanisms of taurocholate transport in canalicular and basolateral rat liver plasma membrane vesicles. Evidence for an electrogenic canalicular organic anion carrier. *J Biol Chem* **259**, 10614-22.
- Meyer zu Schwabedissen, H. E., Jedlitschky, G., Gratz, M., Haenisch, S., Linnemann, K., Fusch, C., Cascorbi, I., and Kroemer, H. K. (2005). Variable expression of MRP2 (ABCC2) in human placenta: influence of gestational age and cellular differentiation. *Drug Metab Dispos* **33**, 896-904.
- Mottino, A. D., Cao, J., Veggi, L. M., Crocenzi, F., Roma, M. G., and Vore, M. (2002). Altered localization and activity of canalicular Mrp2 in estradiol-17beta-D-glucuronide-induced cholestasis. *Hepatology* **35**, 1409-19.
- Mottino, A. D., Hoffman, T., Jennes, L., and Vore, M. (2000). Expression and localization of multidrug resistant protein mrp2 in rat small intestine. *J Pharmacol Exp Ther* **293**, 717-23.
- Naba, H., Kuwayama, C., Kakinuma, C., Ohnishi, S., and Ogihara, T. (2004). Eisai hyperbilirubinemic rat (EHBR) as an animal model affording high drug-exposure in toxicity studies on organic anions. *Drug Metab Pharmacokinet* **19**, 339-51.
- Newton, D. J., Wang, R. W., and Evans, D. C. (2005). Determination of phase I metabolic enzyme activities in liver microsomes of Mrp2 deficient TR- and EHBR rats. *Life Sci* **77**, 1106-15.
- Nezasa, K., Tian, X., Zamek-Gliszczynski, M. J., Patel, N. J., Raub, T. J., and Brouwer, K. L. (2006). Altered hepatobiliary disposition of 5 (and 6)-carboxy-2',7'-dichlorofluorescein in Abcg2 (Bcrp1) and Abcc2 (Mrp2) knockout mice. *Drug Metab Dispos* **34**, 718-23.
- Ng, C., Xiao, Y. D., Lum, B. L., and Han, Y. H. (2005). Quantitative structure-activity relationships of methotrexate and methotrexate analogues transported by the rat multispecific resistance-associated protein 2 (rMrp2). *Eur J Pharm Sci* **26**, 405-13.
- Nies, A. T., and Keppler, D. (2007). The apical conjugate efflux pump ABCC2 (MRP2). *Pflugers Arch* **453**, 643-59.
- Niinuma, K., Takenaka, O., Horie, T., Kobayashi, K., Kato, Y., Suzuki, H., and Sugiyama, Y. (1997). Kinetic analysis of the primary active transport of conjugated metabolites across the bile canalicular membrane: comparative study of S-(2,4-dinitrophenyl)-glutathione and 6-hydroxy-5,7-dimethyl-2-methylamino-

- 4-(3-pyridylmethyl)benzothiazole glucuronide. *J Pharmacol Exp Ther* **282**, 866-72.
- NTP (2006). NTP toxicology and carcinogenesis studies of 3,3',4,4',5-pentachlorobiphenyl (PCB 126) (CAS No. 57465-28-8) in female Harlan Sprague-Dawley rats (Gavage Studies). *Natl Toxicol Program Tech Rep Ser*, 4-246.
- Ogiso, T., Tatematsu, M., Tamano, S., Hasegawa, R., and Ito, N. (1990). Correlation between medium-term liver bioassay system data and results of long-term testing in rats. *Carcinogenesis* **11**, 561-6.
- Paulusma, C. C., Bosma, P. J., Zaman, G. J., Bakker, C. T., Otter, M., Scheffer, G. L., Scheper, R. J., Borst, P., and Oude Elferink, R. P. (1996). Congenital jaundice in rats with a mutation in a multidrug resistance-associated protein gene. *Science* **271**, 1126-8.
- Prueksaritanont, T., Xu, X., Deluna, P., Yamazaki, M., and Lin, J. H. (2003). Stereoselective hepatic disposition of a diastereomeric pair of alphavbeta3 antagonists in rat. *Xenobiotica* **33**, 1125-37.
- Ramsey, J. C., and Andersen, M. E. (1984). A physiologically based description of the inhalation pharmacokinetics of styrene in rats and humans. *Toxicol Appl Pharmacol* **73**, 159-75.
- Rost, D., Kartenbeck, J., and Keppler, D. (1999). Changes in the localization of the rat canalicular conjugate export pump Mrp2 in phalloidin-induced cholestasis. *Hepatology* **29**, 814-21.
- Rost, D., Konig, J., Weiss, G., Klar, E., Stremmel, W., and Keppler, D. (2001). Expression and localization of the multidrug resistance proteins MRP2 and MRP3 in human gallbladder epithelia. *Gastroenterology* **121**, 1203-8.
- Safe, S., Bandiera, S., Sawyer, T., Robertson, L., Safe, L., Parkinson, A., Thomas, P. E., Ryan, D. E., Reik, L. M., Levin, W., and et al. (1985). PCBs: structure-function relationships and mechanism of action. *Environ Health Perspect* **60**, 47-56.
- Safe, S. H. (1994). Polychlorinated biphenyls (PCBs): environmental impact, biochemical and toxic responses, and implications for risk assessment. *Crit Rev Toxicol* **24**, 87-149.
- Sathirakul, K., Suzuki, H., Yasuda, K., Hanano, M., Tagaya, O., Horie, T., and Sugiyama, Y. (1993). Kinetic analysis of hepatobiliary transport of organic anions in Eisai hyperbilirubinemic mutant rats. *J Pharmacol Exp Ther* **265**, 1301-12.

- Schaub, T. P., Kartenbeck, J., Konig, J., Spring, H., Dorsam, J., Staehler, G., Storkel, S., Thon, W. F., and Keppler, D. (1999). Expression of the MRP2 gene-encoded conjugate export pump in human kidney proximal tubules and in renal cell carcinoma. *J Am Soc Nephrol* **10**, 1159-69.
- Schaub, T. P., Kartenbeck, J., Konig, J., Vogel, O., Witzgall, R., Kriz, W., and Keppler, D. (1997). Expression of the conjugate export pump encoded by the *mrp2* gene in the apical membrane of kidney proximal tubules. *J Am Soc Nephrol* **8**, 1213-21.
- Sekine, S., Ito, K., and Horie, T. (2006). Oxidative stress and Mrp2 internalization. *Free Radic Biol Med* **40**, 2166-74.
- Shirai, T. (1997). A medium-term rat liver bioassay as a rapid in vivo test for carcinogenic potential: a historical review of model development and summary of results from 291 tests. *Toxicol Pathol* **25**, 453-60.
- Shoda, J., Miura, T., Utsunomiya, H., Oda, K., Yamamoto, M., Kano, M., Ikegami, T., Tanaka, N., Akita, H., Ito, K., Suzuki, H., and Sugiyama, Y. (2004). Genipin enhances Mrp2 (Abcc2)-mediated bile formation and organic anion transport in rat liver. *Hepatology* **39**, 167-78.
- Solt, D., and Farber, E. (1976). New principle for the analysis of chemical carcinogenesis. *Nature* **263**, 701-3.
- Soroka, C. J., Lee, J. M., Azzaroli, F., and Boyer, J. L. (2001). Cellular localization and up-regulation of multidrug resistance-associated protein 3 in hepatocytes and cholangiocytes during obstructive cholestasis in rat liver. *Hepatology* **33**, 783-91.
- Stockel, B., Konig, J., Nies, A. T., Cui, Y., Brom, M., and Keppler, D. (2000). Characterization of the 5'-flanking region of the human multidrug resistance protein 2 (MRP2) gene and its regulation in comparison with the multidrug resistance protein 3 (MRP3) gene. *Eur J Biochem* **267**, 1347-58.
- St-Pierre, M. V., Serrano, M. A., Macias, R. I., Dubs, U., Hoehli, M., Lauper, U., Meier, P. J., and Marin, J. J. (2000). Expression of members of the multidrug resistance protein family in human term placenta. *Am J Physiol Regul Integr Comp Physiol* **279**, R1495-503.
- Sugie, M., Asakura, E., Zhao, Y. L., Torita, S., Nadai, M., Baba, K., Kitaichi, K., Takagi, K., and Hasegawa, T. (2004). Possible involvement of the drug transporters P-glycoprotein and multidrug resistance-associated protein Mrp2 in disposition of azithromycin. *Antimicrob Agents Chemother* **48**, 809-14.
- Takada, T., Weiss, H. M., Kretz, O., Gross, G., and Sugiyama, Y. (2004). Hepatic transport of PKI166, an epidermal growth factor receptor kinase inhibitor of the

- pyrrolo-pyrimidine class, and its main metabolite, ACU154. *Drug Metab Dispos* **32**, 1272-8.
- Tian, X., Li, J., Zamek-Gliszczynski, M. J., Bridges, A. S., Zhang, P., Patel, N. J., Raub, T. J., Pollack, G. M., and Brouwer, K. L. (2007). Roles of p-glycoprotein, bcrp, and mrp2 in biliary excretion of spiramycin in mice. *Antimicrob Agents Chemother* **51**, 3230-4.
- Trauner, M., Arrese, M., Soroka, C. J., Ananthanarayanan, M., Koepfel, T. A., Schlosser, S. F., Suchy, F. J., Keppler, D., and Boyer, J. L. (1997). The rat canalicular conjugate export pump (Mrp2) is down-regulated in intrahepatic and obstructive cholestasis. *Gastroenterology* **113**, 255-64.
- Treon, S. P., and Chabner, B. A. (1996). Concepts in use of high-dose methotrexate therapy. *Clin Chem* **42**, 1322-9.
- Vlaming, M. L., Mohrmann, K., Wagenaar, E., de Waart, D. R., Elferink, R. P., Lagas, J. S., van Tellingen, O., Vainchtein, L. D., Rosing, H., Beijnen, J. H., Schellens, J. H., and Schinkel, A. H. (2006). Carcinogen and anticancer drug transport by Mrp2 in vivo: studies using Mrp2 (Abcc2) knockout mice. *J Pharmacol Exp Ther* **318**, 319-27.
- Walker, S. E., and Ranatunga, S. K. (2006). Rheumatoid arthritis: A review. *Mo Med* **103**, 539-44.
- Yamada, A., Maeda, K., Kamiyama, E., Sugiyama, D., Kondo, T., Shiroyanagi, Y., Nakazawa, H., Okano, T., Adachi, M., Schuetz, J. D., Adachi, Y., Hu, Z., Kushihara, H., and Sugiyama, Y. (2007). Multiple human isoforms of drug transporters contribute to the hepatic and renal transport of olmesartan, a selective antagonist of the angiotensin II AT1-receptor. *Drug Metab Dispos* (in press).
- Yamazaki, M., Akiyama, S., Ni'inuma, K., Nishigaki, R., and Sugiyama, Y. (1997). Biliary excretion of pravastatin in rats: contribution of the excretion pathway mediated by canalicular multispecific organic anion transporter. *Drug Metab Dispos* **25**, 1123-9.
- Zamek-Gliszczynski, M. J., Hoffmaster, K. A., Humphreys, J. E., Tian, X., Nezasa, K., and Brouwer, K. L. (2006a). Differential involvement of Mrp2 (Abcc2) and Bcrp (Abcg2) in biliary excretion of 4-methylumbelliferyl glucuronide and sulfate in the rat. *J Pharmacol Exp Ther* **319**, 459-67.
- Zamek-Gliszczynski, M. J., Nezasa, K., Tian, X., Kalvass, J. C., Patel, N. J., Raub, T. J., and Brouwer, K. L. (2006b). The important role of Bcrp (Abcg2) in the biliary excretion of sulfate and glucuronide metabolites of acetaminophen, 4-methylumbelliferone, and harmol in mice. *Mol Pharmacol* **70**, 2127-33.

CHAPTER 2

A Possible Role of Multidrug-Resistance-Associated Protein 2 (Mrp2) in Hepatic Excretion of PCB126, an Environmental Contaminant: PBPK/PD Modeling

Manupat Lohitnavy, Yasong Lu, Ornat Lohitnavy, Laura S. Chubb, Shuichi Hirono,
Raymond S. H. Yang

ABSTRACT

PCB126 is a carcinogenic environmental pollutant and its toxicity is mediated through binding with aryl hydrocarbon receptor (AhR). Earlier, we found that PCB126 treated F344 rats had 110-400 times higher PCB126 concentration in the liver than in the fat. Protein binding was suspected to be a major factor for the high liver concentration of PCB126 despite its high lipophilicity. In this research, we conducted a combined pharmacokinetic/pharmacodynamic study in male F344 rats. In addition to blood and tissue pharmacokinetics, we use the development of hepatic preneoplastic foci [glutathione-S-transferase placental form (GSTP)] as a pharmacodynamic endpoint. Experimental data were utilized for building a physiologically-based pharmacokinetic/pharmacodynamic (PBPK/PD) model. PBPK/PD modeling was consistent with the experimental PK and PD data. Salient features of this model include: (1) bindings between PCB126 and hepatic transporter proteins, particularly the multidrug-resistance-associated protein, Mrp2; (2) Mrp2-mediated excretion; and (3) a correlation between area under the curve of PCB126 in the livers (AUC_{Liver}) and GSTP foci development. Mrp2 involvement in PCB126 pharmacokinetics is supported by computational chemistry calculation using a three-dimensional quantitative structure-

activity relationship model of Mrp2 developed by Hirono et al (2005). This work, for the first time, provided a plausible role of a versatile hepatic transporter for drugs, Mrp2, in the disposition of an important environmental pollutant, PCB126. Furthermore, the PK and PD modeling in relation to GSTP foci development created a new opportunity for the application of this PBPK/PD model in the cancer risk assessment process.

1. INTRODUCTION

Polychlorinated biphenyls (PCBs) are halogenated aromatic hydrocarbons that had been widely used in industry. Because of their persistence as environmental pollutants, they had been discontinued from any usage since 1970's. However, significant amount of PCBs is still detectable in foods, human and animal tissues, and in the environment (CDC 2005; Safe *et al.* 1985; Safe 1994). 3,3',4,4',5'-Pentachlorobiphenyl (PCB126) is the most toxic congener of all PCBs with carcinogenic effects. Structurally, PCB126 is capable of binding with aryl hydrocarbon receptor (AhR) and elicits biological effects which include the induction of cytochrome P450A1 and 1A2 (CYP1A1, 1A2), thymic involution, wasting syndrome (Safe 1994), and carcinogenesis in the liver, lung, and mouth in rats (NTP 2006).

Despite its high lipophilicity, the levels of PCB126 in the liver are much higher than those observed in adipose tissue (Chu 1994; Dean *et al.* 2002; Lohitnavy *et al.* 2004). This is similar to those of chlordecone and 2,3,7,8-tetrachlorodibenzo-*p*-dioxin (TCDD) (Abraham *et al.* 1988; Belfiore *et al.* 2007), but at a much higher rate. These results suggested that protein binding is responsible for high levels of PCB126 in the liver. From a different perspective, while PCB126 is known to be persistent in the

environment (Safe 1994), in our laboratory, earlier results demonstrated that PCB126 could attain its steady state fairly rapidly (Lohitnavy *et al.* 2004). An initial pharmacokinetic estimation of half-life for this chemical turned out to be around 3 days (unpublished data). These results suggested that there was a relatively high hepatic clearance of PCB126. Therefore, we further considered the possible involvement of transporter protein(s), specifically the multidrug-resistance-associated protein 2 (Mrp2).

Excretion of xenobiotics can be mediated through several mechanisms, one of which is biliary excretion involving transporter proteins in the liver. This particular mechanism is responsible for excretion of many drugs and chemicals (Petzinger and Geyer 2006; Shitara *et al.* 2006). Mrp2 is an ATP-binding cassette (ABC) transporter, which is responsible for biliary excretion of many drugs and xenobiotics (Borst *et al.* 2006; Jedlitschky *et al.* 2006). Recently, a three-dimensional quantitative structure-activity relationship (3D-QSAR) model of Mrp2 in rats was developed (Hirono *et al.* 2005). Using a number of molecular indices (i.e. steric field, electrostatic field and C log P), and computational chemistry, this 3D-QSAR model is capable of assessing the feasibility of Mrp2 binding, as well as estimating binding affinity (K_m), of chemicals. Although Mrp2 was reported to having significant roles in biliary excretion in many drugs and xenobiotics (Borst *et al.* 2006; Jedlitschky *et al.* 2006), there is thus far no evidence demonstrating that Mrp2 could have a significant role in the disposition of PCB126 or other PCBs. In this paper, for the first time, we demonstrated a possible role of Mrp2 in the disposition of an environmental contaminant, PCB126. By incorporating this suggested role of Mrp2 into PBPK/PD model, the computer simulations were consistent with a number of sets of experimental results from different laboratories.

In this study, we also focused on the pharmacodynamics of PCB126. To test the carcinogenic potential of chemicals, we incorporated pharmacokinetics and pharmacodynamics into the Ito's medium-term liver bioassay (Ito *et al.* 2003; Shirai 1997), one of the most extensively studied cancer bioassay protocols. This bioassay involves a single dose administration of an initiator (diethylnitrosamine, DEN), followed by repeated administration of a promoter (a test chemical; in this case PCB126) to male F344 rats. The promotional effect of this assay is further enhanced by a two-third partial hepatectomy. Based on the development of glutathione-S-transferase placental form (GSTP) foci as a marker for pre-neoplastic lesions, this experimental model has shown excellent capability in predicting liver carcinogenicity in rats (Ogiso *et al.* 1990; Shirai 1997). In our modified protocol, we added multiple time points of sacrifice to observe liver GSTP foci development over time, as well as tissue kinetics for the development of PBPK/PD model.

There had been an earlier attempt of the development of a PBPK model of PCB126 with the incorporation of hepatic protein binding to AhR and CYP1A2 (NTP 2006); however, this model was unable to describe the tissue concentration data accurately (NTP 2006). In the present study, we utilized the available National Toxicology Program (NTP) experimental data (NTP 2006) plus our own results in the building of a new PBPK/PD model. In this model, in addition to protein bindings with AhR and CYP1A2, we incorporated a transporter protein, Mrp2, in the disposition of PCB126 based on supporting evidence from 3D-QSAR and computational chemistry (Hirono *et al.* 2005). The resulting computer simulations were consistent with all the available data.

2. MATERIAL AND METHODS

This study consisted of three parts: (1) development of a PBPK/PD model for PCB126 in the rat under normal physiological conditions with the incorporation of binding between PCB126 and 2 hepatic proteins (i.e. AhR and CYP1A2) and binding/excretion of PCB126 via hepatic Mrp2. The data used in this part were from 3D-QSAR modeling, computational chemistry, and from mining the literature; (2) experimental pharmacokinetic study of PCB126 under the time-course medium-term liver foci bioassay protocol, and simulation of this dataset by incorporation of pathophysiological conditions (i.e. two-third partial hepatectomy and recovery); and (3) correlation between internal dosimetry and experimental liver GSTP foci development.

2.1. Development of a PBPK/PD Model under Normal Physiological Conditions with Incorporation of Binding Between PCB126 and Hepatic Proteins and Excretion of PCB126 via Hepatic Mrp2

2.1.1. Pharmacokinetic studies of PCB126 by the NTP.

Recently the NTP published a 2-year carcinogenic study of PCB126 (NTP 2006). In this report, there were single dose and multiple dose pharmacokinetic studies. As described below, we employed these data as working datasets in PBPK model development in rats without pathological conditions.

2.1.1.1. Single Dose Study

Female Sprague-Dawley rats (SD, 20-22 weeks of age) were orally administered a single dose of 1,000 ng PCB126 in corn oil. PCB126 levels were determined in liver, blood, and fat samples at multiple time points. Group of five rats per time point were bled

and the tissues were collected at 0.5, 1, 1.5, 2, 3, 8, 16, or 24 hours post-PCB126 administration. Tissue samples were analyzed using a validated GC-MS method. These data were available in the NTP Technical Report (NTP 2006).

2.1.1.2. Multiple Dose 2-year Study

Female SD rats were orally administered with corn oil or PCB126 in corn oil at doses of 30, 100, 175, 300, 550, and 1,000 ng/kg body weight (5X per week) for two years. At week 13, 30, 52, and 104, five animals in each group were sacrificed. Livers, blood, and, fat tissue were harvested at the specified time points. Tissue samples were analyzed using a validated GC-MS method. Body weight of the animals was recorded periodically up to two years, and liver weights were reported from interim sacrifices up to one year. In the NTP Technical Report on PCB126, there was a PBPK model of PCB126. However this PBPK model was unable to describe the PCB126 tissue concentration accurately (NTP 2006).

2.1.1.3. Data extraction

The figures illustrating concentration-time courses of the pharmacokinetic studies of PCB126 in the NTP Technical Report (NTP 2006) were utilized. A digiMatic Program (version 2.1; Richmond, Virginia) was used to extract numerical co-ordinates from the concentration-time courses of PCB126 presented in the NTP Technical Report.

2.1.2. Computational Chemistry, 3D-QSAR Modeling of Binding of PCB126 to Mrp2

A 3D-QSAR model for rat Mrp2 was recently developed using ligand-based drug design techniques (Hirono *et al.* 2005). PCB126 is known to be present in the human body at extremely low concentrations (CDC 2005). This congener, being the most toxic of all PCB congeners, is usually studied at very low dose levels in animal experimentation. These realities make *in vitro* binding studies at realistic *in vivo* concentrations difficult due to analytical limitations. Therefore, we chose an *in silico* approach and determined the feasibility of Mrp2 binding by PCB126 based on molecular characteristics, such as molecular steric field, molecular electrostatic field and ClogP calculated by the SYBYL software package (Tripos Inc. St. Louis, USA). With the 3D-QSAR modeling and computational chemistry calculation, we found that Mrp2 binding feasibility is at least as good as or better than that of leukotriene C4, *S*- or *R*-grefapfloxacin glucuronide, temocaprilate, and *L*-methotrexate with a binding affinity constant (K_m) estimated to be 7,760.0 nM ($\log 1/K_m = 5.11$). We believe that, in the present case, the *in silico* approach is a reasonable alternative without the necessity of conducting Mrp2 binding experiments because (1) Hirono and colleagues (Hirono *et al.* 2005), using this same 3D-QSAR modeling and computational chemistry approach, demonstrated that their predicted values of $\log (1/K_m)$ were within 2% of the experimentally determined values for 16 chemicals in their training set. The largest difference of 13% was seen between predicted and experimental values in one of the two chemicals in their test set. Furthermore, according to our sensitivity analyses, varying the above *in silico* derived K_m values by 2X either way resulted in little or no change of

simulation results (unpublished data). Thus, we believe that the *in silico* derived binding affinity constant is adequate for our purpose.

2.1.3. Strategy in PBPK Model Development

The stepwise development of our PBPK model is given below.

2.1.3.1. Overall model scheme

The conceptual PBPK model of PCB126 is illustrated in Fig. 2.1A. The model structure included liver, rapidly perfused, slowly perfused, blood, fat, and GI tract compartments. The model described flow-limited transfer of PCB126 in liver, rapidly perfused, slowly perfused, and fat compartments. All parameters used in the model are summarized in Table 2.1. Physiological parameters were obtained from Brown et al (Brown *et al.* 1997). Partition coefficients of PCB126 in tissues were taken from the NTP Technical Report (NTP 2006).

2.1.3.2. Protein binding

Bindings with AhR and CYP1A2 are responsible for not only toxicological effects of PCB126, but also high levels of PCB126 in the livers. Thus, we incorporated two reversible binding processes between PCB126 and the responsible proteins into our model (Fig. 2.1B). Furthermore, to describe the Mrp2-mediated excretion process, a Michaelis-Menten equation was added in the liver submodel; the utilization of a Michaelis-Menten equation is consistent with the methodology in Hirono et al. (Hirono *et al.* 2005). The binding affinity of Mrp2 (K_m) obtained from the 3D-QSAR calculations was incorporated into the PBPK model, while maximum binding capacity of PCB126 to

Mrp2 was estimated using an optimization process. The equation describing the rate of change in the amount of PCB126 in the liver with Mrp2 excretion was expressed as follows:

$$RAL = QL * (CA - CVL) + KGILV * AGI - ((V_{max} * CVL / (K_m + CVL))) \quad (1)$$

where RAL is rate of change of PCB126 in the liver, QL is blood flow to the liver, CA is PCB126 concentration in arterial blood, CVL is concentration of PCB126 in venous blood coming out of the liver, $KGILV$ is an absorption rate constant of PCB126 from GI tract into the liver, AGI is amount of PCB126 in the GI tract, V_{max} is maximum binding capacity of Mrp2 in PCB126 excretion and K_m is binding affinity constant of Mrp2 to PCB126. In our model, the binding of PCB126 with AhR and CYP1A2 followed the description by Andersen et al (Andersen *et al.* 1993).

2.2. Model Validation

Recently, Fisher et al conducted a single dose PCB126 pharmacokinetic study. In this study, male SD rats were orally administered with a single-dose of PCB126 (7.5, 75, and 275 $\mu\text{g}/\text{kg}$), and liver concentration levels of PCB126 were measured from day 1 up to day 22 post-PCB126 administration (Fisher *et al.* 2006). Since the data concerning changes in body weight of the animals were available, we also incorporated these body weight changes into our model simulations. The data set in this paper which is different from those data sets used in constructing the PBPK model was used for model validation.

TABLE 2.1 Physiological Parameters for the PCB126 PBPK Model.

Model Parameters (unit)	Abbreviations	Single oral gavage ^a	Multiple oral gavage ^a	Time-course medium-term liver bioassay	Parameter estimation
Body weight at start of the experiment (kg)	BW	0.28 ^a	0.184-.185 ^a	0.20 ^b	Literature and experimental data
<i>Tissue volumes (or volume fractions)</i>					
Fat volume fraction	VFC	0.05 ^a	0.05 ^a	0.05 ^a	Literature
Liver volume fraction	VLC	0.38 ^c	N.A. ^d	N.A. ^e	Literature and experimental data
Rapidly perfused (L)	VRC	0.052 ^c	0.052 ^c	0.052 ^c	Literature
Slowly perfused (L)	VSC	0.91 x BW -VF-VL-VB-VR			Literature
Blood volume (L)	VB	0.062 x BW + 0.0012 ^f			
Cardiac Output Constant (L/h/kg)	QCC	14.1 ^c	14.1 ^c	14.1 ^c	Literature
<i>Tissue plasma flow fractions</i>					
Fat	QFC	0.07 ^c	0.07 ^c	0.07 ^c	Literature
Liver	QLC	0.18 ^c	0.18 ^c	0.18 ^c	Literature
Rapidly perfused	QRC	0.58 ^c	0.58 ^c	0.58 ^c	Literature
Slowly perfused	QSC	1.0-QFC-QLC-QRC			
<i>Rate Constants</i>					
Absorption constant (h ⁻¹)	rate KGLV	0.143 ^g	0.143 ^g	0.143 ^g	Optimized

TABLE 2.1(contd.) Physiological Parameters for the PCB126 PBPK Model.

Model Parameters (unit)	Abbreviations	Single oral gavage ^a	Multiple oral gavage ^a	Time-course medium-term liver bioassay	Parameter estimation
<i>Partition Coefficients</i>					
Liver	PL	8.9 ^h	8.9 ^h	8.9 ^h	Literature
Fat	PF	155.0 ^h	155.0 ^h	155.0 ^h	Literature
Rapidly perfused	PR	6.0 ^h	6.0 ^h	6.0 ^h	Literature
Slowly perfused	PS	7.2 ^h	7.2 ^h	7.2 ^h	Literature
<i>Protein Binding</i>					
AhR maximum (nmole/liver)	BM ₁	0.004 ⁱ	0.004 ⁱ	0.004 ⁱ	Literature
AhR affinity (nmole/L)	KB ₁	0.564 ^g	0.564 ^g	0.564 ^g	Optimized
1A2 Basal level (nmole/liver)	BM ₂₀	10.0 ⁱ	10.0 ⁱ	10.0 ⁱ	Literature
1A2 Maximum (nmole/liver)	BM ₂₁	101.3 ^g	N.A.	N.A.	Optimized
1A2 affinity (nmole/L)	KB ₂	5.54 ^g	5.54 ^g	5.54 ^g	Optimized
1A2 induction rate (nmole/h)	slope	N.A.	0.0066 ^g	0.0066 ^g	Optimized
<i>Excretion via MRP2</i>					
Binding affinity (nmole/L)	K _m	7760.0 ^j	7760.0 ^j	7760.0 ^j	Experimental data
MRP2 maximum (nmole/h)	V _{max}	64.6 ^g	64.6 ^g	64.6 ^{g,k}	Optimized

^aBody weight data adopted from the PCB126 NTP Report (NTP 2006).

^bAge-dependent BW adopted from our time-course medium term liver bioassay.

^cParameters adopted from Brown et al (1997) (Brown *et al.* 1997).

^dAge-dependent liver weight adopted from NTP PCB126 Report (NTP 2006).

^eAge-dependent liver weight adopted from our time-course medium term liver bioassay.

^fBlood volume of rats adopted from (Lee and Blaufox 1985).

^gEstimated by ACSL Math.

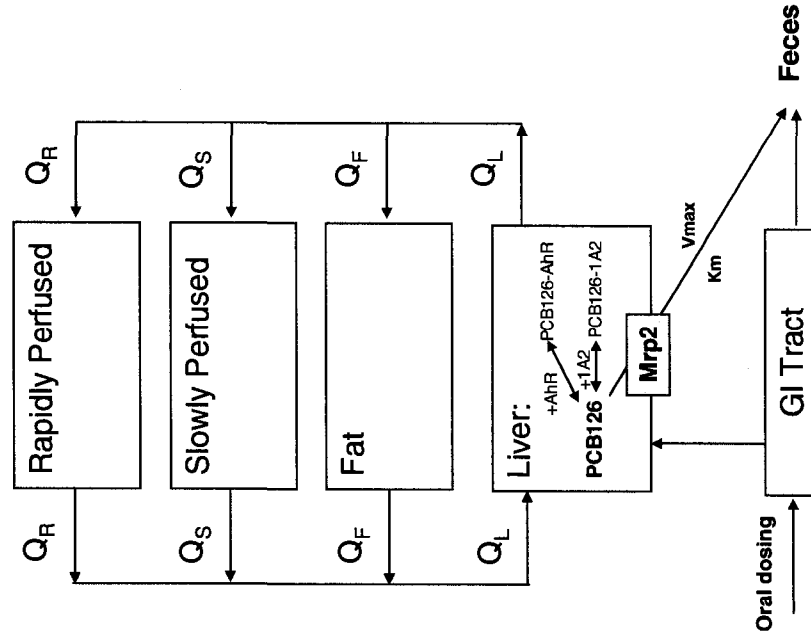
^hAdopted from the PBPK model in the PCB126 NTP Report (NTP 2006).

ⁱAdopted from Andersen et al (1993) (19).

^jCalculated using the 3D-QSAR model and computational chemistry (Hirono *et al.* 2005).

^kAfter PH, from day 21-24, the value of V_{max} was changed to 2,000.0 nmole/h.

(A)



(B)

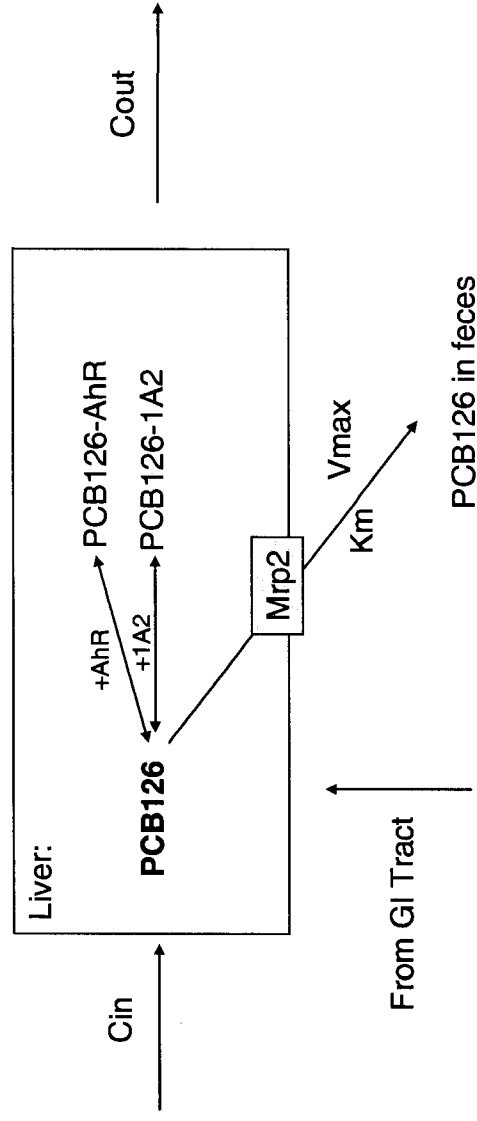


Fig. 2.1. A PBPK model structure of PCB126 (A) and liver subcompartment consisting of binding between PCB126 and AhR, CYP1A2, and excretion via MRP2 (B).

2.3. Sensitivity Analysis

Sensitivity analysis is a useful approach for identifying important parameters affecting a pharmacokinetic measurement (Clewell *et al.* 1994). Log-normalized sensitivity parameters (LSPs) were defined as follows:

$$LSP = \partial \ln R / \partial \ln x' \quad (2)$$

where R is a model output and x is the parameter for which the sensitivity is being tested. This definition quantifies the percentage change in an output value due to the percentage change in a parameter. In this study, the liver concentration (C_L) was an output of most concern. Consequently, we examined the sensitivity of the liver concentration of PCB126 to the parameters related to AhR binding (BM_1 and KB_1), CYP1A2 binding (BM_{2O} , BM_{2I} , KB_2 and slope), Mrp2-mediated excretion (V_{max} and K_m), and partition coefficient in the liver (PL).

2.4. Software

The model code was written and the simulations were performed using ACSL Tox[®] (version 11.8.4; Aegis Technologies Group Inc., Marietta, GA). The sensitivity analysis and parameter optimization were carried out using ACSL Math[®] (version 2.5.4; Aegis Technologies Group Inc., Marietta, GA).

2.5. Pharmacokinetic/Pharmacodynamic Studies of PCB126 under the Time-Course Medium-Term Liver Foci Bioassay Protocol, and Simulation of these Datasets by Incorporating Pathophysiological Conditions

2.5.1. Chemicals

PCB126 (>99% purity) was purchased from AccuStandard (New Haven, CT). 2, 2', 4, 4', 5, 5'-Hexachlorobiphenyl (PCB74; >98% purity) was purchased from Ultra Scientific (North Kingstown, RI) and used as an internal standard for GC analyses. DEN was purchased from Sigma Chemical (St. Louis, MO). Pentane (HPLC grade) and sulfuric acid were supplied by VWR Scientific (Denver, CO). Anhydrous sodium sulfate was purchased from Fisher Scientific (Houston, TX). Florisil was supplied by Alltech Associates (Deerfield, IL).

2.5.2. Animals

Male F344 rats, 30 days of age, supplied by Harlan Sprague-Dawley (Indianapolis, IN), were maintained at the Painter Center, Colorado State University. The Center is fully accredited by the American Association for Accreditation of Laboratory Animal Care. The animals were given food (Harlan Teklad NIH-07 diet; Madison, WI) and water *ad libitum*, and the lighting was set at 12-h light/dark cycle. The study was conducted in accordance with the National Institutes of Health guidelines for the care and use of laboratory animals.

After a 4-week acclimation, the rats were randomly allocated into three groups, and treated according to the time-course medium-term liver foci bioassay (Fig. 2.2). In brief, on day 0, the animals were administered with a single intraperitoneal injection of DEN (200 mg/kg body weight) dissolved in normal saline. On day 14, the rats were

orally administered with a daily oral gavage (5 mL of dosing solution/kg body weight) of corn oil (control), 3.3 µg PCB126/kg body weight (low dose), or 9.8 µg PCB126/kg body weight (high dose) in corn oil until sacrifices. On day 21, a two-third partial hepatectomy (PH) was performed on the rats. On the surgery day and the following 2 days, oral dosing was stopped to decrease stress to the animals while they were recovering from the PH. On day 20, 24, 28, 47, and 56, six rats from each group were sacrificed by aortic exanguination under anesthesia. The body and liver weights from each rat were recorded at the sacrifice (Table 2.2). One piece of a liver (approximately 5 mm thickness) from each liver lobe was collected and fixed in formalin for GSTP foci development analysis. The remaining part of the livers was collected for PCB126 tissue concentration analyses; they were stored at -80°C until chemical analysis.

2.5.3. PCB126 extraction

Liver samples were weighed (approximately 1-2 g/sample). The samples were chopped and 1.5 mL of water added. Subsequently 250 ng PCB74 was added to the samples as an internal standard (I.S.). Then 3 mL of 60% sulfuric acid was added to the samples and mixed vigorously. Following standing overnight at room temperature for complete tissue digestion, 5 mL of pentane was added to the samples and mixed vigorously. The samples were then centrifuged at 3,200 RPM for 15 minutes at 25°C using a Centrifuge Model 5682 (Forma Scientific Inc., Marietta, OH) and the organic layer was collected. Two more extractions were carried out and the organic layers combined. To clean up the extracts, the combined organic layers were passed through a clean-up column consisting of 3.0-g anhydrous sodium sulfate and 500-mg activated florisil. The cleaned up organic extracts were evaporated under nitrogen streams until

dryness. Each sample was reconstituted with 1 mL of pentane (HPLC grade) and analyzed by gas chromatography. The %recovery of PCB126 by this extraction method is about 75%.

2.5.4. Gas chromatographic analyses

An HP-5890 Series II Plus gas chromatograph (Hewlett Packard, Wilmington, DE) with an electron capture detector (ECD) detector was employed to analyze PCB126. A DB-5 (crosslink 5% phenyl methylsilicone, 30 m x 0.53 mm x 0.5 μ m film thickness, Supelco, Bellefonte, PA) capillary column was used. The initial temperature was 80°C for 3 minutes, programmed to 120°C at the rate of 15°C/min and stayed at this temperature level for 5 minute and then programmed to 180°C at the rate of 20°C/min. The flow rate of carrier gas, helium, and the make-up gas, nitrogen, were 5 and 80 mL/min, respectively. The temperature of injector and detector were 225 and 320°C, respectively. The volume of injection was 5-10 μ L per sample. The concentration levels of PCB126 were quantified using an internal standard method. A calibration curve was built and fitted using a linear regression equation. The detection limit of the system was 0.1 ng PCB126.

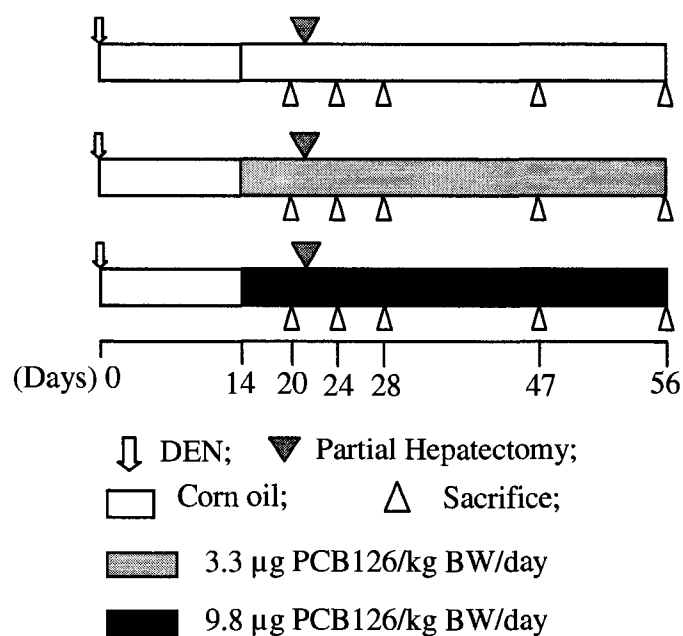


Fig. 2.2. Experimental design of the PCB126 pharmacokinetic study integrated in a time-course liver foci bioassay. A single ip injection of DEN was administered on day 0. Daily oral gavage of corn oil (control) or PCB126 was started from day 14. On day 21, a two-third partial hepatectomy (PH) was performed on the rats. On the surgery day and the following 2 days, PCB126 was not administered to reduce the stress to the animals. Six rats from each treatment group were sacrificed on day 20, 24, 28, 47 and 56. The livers were collected for PCB126 analysis, morphometric analyses of GSTP foci, and PBPK/PD modeling.

TABLE 2.2. Body and Liver Weights and Liver/Body Weight Ratios of the Rats in the Liver Foci Bioassay (mean \pm S.D.)

Days after DEN injection	Body weight (g)		Liver Weight (g)		Liver/body weight ratio (%)	
	Control	Low dose	High dose	Control	Low dose	High dose
20	219.1 \pm 11.3	215.9 \pm 10.9	209.5 \pm 9.2	7.8 \pm 0.6	8.0 \pm 0.5	8.1 \pm 0.5
24	197.9 \pm 13.8	210.2 \pm 7.4	205.9 \pm 9.8	5.7 \pm 1.0	5.9 \pm 0.3	5.8 \pm 0.5
28	208.4 \pm 14.4	210.4 \pm 8.6	213.4 \pm 12.8	6.8 \pm 1.0	7.1 \pm 0.5	7.0 \pm 0.8
47	253.9 \pm 17.3	258.6 \pm 22.1	267.7 \pm 17.3	8.8 \pm 1.3	9.8 \pm 1.1	9.7 \pm 0.6
56	287.6 \pm 18.4	292.0 \pm 11.2	285.6 \pm 29.1	9.3 \pm 0.7	9.9 \pm 0.5	10.3 \pm 1.3
				Control	Low dose	High dose
				3.54 \pm 0.19	3.70 \pm 0.13	3.85 \pm 0.10*
				2.87 \pm 0.42	2.83 \pm 0.20	2.79 \pm 0.15
				3.25 \pm 0.24	3.39 \pm 0.30	3.25 \pm 0.24
				3.51 \pm 0.75	3.82 \pm 0.67	3.63 \pm 0.11
				3.24 \pm 0.05	3.39 \pm 0.08*	3.60 \pm 0.16*

*p<0.05, compared to the concurrent control group.

2.5.5. Development of GSTP foci in the liver

2.5.5.1. Quantification of GSTP foci

Livers were collected at the specified sacrifice time points, fixed in formalin, sliced to 5 μm thickness, and stained for expression of GSTP immunohistochemically. Liver sections were deparaffinized in xylene and rehydrated by passage through an alcohol series. Endogenous peroxidase was quenched in 3% hydrogen peroxide for 10 minutes. Slides were rinsed with deionized water and placed in PBS (pH 7.4; 2.7 mM KCl, 0.14 M NaCl, 1.5mM KH_2PO_4). GSTP foci were detected with a primary GSTP antibody using a standard avidin-biotin complex method. Area and number of GSTP foci were measured using an Olympus BX51 light microscope (Olympus Optical Co., LTD, Tokyo, Japan) coupled with an Optronics DEI-750CE microscope mounted digital camera (Optronics, Coleta, CA) and a stage-mounted Microcode II Digital Readout (Boeackeler Instruments, Inc., Tucson, AZ). Image analysis software was the Bioquant Nova[®] for Windows 98 (Version 5.00.8) computerized histomorphometry program (B&M Biometrics Inc., Nashville, TN), installed in an AOpen PIII-700 computer (AOpen Inc., Taipei, Taiwan). Any GSTP focus larger than two cells (approximately 50 μm diameter) was counted and area of the GSTP focus was recorded. Subsequently the 2 dimensional data of GSTP foci development from the tissue slices were used to calculate numbers and volume of GSTP foci in the livers using STEREO (the McArdle Laboratory, Madison, WI) as described earlier by Xu et al. and Ou et al. (Ou *et al.* 2001; Xu *et al.* 1998).

2.5.5.2. Statistical analyses

Statistical comparisons between treatment groups and the concurrent controls were performed using one-way ANOVA. Values were considered to be statistically significant when $p < 0.05$ (Minitab, Inc., State College, PA).

2.5.6. Correlation Between Internal Dosimetry and Experimental Liver GSTP Foci Development

2.5.6.1. Calculations of internal dose metrics

We selected AUC_{Liver} and %bound AhR as the two most likely candidates for the internal dose metric. Using our PBPK/PD model under the conditions of time-course medium-term liver bioassay, the values of AUC_{Liver} and %bound AhR over time were determined. WinNonlin[®] Professional (version 4.1; Mountain View, CA) was then employed to determine the correlation between the chosen liver internal metrics and the volume of GSTP foci. A simple maximal effect equation was used to describe the correlation between the internal dose metric and the GSTP foci development. The equation can be described as follows:

$$Volume_{GSTP} = \frac{E_{max} AUC_{liver}}{EAUC_{liver,50} + AUC_{liver}} \quad (3)$$

where $Volume_{GSTP}$ is volume of GSTP foci in the liver, E_{max} is the maximal volume of GSTP foci in the liver and $EAUC_{Liver,50}$ is AUC_{Liver} which produces 50% of the maximal volume of GSTP foci in the liver (E_{max}).

3. RESULTS

3.1. Model Performance Under Normal Physiological Conditions

3.1.1. PBPK model simulations: the single dose study

The model simulations of PCB126 concentrations in the liver and fat (Fig. 2.3A) were consistent with the experimental data reported in the NTP Technical Report (NTP 2006). According to our PBPK/PD model, with this dosing scenario (1,000 ng PCB126 oral single dose) at 24 hours post-PCB126 administration, most of PCB126 (about 55.6% of total administered dose) was found in the liver and some of PCB126 (approximately 2.0%) was excreted out from the body via hepatic Mrp2 (Fig. 2.3B).

3.1.2. PBPK model simulations: the multiple-dose study

In the multiple-dose 2-year study, there were 6 dosing levels; 30, 100, 175, 300, 550, and 1,000 ng PCB126/kg body weight. The model simulations of PCB126 concentrations in the liver, fat, and blood were consistent with the experimental data (Fig. 2.4A-F). Further PBPK/PD modeling revealed that %Excretion of PCB126 via Mrp2 was increasing while %PCB126 in the livers was decreasing over time in all dosing levels (Fig. 2.5A and B). For instance, at the dosing level of 30 ng PCB126/kg body weight, at 1, 13, 30, 52, and, 104 weeks, %excretion of PCB126 via Mrp2 was 9.3, 52.4, 73.3, 82.4, and, 88.6%, respectively, while %PCB126 in the liver was 49.6, 27.3, 15.8, 10.7, and, 7.4%, respectively (Fig. 2.5A)

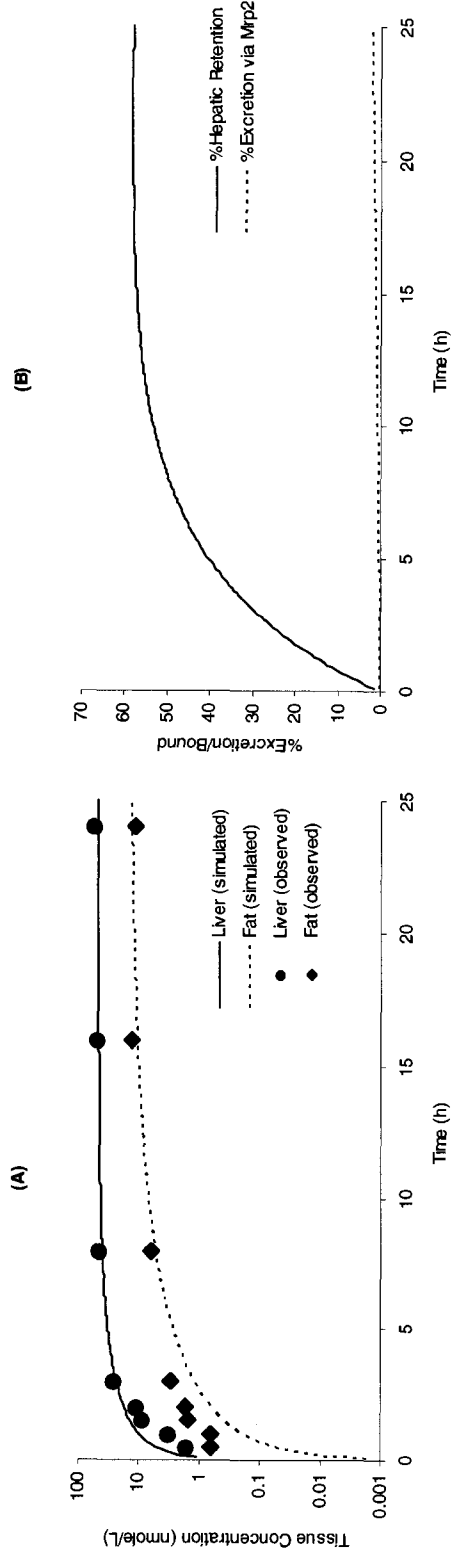


Fig. 2.3. Concentration-time courses of PCB126 in livers (solid line, model simulation; circles, observed data) and fat (dash line, model simulation; diamonds, observed data) of female SD rats orally administered with a single dose of 1000 ng PCB126/kg body weight (A) and model simulations of %PCB126 excretion via MRP2 (dash line) and %hepatic retention of PCB126 in the liver (solid line) compared to the total administered dose (B).

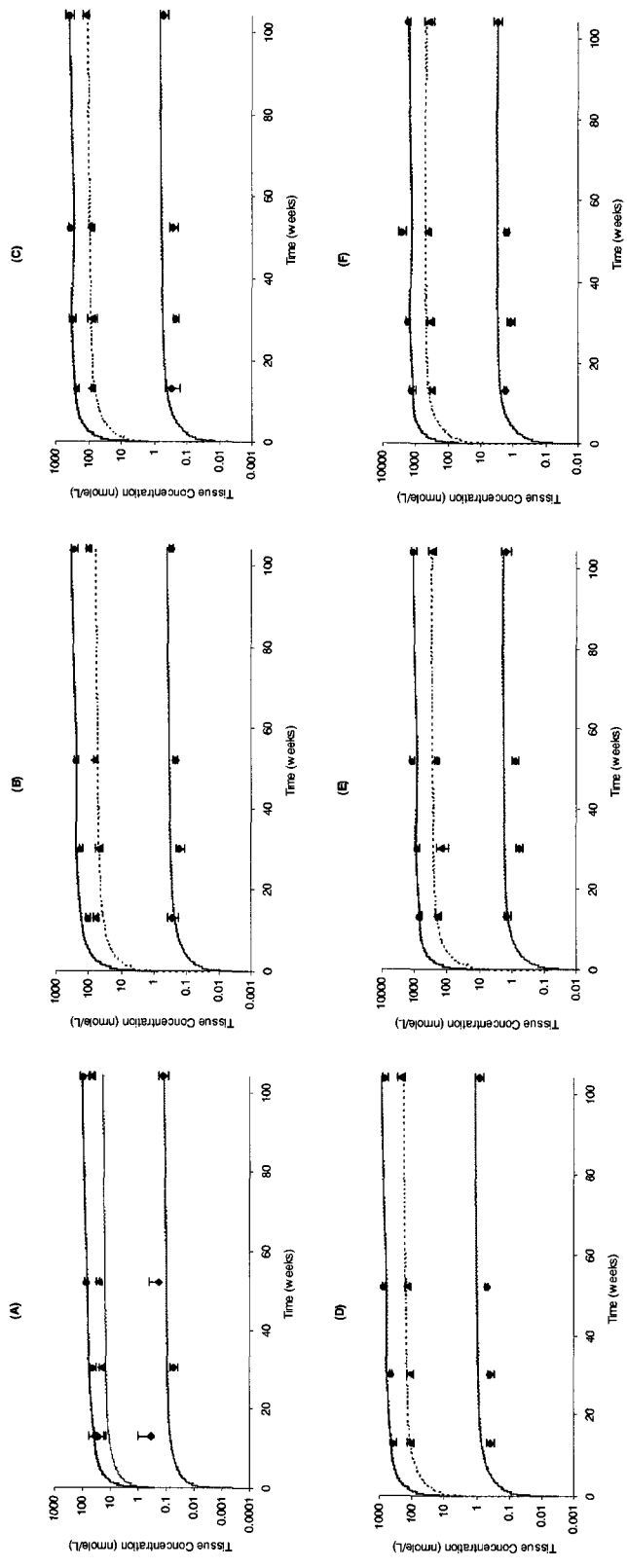


Fig. 2.4. Concentration-time courses of PCB126 in livers (upper curve, solid line, model simulation; closed circles, observed data), fat (middle curve, model simulation; closed triangles, observed data) and blood (lower curve, solid line, model simulation; diamonds, observed data) of female SD rats orally administered with repeated dose of 30 (A), 100 (B), 175 (C), 300 (D), 550 (E), and 1,000 (F) ng PCB126/kg body weight. The data are expressed as mean \pm SD for at least five animals in each group.

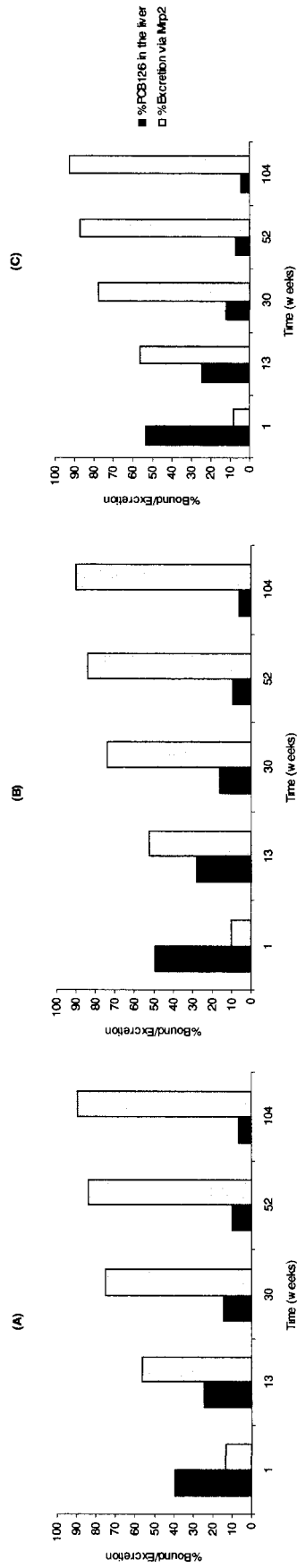


Fig. 2.5. Model simulations of %PCB126 in the livers and %Excretion of PCB126 via MRP2 in female SD rats orally administered with 30 (A), 175 (B), and 1,000 ng PCB126 at various time points. Black and white bars represent %PCB126 in the livers and %Excretion of PCB126 via MRP2 compared total administered dose, respectively.

3.2. PBPK Model Validation

An entirely different data set from a recent study conducted by Fisher et al was used for model validation (Fisher *et al.* 2006). As shown in Fig. 2.6, our PBPK model was utilized to simulate the concentration-time course data taken from this paper. The results, shown in Fig. 2.6, demonstrated fair consistency between the liver concentration-time courses of PCB126 at the dosing levels of 75 and 275 $\mu\text{g}/\text{kg}$. However, at the lowest dosing level of 7.5 $\mu\text{g}/\text{kg}$, the over-prediction of the experimental data was more pronounced (Fig. 2.6). Whether it is due to variability among different laboratories, strains of rats, gender, analytical techniques, and/or dose levels remains unclear.

3.3. Sensitivity Analysis

The sensitivity of hepatic concentration of PCB126 to parameters related to binding with AhR, CYP1A2, and, Mrp2 at various time points in the single dose and multiple-dose (1,000-ng dosing level) studies is summarized in Table 2.3. From the single dose study, at 24 hours post-PCB126 administration, affinity to CYP1A2 (KB_2), capacity of CYP1A2 (BM_{21}), basal level of CYP1A2 (BM_{20}) and the capacity of AhR (BM_1) had the largest effect on the hepatic concentration. Affinity to AhR (KB_1), Mrp2 (K_m), and maximum binding capacity of Mrp2 (V_{max}) had moderate effect while partition coefficient of PCB126 in the liver (PL) had minimal effect on hepatic concentration of PCB126. In the 2-year oral multiple-dose study, at 104 weeks, K_m and V_{max} of Mrp2 had the most prominent effect on concentration of PCB126 in the livers. Induction rate of CYP1A2 (slope), BM_{20} , KB_2 , BM_1 and KB_1 had moderate effect while PL had the weakest effect on PCB126 concentration in the livers.

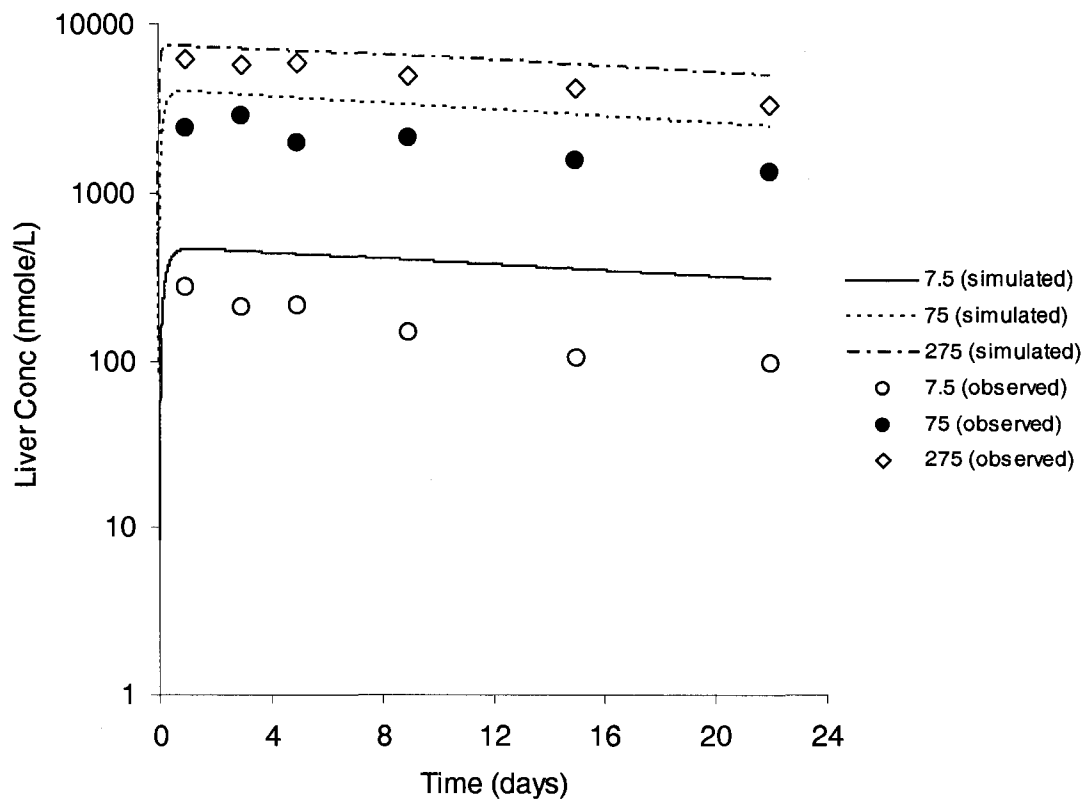


Fig. 2.6. Concentration-time courses of PCB126 in livers of male SD rats orally administered with a single dose of PCB126 (lower line, 7.5 $\mu\text{g}/\text{kg}$; middle line, 75 $\mu\text{g}/\text{kg}$, and; 275 $\mu\text{g}/\text{kg}$ body weight, upper line) compared to liver concentration-time course data taken from Fisher et al (open circles, 7.5 $\mu\text{g}/\text{kg}$; closed circles, 75 $\mu\text{g}/\text{kg}$, and; diamonds, 275 $\mu\text{g}/\text{kg}$).

TABLE 2.3 Log-Normalized Sensitivity Parameter (LSP) Values for PCB126 Liver Concentration in Oral Single Dose and Oral 2-Year Repeated Dose Study.

<i>Oral single dose study (1,000 ng/kg body weight)</i>												
Time (h)	AhR		CYPIA2			Mip2		Partition Coefficient				
	BM ₁	KB ₁	BM ₂₁	BM ₂₀	KB ₂	K _m	V _{max}	PL				
1	0.0262	-0.0194	0.0277	0.0328	-0.0603	0.0012	-0.0012	0.0017				
4	0.0806	-0.0432	0.0930	0.0634	-0.1550	0.0038	-0.0038	0.0034				
8	0.1273	-0.0568	0.1519	0.0879	-0.2368	0.0073	-0.0073	0.0047				
12	0.1574	-0.0643	0.1903	0.1038	-0.2899	0.0109	-0.0109	0.0055				
24	0.1965	-0.0745	0.2400	0.1253	-0.3593	0.0226	-0.0226	0.0067				

<i>Oral 2-year repeated dose study (1,000 ng/kg body weight)</i>												
Time (weeks)	AhR		CYPIA2			Mip2		Partition Coefficient				
	BM ₁	KB ₁	Slope	BM ₂₀	KB ₂	K _m	V _{max}	PL				
1	0.1800	-0.1499	0.0022	0.2593	-0.4458	0.1970	-0.1970	0.0092				
4	0.2620	-0.1699	0.0133	0.2263	-0.5257	0.3981	-0.3981	0.0087				
24	0.4742	-0.1936	0.1239	0.2786	-0.8489	0.9910	-0.9910	0.0137				
52	0.5331	-0.1834	0.2592	0.2317	-0.9009	1.0967	-1.0968	0.0127				
104	0.6022	-0.1982	0.4217	0.1903	-0.9271	1.1383	-1.1383	0.0099				

3.4. Model Performance Under the Conditions of Time-Course Medium-Term Liver Foci Bioassay

Body and liver weight and liver/body weight ratio of the rats in the time-course medium-term liver foci bioassay were summarized in Table 2.2. There was no statistical difference in either body weight or liver weight in all treatment groups as compared to concurrent controls. However, in the low dose group, on day 56, liver/body weight ratio was significantly different compared to concurrent control ($p < 0.05$). In the high dose group, on day 20 and 56, liver/body weight ratio was significantly different compared to the concurrent controls ($p < 0.05$).

With our own experiment, model simulations of PCB126 concentrations in livers were consistent with experimental results (Fig. 2.7A and 2.7B). Oral dosing of PCB126 was started on day 14 until day 21. The dosing was stopped between day 21 and 24. Our PCB126 liver concentration levels on day 24 were lower than the limit of quantification. Using PBPK/PD modeling, %bound AhR in low and high dose group was estimated to be 99.2% and 99.8%, respectively, at 8 weeks, (Fig. 2.8). Area under the curve in the liver (AUC_{Liver}) increased over time in both dosing levels (Fig. 2.9).

3.5. GSTP Foci Development in the Time-Course Medium-Term Liver Foci Bioassay

As shown in Fig. 2.10, when compared to the controls, there was no statistical significance observed in both number and volume of GSTP foci in the rats treated with 3.3 ng PCB126/kg body weight (low dose group). However, in rats treated with 9.8 ng PCB126/kg body weight (high dose group), there were significantly higher numbers of

GSTP foci in the livers on day 24, 28, 47, and, 56 ($p < 0.05$). For instance, on day 56, numbers of GSTP foci in the livers in control and high dose groups were $19,949.0 \pm 6,913.7$ and $35,617.8 \pm 8,806.7$ foci (mean \pm S.D.; $p < 0.05$), respectively, whereas %volume of GSTP foci for control and high dose groups were 0.230 ± 0.062 and $0.520 \pm 0.107\%$ (mean \pm S.D.; $p < 0.05$), respectively.

3.6. Relationship Between AUC_{Liver} and Liver GSTP Foci Development

Using a simple maximal effect equation, AUC_{Liver} correlated well with %volume of GSTP foci in the livers at both dose levels (Fig. 2.11A and 2.11B). Parameters of the maximal effect equation, a reflection of relationship between AUC_{Liver} and %volume of GSTP foci, were summarized in Table 4. In the low and high dose group, maximal volumes of GSTP foci (E_{max}) were 0.402 and 0.717%, respectively, while $EAUC_{Liver}$, 50 in the low and high dose group were 288,096 and 1,413,766 nmole*h/L, respectively.

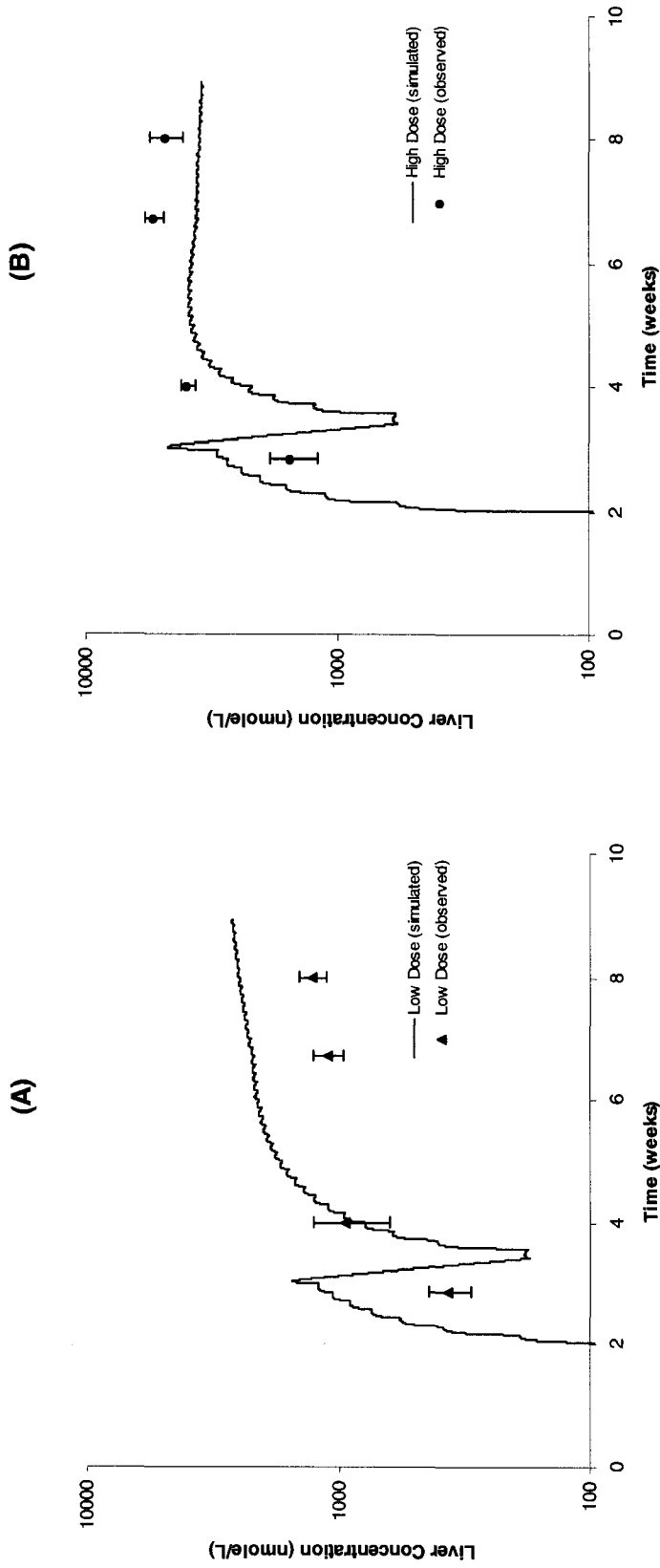


Fig. 2.7. Concentration-time courses of PCB126 in livers of male F344 rats undergone the time-course medium-term initiation-promotion protocol using PCB126 as a chemical promoter. The rats were orally administered with 3.3 (A, solid line, model simulation; triangles, observed data) and 9.8 µg PCB126/day/kg body weight (B, solid line, model simulation; closed circles, observed data) starting on Day14 until sacrifices. The data are expressed as mean ± SD for at least four animals in each group.

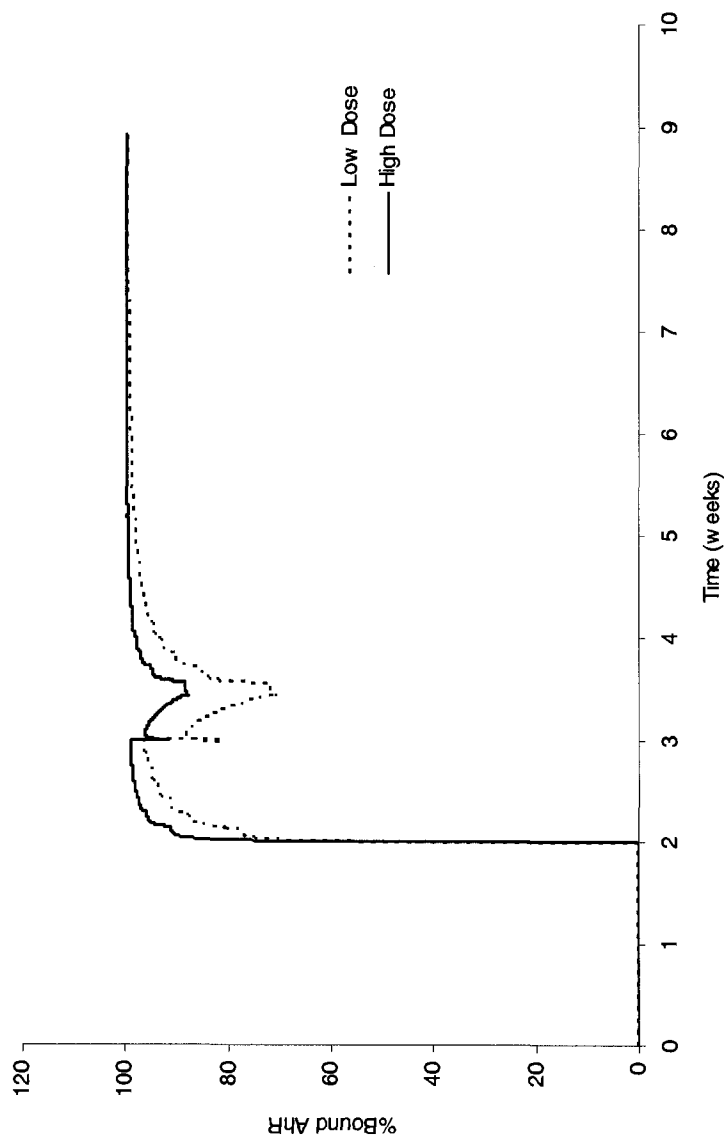


Fig. 2.8. Simulations of % bound aromatic hydrocarbon receptor (AhR) in the livers over time in male F344 rats undergone the time-course medium-term initiation-promotion protocol using PCB126 as a chemical promoter. The rats were orally administered with 3.3 (Low Dose, solid line) and 9.8 μg PCB126/day/kg body weight (High Dose, dash line).

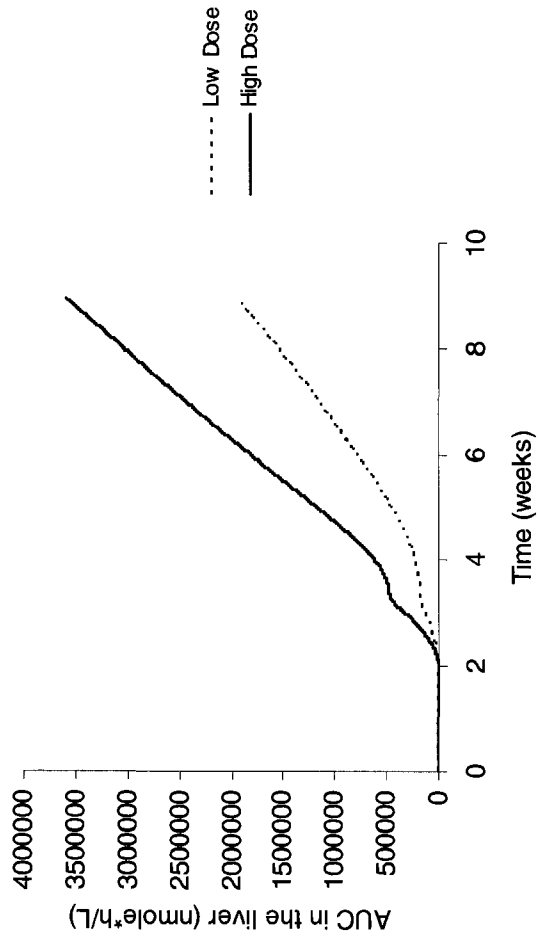


Fig. 2.9. Simulations of area under the curve (AUC) of PCB126 in the livers over time in male F344 rats undergone the time-course medium-term initiation-promotion protocol using PCB126 as a chemical promoter. The rats were orally administered with 3.3 (Low Dose, dash line) and 9.8 $\mu\text{g PCB126/day/kg}$ body weight (High Dose, solid line).

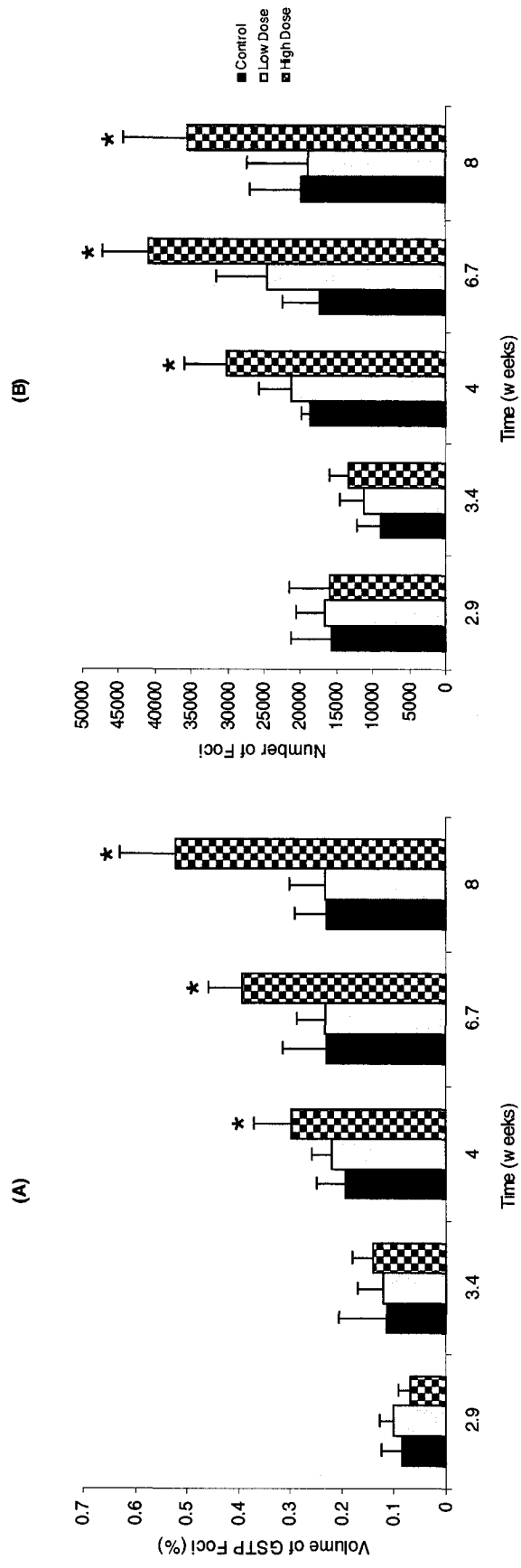


Fig. 2.10. Time-dependent changes in GSTP-positive foci volume (A) and number (B) in male F344 rats subjected to an initiation/promotion protocol using PCB126 as a promoter. The rats were orally administered with corn oil (Control, black solid bars), 3.3 (Low Dose, opened bars), and 9.8 (High Dose, black-patterned bars) μg PCB126/day/kg body weight. The data are expressed as mean \pm SD for at least four animals in each group. *, significantly different from the control group ($P < 0.05$).

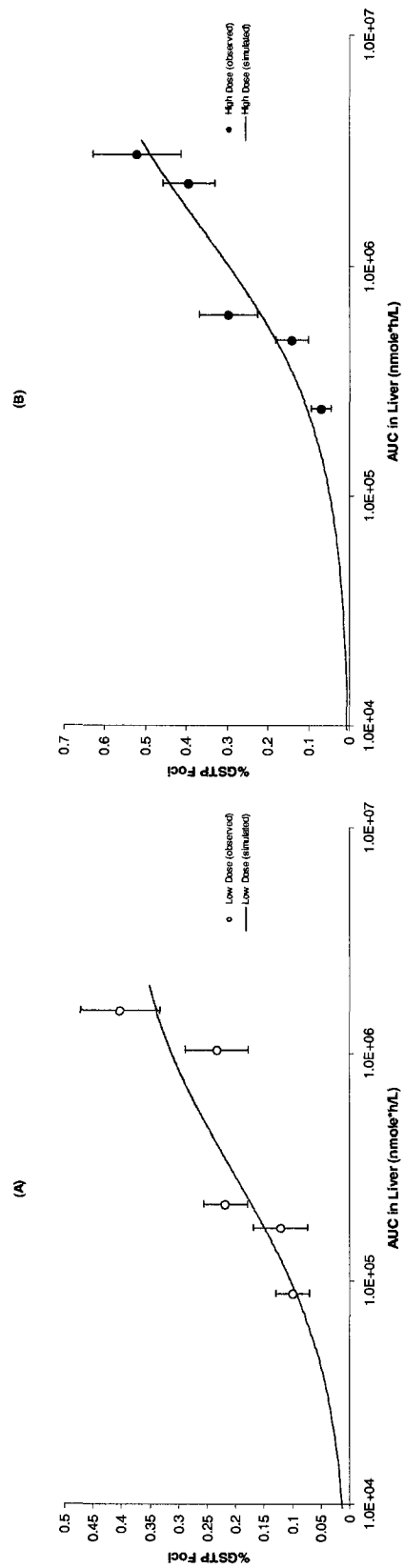


Fig. 2.11. Relationship between area under the curve of PCB126 in the livers (AUC_{Liver}) and GSTP foci development in male F344 rats undergone the time-course medium-term initiation-promotion protocol using PCB126 as a chemical promoter. The rats were orally administered with 3.3 (A) and 9.8 μg PCB126/ day/kg body weight (B). The data are expressed as mean \pm SD for at least four animals in each group.

TABLE 2.4 Summary of pharmacodynamic parameters used in the equation describing the relationship between AUC_{Liver} and GSTP foci development in male F344 rats undergone the time-course medium-term initiation-promotion protocol using PCB126 as a chemical promoter. The rats were orally administered with 3.3 (low dose) or 9.8 (high dose) μg PCB126/kg body weight/day.

Parameters	Treatment group	
	Low dose group	High dose group
E_{max} (%)	0.402	0.717
$EAUC_{Liver, 50}$ (nmole*h/L)	288,096	1,413,766

4. DISCUSSION

For the first time, we demonstrated that the versatile Mrp2 transporter protein in drug disposition is also involved in the excretion of a highly persistent environmental contaminant, PCB126. Furthermore, our PBPK/PD modeling work reported herein has the following significance:

First, our PBPK/PD model is capable of simulating blood and tissue kinetics of PCB126 in rats under many different dosing scenarios. These included the NTP single (Fig. 2.3) and multiple dosing studies up to two years (Fig. 2.4) (NTP 2006), Fisher et al. studies (Fig. 2.6) (Fisher *et al.* 2006), as well as our own studies involving an initiation-promotion experimental protocol (Fig. 2.7).

Second, the much higher hepatic concentration of PCB126 over that in the fat despite high lipophilicity of PCB126 is most likely the result of protein binding. In the liver sub-compartment of our PBPK/PD model, PCB126 binds to AhR and CYP1A2 in a reversible fashion. The level of AhR in the livers was assumed to be constant throughout the testing conditions (Andersen *et al.* 1993), while CYP1A2 was considered to be an inducible protein (Chubb *et al.* 2004; NTP 2006). Using the 3D-QSAR model and computational chemistry developed earlier by Hirono et al (Hirono *et al.* 2005), PCB126 was found to be a good substrate for Mrp2 binding with relatively high affinity. Thus, an Mrp2-mediated excretion process of PCB126 was incorporated into the model. The resulting PBPK/PD model simulations were consistent with a number of experimental data sets from different laboratories.

Third, under pathophysiological conditions involving two-third partial hepatectomy, the model can also satisfactorily simulate the time-course liver

concentrations. PBPK/PD model simulations under our experimental conditions suggested that AUC_{Liver} was a better internal dose metric than the specific binding between PCB126 and AhR. There was a correlation between AUC_{Liver} and the observed liver GSTP foci development.

From this research work, we learned a great deal about the pharmacokinetics and pharmacodynamics of PCB126, particularly regarding the involvement of Mrp2 transporter protein. We would like to share the following thoughts with interested colleagues.

In the current PBPK model of PCB126, we incorporated reversible bindings between PCB126 and hepatic proteins (i.e. AhR and CYP1A2), and an excretion of PCB126 from the liver via Mrp2. From the sensitivity analysis (Table 2.3), in the early period (less than 24 hrs) of the 1,000-ng single oral dose study, the parameters related to the bindings between PCB126 and AhR and CYP1A2 (BM_1 , KB_1 , BM_{21} , BM_{20} , and KB_2) had a stronger effect on PCB126 levels in the liver than those for Mrp2 (K_m and V_{max}). However, when the oral dosing continued, at the same dose level, the parameters related to the Mrp2-mediated excretion became more influential on hepatic concentration of PCB126 than those of AhR and CYP1A2 bindings. It is possible that, at the beginning, absorbed PCB126 from the GI tract entered into the liver and bound preferentially to AhR and CYP1A2 because of their higher binding affinities. As AhR and CYP1A2 had low binding capacities, they became saturated with PCB126. The excess PCB126 in the liver then bound to Mrp2, a transporter protein with lower binding affinity but higher capacity. These Mrp2-bound PCB126 molecules were then excreted from the livers via a biliary excretion process. The above deliberations are also reflected by the fact that at the

later period, when compared to total oral administered dose, the fraction of PCB126 bound to the AhR and CYP1A2 was continuously decreasing, while the fraction of PCB126 excreted via Mrp2 was continually increasing (Fig. 2.5). In model simulations from our initiation-promotion study, the computer modeling results showed a similar trend in increasing fraction of PCB126 in feces via the Mrp2-mediated excretion process (Fig. 2.12A). Computer simulation also demonstrated a decreasing trend of the ratio between hepatic PCB126 levels and the total administered dose (Fig. 2.12B). AhR is considered to be a constitutive protein, although it has been known that the amount of CYP1A2 in the liver can be induced by exposure of PCB126 (Chubb *et al.* 2004; NTP 2006). However the magnitude of the protein induction process may not be sufficient to account for all the protein binding in the liver. Thus, when these binding proteins become saturated with PCB126, the excess PCB126 molecules bind to Mrp2 and are excreted out of the liver by the Mrp2-mediated excretion process.

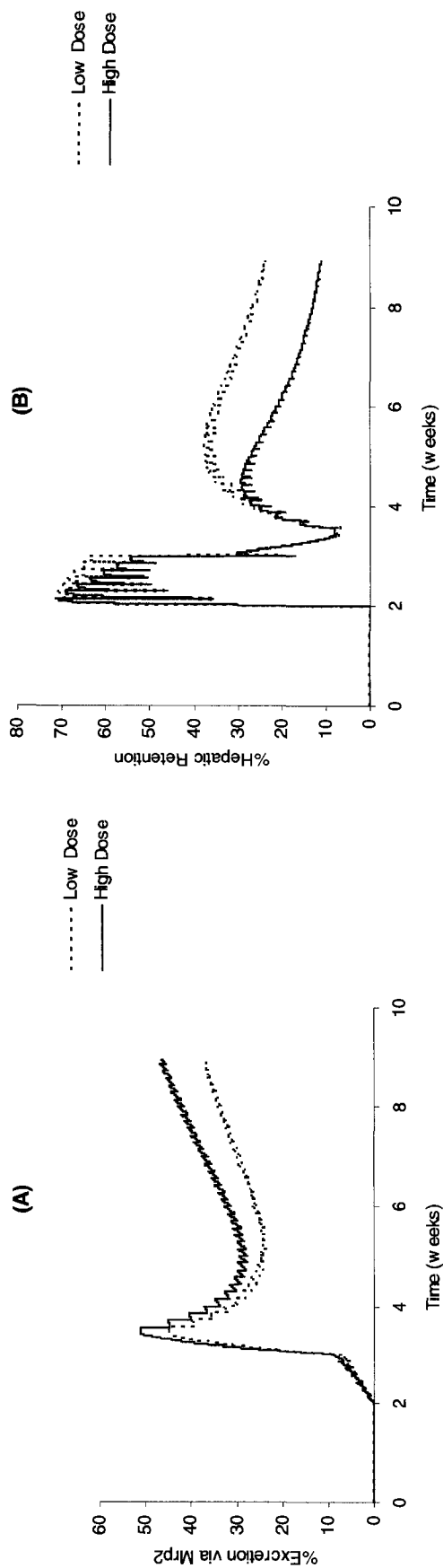


Fig. 2.12. Simulations of percentages of PCB126 excreted into feces compared to total administered dose (A) and simulations of percentages of liver PCB126 retention compared to total administered dose (B) in male F344 rats undergone the time-course medium-term initiation-promotion protocol using PCB126 as a chemical promoter. The rats were orally administered with 3.3 (dash line) and 9.8 μg PCB126/ day/kg body weight (solid line).

In our time-course medium-term liver bioassay study, a two-third partial hepatectomy was performed on all of the animals on day 21. When the two-third liver is removed, the remaining portion of the liver will regenerate (Taub 2004). In our PBPK/PD model, we incorporated this liver regeneration process (Lu *et al.* 2006). To reduce stress to the animals, oral dosing in all of the treatment groups was stopped from day 21 to day 24 (Fig. 2.2). Interestingly, on day 24 (right before the dosing resumed), the liver concentrations of PCB126 in samples harvested from the rats exposed to PCB126 in both dosing levels were lower than the detection limit (Fig. 2.7A and 2.7B). In our modeling, without any changes in Mrp2 affinity or capacity, the model was not able to successfully simulate the liver concentration at this time point. Mrp2 expression was increased by 46% at 12 hours post surgery (Gerloff *et al.* 1999) and bile flow was increased by 73% at 24 hours after PH (Vos *et al.* 1999). In addition, Villanueva *et al.* reported that, after PH, there was an increase in Mrp2-mediated excretion of dinitrophenyl-S-glutathione, a substrate of Mrp2 (Villanueva *et al.* 2005). Thus, in our PBPK/PD model, from day 21 to day 24, the value of the maximal binding capacity of Mrp2 (V_{\max}) was increased from 64.6 to 2,000.0 nmole/h to fit the observed liver concentration data. This result suggested that PH might be a potent stimulator in translocation of Mrp2 from its intracellular storage sites.

It has been recognized that PCB126, a co-planar PCB, exerts its toxicological actions via binding to AhR (Safe *et al.* 1985; Safe 1994). However, it has been hypothesized that there may be other factors contributing to its toxicological effects such as free radical production resulting from CYP1A2 induction (Jin *et al.* 2001; Katynski *et al.* 2004). From our GSTP foci development data, at the dosing level of 9.8 μg

PCB126/kg BW/day, there was a significant difference in GSTP foci development when compared to the controls at 8 weeks (Fig. 2.10). However there was no statistically significant difference in GSTP foci development in rats treated with 3.3 μ g PCB126/kg BW/day at the same period. In our PBPK/PD model simulations, the binding between PCB126 and AhR was similar between the two dose levels (Fig. 2.8). Taken together, these results suggested that specific binding between AhR and PCB126 may not be the only factor contributing to the observed effects in this experimental condition. Thus, using AhR binding as an internal dose metric may not be an appropriate surrogate to describe the GSTP foci development in this study.

It has been suggested that, for chemicals exerting toxicological effects in liver, area under the curve of the chemical can be used as an internal dose metric (MacGregor *et al.* 2001). Hence, we chose AUC_{Liver} as our internal dose metric. The resulting PBPK/PD modeling indicated that AUC_{Liver} has correlation with the liver GSTP foci development (Fig. 2.11A and 2.11B) and is a better internal dose metric for this pharmacodynamic endpoint.

In the past 13 years, a number of clonal growth models were developed to describe liver foci formation in rats treated with carcinogenic chemicals (Conolly and Kimbell 1994; Lu *et al.* 2007; Ou *et al.* 2003; Thomas *et al.* 2000). These biologically-based models were based upon the multistage carcinogenesis theory (Moolgavkar and Knudson 1981). However, up to the present time, these models have not been linked with any pharmacokinetic models. The present study revealed that AUC_{Liver} correlated well with the formation of liver GSTP foci. It would be of considerable utility in risk assessment if the present PBPK/PD model of PCB126 can be incorporated into the clonal

growth model in order to give a more biologically relevant connection between pharmacokinetics to pharmacodynamics.

In summary, Mrp2 is a hepatic transporter responsible for excretion of many drugs and toxicants (Jedlitschky *et al.* 2006). In this study, the feasibility of binding between PCB126 and Mrp2 was assessed and the binding affinity of PCB126 to Mrp2 was predicted using the 3D-QSAR and computational chemistry (Hirono *et al.* 2005). We successfully incorporated the Mrp2-mediated excretion process into our PBPK/PD model. Therefore, the present work provided an illustration of the utility of the computational *in silico* approach. Such an approach would not only conserve research resources, but also minimize animal experimentation. As utilization of computational technologies in biomedical research is generally lagging behind engineering and physical sciences, our work reported herein might serve as a stimulus for moving towards the increasing practice of computational toxicology and pharmacology.

ACKNOWLEDGEMENT

This study is supported by the NIOSH/CDC grant 1 RO1 OH07556, NIEHS Training Grant 1 T32 ES 07321, and scholarships from U.S. Fulbright Foundation and Naresuan University, Thailand. We thank our colleagues in the Quantitative and Computational Toxicology Group for their excellent technical assistance.

REFERENCES

- Abraham, K., Krowke, R., and Neubert, D. (1988). Pharmacokinetics and biological activity of 2,3,7,8-tetrachlorodibenzo-p-dioxin. 1. Dose-dependent tissue distribution and induction of hepatic ethoxyresorufin O-deethylase in rats following a single injection. *Arch Toxicol* **62**, 359-68.
- Andersen, M. E., Mills, J. J., Gargas, M. L., Kedderis, L., Birnbaum, L. S., Neubert, D., and Greenlee, W. F. (1993). Modeling receptor-mediated processes with dioxin: implications for pharmacokinetics and risk assessment. *Risk Anal* **13**, 25-36.
- Belfiore, C. J., Yang, R. S., Chubb, L. S., Lohitnavy, M., Lohitnavy, O. S., and Andersen, M. E. (2007). Hepatic sequestration of chlordecone and hexafluoroacetone evaluated by pharmacokinetic modeling. *Toxicology* **234**, 59-72.
- Borst, P., Zelcer, N., and van de Wetering, K. (2006). MRP2 and 3 in health and disease. *Cancer Lett* **234**, 51-61.
- Brown, R. P., Delp, M. D., Lindstedt, S. L., Rhomberg, L. R., and Beliles, R. P. (1997). Physiological parameter values for physiologically based pharmacokinetic models. *Toxicol Ind Health* **13**, 407-84.
- CDC (2005). Third National Report on Human Exposure to Environmental Chemicals, pp. 186-7. National Center for Environmental Health, Atlanta.
- Chu, I., Villeneuve DC, Yagminas A, LeCavalier P, Poon R, Feeley M, Kennedy SW, Seegal RF, Hakansson H, Ahlborg UG, et al. (1994). Subchronic toxicity of 3,3',4,4',5-pentachlorobiphenyl in the rat. I. Clinical, biochemical, hematological, and histopathological changes. *Fundam Appl Toxicol*. **22**, 457-468.
- Chubb, L. S., Andersen, M. E., Broccardo, C. J., Legare, M. E., Billings, R. E., Dean, C. E., and Hanneman, W. H. (2004). Regional induction of CYP1A1 in rat liver following treatment with mixtures of PCB 126 and PCB 153. *Toxicol Pathol* **32**, 467-73.
- Clewell, H. J., 3rd, Lee, T. S., and Carpenter, R. L. (1994). Sensitivity of physiologically based pharmacokinetic models to variation in model parameters: methylene chloride. *Risk Anal* **14**, 521-31.
- Conolly, R. B., and Kimbell, J. S. (1994). Computer simulation of cell growth governed by stochastic processes: application to clonal growth cancer models. *Toxicol Appl Pharmacol* **124**, 284-95.
- Dean, C. E., Jr., Benjamin, S. A., Chubb, L. S., Tessari, J. D., and Keefe, T. J. (2002). Nonadditive hepatic tumor promoting effects by a mixture of two structurally different polychlorinated biphenyls in female rat livers. *Toxicol Sci* **66**, 54-61.

- Fisher, J. W., Campbell, J., Muralidhara, S., Bruckner, J. V., Ferguson, D., Mumtaz, M., Harmon, B., Hedge, J. M., Crofton, K. M., Kim, H., and Almekinder, T. L. (2006). Effect of PCB 126 on hepatic metabolism of thyroxine and perturbations in the hypothalamic-pituitary-thyroid axis in the rat. *Toxicol Sci* **90**, 87-95.
- Gerloff, T., Geier, A., Stieger, B., Hagenbuch, B., Meier, P. J., Matern, S., and Garton, C. (1999). Differential expression of basolateral and canalicular organic anion transporters during regeneration of rat liver. *Gastroenterology* **117**, 1408-15.
- Hirono, S., Nakagome, I., Imai, R., Maeda, K., Kusuhara, H., and Sugiyama, Y. (2005). Estimation of the three-dimensional pharmacophore of ligands for rat multidrug-resistance-associated protein 2 using ligand-based drug design techniques. *Pharm Res* **22**, 260-9.
- Ito, N., Tamano, S., and Shirai, T. (2003). A medium-term rat liver bioassay for rapid in vivo detection of carcinogenic potential of chemicals. *Cancer Sci* **94**, 3-8.
- Jedlitschky, G., Hoffmann, U., and Kroemer, H. K. (2006). Structure and function of the MRP2 (ABCC2) protein and its role in drug disposition. *Expert Opin Drug Metab Toxicol* **2**, 351-66.
- Jin, X., Kennedy, S. W., Di Muccio, T., and Moon, T. W. (2001). Role of oxidative stress and antioxidant defense in 3,3',4,4',5-pentachlorobiphenyl-induced toxicity and species-differential sensitivity in chicken and duck embryos. *Toxicol Appl Pharmacol* **172**, 241-8.
- Katynski, A. L., Vijayan, M. M., Kennedy, S. W., and Moon, T. W. (2004). 3,3',4,4',5-Pentachlorobiphenyl (PCB 126) impacts hepatic lipid peroxidation, membrane fluidity and beta-adrenoceptor kinetics in chick embryos. *Comp Biochem Physiol C Toxicol Pharmacol* **137**, 81-93.
- Lee, H. B., and Blafox, M. D. (1985). Blood volume in the rat. *J Nucl Med* **26**, 72-6.
- Lohitnavy, M., Chubb, L. S., Lohitnavy, O., Yang, C. C., Homberg, J., Campaign, J. A., and Yang, R. S. (2004). Pharmacokinetic (PK)/Pharmacodynamic (PD) Relationship of PCB126 Under the Conditions of Modified Medium-Term Liver Bioassay. *Toxicologist* **78**, 271.
- Lu, Y., Lohitnavy, M., Reddy, M., Lohitnavy, O., Eickman, E., Ashley, A., Gerjevic, L., Xu, Y., Conolly, R. B., and Yang, R. S. H. (2007). Quantitative analysis of liver GST-P foci promoted by a chemical mixture of hexachlorobenzene and PCB 126: Implication of size-dependent cellular growth kinetics. *Arch Toxicol* (in press).
- Lu, Y., Lohitnavy, M., Reddy, M. B., Lohitnavy, O., Ashley, A., and Yang, R. S. (2006). An Updated Physiologically Based Pharmacokinetic Model for

Hexachlorobenzene: Incorporation of Pathophysiological States following Partial Hepatectomy and Hexachlorobenzene Treatment. *Toxicol Sci* **91**, 29-41.

- MacGregor, J. T., Collins, J. M., Sugiyama, Y., Tyson, C. A., Dean, J., Smith, L., Andersen, M., Curren, R. D., Houston, J. B., Kadlubar, F. F., Kedderis, G. L., Krishnan, K., Li, A. P., Parchment, R. E., Thummel, K., Tomaszewski, J. E., Ulrich, R., Vickers, A. E., and Wrighton, S. A. (2001). In vitro human tissue models in risk assessment: report of a consensus-building workshop. *Toxicol Sci* **59**, 17-36.
- Moolgavkar, S. H., and Knudson, A. G., Jr. (1981). Mutation and cancer: a model for human carcinogenesis. *J Natl Cancer Inst* **66**, 1037-52.
- NTP (2006). NTP toxicology and carcinogenesis studies of 3,3',4,4',5-pentachlorobiphenyl (PCB 126) (CAS No. 57465-28-8) in female Harlan Sprague-Dawley rats (Gavage Studies). *Natl Toxicol Program Tech Rep Ser*, 4-246.
- Ogiso, T., Tatematsu, M., Tamano, S., Hasegawa, R., and Ito, N. (1990). Correlation between medium-term liver bioassay system data and results of long-term testing in rats. *Carcinogenesis* **11**, 561-6.
- Ou, Y. C., Conolly, R. B., Thomas, R. S., Gustafson, D. L., Long, M. E., Dobrev, I. D., Chubb, L. S., Xu, Y., Lapidot, S. A., Andersen, M. E., and Yang, R. S. (2003). Stochastic simulation of hepatic preneoplastic foci development for four chlorobenzene congeners in a medium-term bioassay. *Toxicol Sci* **73**, 301-14.
- Ou, Y. C., Conolly, R. B., Thomas, R. S., Xu, Y., Andersen, M. E., Chubb, L. S., Pitot, H. C., and Yang, R. S. (2001). A clonal growth model: time-course simulations of liver foci growth following penta- or hexachlorobenzene treatment in a medium-term bioassay. *Cancer Res* **61**, 1879-89.
- Petzinger, E., and Geyer, J. (2006). Drug transporters in pharmacokinetics. *Naunyn Schmiedebergs Arch Pharmacol* **372**, 465-75.
- Safe, S., Bandiera, S., Sawyer, T., Robertson, L., Safe, L., Parkinson, A., Thomas, P. E., Ryan, D. E., Reik, L. M., Levin, W., and et al. (1985). PCBs: structure-function relationships and mechanism of action. *Environ Health Perspect* **60**, 47-56.
- Safe, S. H. (1994). Polychlorinated biphenyls (PCBs): environmental impact, biochemical and toxic responses, and implications for risk assessment. *Crit Rev Toxicol* **24**, 87-149.
- Shirai, T. (1997). A medium-term rat liver bioassay as a rapid in vivo test for carcinogenic potential: a historical review of model development and summary of results from 291 tests. *Toxicol Pathol* **25**, 453-60.

- Shitara, Y., Horie, T., and Sugiyama, Y. (2006). Transporters as a determinant of drug clearance and tissue distribution. *Eur J Pharm Sci* **27**, 425-46.
- Taub, R. (2004). Liver regeneration: from myth to mechanism. *Nat Rev Mol Cell Biol* **5**, 836-47.
- Thomas, R. S., Conolly, R. B., Gustafson, D. L., Long, M. E., Benjamin, S. A., and Yang, R. S. (2000). A physiologically based pharmacodynamic analysis of hepatic foci within a medium-term liver bioassay using pentachlorobenzene as a promoter and diethylnitrosamine as an initiator. *Toxicol Appl Pharmacol* **166**, 128-37.
- Villanueva, S. S., Ruiz, M. L., Luquita, M. G., Sanchez Pozzi, E. J., Catania, V. A., and Mottino, A. D. (2005). Involvement of Mrp2 in hepatic and intestinal disposition of dinitrophenyl-S-glutathione in partially hepatectomized rats. *Toxicol Sci* **84**, 4-11.
- Vos, T. A., Ros, J. E., Havinga, R., Moshage, H., Kuipers, F., Jansen, P. L., and Muller, M. (1999). Regulation of hepatic transport systems involved in bile secretion during liver regeneration in rats. *Hepatology* **29**, 1833-9.
- Xu, Y. H., Dragan, Y. P., Campbell, H. A., and Pitot, H. C. (1998). STEREO: a program on a PC-Windows 95 platform for recording and evaluating quantitative stereologic investigations of multistage hepatocarcinogenesis in rodents. *Comput Methods Programs Biomed* **56**, 49-63.

CHAPTER 3

Hepatic Enzyme and Receptor Expression as Biomarkers for Carcinogenicity in Rats Exposed to PCB126, Hexachlorobenzene, and, Their Mixture

Manupat Lohitnavy, Stephen A. Benjamin, Elizabeth Eickman, Lisa N. Gerjevic, Ornrat Lohitnavy, Yasong Lu, Jon T. Painter, and Raymond S.H. Yang.

ABSTRACT

3,3',4,4',5-Pentachlorobiphenyl (PCB126) and hexachlorobenzene (HCB) are potential human carcinogens. Since both compounds are persistent environmental pollutants, co-exposure to PCB126 and HCB is realistic as is interest in evaluating carcinogenic potential of a mixture of these two chemicals. Using a time-course medium-term liver bioassay protocol, male F344 rats were given a single i.p. dose of 200 mg/kg of diethylnitrosamine (DEN) as an initiator on day 0. Oral dosing (1X/day; 5 days/week) of PCB126 (9.8 µg/kg BW/dose), HCB (28.5 mg/kg BW/dose) or their mixture (9.8 µg of PCB126/kg BW/dose and 28.5 mg of HCB/kg BW/dose) or corn oil (control group) was carried out from week 2 to 24 weeks. On day 21, a two-thirds partial hepatectomy (PH) was performed to induce hepatocyte proliferation. Rats were sacrificed on day 20, and at 4, 8, 12, 18 and 24 weeks post-DEN injection. Three days before sacrifices, an osmotic minipump filled with bromodeoxyurine (BrDU) solution was surgically inserted into each rat. The time-course development of foci expressing glutathione-S-transferase placental form positive (GSTP⁺), transforming growth factor-α positive (TGFα⁺), or transforming

growth factor- β 2 receptor negative (TGF β 2Rc $^-$) in the liver was evaluated using morphometric analyses. Percent Labeling Indices (%L.I.) of BrDU incorporated cells were determined in the whole liver and within GSTP $^+$ foci categorized into 4 different phenotypes. PCB126, HCB, and their mixture significantly increased GSTP $^+$, TGF α^+ , and TGF β 2Rc $^-$ foci in both numbers and size. TGF α^+ and TGF β 2Rc $^-$ foci formation was statistically significant at the later time points suggesting that they are markers for carcinogenesis in the late promotion or early progression stages. Four different phenotypes of GSTP $^+$ foci demonstrated statistical differences in their growth characteristics suggesting that there is more than one population of pre-neoplastic cells.

1. INTRODUCTION

Polychlorinated biphenyls (PCBs) are halogenated aromatic hydrocarbons that had been widely used in industry and are persistent environmental pollutants. While their use has been discontinued since the 1970's, significant amounts of PCBs are still detectable in foods, human and animal tissues, and, in the environment (Safe *et al.* 1985; Safe 1994). 3,3',4,4',5'-Pentachlorobiphenyl (PCB126) is the most toxic PCB congener and is a demonstrated carcinogen. Structurally, PCB126 is capable of binding with aryl hydrocarbon receptor (AhR). Its toxicological effects include induction of cytochrome P4501A1 and 1A2 (CYP1A1 and 1A2), respectively (Safe *et al.* 1985; Safe 1994), and carcinogenesis in several organs (i.e. liver, lung, and mouth) in rats (NTP 2006).

Hexachlorobenzene (HCB) was originally used as a fungicide, but its commercial production and use have been discontinued. However, HCB is still detectable in the environment due to its chemical and thermal stability. As a highly lipophilic chemical,

HCB primarily accumulates in the adipose tissue in the body. HCB is toxic in laboratory animals and humans (Alvarez *et al.* 1999; Gocmen *et al.* 1986; Ralph *et al.* 2003; Smith *et al.* 1987a; Vos 1986). Despite the lack of genotoxicity, HCB-induced carcinogenicity was observed in laboratory animals with the liver being one of the main target organs (Smith *et al.* 1985). HCB has been classified as “reasonably anticipated to be a human carcinogen” (NTP 2001). Since both PCB126 and HCB are persistent in the environment, co-exposure to these carcinogens is realistic and may pose toxicological hazards to humans.

Many experimental animal models have been proven to be useful in studying chemical carcinogenesis (Shirai 1997; Solt and Farber 1976). Initiation-promotion models, involving a single dose administration of an initiator, followed by repeated administration of a promoter, can reveal the capability of chemicals to cause cancer. Ito’s medium-term liver bioassay is one of the most extensively studied protocols (Ito *et al.* 2003; Shirai 1997). Based on development of glutathione-S-transferase placental form positive (GSTP⁺) foci as a pre-neoplastic marker, this experimental model accurately predicts liver carcinogenicity in rats (Ogiso *et al.* 1990; Shirai 1997).

Apart from using GSTP as a pre-neoplastic marker, other tumor markers such as overt expression of tumor growth factors such as transforming growth factor (TGF)- α and absence of the expression of transforming growth factor β Type 2 receptor (TGF β 2Rc) are well-established tumor markers in many kinds of cancers in humans and experimental animals. TGF- α is expressed in viral hepatitis (Chung *et al.* 2000) and many human tumors (Bates *et al.* 1988; Chung *et al.* 2000; Derynck *et al.* 1987; Mydlo *et al.* 1989; Smith *et al.* 1987b; Yeh *et al.* 1987), including liver tumors (Bates *et al.* 1988; Chung *et*

al. 2000; Derynck *et al.* 1987; Mydlo *et al.* 1989; Yeh *et al.* 1987) and in chemically induced animal tumors (Luetke *et al.* 1988). TGF- α has been used as a tumor marker in rats (Dragan *et al.* 1995; Steinmetz and Klaunig 1996) and is suggested to be a tumor marker for carcinogenic progression (Dragan *et al.* 1995). In TGF- α transgenic mice, hepatocellular carcinoma was observed at 10-15 months (Jhappan *et al.* 1990). Co-expression of c-myc in TGF- α transgenic animals resulted in a synergistic effect on liver tumor development, including shorter latency period and a more aggressive phenotype (Calvisi and Thorgeirsson 2005).

Transforming growth factor (TGF)- β is a cytokine in the TGF- β superfamily. TGF- β ligands elicit different cellular responses via binding and activation through their receptors at the cell membrane. Lower expression or lack of function of its receptor, transforming growth factor- β Type 2 receptor (TGF β 2Rc), is associated with many kinds of human cancers such as colorectal cancer (Brattain *et al.* 1996; Markowitz *et al.* 1995) and hepatocellular carcinoma (Sue *et al.* 1995). Mutations leading to lack of function phenotype may play a role in cancer development. In addition, knockout experiments indicated that lack of the *TGF β 2Rc* gene can accelerate cancer development and lead to more aggressive phenotypes in these animals (Cheng *et al.* 2005; Forrester *et al.* 2005; Huntley *et al.* 2004). The TGF β 2Rc knockout animals showed a significantly higher hepatocyte proliferation rate with a concomitant lowering of apoptotic rate compared to its wild-type counterparts (Tang *et al.* 1998). When the knockout animals were co-treated with DEN and phenobarbital, tumor incidences, size of the tumors, and tumor malignancy in chemical-treated animals were higher compared to knockout animals without chemical treatment (Tang *et al.* 1998). Interestingly, in female transgenic mice

expressing a dominant-negative mutant TGF β 2Rc alone, mammary tumors developed spontaneously with a long median latency (27.5 months) (Gorska *et al.* 2003). The major difference in mammary tumors arising in TGF- α transgene alone animals compared to bigenic TGF β 2Rc^{-/-}/TGF- α was the marked suppression of tumor invasion. These result suggested that over-expression of TGF- α and absence of TGF β 2Rc function could lead to an overt growth and a more aggressive phenotype of tumors (Gorska *et al.* 2003).

In our laboratory, to further investigate the carcinogenic effects of chemicals in the development of GSTP⁺ foci in the initiation-promotion protocol, we have modified the original Ito's medium-term liver bioassay by adding multiple sacrificing time points, as well as the utilization of multiple markers for carcinogenic effects (Dean *et al.* 2002; Lohitnavy *et al.* 2004; Lu *et al.* 2007; Ou *et al.* 2003; Ou *et al.* 2001). We exposed F344 male rats to PCB126, HCB, and their mixture and investigated tumor markers (i.e. GSTP, TGF α , and TGF β 2Rc) at sequential time points. The objectives of this study were to: 1) assess time-dependent changes in GSTP⁺, TGF α ⁺, and TGF β 2Rc⁻ foci development after exposure to PCB126, HCB, and their mixture, and; 2) investigate the growth characteristics of the GSTP⁺ foci based on their TGF- α and TGF β 2Rc expressing phenotype.

2. MATERIAL AND METHODS

2.1. Chemicals

PCB126 was purchased from AccuStandard Inc. (New Haven, CT). HCB was purchased from Aldrich Chemical (Milwaukee, WI). DEN and BrDU were purchased from Sigma Chemical Co. (St. Louis, MO).

2.2. Animals and treatment

Male F344 rats, 30 days of age, from Harlan Sprague Dawley (Indianapolis, IN) were acclimated for 4 weeks before the start of the experimentation. The rats were randomized by weight and allocated into four treatment groups (Fig. 3.1). On day 0, the animals received a single i.p. injection of DEN (200 mg/kg) dissolved in 0.9% saline. On day 14, the animals received gavage (5 days per week) administration of corn oil or 9.8 μg PCB126 /kg or HCB (28.5 mg/kg/day, 5X/week) or their mixture (28.5 mg HCB/kg/day and 9.8 μg PCB126/kg/day, 5X/week) in a corn oil vehicle through the remainder of the 24-week study. On day 21, a two-thirds partial hepatectomy was performed on all animals. Animals were given food (Harlan Teklad NIH-07 Diet; Madison, WI) and water *ad libitum*, and lighting was set on a 12-h light/dark cycle. On days 20, and at week 4, 8, 12, 18 and 24, the animals from each treatment group were sacrificed by aortic exsanguination (Fig. 3.1). The whole liver was removed; tissues were fixed in 10% neutral-buffered formalin, embedded in paraffin, and serially sectioned at 5 μm . The studies were conducted in accordance with the NIH guidelines for the care and use of laboratory animals. The animals were maintained in a fully accredited animal care facility by the American Association for Accreditation of Laboratory Animal Care.

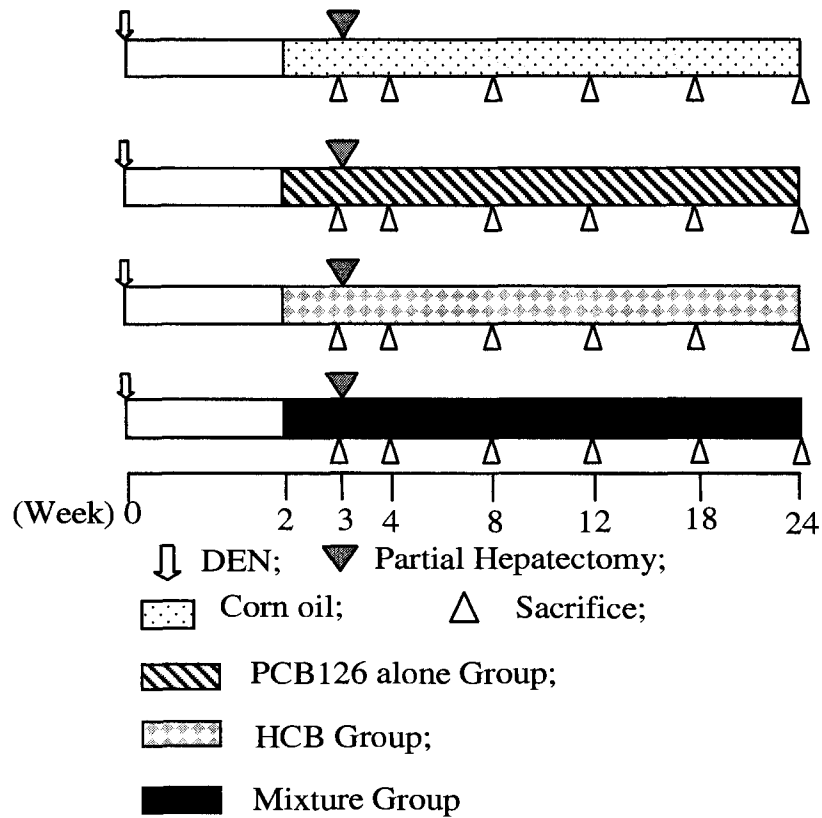


Fig. 3.1. Experimental design of the time-course liver foci bioassay. A single intraperitoneal injection of 200 mg/kg DEN was given on day 0. Daily oral gavage of corn oil or chemical (PCB126, HCB, and their mixture) solution started at week 2 (day 14) until sacrifice. On week 3, a two-thirds partial hepatectomy was performed on the rats. On the day of surgery and the following three days the gavage dosing was suspended to reduce the stress to the animals. Six rats from each treatment group were sacrificed on days 20 and week 4, 8, 12, 18 and 24. The liver was sectioned and saved for GSTP⁺ foci measurement and other analyses.

2.3. Quantification of GSTP⁺ foci

Formalin-fixed tissues from all animals were used for the immunohistochemical identification of GSTP⁺ foci. Liver sections were deparaffinized in xylene and rehydrated by passage through an alcohol series. Endogenous peroxidase was quenched in 3% hydrogen peroxide for 10 min. The slides were rinsed with deionized water and placed in PBS (pH 7.4; 2.7 mM KCl, 0.14 M NaCl, 1.5 mM KH₂PO₄, and 8.1 mM Na₂PO₄). A standard avidin-biotin complex method protocol (Vector Labs, Burlingame, CA) was followed, and foci were detected with GSTP primary antibody (Binding Site, San Diego, CA). GSTP⁺ foci were measured using a Leitz light microscope coupled with the BioQuant image analysis system (version 5; R&M Biometrics, Nashville, TN). The foci consisting of more than two cells, roughly corresponding to 50 μm in diameter, were recorded.

2.4. Quantification of TGFα⁺ and TGFβ2Rc⁻ foci

Formalin-fixed tissues from the animals sacrificed at week 12, 18 and 24 were used for the immunohistochemical identification of TGFα⁺ foci. Liver sections were deparaffinized in xylene and rehydrated by passage through an alcohol series. Endogenous peroxidase was quenched in 3% hydrogen peroxide for 5 min. The slides were rinsed with deionized water and placed in PBS (pH 7.4; 2.7 mM KCl, 0.14 M NaCl, 1.5 mM KH₂PO₄, and 8.1 mM Na₂PO₄). A standard avidin-biotin complex method protocol (Vector Labs, Burlingame, CA) was followed. A tissue slide was individually treated with TGF-α primary antibody (Santa Cruz Biotechnology, Inc., Santa Cruz, CA) and TGF-β2 receptor primary antibody (Santa Cruz Biotechnology, Inc., Santa Cruz, CA). Subsequently TGFα⁺ and TGFβ2Rc⁻ foci were measured using a Leitz light

microscope coupled with the BioQuant image analysis system (version 5; R&M Biometrics, Nashville, TN). The foci with more than two cells, roughly corresponding to 50 μm in diameter, were recorded.

2.5. Determination of cell division rate of the liver

Three days before the sacrifices, an osmotic minipump (Alzet model 2ML1, 10 $\mu\text{l/hr}$; Alza Corporation, Palo Alto, CA), filled with bromodeoxyuridine (BrDU) (20 mg/ml), was implanted subcutaneously over the dorsal midscapular region. The animals were anesthetized with isoflurane (Anaquest, Madison, WI), and the incision was closed using stainless steel wound clips. Detection of BrDU-labeled cells was performed on formalin-fixed liver sections using standard avidin/biotin complex method immunoperoxidase kits (Vector Labs, Burlingame, CA) with primary BrDU antibody (Biogenex Labs, San Ramon, CA) and 3-amino-9-ethylcarbazole (Biomedica, Foster City, CA). At least 1,000 cells/animal and four animals/group were counted. The labeling index (LI) was calculated as the number of cells labeled divided by the total number of cells counted. The cell division rate (α ; day^{-1}) was calculated as described by Moolgavkar and Luebeck:

$$\alpha = \frac{1}{2t} \times \ln \left[\frac{1}{1 - LI} \right] \quad (1)$$

, where t is the number of days of exposure to BrDU.

2.6. Determination of cell division rate within GSTP⁺ foci

One hundred and two of large GSTP⁺ foci (area of the foci larger than $3.2 \times 10^5 \mu\text{m}^2$) were randomly selected from the liver sections. The areas of GSTP⁺ foci were

recorded. Three liver serial sections were individually stained with TGF- α , TGF- β 2 receptor, and BrDU, respectively. Evaluations of TGF- α and TGF- β 2 receptor expressions of the corresponding areas to the GSTP⁺ foci were performed. The corresponding areas of GSTP⁺ foci in BrDU-stained slides were recorded. Images from the areas were taken. BrDU incorporated cells and total cell number were counted. Percent L.I. and division rate (α ; day⁻¹) of the foci was calculated as described earlier in Equation 1.

3. RESULTS

3.1. Effects of the Chemicals on Body Weight and Liver Weight

PCB 126, HCB and their mixture significantly affected both body weight and liver weight of the animals at week 24 (Table 3.1 and 3.2). All three groups showed body weight reduction with time: the PCB126 and mixture groups were more markedly affected. In contrast, liver weights were increased in all three treatment groups on a time course basis (Table 3.2). Due to drastic weight loss in rats treated with PCB126 and the mixture, oral gavage in all treatment groups was stopped at week 16. All animals were maintained until their final sacrifices.

3.2. A Hepatocellular Adenoma in a Rat Treated with PCB126

One of the rats treated with PCB126 for 18 weeks developed a hepatocellular adenoma. The mass was GSTP⁺, TGF α ⁺, and TGF β 2Rc⁻ (Fig. 3.2). The %L.I. and division rate within the tumor were 40.7% and 0.0872 day⁻¹, respectively, whereas %L.I. and division rate outside the tumor were 19.0% and 0.0350 day⁻¹, respectively.

TABLE 3.1. Effect of PCB126, HCB, and their mixture on body weight (g) of male F344 rats.

Treatment Group	Time after DEN (weeks)						
	0	2.86	4	8	12	18	24
Control	197.7 ± 21.2	225.9 ± 22.2	230.4 ± 8.6	279.2 ± 13.4	301.9 ± 16.3	377.9 ± 26.5	422.2 ± 9.1
HCB	191.5 ± 19.8	228.0 ± 8.7	226.3 ± 23.2	274.6 ± 22.4	328.6 ± 14.4*	334.4 ± 17.6*	389.7 ± 22.7*
PCB126	192.2 ± 23.3	224.6 ± 14.1	209.2 ± 15.8*	237.8 ± 20.2*	279.4 ± 13.9*	233.8 ± 17.4*	253.2 ± 8.3*
Mixture	193.6 ± 25.9	215.9 ± 17.1	195.8 ± 16.1*	206.9 ± 8.5*	211.3 ± 25.4*	234.4 ± 24.2*	254.8 ± 15.1*

NOTE: Values represent the mean ± S.D. *p<0.05, significantly different from the concurrent controls.
Dosing was stopped at week 16 due to overt toxicity in the form of marked body weight reduction.

TABLE 3.2. Effect of PCB126, HCB, and their mixture on liver weight (g) of male F344 rats undergone the modified Ito's liver bioassay.

Treatment Group	Time after DEN (weeks)					
	2.86	4	8	12	18	24
Control	7.69 ± 1.25	6.79 ± 0.35	9.60 ± 0.49	9.37 ± 0.87	12.10 ± 1.50	11.90 ± 0.40
HCB	8.51 ± 0.24	8.36 ± 0.64*	13.37 ± 1.46*	17.56 ± 1.52*	15.00 ± 0.90*	15.80 ± 1.30*
PCB126	10.36 ± 0.74*	9.32 ± 0.67*	11.92 ± 1.53*	15.96 ± 0.87*	11.80 ± 0.90	13.40 ± 1.30*
Mixture	10.03 ± 1.06*	8.69 ± 0.66*	13.29 ± 1.16*	14.37 ± 2.63*	15.00 ± 1.40*	17.00 ± 1.40*

NOTE: Values represent the mean ± S.D. *p<0.05, significantly different from the concurrent controls; Dosing was stopped at week 16 due to overt toxicity in the form of marked body weight reduction.



Fig. 3.2. A serial section of a hepatocellular adenoma in a male F344 rat treated with PCB126. The tumor is GSTP⁺ (A), TGF-α⁺ (B) and TGFβ2Rc⁻ (C). Notably, this mass is a GSTP⁺ focus with the G⁺/α⁺/β⁻ phenotype.

3.3. Development of GSTP⁺ Foci

Time-dependent changes in GSTP⁺ foci development were observed in all treatment groups (Fig. 3.3). HCB, PCB126, and their mixture statistically increased both size and number of GSTP⁺ foci (Fig. 3.3). For instance, in HCB treated group, time-dependent changes in GSTP⁺ foci development were also observed. For example, at week 24, %GSTP⁺ foci area in control and HCB treated group were 0.79 ± 0.26 and $2.64 \pm 0.42\%$ (mean \pm S.D.; $p < 0.05$), respectively, whereas numbers of the foci for control and PCB126 treated rats were 142.3 ± 22.3 and 320.2 ± 71.3 foci/ μm^2 (mean \pm S.D.; $p < 0.05$), respectively.

At week 24, %GSTP⁺ foci area in control and PCB126 treated group were 0.79 ± 0.26 and $2.47 \pm 0.47\%$ (mean \pm S.D.; $p < 0.05$), respectively, whereas numbers of the foci for control and PCB126 treated rats were 142.3 ± 22.3 and 360.0 ± 124.5 foci/ μm^2 (mean \pm S.D.; $p < 0.05$), respectively.

In mixture treated group, time-dependent changes in GSTP⁺ foci development were also observed. For example, at week 24, %GSTP⁺ foci area in control and mixture treated group were 0.79 ± 0.26 and $2.32 \pm 1.09\%$ (mean \pm S.D.; $p < 0.05$), respectively, whereas numbers of the foci for control and PCB126 treated rats were 142.3 ± 22.3 and 507.9 ± 122.2 foci/ μm^2 (mean \pm S.D.; $p < 0.05$), respectively.

3.4. Development of TGF α ⁺ Foci

PCB126 significantly increased the area of TGF α ⁺ foci at week 18 and 24. At week 24, % area of TGF α ⁺ foci in control and PCB126 treated rats were 0.018 ± 0.009 and $1.268 \pm 1.023\%$ (mean \pm S.D.; $p < 0.05$), respectively, whereas numbers of TGF α ⁺

foci in control and PCB126 treated rats were 14.0 ± 6.6 and 247.5 ± 37.5 foci/ μm^2 (mean \pm S.D.; $p < 0.05$), respectively (Fig. 3.4).

In the HCB group, at week 24, % area of TGF α^+ foci in control and HCB treated rats were 0.018 ± 0.009 and $0.291 \pm 0.296\%$ (mean \pm S.D.; $p < 0.05$), respectively, whereas numbers of TGF α^+ foci in control and HCB treated rats were 14.0 ± 6.6 and 64.5 ± 50.5 foci/ μm^2 (mean \pm S.D.; $p < 0.05$), respectively (Fig. 3.4).

In the mixture treated group, at week 24, % area of TGF α^+ foci in control and mixture treated rats were 0.018 ± 0.009 and $0.277 \pm 0.202\%$ (mean \pm S.D.; $p < 0.05$), respectively, whereas numbers of TGF α^+ foci in control and mixture treated rats were 14.0 ± 6.6 and 94.1 ± 75.0 foci/ μm^2 (mean \pm S.D.; $p < 0.05$), respectively (Fig. 3.4).

3.5. TGF β 2Rc $^-$ Foci Formation

PCB126 significantly increased the area of TGF β 2Rc $^-$ foci at week 18 and 24, and increased the number of TGF β 2Rc $^-$ foci at week 24 ($p < 0.05$) (Fig. 3.5). At week 24, % area TGF β 2Rc $^-$ foci in control and PCB126 treated rats were 0.015 ± 0.037 and $0.420 \pm 0.396\%$ (mean \pm S.D.; $p < 0.05$), respectively, whereas numbers of TGF β 2Rc $^-$ foci in control and PCB126 treated rats were 0.2 ± 0.4 and 5.5 ± 4.9 foci/ μm^2 (mean \pm S.D.; $p < 0.05$), respectively (Fig. 3.5).

Neither HCB nor the mixture produces any significant difference in TGF β 2Rc $^-$ foci development.

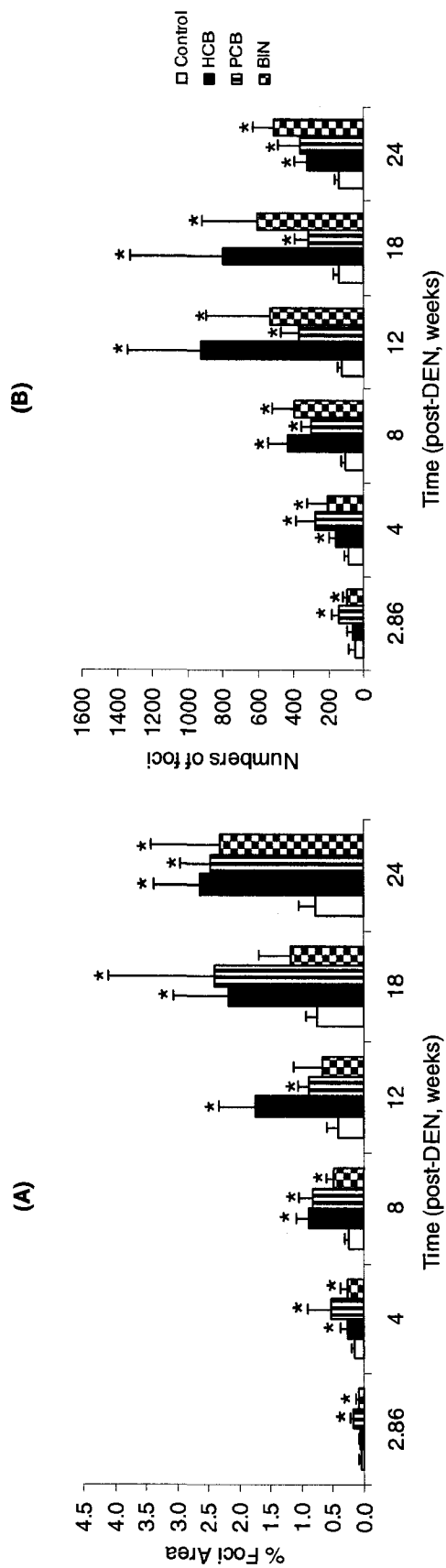


Fig. 3.3. Time-dependent changes in liver GSTP⁺ foci relative area and number in male F344 rats subjected to an initiation/promotion protocol using diethylnitrosamine (DEN) as an initiator and using corn oil (Control; white bars), HCB (black bars), PCB126 (striped bars) or mixture (BIN; checkered bars) as the promoting agents. The data are expressed as mean \pm S.D. *, significantly different from the control group ($P < 0.05$).

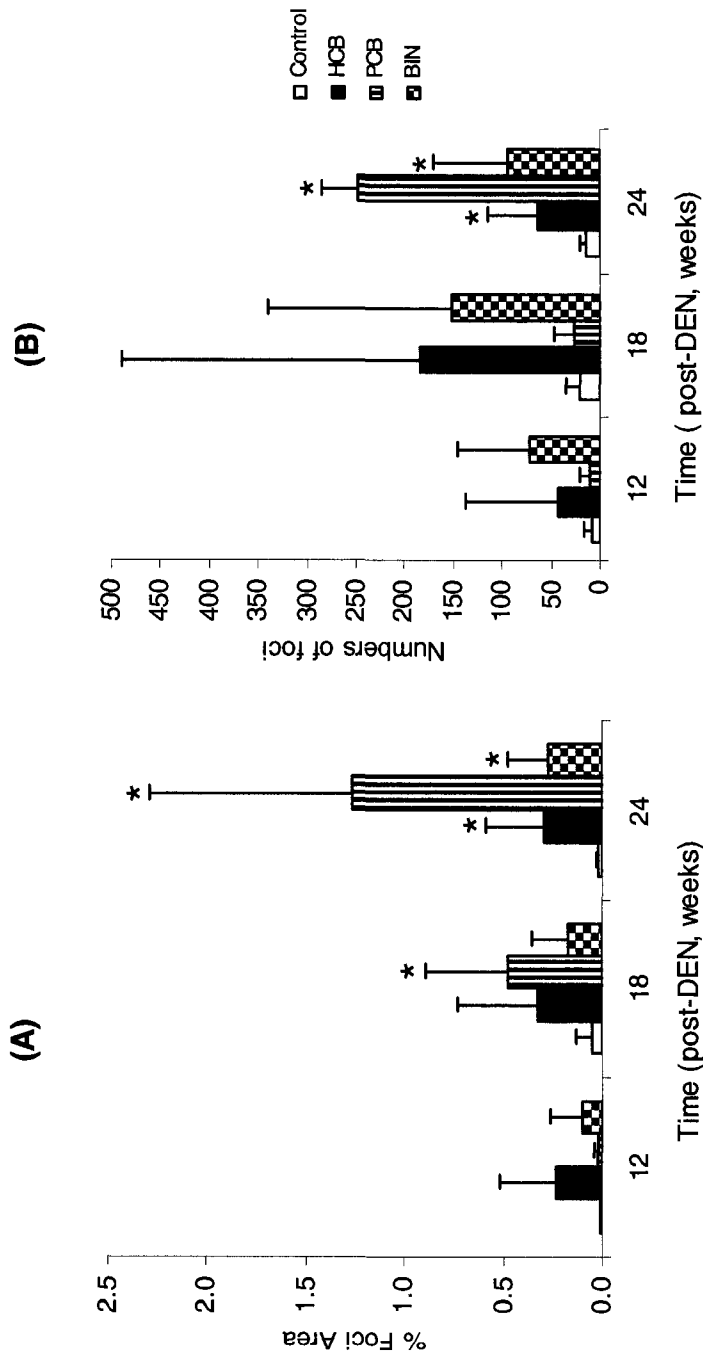


Fig. 3.4. Time-dependent changes in liver TGF α ⁺ foci relative area and number in male F344 rats subjected to an initiation/promotion protocol using diethylnitrosamine (DEN) as an initiator and using corn oil (Control; white bars), HCB (black bars), PCB126 (striped bars) or mixture (BIN; checkered bars) as the promoting agents. The data are expressed as mean \pm S.D. *, significantly different from the control group ($P < 0.05$).

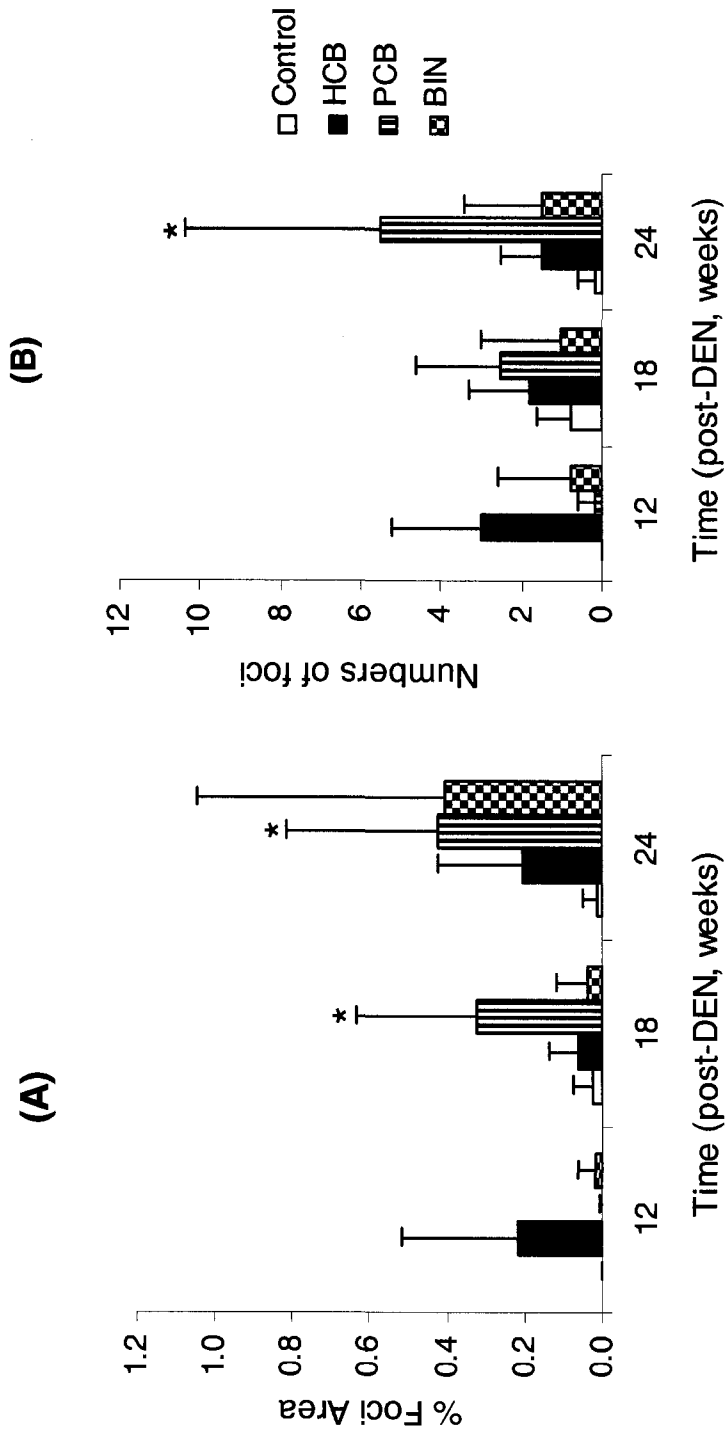


Fig. 3.5. Time-dependent changes in liver TGFβ2Rc foci relative area and number in male F344 rats subjected to an initiation/promotion protocol using diethylnitrosamine (DEN) as an initiator and using corn oil (Control; white bars), HCB (black bars), PCB126 (striped bars) or mixture (BIN; checkered bars) as the promoting agents. The data are expressed as mean ± S.D. *, significantly different from the control group ($P < 0.05$).

3.6. Hepatocyte Proliferation

Time-dependent changes in the %L.I. of the whole livers and calculated division rate were observed in PCB126 and mixture group, whereas there was no significant changes observed in HCB treated group (Fig. 3.6). At week 24, %L.I. of the liver in control and PCB126 treated rats were 1.80 ± 1.45 and $11.0 \pm 9.5\%$ (mean \pm S.D.; $p < 0.05$), respectively, whereas the calculated division rate of the liver in control and PCB126 treated rats were 0.0028 ± 0.0023 and $0.0200 \pm 0.0178 \text{ day}^{-1}$ (mean \pm S.D.; $p < 0.05$), respectively.

In mixture treated group, at week 24, %L.I. of the liver in control and mixture treated rats were 1.80 ± 1.45 and $8.5 \pm 5.2\%$ (mean \pm S.D.; $p < 0.05$), respectively, whereas the calculated division rate of the liver in control and PCB126 treated rats were 0.0028 ± 0.0023 and $0.0158 \pm 0.0097 \text{ day}^{-1}$ (mean \pm S.D.; $p < 0.05$), respectively.

3.7. Growth Characteristics in Four Different Phenotypes of GSTP⁺ Foci

Growth characteristics of four different GSTP⁺ foci based on their differential expression in TGF- α and TGF β 2Rc are summarized in Table 3.3 and 3.4, respectively. Overall, GSTP⁺ foci with G⁺/ α ⁺/ β ⁻ phenotype (GSTP⁺ foci with TGF- α ⁺ and TGF β 2Rc⁻) had the highest %L.I. compared to other phenotypes. At week 24, %L.I. of GSTP⁺ foci with G⁺/ α ⁻/ β ⁺ and G⁺/ α ⁺/ β ⁻ phenotype were 3.67 ± 2.39 and $18.10 \pm 11.54\%$ (mean \pm S.D.; $p < 0.05$), respectively. When the foci sorted by exposure period, time-dependent changes in their growth characteristics were observed in GSTP⁺ foci with G⁺/ α ⁺/ β ⁻ and G⁺/ α ⁺/ β ⁺ phenotype. Among the GSTP⁺ foci with G⁺/ α ⁺/ β ⁻ phenotype, PCB126 is the

most potent agent in increasing the %L.I. within the GSTP⁺ foci, while HCB has the weakest effect.

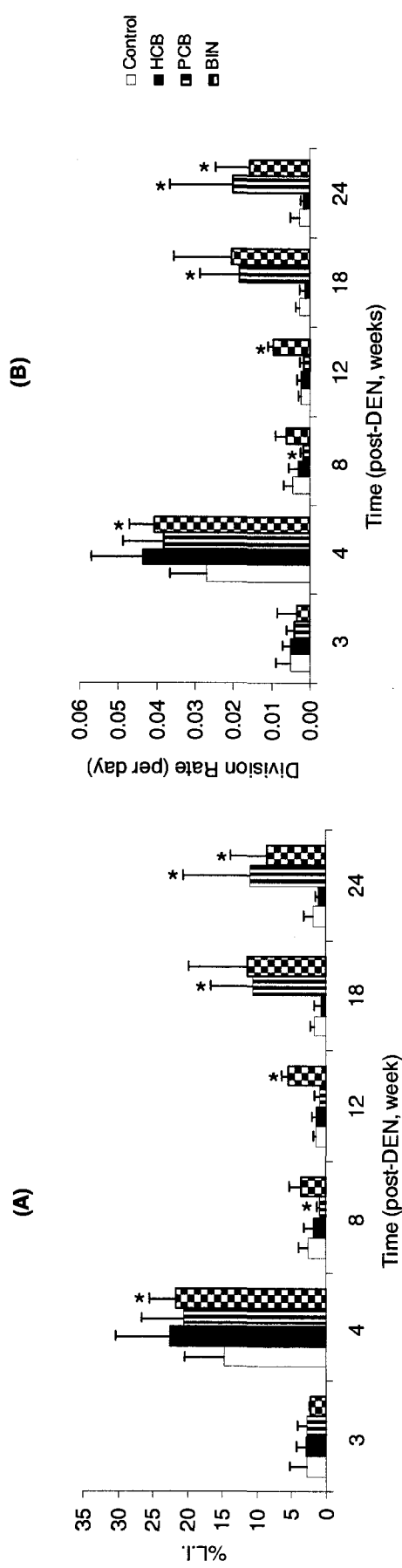


Fig. 3.6. Time-dependent changes in %L.I. of BrDU incorporated cells (A) and average cell division rates of the livers (B) of male F344 rats to an initiation/promotion protocol using diethylnitrosamine (DEN) as an initiator and using corn oil (Control; white bars), HCB (black bars), PCB126 (striped bars) or mixture (BIN; checkered bars) as the promoting agents. The data are expressed as mean \pm S.D. *, significantly different from the control group ($P < 0.05$).

TABLE 3.3. Size-dependent changes in % labeling index of GSTP⁺ foci with different TGF- α and TGF β 2Rc expressing phenotypes.

Area of Foci (A, μm^2)	Differential Expression			Differential Expression			Differential Expression		
	GSTP ⁺	TGF α	TGF β 2Rc ⁺	GSTP ⁺	TGF α	TGF β 2Rc ⁺	GSTP ⁺	TGF α	TGF β 2Rc ⁺
	G ⁺	α^+	β^+	G ⁺	α^+	β^+	G ⁺	α^+	β^+
A < 3.2 x 10 ⁵	1.94 ± 1.71 (n= 15) (Control: 1.35 ± 0.80, n= 6) (HCB: 1.63 ± 0.68, n= 6) (PCB: 1.88 ± 1.38, n= 2) (BIN: 7.5, n= 1)	18.62 ± 9.78* (n= 10) (Control: N.A., n= 0) (HCB: 9.36 ± 7.12, n= 2) (PCB: 25.42 ± 8.76, n= 5) (BIN: 13.45 ± 3.19, n= 3)	22.18 ± 10.82* (n= 8) (Control: N.A., n= 0) (HCB: N.A., n= 0) (PCB: 23.96 ± 10.35, n= 7) (BIN: 9.74, n= 1)	5.05 ± 5.70 (n= 5) (Control: N.A., n= 0) (HCB: 2.52 ± 0.77, n= 4) (PCB: N.A., n= 0) (BIN: 15.17, n= 1)					
3.2 x 10 ⁵ < A < 6.4 x 10 ⁵	2.76 ± 1.70 (n= 5) (Control: 5.52, n= 1) (HCB: 2.10 ± 1.44, n= 2) (PCB: 2.07, n= 1) (BIN: 2.04, n= 1)	21.14 ± 11.13* (n= 12) (Control: 14.22, n= 1) (HCB: 9.82 ± 10.62, n= 3) (PCB: 26.25 ± 8.41, n= 8) (BIN: N.A., n= 0)	12.98 ± 8.78* (n= 8) (Control: 4.73, n= 1) (HCB: 4.57, n= 1) (PCB: 31.01, n= 1) (BIN: 12.70 ± 4.31, n= 5)	6.33 ± 6.06 (n= 6) (Control: 7.07 ± 6.53, n= 2) (HCB: 2.59 ± 1.13, n= 3) (PCB: 16.08, n= 1) (BIN: N.A., n= 0)					
A > 6.4 x 10 ⁵	4.81 ± 2.26 (n= 6) (Control: N.A., n= 0) (HCB: 2.15 ± 0.80, n= 2) (PCB: N.A., n= 0) (BIN: 6.14 ± 1.12, n= 4)	16.43 ± 10.47* (n= 19) (Control: 6.17 ± 2.17, n= 2) (HCB: 9.49 ± 5.68, n= 6) (PCB: 28.19 ± 6.14, n= 7) (BIN: 11.38 ± 1.88, n= 4)	12.74 ± 14.20 (n= 2) (Control: N.A., n= 0) (HCB: 2.70, n= 1) (PCB: 22.78, n= 1) (BIN: N.A., n= 0)	15.99 ± 9.47* (n= 6) (Control: N.A., n= 0) (HCB: 1.8, n= 1) (PCB: 19.36 ± 3.41, n= 3) (BIN: 18.04 ± 13.45, n= 2)					
All	2.76 ± 2.13 (n= 26) (Control: 1.95 ± 1.74, n= 7) (HCB: 1.82 ± 0.79, n= 10) (PCB: 1.94 ± 0.98, n= 3) (BIN: 5.68 ± 2.06, n= 6)	18.34 ± 10.44* (n= 41) (Control: 8.85 ± 4.90, n= 3) (HCB: 9.55 ± 6.62, n= 11) (PCB: 26.72 ± 7.45, n= 20) (BIN: 12.27 ± 2.53, n= 7)	17.04 ± 10.69* (n= 18) (Control: 4.73, n= 1) (HCB: 3.64 ± 1.32, n= 2) (PCB: 24.62 ± 9.29, n= 9) (BIN: 12.21 ± 4.04, n= 6)	9.36 ± 8.56* (n= 17) (Control: 7.07 ± 6.53, n= 2) (HCB: 2.45 ± 0.83, n= 8) (PCB: 18.54 ± 3.23, n= 4) (BIN: 17.09 ± 9.66, n= 3)					

NOTE: Values represent the mean ± S.D. *p<0.05, significantly different from the GSTP⁺ foci with G⁺/ α / β ⁺ phenotype group.

Abbreviations: n, numbers of GSTP⁺ foci analyzed;

N.A., not available;

Control, foci from the control group;

HCB, foci from the HCB group; PCB, foci from the PCB126 group; BIN, foci from the mixture group.

TABLE 3.4. Time-dependent changes in % labeling index of GSTP⁺ foci with different TGF- α and TGF β 2Rc expressing phenotypes.

Time (weeks)	Differential Expression		Differential Expression		Differential Expression		Differential Expression	
	GSTP ⁺	TGF α	GSTP ⁺	TGF α	GSTP ⁺	TGF α	GSTP ⁺	TGF α
	G ⁺	β^+	G ⁺	β^+	G ⁺	β^+	G ⁺	β^+
12	1.76 ± 0.67 (n= 10) (Control: 1.52 ± 0.53, n= 3) (HCB: 1.80 ± 0.66, n= 4) (PCB: 1.94 ± 0.98, n= 3) (BIN: N.A., n= 0)	13.22 ± 6.39* (n= 7) (Control: N.A., n= 0) (HCB: 13.23 ± 7.50, n= 5) (PCB: N.A., n= 0) (BIN: 13.20 ± 4.46, n= 2)	11.25 ± 2.12* (n= 2) (Control: N.A., n= 0) (HCB: N.A., n= 0) (PCB: N.A., n= 0) (BIN: 11.25 ± 2.12, n= 2)	5.95 ± 5.67 (n= 7) (Control: 11.69., n= 1) (HCB: 2.75 ± 0.95, n= 5) (PCB: 16.21, n= 1) (BIN: N.A., n= 0)				
18	2.76 ± 2.87 (n= 5) (Control: 0.68 ± 0.96, n= 2) (HCB: 2.48 ± 0.89, n= 2) (PCB: : N.A., n= 0) (BIN: 7.50, n= 1)	20.41 ± 10.50* (n= 19) (Control: 9.42 ± 6.78, n= 2) (HCB: 5.71 ± 4.78, n= 3) (PCB: 26.18 ± 6.41, n= 13) (BIN: 11.56, n= 1)	22.69 ± 11.24* (n= 8) (Control: N.A., n= 0) (HCB: 4.57, n= 1) (PCB: 26.45 ± 9.50, n= 6) (BIN: 18.25, n= 1)	2.03 (n= 1) (Control: N.A., n= 0) (HCB: 2.03, n= 1) (PCB: N.A., n= 0) (BIN: N.A., n= 0)				
24	3.67 ± 2.39 (n= 11) (Control: 3.86 ± 2.35, n= 2) (HCB: 1.52 ± 0.87, n= 4) (PCB: N.A., n= 0) (BIN: 5.32 ± 2.07, n= 5)	18.10 ± 11.54* (n= 15) (Control: 6.17 ± 2.17, n= 2) (HCB: 9.49 ± 5.68, n= 6) (PCB: 28.19 ± 6.14, n= 7) (BIN: 11.38 ± 1.88, n= 4)	12.85 ± 9.17* (n= 8) (Control: 4.73, n= 1) (HCB: 2.70, n= 1) (PCB: 20.94 ± 9.44, n= 3) (BIN: 10.84 ± 4.07, n= 3)	12.83 ± 9.60 (n= 9) (Control: 2.45, n= 1) (HCB: 1.91 ± 0.16, n= 2) (PCB: 19.31 ± 3.47, n= 3) (BIN: 17.09 ± 9.66, n= 3)				
All	2.76 ± 2.13 (n= 26) (Control: 1.95 ± 1.74, n= 7) (HCB: 1.82 ± 0.79, n= 10) (PCB: 1.94 ± 0.98, n= 3) (BIN: 5.68 ± 2.06, n= 6)	18.34 ± 10.44* (n= 41) (Control: 8.85 ± 4.90, n= 3) (HCB: 9.55 ± 6.62, n= 11) (PCB: 26.72 ± 7.45, n= 20) (BIN: 12.27 ± 2.53, n= 7)	17.04 ± 10.69* (n= 18) (Control: 4.73, n= 1) (HCB: 3.64 ± 1.32, n= 2) (PCB: 24.62 ± 9.29, n= 9) (BIN: 12.21 ± 4.04, n= 6)	9.36 ± 8.56* (n= 17) (Control: 7.07 ± 6.53, n= 2) (HCB: 2.45 ± 0.83, n= 8) (PCB: 18.54 ± 3.23, n= 4) (BIN: 17.09 ± 9.66, n= 3)				

NOTE: Values represent the mean ± S.D. *p<0.05, significantly different from the GSTP⁺ foci with G⁺/ α / β ⁺ phenotype group.

Abbreviations: n, numbers of GSTP⁺ foci analyzed; N.A., not available; Control, foci from the control group;

HCB, foci from the HCB group; PCB, foci from the PCB126 group; BIN, foci from the mixture group.

4. DISCUSSION

This study, for the first time, examined the growth characteristics of GSTP⁺ hepatic foci based on their differential expression of TGF α and TGF β 2Rc in male F344 rats treated with PCB126, HCB, or their mixture. Our results clearly demonstrated that the GSTP⁺ foci with TGF α expression with the absence of TGF β 2Rc expression had the highest division rate compared to other types of GSTP⁺ foci (Table 3.3 and 3.4). Thus, it is possible that the GSTP⁺ foci with this specific phenotype acquire growth advantages and transform to tumors. This hypothesis was also supported by our finding that the hepatocellular adenoma found in a rat treated with PCB126 was also a GSTP⁺ focus with TGF α expression with the absence of TGF β 2Rc expression (Fig. 3.2).

Time-dependent changes in hepatic GSTP⁺, TGF α ⁺, and TGF β 2Rc⁻ foci also were observed. Increases in GSTP⁺ foci were observed in all treatment groups as early as 4 weeks post-DEN administration (Fig. 3.3), while increases in TGF α ⁺ foci and TGF β 2Rc⁻ foci were seen only at later times. Increases in TGF α ⁺ foci were observed at week 24 in all treatment groups (Fig. 3.4), however, increases in TGF β 2Rc⁻ foci were observed only in rats treated with PCB126 (Fig. 3.5).

Time-dependent changes in %L.I. and the division rates of the liver were observed in PCB126 and the mixture group, whereas there was no significant changes observed in the HCB treated group (Fig. 3.6). These results suggested that while HCB could increase the development of GSTP⁺ and TGF α ⁺ foci, it had no demonstrable effect on liver cell division, whereas PCB126 could contribute to these mitogenic effects in rats treated with PCB126.

The GSTP⁺ foci with TGF- α expression and without TGF β 2Rc expression demonstrated significantly higher cell division rates as shown by BrDU labeling indices (Table 3.3 and 3.4). These particular GSTP⁺ foci with the G⁺/ α ⁺/ β ⁻ phenotype had a division rate 6-7 fold higher than the GSTP⁺ foci without TGF- α expression and with TGF β 2Rc expression, the G⁺/ α ⁻/ β ⁺ phenotype. Among the G⁺/ α ⁺/ β ⁻ phenotype, PCB126 had the highest potency in increasing the %L.I. within the GSTP⁺ foci (Table 3.3 and 3.4). This suggests that, PCB126-induced, foci with G⁺/ α ⁺/ β ⁻ phenotype had significantly higher growth advantage compared to the GSTP⁺ foci with G⁺/ α ⁻/ β ⁺ phenotype. One hepatocellular adenoma was observed in a PCB126-treated rat at week 18. This tumor was classified as a GSTP⁺ focus with G⁺/ α ⁺/ β ⁻ phenotype (Fig. 3.2). Its %L.I. and division rate within the tumor were much higher than outside the tumor. Our current results supported the earlier findings in transgenic mice with bigenic TGF β 2Rc⁻/TGF- α (Gorska *et al.* 2003). These results suggest that expression TGF- α and lack of expression of TGF β 2Rc may predispose preneoplastic cells to progress to malignancy.

Phenotypic differences of GSTP⁺ foci based on TGF- α and TGF β 2Rc expression can be useful in classification of hepatic preneoplastic and neoplastic growth characteristics of as seen in this study and others (Farber 1984). Using a computer modeling approach, it has been suggested that there are at least two cell populations with different growth characteristics (Conolly and Andersen 1997; Lu *et al.* 2007; Ou *et al.* 2003; Ou *et al.* 2001). Cells advancing to the later stages of carcinogenesis (presumably GSTP⁺, TGF- α ⁺ and TGF β 2Rc⁻ phenotype) would have a growth advantage over those that are TGF- α ⁻ and TGF β 2Rc⁺ because of the over-expression of the mitogenic cytokine and the absence of response to apoptotic signals and could reflect an increasingly

malignant hepatocyte population. The approach of determining division rates in phenotypically different liver GSTP⁺ foci can be incorporated into computer models to predict time-dependent changes in liver foci development after exposure to a variety of chemicals and chemical mixtures.

In summary, the GSTP⁺ foci with TGF- α expression and an absence of TGF β 2Rc expression had the highest hepatocyte division rate and might be the cell population which evolves from preneoplasia to malignancy. In that sense, they may serve as excellent biomarkers for carcinogenicity in the liver.

ACKNOWLEDGEMENT

This study is supported by the NIOSH/CDC grant 1 RO1 OH07556, NIEHS Training Grant 1 T32 ES 07321, and scholarships from U.S. Fulbright Foundation and Naresuan University, Thailand. We thank our colleagues in the Quantitative and Computational Toxicology Group for their excellent technical assistance.

REFERENCES

- Alvarez, L., Randi, A., Alvarez, P., Kolliker Frers, R., and Kleiman de Pisarev, D. L. (1999). Effect of hexachlorobenzene on NADPH-generating lipogenic enzymes and L-glycerol-3-phosphate dehydrogenase in brown adipose tissue. *J Endocrinol Invest* **22**, 436-445.
- Bates, S. E., Davidson, N. E., Valverius, E. M., Freter, C. E., Dickson, R. B., Tam, J. P., Kudlow, J. E., Lippman, M. E., and Salomon, D. S. (1988). Expression of transforming growth factor alpha and its messenger ribonucleic acid in human breast cancer: its regulation by estrogen and its possible functional significance. *Mol Endocrinol* **2**, 543-55.
- Brattain, M. G., Markowitz, S. D., and Willson, J. K. (1996). The type II transforming growth factor-beta receptor as a tumor-suppressor gene. *Curr Opin Oncol* **8**, 49-53.
- Calvisi, D. F., and Thorgeirsson, S. S. (2005). Molecular mechanisms of hepatocarcinogenesis in transgenic mouse models of liver cancer. *Toxicol Pathol* **33**, 181-4.
- Cheng, N., Bhowmick, N. A., Chytil, A., Gorksa, A. E., Brown, K. A., Muraoka, R., Arteaga, C. L., Neilson, E. G., Hayward, S. W., and Moses, H. L. (2005). Loss of TGF-beta type II receptor in fibroblasts promotes mammary carcinoma growth and invasion through upregulation of TGF-alpha-, MSP- and HGF-mediated signaling networks. *Oncogene* **24**, 5053-68.
- Chung, Y. H., Kim, J. A., Song, B. C., Lee, G. C., Koh, M. S., Lee, Y. S., Lee, S. G., and Suh, D. J. (2000). Expression of transforming growth factor-alpha mRNA in livers of patients with chronic viral hepatitis and hepatocellular carcinoma. *Cancer* **89**, 977-82.
- Conolly, R. B., and Andersen, M. E. (1997). Hepatic foci in rats after diethylnitrosamine initiation and 2,3,7,8-tetrachlorodibenzo-p-dioxin promotion: evaluation of a quantitative two-cell model and of CYP 1A1/1A2 as a dosimeter. *Toxicol Appl Pharmacol* **146**, 281-93.
- Dean, C. E., Jr., Benjamin, S. A., Chubb, L. S., Tessari, J. D., and Keefe, T. J. (2002). Nonadditive hepatic tumor promoting effects by a mixture of two structurally different polychlorinated biphenyls in female rat livers. *Toxicol Sci* **66**, 54-61.
- Derynck, R., Goeddel, D. V., Ullrich, A., Gutterman, J. U., Williams, R. D., Bringman, T. S., and Berger, W. H. (1987). Synthesis of messenger RNAs for transforming growth factors alpha and beta and the epidermal growth factor receptor by human tumors. *Cancer Res* **47**, 707-12.

- Dragan, Y., Teeguarden, J., Campbell, H., Hsia, S., and Pitot, H. (1995). The quantitation of altered hepatic foci during multistage hepatocarcinogenesis in the rat: transforming growth factor alpha expression as a marker for the stage of progression. *Cancer Lett* **93**, 73-83.
- Farber, E. (1984). Cellular biochemistry of the stepwise development of cancer with chemicals: G. H. A. Clowes memorial lecture. *Cancer Res* **44**, 5463-74.
- Forrester, E., Chytil, A., Bierie, B., Aakre, M., Gorska, A. E., Sharif-Afshar, A. R., Muller, W. J., and Moses, H. L. (2005). Effect of conditional knockout of the type II TGF-beta receptor gene in mammary epithelia on mammary gland development and polyomavirus middle T antigen induced tumor formation and metastasis. *Cancer Res* **65**, 2296-302.
- Gocmen, A., Peters, H. A., Cripps, D. J., Morris, C. R., and Dogramaci, I. (1986). Porphyria turcica: hexachlorobenzene-induced porphyria. *IARC Sci Publ*, 567-573.
- Gorska, A. E., Jensen, R. A., Shyr, Y., Aakre, M. E., Bhowmick, N. A., and Moses, H. L. (2003). Transgenic mice expressing a dominant-negative mutant type II transforming growth factor-beta receptor exhibit impaired mammary development and enhanced mammary tumor formation. *Am J Pathol* **163**, 1539-49.
- Huntley, S. P., Davies, M., Matthews, J. B., Thomas, G., Marshall, J., Robinson, C. M., Eveson, J. W., Paterson, I. C., and Prime, S. S. (2004). Attenuated type II TGF-beta receptor signalling in human malignant oral keratinocytes induces a less differentiated and more aggressive phenotype that is associated with metastatic dissemination. *Int J Cancer* **110**, 170-6.
- Ito, N., Tamano, S., and Shirai, T. (2003). A medium-term rat liver bioassay for rapid in vivo detection of carcinogenic potential of chemicals. *Cancer Sci* **94**, 3-8.
- Jhappan, C., Stahle, C., Harkins, R. N., Fausto, N., Smith, G. H., and Merlino, G. T. (1990). TGF alpha overexpression in transgenic mice induces liver neoplasia and abnormal development of the mammary gland and pancreas. *Cell* **61**, 1137-46.
- Lohitnavy, M., Chubb, L. S., Lohitnavy, O., Yang, C. C., Homberg, J., Campain, J. A., and Yang, R. S. (2004). Pharmacokinetic (PK)/Pharmacodynamic (PD) Relationship of PCB126 Under the Conditions of Modified Medium-Term Liver Bioassay. *Toxicologist* **78**, 271.
- Lu, Y., Lohitnavy, M., Reddy, M. B., Lohitnavy, O., Eickman, E., Ashley, A., Gerjevic, L., Xu, Y., Conolly, R. B., and Yang, R. S. H. (2007). Quantitative Analysis of Liver GST-P Foci Promoted by a Chemical Mixture of Hexachlorobenzene and PCB 126: Implication of Size-dependent Cellular Growth Kinetics. *Arch Toxicol*, (in press).

- Luetke, N. C., Michalopoulos, G. K., Teixido, J., Gilmore, R., Massague, J., and Lee, D. C. (1988). Characterization of high molecular weight transforming growth factor alpha produced by rat hepatocellular carcinoma cells. *Biochemistry* **27**, 6487-94.
- Markowitz, S., Wang, J., Myeroff, L., Parsons, R., Sun, L., Lutterbaugh, J., Fan, R. S., Zborowska, E., Kinzler, K. W., Vogelstein, B., and et al. (1995). Inactivation of the type II TGF-beta receptor in colon cancer cells with microsatellite instability. *Science* **268**, 1336-8.
- Mydlo, J. H., Michaeli, J., Cordon-Cardo, C., Goldenberg, A. S., Heston, W. D., and Fair, W. R. (1989). Expression of transforming growth factor alpha and epidermal growth factor receptor messenger RNA in neoplastic and nonneoplastic human kidney tissue. *Cancer Res* **49**, 3407-11.
- NTP (2001). Ninth report on carcinogenesis: Hexachlorobenzene. National Toxicology Program.
- NTP (2006). NTP toxicology and carcinogenesis studies of 3,3',4,4',5-pentachlorobiphenyl (PCB 126) (CAS No. 57465-28-8) in female Harlan Sprague-Dawley rats (Gavage Studies). *Natl Toxicol Program Tech Rep Ser*, 4-246.
- Ogiso, T., Tatematsu, M., Tamano, S., Hasegawa, R., and Ito, N. (1990). Correlation between medium-term liver bioassay system data and results of long-term testing in rats. *Carcinogenesis* **11**, 561-6.
- Ou, Y. C., Conolly, R. B., Thomas, R. S., Gustafson, D. L., Long, M. E., Dobrev, I. D., Chubb, L. S., Xu, Y., Lapidot, S. A., Andersen, M. E., and Yang, R. S. (2003). Stochastic simulation of hepatic preneoplastic foci development for four chlorobenzene congeners in a medium-term bioassay. *Toxicol Sci* **73**, 301-14.
- Ou, Y. C., Conolly, R. B., Thomas, R. S., Xu, Y., Andersen, M. E., Chubb, L. S., Pitot, H. C., and Yang, R. S. (2001). A clonal growth model: time-course simulations of liver foci growth following penta- or hexachlorobenzene treatment in a medium-term bioassay. *Cancer Res* **61**, 1879-89.
- Ralph, J. L., Orgebin-Crist, M. C., Lareyre, J. J., and Nelson, C. C. (2003). Disruption of androgen regulation in the prostate by the environmental contaminant hexachlorobenzene. *Environ Health Perspect* **111**, 461-466.
- Safe, S., Bandiera, S., Sawyer, T., Robertson, L., Safe, L., Parkinson, A., Thomas, P. E., Ryan, D. E., Reik, L. M., Levin, W., and et al. (1985). PCBs: structure-function relationships and mechanism of action. *Environ Health Perspect* **60**, 47-56.

- Safe, S. H. (1994). Polychlorinated biphenyls (PCBs): environmental impact, biochemical and toxic responses, and implications for risk assessment. *Crit Rev Toxicol* **24**, 87-149.
- Shirai, T. (1997). A medium-term rat liver bioassay as a rapid in vivo test for carcinogenic potential: a historical review of model development and summary of results from 291 tests. *Toxicol Pathol* **25**, 453-60.
- Smith, A. G., Dinsdale, D., Cabral, J. R., and Wright, A. L. (1987a). Goitre and wasting induced in hamsters by hexachlorobenzene. *Arch Toxicol* **60**, 343-349.
- Smith, A. G., Francis, J. E., Dinsdale, D., Manson, M. M., and Cabral, J. R. (1985). Hepatocarcinogenicity of hexachlorobenzene in rats and the sex difference in hepatic iron status and development of porphyria. *Carcinogenesis* **6**, 631-636.
- Smith, J. J., Derynck, R., and Korc, M. (1987b). Production of transforming growth factor alpha in human pancreatic cancer cells: evidence for a superagonist autocrine cycle. *Proc Natl Acad Sci U S A* **84**, 7567-70.
- Solt, D., and Farber, E. (1976). New principle for the analysis of chemical carcinogenesis. *Nature* **263**, 701-3.
- Steinmetz, K. L., and Klaunig, J. E. (1996). Transforming growth factor-alpha in carcinogen-induced F344 rat hepatic foci. *Toxicol Appl Pharmacol* **140**, 131-45.
- Sue, S. R., Chari, R. S., Kong, F. M., Mills, J. J., Fine, R. L., Jirtle, R. L., and Meyers, W. C. (1995). Transforming growth factor-beta receptors and mannose 6-phosphate/insulin-like growth factor-II receptor expression in human hepatocellular carcinoma. *Ann Surg* **222**, 171-8.
- Tang, B., Bottinger, E. P., Jakowlew, S. B., Bagnall, K. M., Mariano, J., Anver, M. R., Letterio, J. J., and Wakefield, L. M. (1998). Transforming growth factor-beta1 is a new form of tumor suppressor with true haploid insufficiency. *Nat Med* **4**, 802-7.
- Vos, J. G. (1986). Immunotoxicity of hexachlorobenzene. *IARC Sci Publ*, 347-56.
- Yeh, Y. C., Tsai, J. F., Chuang, L. Y., Yeh, H. W., Tsai, J. H., Florine, D. L., and Tam, J. P. (1987). Elevation of transforming growth factor alpha and its relationship to the epidermal growth factor and alpha-fetoprotein levels in patients with hepatocellular carcinoma. *Cancer Res* **47**, 896-901.

CHAPTER 4

A Novel Physiologically-Based Pharmacokinetic Model of Methotrexate Incorporating Hepatic Excretion via Multidrug-Resistance-Associated Protein 2 (Mrp2) in Mice, Rats, Dogs, and Humans

Manupat Lohitnavy, Yasong Lu, Ornrat Lohitnavy, Mike A. Lyons, and,
Raymond S. H. Yang

ABSTRACT

A novel physiologically-based pharmacokinetic (PBPK) model of methotrexate (MTX) was built based on an earlier model developed by Bischoff et al. (1971). MTX is known to be a substrate of multidrug-resistance-associated protein 2 (Mrp2). More recently, a three-dimensional quantitative structure-activity relationship model (3D-QSAR) of Mrp2 was developed by Hirono et al. (2005) in Japan. In our updated PBPK model of MTX, using the computational chemistry-derived binding affinity (K_m), a Mrp2-mediated biliary excretion process was incorporated as the MTX excretory pathway. Our model simulation results are consistent with numerous datasets obtained from mice, rats, dogs, and humans, at a variety of dose levels. Comparisons were made between our updated PBPK model and the earlier one from Bischoff et al. using a PBPK Index approach. Our new PBPK model was further verified against additional pharmacokinetic datasets from rats under special experimental conditions (cannulated bile duct) and Eisai hyperbilirubinemic rats.

1. INTRODUCTION

Methotrexate (MTX) is a dihydrofolate reductase (DHFR) inhibitor which has been widely used in cancer treatment and rheumatoid arthritis (Treon and Chabner 1996; Walker and Ranatunga 2006). MTX exerts its pharmacological effects via an irreversible binding to DHFR resulting in its cytotoxic effects. Bischoff et al. reported a physiologically-based pharmacokinetic (PBPK) model of MTX (Bischoff *et al.* 1971). That model was one of the earliest PBPK models published in the literature. It was able to describe a variety of dose levels of MTX in several species, including mice, rats, dogs, and humans. The original model consisted of plasma, liver, kidney, muscle, gut lumen, and gut tissue compartments. Entero-hepatic recirculation behavior of MTX was also mathematically incorporated into the model. In the liver sub-compartment, MTX was excreted into bile using biliary secretion. MTX was then secreted into the gut lumen and reabsorbed thereby completing its entero-hepatic recirculation. Since it has been 36 years, the original computer code was not available. Thus, in our present study, we recreated the code based on the conceptual model in the publication.

Multidrug-resistance-associated protein 2 (Mrp2), a transporter protein, was recently identified as a molecular entity responsible for this biliary excretion of MTX (Han *et al.* 2001). A mutation at Trp1254 of *Mrp2* gene resulted in a loss of MTX transport activity in a cell culture system (Ito *et al.* 2001). A three-dimensional quantitative structure-activity relationship (3D-QSAR) model of Mrp2 was developed by Hirono and colleagues in Japan (Hirono *et al.* 2005). In that paper, the authors reported a binding affinity (K_m) value [$\log(1/K_m) = 3.47$ L/mole] between MTX and Mrp2 using a computational chemistry technique. We integrated these biochemical and molecular

characteristics of MTX into a newly updated PBPK model of MTX. Thus, this paper: 1) recounts our conceptual development of the involvement of Mrp2 in MTX pharmacokinetics; 2) builds a novel PBPK model of MTX by incorporating an Mrp2-mediated biliary excretion process into the Bischoff et al. 1971 model; 3) compares the performances of the newly built PBPK model with the reconstructed Bischoff et al. 1971 PBPK model, and 4) verifies of the updated PBPK model using additional special and relevant experimental datasets.

2. MATERIAL AND METHODS

2.1. A Reconstruction of the PBPK Model of MTX Earlier Developed by Bischoff et al (1971)

2.1.1. Pharmacokinetic Studies in Bischoff et al (1971)

Since the Bischoff et al. (1971) paper was over 36 years old, we had to re-code the PBPK model based on the conceptual model presented in the paper. The original PBPK model of MTX consists of plasma, liver, gut tissue, kidney, and muscle compartments (Bischoff *et al.* 1971). All parameters used in the model are summarized in Table 4.1. The reconstructed model code was written and the simulations were performed using ACSL Tox[®] (version 11.8.4; Aegis Technologies Group Inc., Marietta, GA). Parameter optimization was performed using ACSL Math[®] (version 2.5.4; Aegis Technologies Group Inc., Marietta, GA). This earlier model featured an entero-hepatic recirculation of MTX via excretion of MTX into the bile, then, MTX was re-absorbed into the gut tissue, and re-entered into the liver through the hepatic vein. In a reconstructed PBPK model of MTX, a biliary excretion process with a first-order excretion kinetics was assumed. In the Bischoff et al. paper, figures of the concentration-

time courses of MTX in mice, rats, dogs, and humans were presented. Mice were intravenously administered with 3.0 and 300.0 mg MTX/kg BW. Rats were given with an i.p. single-dose of 0.5, 6.0, and 25.0 mg MTX/kg BW. Dogs were intravenously administered with 3.0 mg MTX/kg BW. Two human volunteers also participated in the study; they were intravenously administered with a single dose of 1.0 mg MTX/kg BW. MTX concentration-time courses were shown separately for each human subject. Tissue samples (plasma, liver, kidney, muscle, and gut tissue in mice, rats, and dogs; plasma only in humans) from multiple time points were collected and analyzed for MTX concentration levels.

2.1.2. Data extraction

DigiMatic Program (version 2.1; Richmond, Virginia) was used to extract numerical co-ordinates from the concentration-time courses of MTX presenting in the figures published by Bischoff et al (Bischoff *et al.* 1971).

2.2. Incorporation of an Mrp2-Mediated Biliary Secretion into the Reconstructed Bischoff et al. Model

Multidrug-resistance-associated protein 2 (Mrp2), a transporter protein, was identified in 2001 to play an important role in the biliary excretion of MTX by Han et al. (2001). Such a molecular excretory role of Mrp2 in MTX pharmacokinetics was indirectly substantiated by Ito et al. (2001) because a mutation at Trp1254 of Mrp2 gene resulted in a loss of MTX transport activity in a cell culture system. A few years later, a 3D-QSAR model for rat Mrp2 was developed by Hirono et al. (2005) based on molecular characteristics such as molecular steric field, molecular electrostatic field and ClogP calculated by SYBYL software package (Tripos Inc., St. Louis, USA) (Hirono *et al.*

2005). These investigators demonstrated that their predicted values of $\log(1/K_m)$, which are measurements for binding affinity to Mrp2, were within 2% of the experimentally determined values for 16 chemicals, including MTX, in their training set (Hirono *et al.* 2005). The largest difference of 13% was seen between predicted and experimental values in one of the two chemicals in their test set (Hirono *et al.* 2005). Thus, we believe that the *in silico* derived binding affinity constant, K_m , is adequate for our purpose.

Armed with this newly emerged scientific information, we started to develop our PBPK model of MTX with Mrp2-mediated excretion in the rats first and then proceeded to mice, dogs, and humans, respectively. A schematic diagram of PBPK of MTX with the incorporation of an Mrp2-mediated secretion process is presented in Fig. 4.1. Since in Hirono *et al.* study (Hirono *et al.* 2005) a Michaelis-Menten equation was used for the derivation of the MTX-Mrp2 binding affinity constant, K_m , the first order biliary excretion process used in the reconstructed Bischoff *et al.* MTX model was replaced by a Michaelis-Menten equation. The computational chemistry-derived K_m value by Hirono *et al.* was employed. A maximum binding capacity (V_{max}) value between MTX and Mrp2 in rats was estimated using an optimization process while all of other physiological parameters were identical to those of the reconstructed Bischoff *et al.* model. After a PBPK model in rats was developed, we then proceeded to our model development for mice, dogs and humans, respectively. To determine the values of K_m and V_{max} in these species, a stepwise optimization was performed. In humans, since individual datasets for each of the human volunteers were available, an optimization for the values of V_{max} and K_m in each subject was performed. The values of K_m and V_{max} of Mrp2 in mice, rats, dogs, and humans are summarized in Table 4.1.

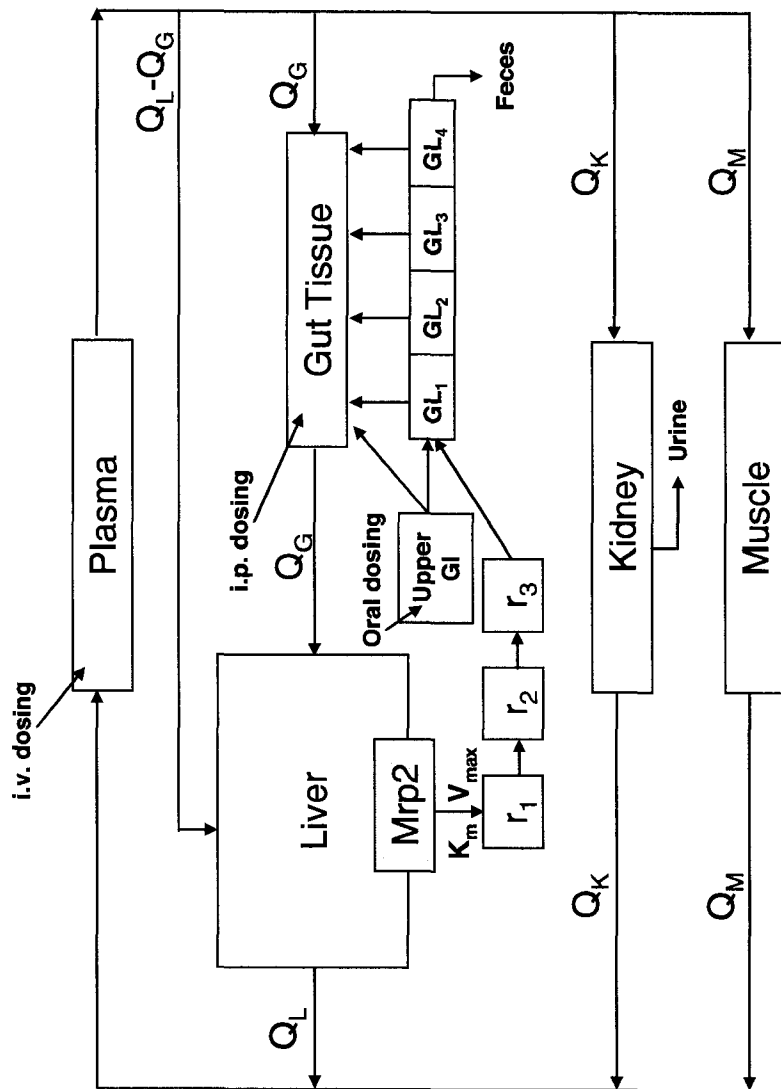


Fig. 4.1. A schematic diagram of a PBPK model of methotrexate (MTX) with MRP2-mediated biliary excretion. In this model, MTX can be administered into the body via intravenous, intraperitoneal and oral administration. The model consists of kidney, muscle, plasma, gut tissue, gut lumen (upper GI and lower GI consisting of GL₁, GL₂, GL₃ and GL₄), liver, and biliary secretion pathway (r₁, r₂ and r₃). MTX can be excreted from the liver into bile via an MRP2-mediated excretion process. Once excreted into the bile, MTX moves along the biliary excretion pathway (r₁, r₂ and r₃) and secreted into the gut lumen at the GL₁ segment. In GL₁, GL₂, GL₃ and GL₄ segment, MTX can be reabsorbed into the gut tissue, transferred to the adjacent segment, or excreted out of the body in feces.

Table 4.1. Physiological Parameters for the MTX PBPK Models.

Parameters	Bischoff et al. model				Updated Mrp2 model				
	Mice	Rats	Dogs	Humans	Mice	Rats	Dogs	Human 1	Human 2
Body Weight (kg)	0.022	0.2	17.0	70.0	0.022	0.2	17.0	70.0	70.0
<i>Volume of Organs (L)</i>									
Plasma	0.001	0.009	0.65	3.0	0.001	0.009	0.65	3.0	3.0
Muscle	0.01	0.1	7.5	35.0	0.01	0.1	7.5	35.0	35.0
Kidney	0.00034	0.0019	0.076	0.28	0.00034	0.0019	0.076	0.28	0.28
Liver	0.0013	0.0083	0.36	1.35	0.0013	0.0083	0.36	1.35	1.35
Gut Tissue	0.0015	0.011	0.64	2.1	0.0015	0.011	0.64	2.1	2.1
Gut Lumen	0.0015	0.011	0.64	2.1	0.0015	0.011	0.64	2.1	2.1
<i>Blood Flow (L/h)</i>									
Muscle	0.03	0.18	8.4	25.2	0.03	0.18	8.4	25.2	25.2
Kidney	0.48	0.30	11.4	42.0	0.48	0.30	11.4	42.0	42.0
Liver	0.066	0.39	13.2	48.0	0.066	0.39	13.2	48.0	48.0
Gut tissue	0.054	0.318	11.4	42.0	0.054	0.318	11.4	42.0	42.0
<i>Partition Coefficient</i>									
Muscle	0.15	0.15	0.15	0.15	0.15	0.15	0.15	0.15	0.15
Kidney	3.0	3.0	14.0	3.0	3.0	3.0	14.0	3.0	3.0
Liver	3.0	3.0	2.0	3.0	3.0	3.0	2.0	3.0	3.0
Gut tissue	1.0	1.0	1.0	1.0	1.0	1.0	1.0	1.0	1.0
<i>Clearance (L/h)</i>									
Kidney	0.012	0.066	3.36	11.4	0.012	0.066	3.36	11.4	11.4
Bile	0.024	0.18	0.48	12.0	N.A.	N.A.	N.A.	N.A.	N.A.
<i>Mrp2-mediated biliary secretion</i>									
Binding Affinity (mg/L)	N.A.	N.A.	N.A.	N.A.	154.0	154.0 ^a	154.0	150.2	150.2
Maximum binding capacity (mg/h)	N.A.	N.A.	N.A.	N.A.	5.70	36.20	160.11	3888.9	2188.8
<i>GI absorption parameters</i>									
Capacity (mg/h)	0.012	1.2	90.0	114.0	0.012	1.2	90.0	114.0	114.0
Affinity (mg/L)	6.0	200	200	200	6.0	200	200	200	200
K _{abs} (hour ⁻¹)	0.00006	0.00006	0.0006	0.00006	0.00006	0.00006	0.0006	0.00006	0.00006
Mass transfer in lower GI (hour ⁻¹)	0.60	0.60	0.09	0.06	0.60	0.60	0.09	0.06	0.06
Absorption rate constant at the upper GI (hour ⁻¹)	N.A.	N.A.	N.A.	N.A.	N.A.	N.A.	0.05	N.A.	N.A.
Mass transfer from upper GI to lower segment (hour ⁻¹)	N.A.	N.A.	N.A.	N.A.	N.A.	N.A.	0.418	N.A.	N.A.

^a In Eisai hyperbilirubinemic rats (EHBR), the maximum binding capacity of Mrp2 to MTX (V_{max}) was set as zero.

2.3. Comparisons Between the Bischoff et al. Model and Our Updated PBPK Model with the Mrp2-Mediated Excretion Process

A comparison between PBPK models using a “PBPK Index” was earlier proposed by Krishnan et al (Krishnan *et al.* 1995). In brief, the PBPK index is a statistical evaluation of the degree of concordance between simulations and experimental data. It provides a more decisive means to determine the best-fit model. The PBPK Index can be calculated by using the following stepwise calculations (Krishnan *et al.* 1995):

$$et = |St - Et| \quad (1)$$

Where, et is absolute error, St is a simulated datum from a tested PBPK model, and Et is an observed datum from an experiment.

$$RMet^2 = \sqrt{\sum et^2 / N} \quad (2)$$

Where, $RMet^2$ is root mean of error square, N is number of data pairs in the dataset, and et^2 are the square of the error estimates.

$$I_I = RMet_{Simulated}^2 / RMet_{Observed}^2 \quad (3)$$

Where, I_I is an initial index and $RMet_{Simulated}^2$ and $RMet_{Observed}^2$ is root mean of the square of simulated and experimental data, respectively.

$$I_c = \left[I_a \times \left(N_a / \sum_{i=1}^n N_i \right) \right] + \left[I_b \times \left(N_b / \sum_{i=1}^n N_i \right) \right] \quad (4)$$

Where, I_c is consolidated discrepancy index (provide an indication of the overall, weighted average of the discrepancy between PBPK model simulations and experimental data), I_a and I_b are the discrepancy indices obtained from end points a and b, respectively

(from a single study), N_a and N_b are number of data points in the time-course curve for endpoints a and b, respectively. Finally, The PBPK Index can be calculated by averaging the I_c 's obtained from multiple studies (i.e. exposure concentrations, routes, scenarios, or species). In general, the lower the PBPK Index is, the better the performance of the model is.

2.4. Verifying the Updated PBPK Model of MTX With Additional Special and Relevant Experimental Datasets

To further test the capability of our updated PBPK model, we selected two additional datasets from the literatures. The first dataset was a pharmacokinetic study of MTX with oral dosing in male Sprague-Dawley (SD) rats and in male Eisai hyperbilirubinemic rats (EHBR) which was a mutant strain deficient in Mrp2 expression (Naba *et al.* 2004). In this study, the animals were orally administered with a single dose of 0.2 or 0.6 mg MTX/kg BW. Subsequently, serial plasma samples were collected through jugular vein cannulation for up to 12 hours, and the samples were analyzed for MTX levels using an LC-MS method. Since the earlier PBPK model simulations involved intravenous and intraperitoneal dosing (see Section 2.1), with this oral dosing condition, we incorporated an upper GI tract with a different absorption rate constant and a luminal mass transfer rate into the existing model (Fig. 4.1). The values of these two parameters were obtained from optimization processes (Table 4.1). To simulate the experimental conditions in EHBR, the value of V_{\max} in these rats was assumed to be zero resulting in an absence of MTX biliary excretion.

The second dataset was taken from Chen et al (Chen *et al.* 2003). In that study, a role of Mrp2 in biliary excretion of MTX was investigated using SD rats and EHBR. To

collect bile from the animals, bile duct was cannulated, and an intravenous MTX infusion at an infusion rate of 60 µg MTX/minute was delivered to the rats for two hours. Subsequently, the infusion was stopped and bile was continuously collected for up to 2 hours. Cumulative MTX levels in the bile were determined using an LC-MS/MS technique. To simulate this experimental condition (i.e. bile duct cannulation), MTX was assumed to be secreted from the liver out of the body bypassing the entero-hepatic recirculation process. All data points from these two datasets were extracted from the figures of those studies using the DigiMatic Program as described earlier.

2.5. Sensitivity Analysis

Sensitivity analysis is a useful approach for identifying important parameters affecting a pharmacokinetic measurement (Clewel *et al.* 1994). Log-normalized sensitivity parameters (LSPs) were defined as follows:

$$LSP = \partial \ln R / \partial \ln x' \quad (5)$$

Where, R is a model output and x is the parameter for which the sensitivity is being tested. This definition quantifies the percentage change in an output value due to the percentage change in a parameter. To demonstrate the significance of parameters affecting the MTX concentrations in rat liver, sensitivity analyses were performed under two different experimental conditions: 1) a single i.p. dose (6 mg MTX/kg BW) in normal rats, and; 2) the continuous infusion (60 µg MTX/kg BW/min. for 2 hours) in rats with bile duct cannulation. Sensitivity analysis was performed using ACSL Math[®] (version 2.5.4; Aegis Technologies Group Inc., Marietta, GA). Parameters involving partition coefficient (partition coefficient of the liver, PL), Mrp2-mediated excretion (V_{\max} and K_m), and blood flow (QGT and QL) were evaluated in these analyses.

3. RESULTS

3.1. Performances of the Reconstructed Bischoff et al. Model and Our Updated PBPK Model with an Mrp2-Mediated Biliary Excretion Process

Comparisons between the two models are shown as time-course tissue MTX simulation plots in mice (Fig. 4.2 and 4.3), rats (Fig. 4.4 and 4.5), dogs (Fig. 4.6), and humans (Fig. 4.7 and 4.8). Both models are able to successfully describe the datasets obtained from Bischoff et al (1971). The quality of fit as judged by PBPK Indices in all four species is presented in Table 4.2. PBPK indices of the Bischoff et al. model and our updated PBPK model are 18.23 and 19.90, respectively. In general, using the PBPK Index approach, our new MTX PBPK model is comparable to the Bischoff et al. model in describing MTX concentration-time courses in mice, rats, dogs, and humans. However, it should be emphasized that our updated PBPK model contains the latest scientific information on biliary excretion involving Mrp2.

3.2. Performances of Our Updated PBPK Model Against Additional Datasets Involving Special Experimental Conditions

Plasma concentration-time courses of MTX in SD rats and EHBR administered with an oral single-dose of MTX (0.2 or 0.6 mg MTX/kg BW) are presented in Fig. 4.9A and 4.9B, respectively. In SD rats administered with MTX intravenous infusion (60 μ g MTX/kg BW) for two hours, a simulation curve and the observed data of % cumulative MTX in are illustrated in Fig. 4.10.

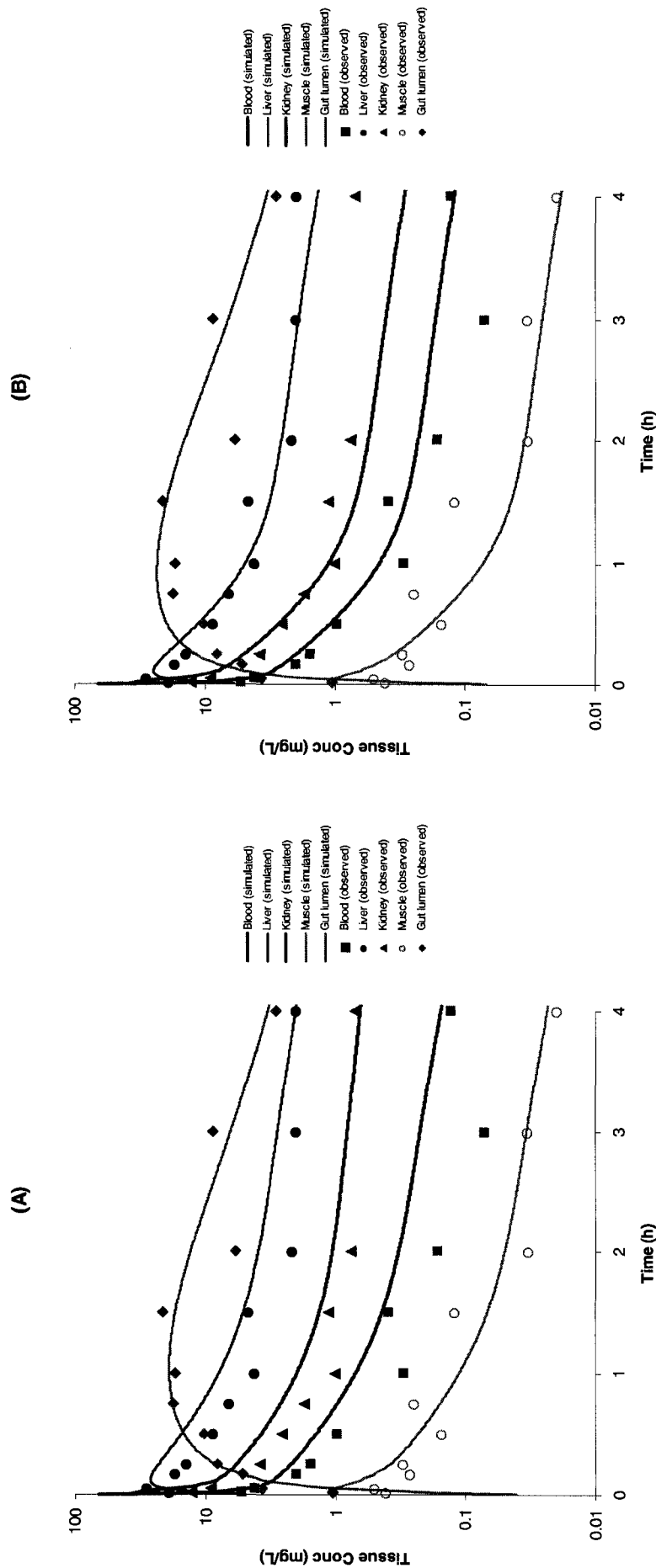


Fig. 4.2. Model simulations of tissue methotrexate (MTX) concentrations in mice administered with 3.0 mg/kg i.v. MTX from the reconstructed Bischoff et al. PBPK model (A) and from our updated PBPK model with an incorporation of MRP2-mediated excretion (B).

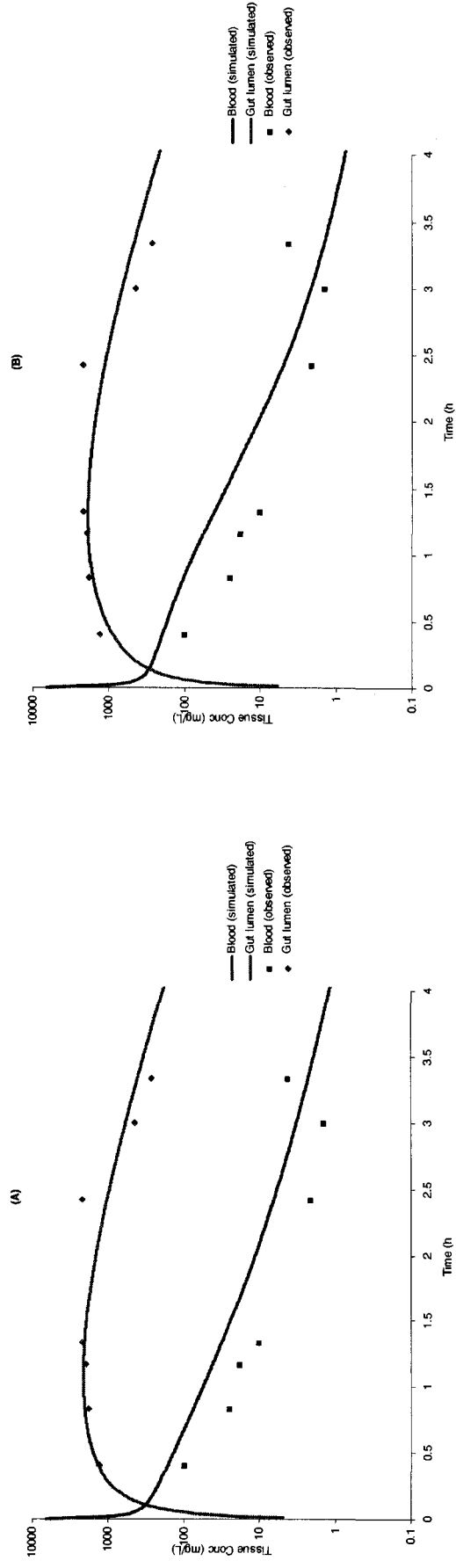


Fig. 4.3. Model simulations of tissue methotrexate (MTX) concentrations in mice administered with 300 mg/kg i.v. MTX from the reconstructed Bischoff et al. model (A) and from our updated PBPK model with an incorporation of MRP2-mediated excretion (B).

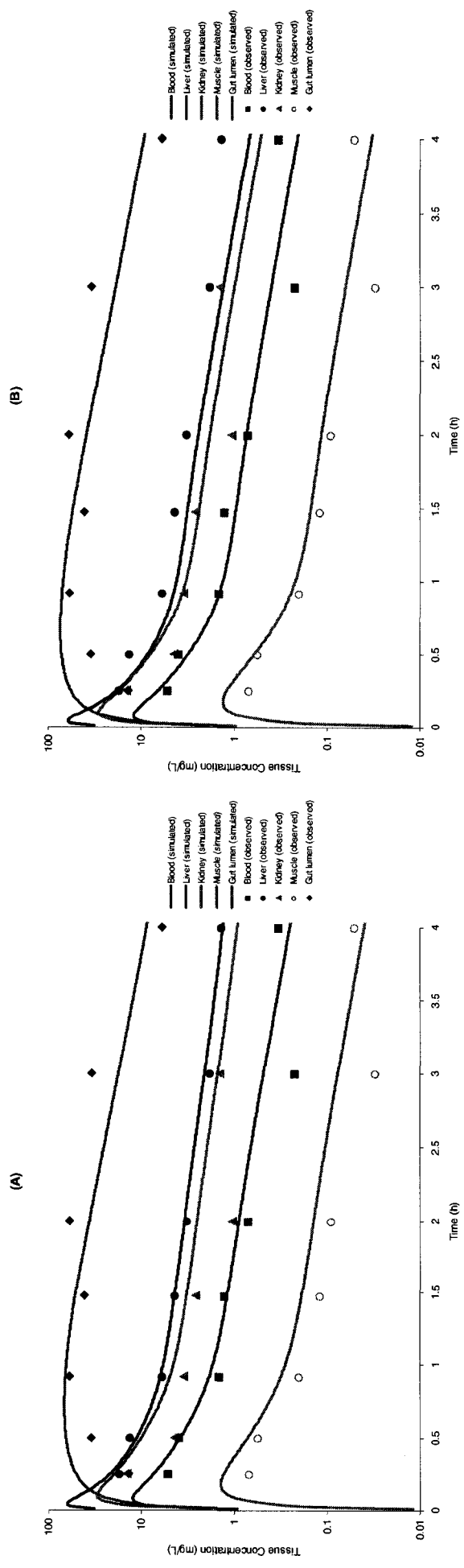


Fig. 4.4. Model simulations of tissue methotrexate (MTX) concentrations in rats administered with 6.0 mg/kg i.p. MTX from the reconstructed Bischoff et al. model (A) and from our updated PBPK model with an incorporation of MRP2-mediated excretion (B).

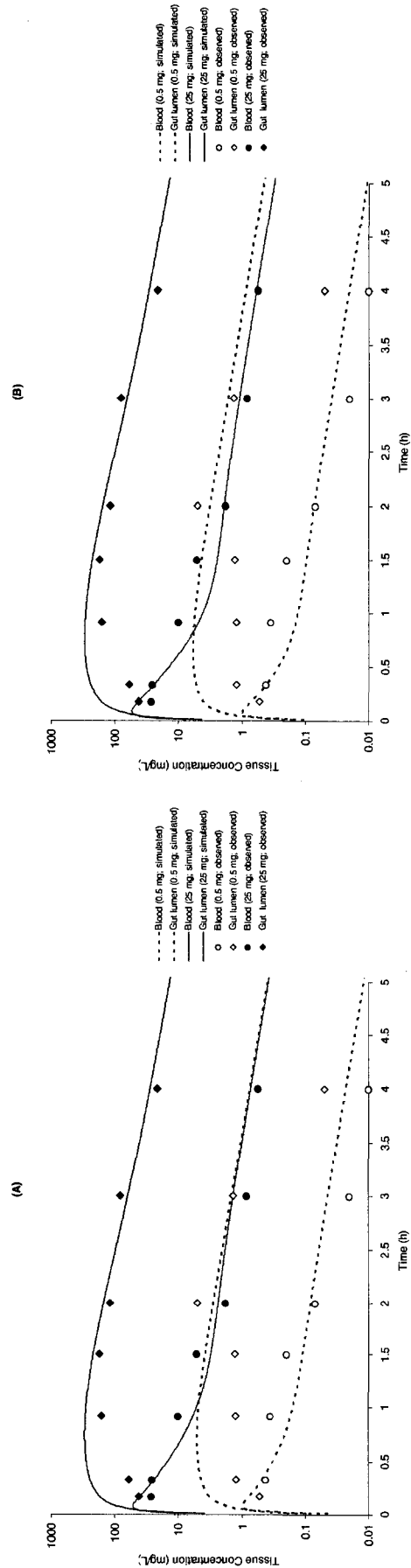


Fig. 4.5. Model simulations of tissue methotrexate (MTX) concentrations in rats administered with 0.5 and 25.0 mg/kg i.p. MTX from the reconstructed Bischoff et al. model (A) and from our updated PBPK model with an incorporation of MRP2-mediated excretion (B).

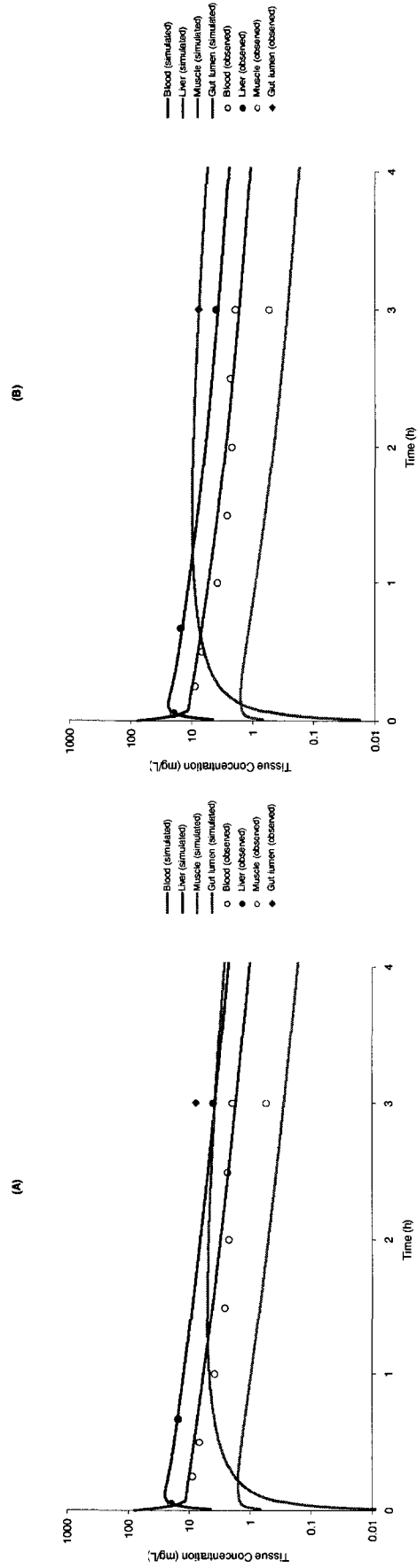


Fig. 4.6. Model simulations of tissue methotrexate (MTX) concentrations in a dog administered with 3.0 mg/kg i.v. MTX from the reconstructed Bischoff et al. model (A) and from our updated PBPK model with an incorporation of MRP2-mediated excretion (B).

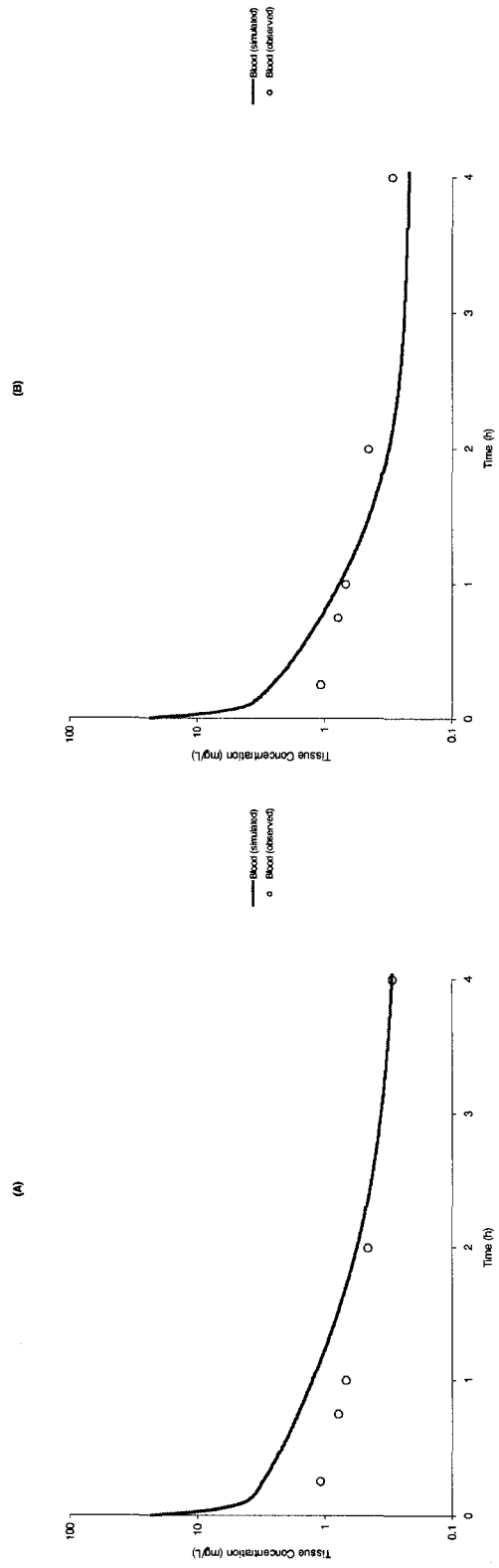


Fig. 4.7. Model simulations of tissue methotrexate (MTX) concentrations in a human administered with 1.0 mg/kg i.v. MTX from the reconstructed Bischoff et al. model (A) and from our updated PBPK model with an incorporation of MRP2-mediated excretion (B).

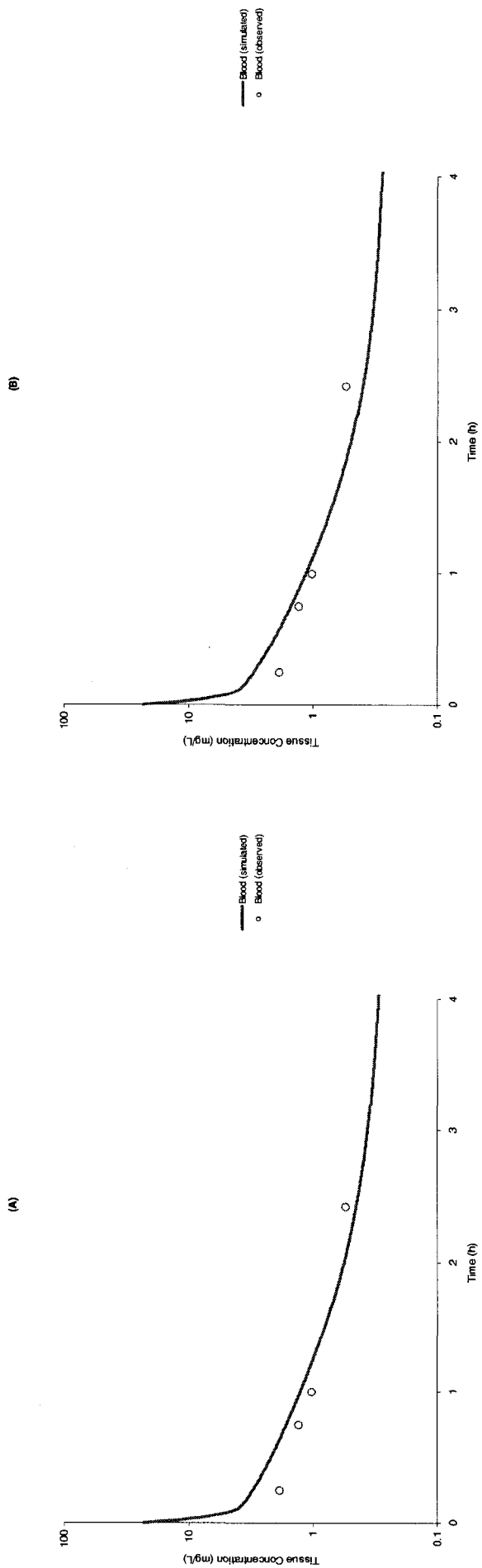


Fig. 4.8. Model simulations of tissue methotrexate (MTX) concentrations in a human administered with 1.0 mg/kg i.v. MTX from the reconstructed Bischoff et al. model (A) and from our updated PBPK model with an incorporation of Mip2-mediated excretion (B).

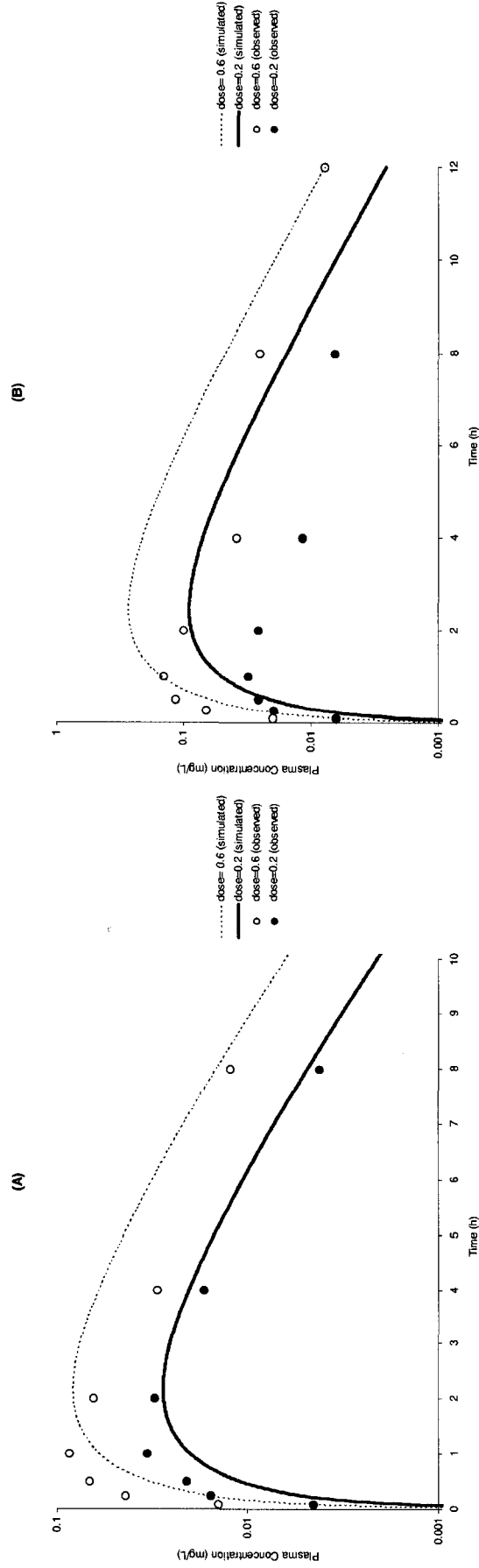


Fig. 4.9. Concentration-time courses of methotrexate (MTX) in plasma of SD rats (A) and Eisai rats (B) orally administered with 0.2 (solid line and close circles) and 0.6 mg/kg (dash line and open circles) using our updated PBPK model with an incorporation of MRP2-mediated excretion.

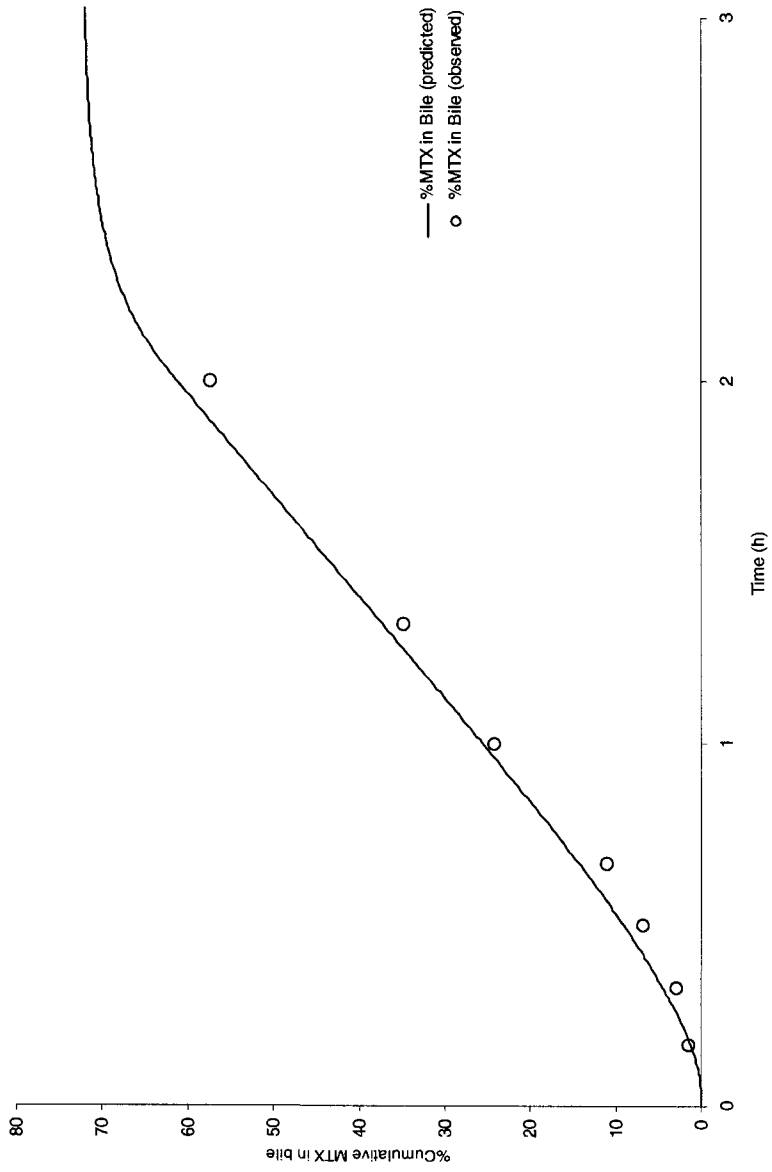


Fig. 4.10. Accumulation of methotrexate (MTX) in bile compared to administered dose in SD rats (solid line, model simulation; open circles, experimental data). Bile duct cannulation was performed in all of the animals. MTX was intravenously infused to the animals at an infusion rate of 60 μg MTX/min for 2 hours. The simulation line was an output from our updated PBPK model with an incorporation of MRP2-mediated excretion.

Table 4.2. Comparison of PBPK indices of MTX PBPK in mice, rats, dogs, and humans from the Bischoff et al. model and our updated PBPK model.

<i>Species (dosing level)</i>	PBPK Indices (Bischoff et al. model)	PBPK Indices (our updated model)
<i>Mice (3.0 mg MTX/kg BW)</i>		
Plasma	0.35	0.86
Liver	0.35	1.10
Kidney	0.34	0.95
Muscle	0.47	0.39
Gut tissue	0.83	0.61
Total	2.34	3.91
<i>Mice (300 mg MTX/kg BW)</i>		
Plasma	0.26	0.17
Gut tissue	1.71	1.79
Total	1.97	1.96
<i>Rats (6.0 mg MTX/kg BW)</i>		
Plasma	1.71	1.03
Liver	1.69	0.62
Kidney	0.34	0.59
Muscle	0.57	1.48
Gut tissue	0.50	0.44
Total	4.81	4.16
<i>Rats (25.0 mg MTX/kg BW)</i>		
Plasma	2.76	2.30
Gut tissue	0.62	0.61
Total	3.38	2.91
<i>Rats (0.5 mg MTX/kg BW)</i>		
Plasma	1.28	1.14
Gut tissue	0.51	0.43
Total	1.79	1.57
<i>Dogs (3.0 mg MTX/kg BW)</i>		
Plasma	2.84	3.82
Total	2.84	3.82
<i>Humans (1.0 mg MTX/kg BW)</i>		
Subject 1- Plasma	0.38	0.56
Subject 2- Plasma	0.90	1.00
Total	1.28	1.56
<i>All 4 species</i>		
Mice	4.31	5.87
Rats	9.98	8.65
Dogs	2.84	3.82
Humans	1.28	1.56
Total	18.41	19.90

3.3. Sensitivity Analysis

Effects of the parameters on liver concentrations of MTX are presented in Table 4.3. In rats administered with a single-dose i.p. injection (6.0 mg MTX/kg BW), PL, V_{\max} , and K_m have strong effects on the liver MTX concentrations. In comparison, QGT and QL have a weak effect on liver MTX concentrations.

In the bile duct cannulated rats administered with a continuous infusion of MTX (60 μ g MTX/kg BW/min. for 2 hours), once again, PL, V_{\max} , and K_m have the strongest effects on liver MTX concentrations. As shown in Table 4.3, while the general trend of the sensitive parameter remained unchanged, there appeared to be a time-dependence regarding the magnitude of sensitivity. For instance, at 4 hours, PL has moderate effect while V_{\max} and K_m have the strongest effects on liver MTX concentrations.

Table 4.3. Log-Normalized Sensitivity (LSP) Parameter Values for Liver Concentration of Methotrexate (MTX) Under Two Different Experimental Conditions.

<i>I.P. dose in normal rats (6.0 mg MTX/kg BW)</i>					
	Partition Coefficient	Mrp2-mediated excretion		Blood flow	
Time	PL	V_{max}	K_m	QGT	QL
0.5	1.212	-1.235	1.171	-0.071	0.078
1.0	1.127	-1.016	0.999	-0.025	-0.030
1.5	1.078	-0.823	0.817	-0.024	-0.034
2.0	1.090	-0.787	0.784	-0.033	-0.030
3.0	1.140	-0.777	0.776	-0.051	-0.033
4.0	1.186	-0.750	0.750	-0.067	-0.039

<i>I.V. infusion in rats with bile duct cannulation (60 μg MTX/min. for 2 hours)</i>					
	Partition Coefficient	Mrp2-mediated excretion		Blood flow	
Time	PL	V_{max}	K_m	QGT	QL
0.5	0.883	-0.617	0.585	0.006	0.168
1.0	0.967	-0.793	0.741	0.002	0.119
1.5	0.991	-0.851	0.791	0.001	0.109
2.0	0.998	-0.867	0.805	0.000	0.107
3.0	1.923	-2.981	2.894	-0.060	-0.318
4.0	2.700	-4.997	4.909	-0.129	-0.597

4. DISCUSSION

In this report, we present a novel and updated PBPK model of MTX. A prominent feature of this new model is the addition of a biologically relevant mode of MTX biliary excretion. It has been recognized that MTX is a substrate of Mrp2, a protein transporter, with a relatively high affinity (Hirono *et al.* 2005). By binding with this transporter protein in the liver, MTX is excreted into the bile (Han *et al.* 2001; Ito *et al.* 2001). Using a binding affinity (K_m) reported by Hirono et al (Hirono *et al.* 2005), the newly developed model can successfully describe numerous datasets obtained from mice, rats, dogs, and humans. Furthermore, the capability of the new model was extended to describe additional datasets obtained from special pharmacokinetic studies with intravenous infusion and oral dosing scenarios in bile duct-cannulated rats and Eisai hyperbilirubinemic rats.

From the sensitivity analyses, in normal rats administered with a single i.p. dose of MTX (6 mg MTX/kg BW), the partition coefficient of MTX in the livers (PL) had the strongest effect on the liver MTX concentrations while the parameters related to the Mrp2-mediated biliary secretion (V_{max} and K_m) had a moderate effect (Table 4.3). However, in the rats with a cannulated bile duct, V_{max} and K_m had the strongest effect while PL had a moderate effect on the liver MTX concentrations. In these animals, the entero-hepatic recirculation process was “by-passed”. MTX was being secreted into the bile and continually collected. Thus, there was no MTX excreted into the GI tract and none re-absorbed into the body. These results suggested a significant role of the entero-hepatic recirculation and the Mrp2-mediated biliary secretion in MTX pharmacokinetics.

In our new model, an upper GI compartment was added and served as an absorption site for MTX oral administration. Interestingly, the absorption rate constant at this particular site of the GI lumen was much higher than those of the lower GI lumen (Fig. 4.1). In some drugs with high molecular weight, such as itraconazole which has a similar molecular weight to MTX, the drug showed two distinct sites of drug absorption with two different absorption rate constants (Lohitnavy *et al.* 2005; Lohitnavy *et al.* 2006).

Another prominent feature included in this updated PBPK model was its capability in predicting of MTX concentration-time courses in EHBR. These EHBR, a mutant strain of rats deficient in Mrp2 expression, have long been used in pharmacokinetic studies revealing the significance of Mrp2 in pharmacokinetics of drugs (Chu *et al.* 1997; Sathirakul *et al.* 1993; Yamazaki *et al.* 1997). From our model simulations, for EHBR, we “turned off” the Mrp2-mediated excretion by setting the V_{\max} value to zero resulting in differences in MTX concentration-time courses when compared to their normal counterparts (Fig. 4.9A and 4.9B). In SD rats with a cannulated bile duct, MTX infusion was delivered to the animals. To simulate this experimental condition, we assumed that MTX was being excreted into the bile out of the body and there was no entero-hepatic recirculation. As shown in Fig. 4.10, The simulation results showed a good agreement with the observed data (Chen *et al.* 2003). When a simulation of this testing condition was performed in EHBR, Mrp2-mediated excretion was “turned off” resulting in no MTX recovery in the collected bile (data not shown). Taken together, these results suggested that Mrp2 may be the most predominant pathway responsible for the biliary excretion of MTX.

In our model developments, the values of V_{\max} and K_m in all four species were obtained either from the literature or from optimization processes. Interestingly, from model developments in mice, rats, dogs and humans, there were a strong linear correlation ($r^2 > 0.99$) between log body weight and log V_{\max} of Mrp2 (Fig. 4.11). Experimentally, determination of an *in vivo* maximum binding capacity (V_{\max}) of Mrp2 is difficult, therefore utilization of scaling techniques suggested by Boxenbaum (Boxenbaum 1984) may be a useful and practical methodology in approximating V_{\max} of Mrp2 of other substrates.

Since there were two datasets in humans shown in Bischoff et al. (1971) studies, we used an optimization approach to determine the values of V_{\max} and K_m of Mrp2 to fit the available datasets individually (Fig. 4.7B and 4.8B). With this approach, plasma MTX concentration-time courses in both subjects were successfully described. These results suggested that there might be interpersonal variations in Mrp2-mediated excretion of MTX in humans. Interpersonal variations (e.g. genetics, age, genders, and pathophysiological conditions) are known to affect pharmacokinetics of drugs and chemicals (Dorado *et al.* 2006; Engen *et al.* 2006; Hopkins and Martin 2006; Ribeiro and Cavaco 2006). Thus, an individual parameter optimization technique may be a useful tool in estimating the parameters affecting individual pharmacokinetics of drugs and chemicals. With this approach, individualizations of MTX dosing regimens are possible and may be applied in personal therapeutic monitoring of MTX in humans.

Recently, our group successfully developed a PBPK model of 3,3',4,4',5-pentachlorobiphenyl (PCB126) (Lohitnavy *et al.* 2007), an important environmental contaminant. In this PBPK model of PCB126, an Mrp2-mediated excretion process was

also incorporated into the liver compartment. PCB126 binds to Mrp2 with a relatively higher affinity than MTX. Thus, it is possible that, when these two chemical are concomitantly present in the body, the chemicals may competitively interact with each other at the level of hepatic Mrp2. This competitive interaction might result in changes in pharmacokinetics of PCB126 and/or MTX with possible overt toxicities of PCB126 and/or MTX. To verify this hypothesis, *in vivo* experiments involving concomitant administrations of PCB126 and MTX and the construction of a PBPK model incorporated with a pharmacokinetic interaction at the hepatic Mrp2 level are ongoing in our laboratory.

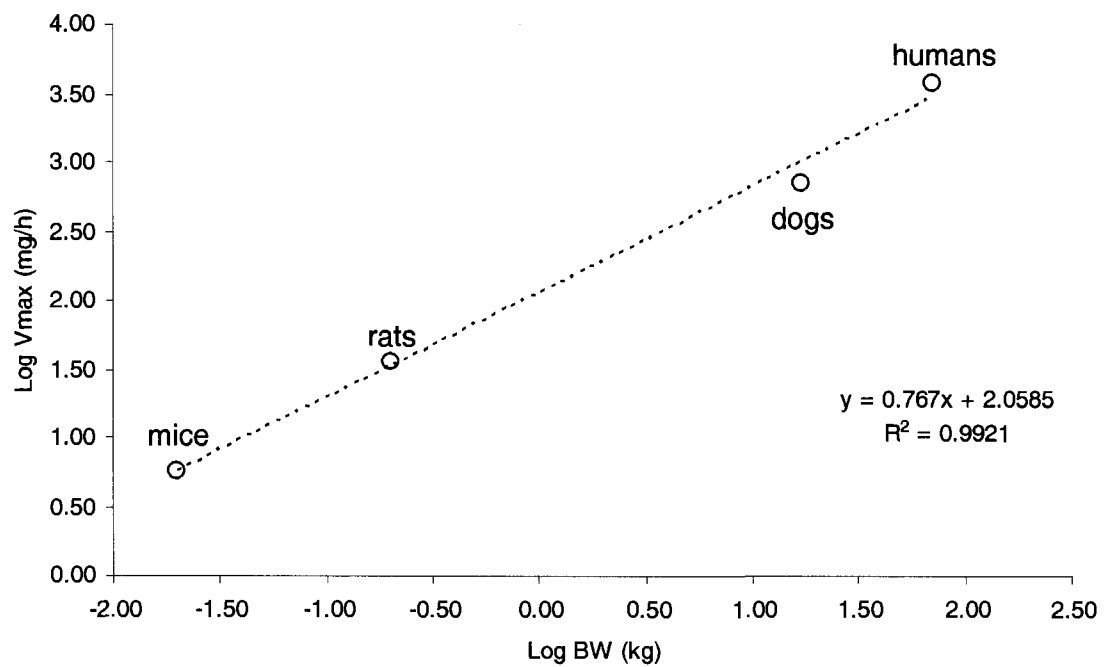


Fig. 4.11. Relationship between log V_{\max} and log body weight in mice, rats, dogs, and humans.

ACKNOWLEDGEMENT

This study is supported by the NIOSH/CDC grant 1 RO1 OH07556, and scholarships from the U.S. Fulbright Foundation and Naresuan University, Thailand. We thank our colleagues in the Quantitative and Computational Toxicology Group for their excellent technical assistance.

REFERENCES

- Bischoff, K. B., Dedrick, R. L., Zaharko, D. S., and Longstreth, J. A. (1971). Methotrexate pharmacokinetics. *J Pharm Sci* **60**, 1128-33.
- Boxenbaum, H. (1984). Interspecies pharmacokinetic scaling and the evolutionary-comparative paradigm. *Drug Metab Rev* **15**, 1071-121.
- Chen, C., Scott, D., Hanson, E., Franco, J., Berryman, E., Volberg, M., and Liu, X. (2003). Impact of Mrp2 on the biliary excretion and intestinal absorption of furosemide, probenecid, and methotrexate using Eisai hyperbilirubinemic rats. *Pharm Res* **20**, 31-7.
- Chu, X. Y., Kato, Y., Niinuma, K., Sudo, K. I., Hokusui, H., and Sugiyama, Y. (1997). Multispecific organic anion transporter is responsible for the biliary excretion of the camptothecin derivative irinotecan and its metabolites in rats. *J Pharmacol Exp Ther* **281**, 304-14.
- Clewell, H. J., 3rd, Lee, T. S., and Carpenter, R. L. (1994). Sensitivity of physiologically based pharmacokinetic models to variation in model parameters: methylene chloride. *Risk Anal* **14**, 521-31.
- Dorado, P., Berecz, R., Penas-Lledo, E. M., Caceres, M. C., and Llerena, A. (2006). Clinical implications of CYP2D6 genetic polymorphism during treatment with antipsychotic drugs. *Curr Drug Targets* **7**, 1671-80.
- Engen, R. M., Marsh, S., Van Booven, D. J., and McLeod, H. L. (2006). Ethnic differences in pharmacogenetically relevant genes. *Curr Drug Targets* **7**, 1641-8.
- Han, Y. H., Kato, Y., Haramura, M., Ohta, M., Matsuoka, H., and Sugiyama, Y. (2001). Physicochemical parameters responsible for the affinity of methotrexate analogs for rat canalicular multispecific organic anion transporter (cMOAT/MRP2). *Pharm Res* **18**, 579-86.

- Hirono, S., Nakagome, I., Imai, R., Maeda, K., Kusuhara, H., and Sugiyama, Y. (2005). Estimation of the three-dimensional pharmacophore of ligands for rat multidrug-resistance-associated protein 2 using ligand-based drug design techniques. *Pharm Res* **22**, 260-9.
- Hopkins, M. M., and Martin, P. A. (2006). Role of pharmacogenetics in the use of CNS drugs: from drug pipeline to primary care? *Expert Rev Neurother* **6**, 1765-7.
- Ito, K., Oleschuk, C. J., Westlake, C., Vasa, M. Z., Deeley, R. G., and Cole, S. P. (2001). Mutation of Trp1254 in the multispecific organic anion transporter, multidrug resistance protein 2 (MRP2) (ABCC2), alters substrate specificity and results in loss of methotrexate transport activity. *J Biol Chem* **276**, 38108-14.
- Krishnan, K., Haddad, S., and Pelekis, M. (1995). A simple index for representing the discrepancy between simulations of physiological pharmacokinetic models and experimental data. *Toxicol Ind Health* **11**, 413-22.
- Lohitnavy, M., Lohitnavy, O., Thangkeattayanon, O., and Srichai, W. (2005). Reduced oral itraconazole bioavailability by antacid suspension. *J Clin Pharm Ther* **30**, 201-6.
- Lohitnavy, M., Lu, Y., and Lohitnavy, O. (2006). A pharmacokinetic model of the gastrointestinal tract consisting of two segments can describe the concentration-time course of itraconazole. *Int J Clin Pharmacol Ther* **44**, 394-6.
- Lohitnavy, M., Lu, Y., Lohitnavy, O., Chubb, L., Hirono, S., and Yang, R. S. H. (2007). A Possible Role of Multidrug-Resistance-Associated Protein 2 (Mrp2) in Hepatic Excretion of PCB126, an Environmental Contaminant; PBPK/PD Modeling. *Toxicol Sci* (submitted).
- Naba, H., Kuwayama, C., Kakinuma, C., Ohnishi, S., and Ogihara, T. (2004). Eisai hyperbilirubinemic rat (EHBR) as an animal model affording high drug-exposure in toxicity studies on organic anions. *Drug Metab Pharmacokinet* **19**, 339-51.
- Ribeiro, V., and Cavaco, I. (2006). Pharmacogenetics of cytochromes P450 in tropical medicine. *Curr Drug Targets* **7**, 1709-19.
- Sathirakul, K., Suzuki, H., Yasuda, K., Hanano, M., Tagaya, O., Horie, T., and Sugiyama, Y. (1993). Kinetic analysis of hepatobiliary transport of organic anions in Eisai hyperbilirubinemic mutant rats. *J Pharmacol Exp Ther* **265**, 1301-12.
- Treon, S. P., and Chabner, B. A. (1996). Concepts in use of high-dose methotrexate therapy. *Clin Chem* **42**, 1322-9.
- Walker, S. E., and Ranatunga, S. K. (2006). Rheumatoid arthritis: A review. *Mo Med* **103**, 539-44.

Yamazaki, M., Akiyama, S., Ni'inuma, K., Nishigaki, R., and Sugiyama, Y. (1997).
Biliary excretion of pravastatin in rats: contribution of the excretion pathway
mediated by canalicular multispecific organic anion transporter. *Drug Metab
Dispos* **25**, 1123-9.

CHAPTER 5

Pharmacokinetic Interactions at the Level of Multidrug-Resistance-Associated Protein 2 (Mrp2) Among Methotrexate, 3,3',4,4',5-Pentachlorobiphenyl (PCB126), and Genipin in Rats: A Physiologically-Based Pharmacokinetic Model

Manupat Lohitnavy, Brad Reisfeld, Omrat Lohitnavy, Yasong Lu, Arthur N. Mayeno,

Raymond S. H. Yang

ABSTRACT

Multidrug-resistance-associated protein 2 (Mrp2) is a protein transporter responsible for biliary excretion of many xenobiotics. When Mrp2 substrates are simultaneously present in the body, pharmacokinetic interactions are possible. In this study, we investigate pharmacokinetic fate of methotrexate (MTX) with and without the influence of the co-treatment of 3,3',4,4',5-pentachlorobiphenyl (PCB126), another Mrp2 substrate, and genipin, a Mrp2 translocation enhancer. F344 rats were allocated into 4 treatment groups (MTX alone, MTX+PCB126, MTX+genipin, and MTX+PCB126+genipin). Following dosing, the animals were sacrificed and liver samples were collected at 0.5, 1, 2, 6, and 12 hours. Hepatic MTX levels were determined using HPLC-UV. When compared to the MTX alone group, significant differences in liver MTX concentration levels were observed in MTX+genipin and MTX+genipin+PCB126 group. A physiologically-based pharmacokinetic (PBPK) model incorporating a competitive inhibition process between MTX and PCB126 for hepatic Mrp2 was developed, and this model consistently simulated the concentration-time courses of MTX and PCB126 in livers. Thus, our model suggests that inhibition mechanism of MTX by PCB126 modifies MTX concentration-time courses. Application

of similar PBPK modeling approaches may be useful to quantitatively predict the pharmacokinetic interactions between other Mrp2 substrates.

1. INTRODUCTION

Pharmacokinetic interactions between drugs and chemicals from foods are well-documented and pose many potential therapeutic problems, including adverse drug reactions and possible therapeutic failures. These pharmacokinetic interactions are due to many underlying mechanisms which change the pharmacokinetics of drugs (Beique *et al.* 2007; Fujita 2004; Mallet *et al.* 2007; Singh 1999; Walubo 2007; Zhou *et al.* 2007). Many xenobiotics can affect absorption, distribution, metabolism, and excretion of other chemicals and drugs, resulting in changes in their pharmacokinetics (Beique *et al.* 2007; Brown 1993; Lohitnavy *et al.* 2005; Otagiri 2005; Walubo 2007).

Excretion of xenobiotics can be mediated through several mechanisms, one of which is biliary excretion involving hepatic transporters. This particular mechanism is responsible for the excretion of many drugs and chemicals (Petzinger and Geyer 2006; Shitara *et al.* 2006). Multidrug-resistance-associated protein 2 (Mrp2) is an ATP-binding cassette (ABC) transporter which is responsible for biliary excretion (Borst *et al.* 2006; Jedlitschky *et al.* 2006). Concurrent administrations of Mrp2 substrates can lead to changes in xenobiotics disposition. For example, a concomitant administration of two Mrp2 substrates, curcumin (a plant-derived chemical from *Curcuma longa*) and talinolol resulted in significant changes in pharmacokinetics of talinolol. The mechanism of a possible pharmacokinetic interaction at the Mrp2 level was suggested (Juan *et al.* 2007). Some other examples of the Mrp2 substrates are methotrexate (MTX) and 3,3',4,4',5-

pentachlorobiphenyl (PCB126) (Hirono *et al.* 2005; Jedlitschky *et al.* 2006; Lohitnavy *et al.* 2007b).

MTX is a dihydrofolate reductase (DHFR) inhibitor widely used in cancer treatments and rheumatoid arthritis (Treon and Chabner 1996; Walker and Ranatunga 2006). MTX exerts its pharmacological effects via an irreversible binding to DHFR resulting in its cytotoxic effects. In 1971, Bischoff *et al.* reported a physiologically-based pharmacokinetic (PBPK) model of MTX (Bischoff *et al.* 1971). This model was able to describe a variety of dose levels of MTX in several species. The original model consisted of plasma, liver, kidney, muscle, gut lumen, and gut tissue compartments. In the liver sub-compartment, MTX is excreted into bile via biliary secretion with an unknown biological entity. It was later discovered that MTX is a substrate of Mrp2 with relatively high binding affinity (Han *et al.* 2001; Hirono *et al.* 2005). Based on this novel information regarding the significant role of Mrp2 in MTX pharmacokinetics, an updated PBPK model of MTX was developed (Lohitnavy *et al.* 2007b). In this updated PBPK model of MTX, the empirical biliary excretion process was replaced by a Mrp2-mediated excretion process. The biochemical characteristics of MTX to Mrp2 as predicted by a three-dimensional quantitative structure-activity relationship (3D-QSAR) modeling approach was incorporated into the model (Hirono *et al.* 2005). This MTX PBPK model could satisfactorily describe numerous datasets from different dosing scenarios. The utility of the updated model was extended by studying MTX concentration-time courses in additional different dosing scenarios (e.g. oral dosing and continuous IV infusion), under special experimental conditions (i.e. rats with bile duct cannulation), and, in a

specific animal model (e.g. Eisai hyperbilirubinemic rats, a special strain of rats lacking Mrp2 expression) (Lohitnavy *et al.* 2007b).

PCB126, a persistent environmental contaminant, is the most toxic PCB congener and a demonstrated carcinogen. PCB126 is capable of binding with aryl hydrocarbon receptor (AhR) and exerts its toxicological effects including induction of cytochrome P450 (CYP) 1A1 and 1A2 (Safe *et al.* 1985; Safe 1994), and carcinogenic effects in several organs (i.e. liver, lung, and mouth) in rats (NTP 2006). Recently, a PBPK/PD model of PCB126 was reported (Lohitnavy *et al.* 2007a). Using a 3D-QSAR computational approach (Hirono *et al.* 2005), a Mrp2-mediated excretion process of PCB126 was identified and incorporated into the model. The PBPK/PD model could describe many pharmacokinetic datasets obtained under several different experimental conditions in different laboratories (Lohitnavy *et al.* 2007a).

Genipin, an intestinal metabolite of geniposide (a plant-derived glycoside), is known to have a strong effect on enhancing localization of Mrp2 to the liver canalicular membrane, and, thereby, enhances biliary excretion of Mrp2 substrates (Shoda *et al.* 2004). Since MTX and PCB126 are both Mrp2 substrates and genipin is able to enhance Mrp2 translocations, these three chemicals, when concomitantly presenting in the body, may alter each other's pharmacokinetic behaviors and their disposition. In this study, we specifically study MTX pharmacokinetic behaviors with and without the influence of PCB126, and/or genipin.

2. MATERIAL AND METHODS

2.1. Chemicals

MTX (98% purity) was purchased from Sigma-Aldrich (Steinheim, Germany). PCB126 (>99% purity) was purchased from AccuStandard (New Haven, CT). 2,2',4,4',5,5'-Hexachlorobiphenyl (PCB74; >98% purity) was purchased from Ultra Scientific (North Kingstown, RI) and used as an internal standard for GC analyses of PCB126. Genipin was purchased from Wako Chemicals USA, Inc. (Richmond, VA). Pentane and sulfuric acid were supplied by VWR Scientific (Denver, CO). Ethyl acetate was purchased from Fisher Scientific (Houston, TX). Florisil and anhydrous sodium sulfate drying columns were obtained from Alltech Associates (Deerfield, IL). All reagents were of analytical grade or higher.

2.2. Animals

Male F344 rats (body weight, 262-308 gm), about 30 days of age, supplied by Harlan Sprague-Dawley (Indianapolis, IN), were maintained at the Painter Center, Colorado State University. The Center is fully accredited by the American Association for Accreditation of Laboratory Animal Care. The animals were given food (Harlan Teklad NIH-07 diet; Madison, WI) and water *ad libitum*, and the lighting was set at a 12-h light/dark cycle. The study was conducted in accordance with the National Institutes of Health guidelines for the care and use of laboratory animals.

2.3. Study Design

The rats were divided into 4 treatment groups (n=15 in each group): MTX alone, MTX+PCB126, MTX+genipin, and MTX+PCB126+genipin. In the MTX alone group, the rats were orally administered with a single dose of MTX (3 mg/kg). In the

MTX+PCB126 group, the rats were orally administered with PCB126 (9.8 µg/kg/day) in corn oil 4 days prior to the MTX administration. On the fifth day of the experiment, a single oral dose of MTX (3 mg/kg) was administered to the rats. In the MTX+genipin group, genipin (10 µmole/min/kg) in normal saline was slowly infused through a tail vein for 30 minutes before MTX oral dosing. In the MTX+PCB126+genipin group, four oral doses of PCB126 (9.8 µg/kg/day) in corn oil were administered to each rat. Thirty minutes before MTX oral dosing (3 mg/kg), genipin solution (10 µmole/min/kg) in normal saline was slowly infused through a tail vein for 30 minutes. Subsequently, the animals were sacrificed at 0.5, 1.0, 2.0, 6.0, and 12.0 hours post-MTX administration (n=3 at each sacrificing time point). Liver samples were collected and stored at -80°C until chemical analyses.

2.4. Chemical Analysis

2.4.1. MTX Analysis.

A liquid-liquid extraction method and HPLC conditions were modified from the methods previously reported by Alkaysi et al (Alkaysi *et al.* 1990). In brief, liver samples (0.4-0.6 g) were weighed, added with 1 mL of water, and ground into a suspension. Then, 0.6 mL of 15% trichloroacetic and 1 mL of glacial acetic were added into the samples and mixed vigorously. Subsequently, 5 mL of ethyl acetate was added into the samples, mixed vigorously, and left standing for 12 hours. The samples were centrifuged and the organic layer was collected. The samples were extracted with 3 mL of ethyl acetate two more times, the organic layers from each sample were pooled together. The combined organic extracts were evaporated under a nitrogen stream until dryness. Then, the dried extracts were reconstituted with 300 µL of water, and 100 µL of the reconstituted

samples was injected to an HPLC system. The HPLC system consisted of an L-6200A Intelligent Pump[®], an L-4250 UV-VIS Detector[®], a D-6000 Interface[®], and an AS-2000 Autosampler[®] (Hitachi Instrument Inc., Tokyo, Japan). Mobile phase [91% ammonium acetate buffer (pH 5.0): 4.5% acetonitrile: 4.5% methanol] was delivered with an isocratic fashion at a rate of 1.3 mL/min through a C-18 Luna[®] analytical column (3 μ m, 150 x 4.60 mm; Phenomenex, Torrance, CA, USA) with a C-18 SecurityGuard[®] (4 x 3.0 mm; Phenomenex, Torrance, CA, USA). Measurement of MTX was performed at the wavelength of 305 nm and data were analyzed using D-7000 HPLC System Manager[®] (version 4.0; Hitachi Instrument Inc., Tokyo, Japan). A calibration curve of MTX extracted from liver samples constructed at a concentration range of 0-1,000 ng MTX/g liver showed linearity with $r^2 > 0.99$.

2.4.2. PCB126 Analysis

Liver samples were weighed (approximately 1.5 g/sample) and chopped and 1.5 mL of water added to each sample. Subsequently 250 ng PCB74 was added to each samples as an internal standard (I.S.), followed by 3 mL of 60% sulfuric acid, and the contents mixed vigorously. After standing overnight at room temperature for complete tissue digestion, 5 mL of pentane was added to each sample and mixed vigorously. The samples were then centrifuged at 3,200 RPM for 15 minutes at 25°C using a Centrifuge Model 5682 (Forma Scientific Inc., Marietta, OH), and the organic layer was collected. Two more extractions were carried out and the organic layers combined. To clean up the extracts, the combined organic layers were passed through a clean-up column consisting of 3.0 g anhydrous sodium sulfate and 500 mg activated florisil. The cleaned up organic extracts were evaporated under nitrogen streams to dryness. Each sample was

reconstituted with 1 mL of pentane (HPLC grade) and analyzed by gas chromatography. The % recovery of PCB126 by this extraction method is about 75%. An HP-5890 Series II Plus gas chromatograph (Hewlett Packard, Wilmington, DE) with an electron capture detector (ECD) detector was employed to analyze PCB126. An analytical capillary column (Zebron ZB-5[®]; crosslink 5% phenyl methylsilicone, 30 m x 0.53 mm x 0.5 µm film thickness, Phenomenex, Torrance, CA) protected with a guard capillary column (Zebron[®]; crosslink 5% phenyl methylsilicone, 5 m x 0.53 mm x 0.5 µm film thickness, Phenomenex, Torrance, CA) was employed. The GC temperature conditions were as follows: The initial temperature was 80°C for 3 minutes, programmed to 120°C at the rate of 15°C/min, remained at this temperature level for 5 minute, and then programmed to increase at the rate of 20°C/min to the final temperature level of 220°C. The flow rate of helium, carrier gas, and the make-up gas, nitrogen, were 5 and 80 mL/min, respectively. The temperatures of injector and detector were 250°C and 300°C, respectively. The volume of injection was 1-2 µL per sample. The concentration levels of PCB126 were quantified using an internal standard method. The retention times of PCB126 and I.S. were at 21.2 and 22.9 minutes, respectively. A calibration curve was built and fitted using a linear regression equation with linearity (r^2) > 0.99. The detection limit of the system was 0.1 ng PCB126.

2.5. PBPK Modeling of MTX Pharmacokinetics With or Without Co-Treatment of PCB126

2.5.1. Strategies in PBPK model development

PBPK models of MTX and PCB126 with an incorporation of the Mrp2-mediated excretion process were recently developed in our laboratory (Lohitnavy *et al.* 2007a;

Lohitnavy *et al.* 2007b). Individual PBPK model structures, their computer codes, and all parameters used in these two PBPK models were detailed in these publications (Lohitnavy *et al.* 2007a; Lohitnavy *et al.* 2007b). To simulate our experimental conditions in which MTX and PCB126 were concomitantly present in the animals, the two PBPK models were integrated. A schematic diagram of the PBPK model with pharmacokinetic interaction between these two chemicals is depicted in Fig. 5.1. All parameters used in the current PBPK model are summarized in Table 5.1. To describe pharmacokinetic interactions between MTX and PCB126 at Mrp2 in the liver, a Michaelis-Menten equation describing competitive inhibition behavior was incorporated into the liver sub-models for both chemicals (Haddad *et al.* 2001). The competitive inhibition equations between MTX and PCB126 at hepatic Mrp2 excretion sites were described as follows:

$$RBile_{MTX} = (V_{max, MTX} * CVL_{MTX}) / [K_{m, MTX} * (1 + CVL_{PCB126}/KIM) + CVL_{MTX}] \quad (1)$$

$$RBile_{PCB126} = (V_{max, PCB126} * CVL_{PCB126}) / [K_{m, PCB126} * (1 + CVL_{MTX}/KIP) + CVL_{PCB126}] \quad (2)$$

where $RBile_{MTX}$ and $RBile_{PCB126}$ are rates of biliary excretion of MTX and PCB126 via the Mrp2-mediated excretion processes, respectively. $V_{max, MTX}$ and $V_{max, PCB126}$ are maximal binding capacities between Mrp2 and MTX, and Mrp2 and PCB126, respectively. CVL_{MTX} and CVL_{PCB126} are concentration levels of MTX and PCB126 in venous blood in the liver, respectively. $K_{m, MTX}$ and $K_{m, PCB126}$ are binding affinities between Mrp2 and MTX and PCB126, respectively. KIM and KIP are the constants describing competitive inhibition of Mrp2-mediated excretion of MTX by PCB126 and

PCB126 by MTX, respectively. The values of KIM and KIP were estimated using optimization procedures. When PBPK modeling of MTX alone was implemented, all the commands and parameters related to PCB126 were turned off.

2.5.2. Sensitivity Analysis

Sensitivity analysis is a useful approach for identifying important parameters affecting a pharmacokinetic measurement (Clewell *et al.* 1994). Log-normalized sensitivity parameters (LSPs) were defined as follows:

$$LSP = \partial \ln R / \partial \ln x' \quad (3)$$

where R is a model output and x is the parameter for which the sensitivity is being tested. This definition quantifies the percentage change in an output value due to the percentage change in a parameter. In this study, the liver concentration of MTX and PCB126 were outputs of most concern. Thus, we examined the sensitivity of the liver concentration of MTX to the parameters related to competitive inhibition (KIM), blood flow (QGT_{MTX} and QL_{MTX}), Mrp2-mediated MTX excretion ($V_{max, MTX}$ and $K_{m, MTX}$), and partition coefficient of MTX in the liver (PL_{MTX}).

For PCB126, we examined the sensitivity of the liver concentration of PCB126 to the parameters related to competitive inhibition (KIP), AhR binding (BM_1 and KB_1), CYP1A2 binding (BM_{2O} , KB_2 and slope), Mrp2-mediated PCB126 excretion ($V_{max, PCB126}$ and $K_{m, PCB126}$), and partition coefficient of PCB126 in the liver (PL_{PCB126}).

2.5.3. Software

The model code was written and the simulations were performed using ACSL Tox[®] (version 11.8.4; Aegis Technologies Group Inc., Marietta, GA). Parameter optimizations were performed using ACSL Math[®] (version 2.5.4; Aegis Technologies

Group Inc., Marietta, GA). The sensitivity analysis and parameter optimization were carried out using ACSL Math[®] (version 2.5.4; Aegis Technologies Group Inc., Marietta, GA).

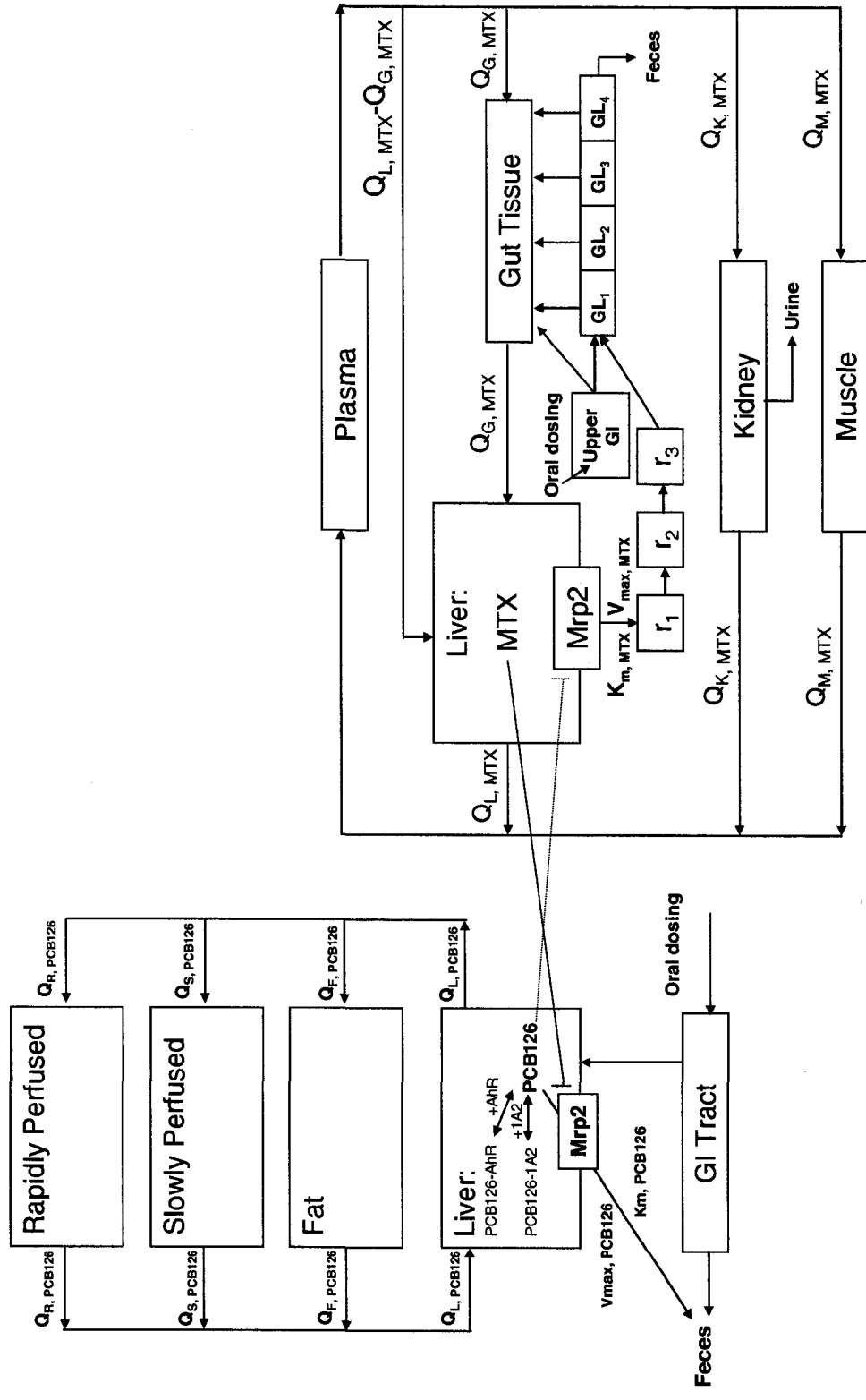


Fig. 5.1. A schematic diagram of the PBPK model structure with a description of pharmacokinetic interactions between methotrexate (MTX) and 3,3',4,4',5-pentachlorobiphenyl (PCB126). Competitive inhibition between these two Mrp2 substrates occurs at Mrp2 in the liver. The symbols (⊥) represent competitive inhibition processes, resulting from the co-presence of MTX and PCB126.

TABLE 5.1. Summary of all parameters used in the MTX-PCB126 interaction model: PCB126 Section.

Model Parameters (unit)	Abbreviations	Parameter Values
Body weight (kg)	BW	0.277
<i>Tissue volumes (or volume fractions):</i>		
Fat volume fraction	VFC _{PCB126}	0.05
Liver volume fraction	VLC _{PCB126}	0.038
Rapidly perfused (L)	VRC _{PCB126}	0.052
Slowly perfused (L)	VSC _{PCB126}	0.91 x BW - VF-VL-VB-VR
Blood volume (L)	VB _{PCB126}	0.062 x BW + 0.0012
Cardiac Output Constant (L/hr/kg)	QCC _{PCB126}	14.1
<i>Tissue plasma flow fractions:</i>		
Fat	QFC _{PCB126}	0.07
Liver	QLC _{PCB126}	0.18
Rapidly perfused	QRC _{PCB126}	0.58
Slowly perfused	QSC _{PCB126}	1.0-QFC-QLC-QRC
<i>Rate Constants:</i>		
Absorption rate constant (hr ⁻¹)	KGILV _{PCB126}	0.143
<i>Partition Coefficients:</i>		
Liver	PL _{PCB126}	8.9
Fat	PF _{PCB126}	155.0
Rapidly perfused	PR _{PCB126}	6.0
Slowly perfused	PS _{PCB126}	7.2
<i>Protein Binding:</i>		
AhR maximum (nmole/liver)	BM ₁	0.004
AhR affinity (nM)	KB ₁	0.564
1A2 Basal level (nmole/liver)	BM ₂₀	10.0
1A2 affinity (nM)	KB ₂	5.54
1A2 induction rate (nmole/hr)	slope	0.0066
<i>PCB126 Excretion via Mrp2:</i>		
Binding affinity (nM)	K _{m, PCB126}	7,760.0
Maximal binding capacity of Mrp2 (nmole/hr)	V _{max, PCB126}	64.6
<i>Competitive inhibition:</i>		
Inhibition constant of MTX by PCB126 (nM)	KIM	12.07 ^a
Inhibition constant of PCB126 by MTX (nM)	KIP	3,926.3 ^a

^a Optimized values.

TABLE 5.1(contd.) Summary of all parameters used in the MTX-PCB126 interaction model: Methotrexate Section.

Model Parameters (unit)	Abbreviations	Parameter Values
<i>Volume of Organs (L):</i>		
Plasma	VP_{MTX}	0.009
Muscle	VM_{MTX}	0.1
Kidney	VK_{MTX}	0.0019
Liver	VL_{MTX}	0.0083
Gut Tissue	VGT_{MTX}	0.011
Gut Lumen	VGL_{MTX}	0.011
<i>Blood Flow (L/hr):</i>		
Muscle	QM_{MTX}	0.18
Kidney	QK_{MTX}	0.30
Liver	QL_{MTX}	0.39
Gut tissue	QGT_{MTX}	0.318
<i>Partition Coefficients:</i>		
Muscle	PM_{MTX}	0.15
Kidney	PK_{MTX}	3.0
Liver	PL_{MTX}	3.0
Gut tissue	PGT_{MTX}	1.0
<i>Urinary excretion:</i>		
Kidney clearance (l/hr)	$CL_{Urine, MTX}$	0.066
<i>Mrp2-mediated biliary secretion:</i>		
Maximum binding capacity (nmole/hr)	$V_{max, MTX}$	79,658.5
Binding Affinity (nM)	$K_{m, MTX}$	338,834.6
<i>Absorption and GI Motility Rate Constants:</i>		
Capacity (nmole/hr)	$V_{max, GI, MTX}$	2,640.6
Affinity (nM)	$K_{m, GI, MTX}$	440,102.1
Absorption constant from the lower GI tract (hr^{-1})	$KABS_{MTX}$	0.00006
Mass transfer in lower GI (hr^{-1})	$KMASS_{MTX}$	0.6
Absorption rate constant at the upper GI (hr^{-1})	$KGILV_{MTX}$	0.05
Mass transfer from upper GI to lower segment (hr^{-1})	$KMOV_{MTX}$	0.418

3. RESULTS

Kidney weight, liver weight, and % liver weight of the animals at sacrifice in all treatment groups are summarized in Table 5.2. When compared to MTX alone group, statistical difference in absolute kidney weight was observed in MTX+PCB126+genipin group ($p<0.05$). Percent Liver weights in MTX+PCB126 and MTX+PCB126+genipin were statistically different when compared to the MTX alone group ($p<0.05$).

3.1. Effect of PCB126 and/or Genipin on Liver MTX Concentration-Time Courses

Liver concentration-time courses of MTX in rats treated with MTX alone, MTX+PCB126, MTX+genipin, and MTX+PCB126+genipin are illustrated in Fig. 5.2. At 0.5 hours, hepatic concentrations of MTX in rats treated with MTX+PCB126 and MTX+genipin were significantly lower than those in rats treated with MTX alone ($p<0.05$). At 2 hours, liver MTX concentrations in rats treated with MTX+genipin infusion were significantly lower than those in the MTX alone group ($p<0.05$). At 6 hours, in MTX+PCB126+genipin group, liver MTX concentrations were significantly decreased when compared to those in the MTX alone group ($p<0.05$). At 12 hours, in MTX+genipin, and, MTX+PCB126+genipin group, hepatic MTX concentration levels were significantly decreased when compared to the MTX alone group ($p<0.05$).

TABLE 5.2. Summary of kidney weight and liver weight of male F344 rats treated with a single oral dose of methotrexate (MTX; 3 mg/kg), with MTX and 3,3',4,4',5-pentachlorobiphenyl (PCB126; 9.8 µg/kg/day/dose for 4 doses), with MTX and genipin infusion (10 µmole/min/kg for 30 minutes before MTX dosing), and MTX with PCB126 (9.8 µg/kg/day/dose for 4 doses) and genipin infusion (10 µmole/min/kg for 30 minutes before MTX dosing). The data represent mean ± SD (n=15; at each sacrificing time point). *, significantly different from the MTX alone group ($P < 0.05$).

Treatment Group	Body weight (g)	Kidney weight (g)	Liver weight (g)	%Liver weight
MTX alone	298 ± 6	1.87 ± 0.08	10.28 ± 1.15	3.45 ± 0.33
MTX + PCB126	277 ± 7	1.87 ± 0.11	10.96 ± 0.92	4.08 ± 0.23*
MTX + genipin	278 ± 7	1.83 ± 0.09	9.85 ± 0.75	3.28 ± 0.96
MTX + PCB126 + genipin	274 ± 3 298 ± 6	1.77 ± 0.08*	10.89 ± 0.52	3.98 ± 0.18*

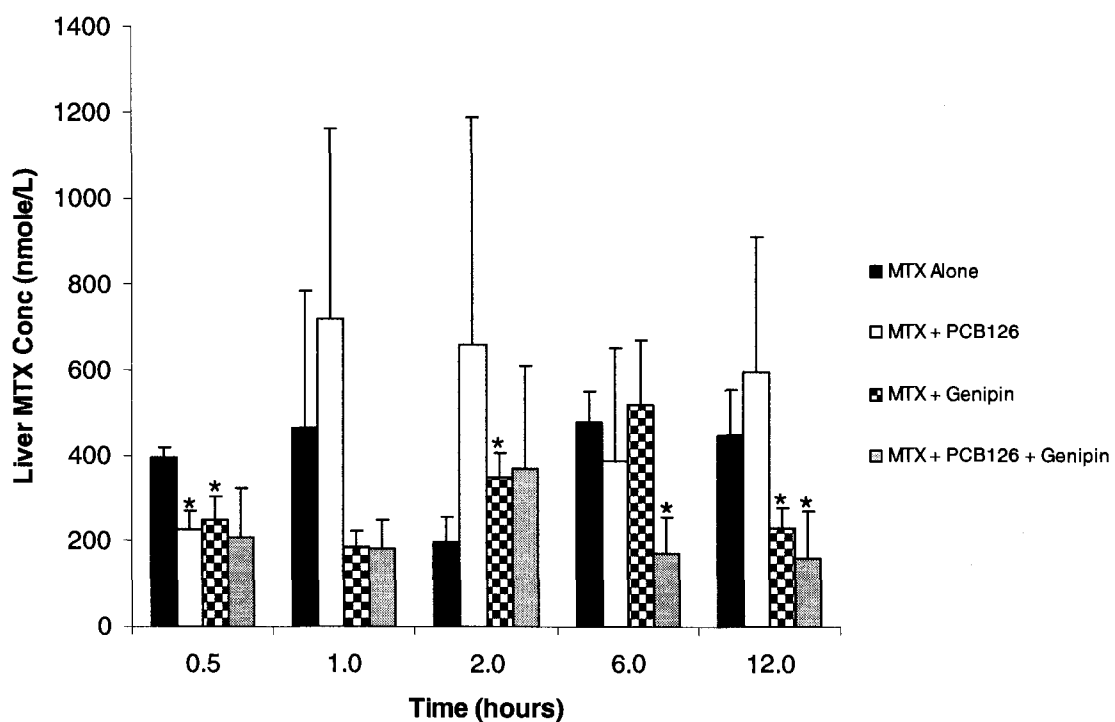


Fig. 5.2. Liver methotrexate (MTX) concentration-time courses in male F344 rats (n=3 at each sacrificing time point) treated with MTX alone (black bars), MTX+PCB126 (white bars), MTX+genipin (checker-patterned bars), and, MTX+PCB126+genipin (gray bars). The data are expressed as mean \pm S.D. *, significantly different from the MTX alone group ($P < 0.05$).

3.2. Computer Simulations of MTX and PCB126 Concentration-Time Courses in Livers of Male F344 Rats Using PBPK Modeling Approaches.

Model simulations of concentration-time courses of MTX and/or PCB126 of rats in MTX alone, MTX+PCB126, and MTX+PCB126+genipin group are illustrated in Fig. 5.3A-C. In Fig. 5.3A-C, the figures show model simulations of liver concentration-time courses of MTX and PCB126 assuming that there were pharmacokinetic interactions at hepatic Mrp2.

The PBPK model can describe our experimental data reasonably well in rats treated with MTX alone (Fig. 5.3A), in rats treated with MTX+PCB126 (Fig. 5.3B), and, in rats treated with MTX+PCB126+genipin (Fig. 5.3C). Using an optimization approach, the constants describing competitive inhibition of the Mrp2-mediated excretion of MTX by PCB126 and PCB126 by MTX (KIM and KIP) were estimated at 12.07 nmole/L and 3,926.3 nmole/L, respectively.

In MTX+PCB126+genipin group, since lowered liver MTX concentration levels were observed, we used an optimization process to estimate maximal binding capacity of MTX ($V_{\max, \text{MTX}}$) and PCB126 ($V_{\max, \text{PCB126}}$). $V_{\max, \text{MTX}}$ and $V_{\max, \text{PCB126}}$ were 144,600.0 nmole/hr and 62.6 nmole/hr, respectively. These V_{\max} values were used only in the MTX+PCB126+Genipin group. Model simulations compared to our analytical data of this experimental data are shown in Fig. 5.3C.

3.4. Sensitivity Analysis

The sensitivities of hepatic concentrations of MTX and PCB126 related to certain selected physiological parameters at various time points are summarized in Table 5.3 and

5.4, respectively. For liver MTX concentration, at 24 hours post-MTX administration, $K_{m, MTX}$, $V_{max, MTX}$, and PL_{MTX} had the largest effect on the hepatic MTX concentration, while KIM had moderate effect and QGT_{MTX} and QL_{MTX} have the weakest effect on the hepatic MTX concentration (Table 5.3).

For liver PCB126 concentration, at 24 hours post-MTX administration, BM_1 , KB_1 , BM_{20} , KB_2 and Slope have the most prominent effect on the hepatic PCB126 concentration, while $K_{m, PCB126}$, $V_{max, PCB126}$, and PL_{PCB126} have moderate effect and KIP has minimal effect on the liver PCB126 concentration (Table 5.4).

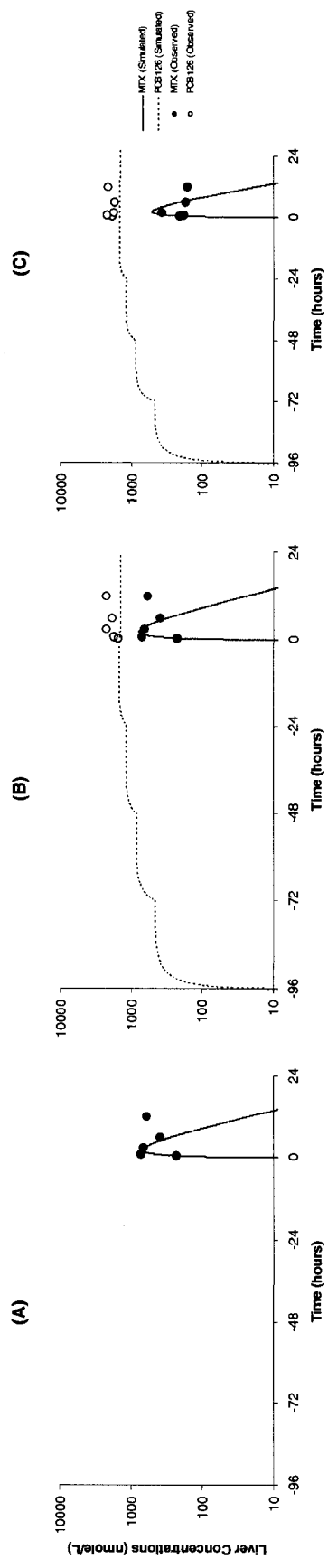


Fig. 5.3. Liver concentration time-courses of rats in MTX alone group (A), MTX+PCB126 group (B), and MTX+PCB126+genipin group (C). Liver concentration data from our current studies (MTX, closed circles; PCB126, open circles) were compared to simulation results (MTX, smooth lines; PCB126, dotted lines) using our PBPK model incorporated with competitive inhibition processes between MTX and PCB126 at the level of hepatic MRP2.

Table 5.3. Log-Normalized Sensitivity Parameter (LSP) Values for MTX Liver Concentration.

Time (hrs)	Competitive Inhibition		Mrp2-mediated Excretion		Blood Flow		Partition Coefficient
	K _{IM}	K _{m, MTX}	V _{max, MTX}	QGT _{MTX}	QL _{MTX}	PL _{MTX}	
0	0	0	0	0	0	0	0
0.5	-0.11936	0.4480	-0.4481	0.0674	-0.0776	0.8052	0.8052
1	-0.14791	0.5555	-0.5557	0.0339	-0.0526	0.8863	0.8863
2	-0.16740	0.6295	-0.6298	0.0109	-0.0417	0.9562	0.9562
4	-0.17180	0.6477	-0.6479	-0.0089	-0.0419	1.0253	1.0253
8	-0.16361	0.6201	-0.6202	-0.0326	-0.0498	1.1117	1.1117
12	-0.15567	0.5931	-0.5931	-0.0481	-0.0563	1.1684	1.1684
24	-0.14381	0.5559	-0.5559	-0.0678	-0.0652	1.2407	1.2407

Table 5.4. Log-Normalized Sensitivity Parameter (LSP) Values for PCB126 Liver Concentrations.

Time (hrs)	Competitive Inhibition		Mrp2-mediated Excretion		AhR			CYP 1A2		Partition Coefficient PL_{PCB126}
	KIP	$K_m, PCB126$	$K_m, PCB126$	$V_{max, PCB126}$	BM_1	KB_1	BM_{20}	KB_2	Slope	
-72	0	-0.0209	0.0209	0.0209	0.2265	-0.1305	0.1368	-0.3801	0.0005	0.0083
-48	0	-0.0312	0.0311	0.0311	0.2691	-0.0756	0.1600	-0.3896	0.0013	0.0113
-24	0	-0.0402	0.0402	0.0402	0.3062	-0.0550	0.1810	-0.3845	0.0022	0.0147
0	0	-0.0479	0.0479	0.0479	0.3377	-0.0438	0.1988	-0.3713	0.0033	0.0184
0.5	-0.00002	-0.0483	0.0483	0.0483	0.3378	-0.0439	0.1988	-0.3715	0.0033	0.0184
1	-0.00006	-0.0487	0.0487	0.0487	0.3378	-0.0439	0.1988	-0.3717	0.0033	0.0184
2	-0.00016	-0.0494	0.0494	0.0494	0.3379	-0.0440	0.1988	-0.3720	0.0034	0.0184
4	-0.00031	-0.0510	0.0510	0.0510	0.3381	-0.0442	0.1989	-0.3727	0.0034	0.0184
8	-0.00034	-0.0544	0.0544	0.0544	0.3385	-0.0445	0.1991	-0.3742	0.0036	0.0184
12	-0.00030	-0.0579	0.0578	0.0578	0.3390	-0.0448	0.1993	-0.3757	0.0037	0.0183
24	-0.00027	-0.0681	0.0681	0.0681	0.3403	-0.0458	0.2000	-0.3801	0.0041	0.0183

4. DISCUSSION

Our original objective was to investigate MTX pharmacokinetics with or without the influence of co-treatment of PCB126 and/or genipin. As demonstrated in the Results section, MTX liver concentrations, on a time-course basis, were affected by the presence of PCB126 and/or genipin. More detailed discussion is given below.

4.1. Effects of PCB126 and/or Genipin on Liver MTX and PCB126 Concentration

At the earlier period post-MTX oral administration, PCB126 significantly decreased liver MTX concentration levels while there was no statistical difference observed at the later time points (Fig. 5.2).

However, at the later time points, on a time-course basis, liver MTX levels in the MTX+PCB126 group was slightly higher than those in the MTX alone group (Fig. 5.2). It is possible that, with a higher binding affinity to Mrp2 compared to MTX, PCB126 preferentially bound to Mrp2 and, thereby, inhibited the Mrp2-mediated excretion process of MTX, resulting in the changes of MTX concentration levels in the livers. However, when MTX was continuously excreted into the GI lumen via the Mrp2 biliary excretion process, it could be reabsorbed into the body. Thus, the competitive inhibition effect of PCB126 on the hepatic transporter became less pronounced in the later time points.

Interestingly, in the MTX+PCB126+genipin group, at 6.0 and 12.0 hours, MTX concentration levels were statistically lowered than those in MTX alone group, while, in the MTX+genipin group, lower hepatic MTX concentration levels were observed at 12.0 hours only. These results suggest that, with the co-administration of PCB126, genipin could enhance biliary excretion of MTX. This facilitating effect of PCB126 in lowering

hepatic MTX concentration levels may be due to an Mrp2 induction effect of PCB126 (Maher *et al.* 2005). It is plausible that, in the MTX+PCB126 group, although PCB126 can induce the total expression of hepatic Mrp2, it may not increase the Mrp2 levels at liver canalicular membrane. Once genipin, an Mrp2 translocation enhancer, was concomitantly administered, it enhanced the Mrp2 translocation process, thereby increasing Mrp2 levels at the excretion site and resulting in lowered hepatic MTX concentration levels.

Mechanistically, genipin can increase the presence of Mrp2 at the liver canalicular membrane (Shoda *et al.* 2004). For instance, at 2.0 hours, the hepatic concentration levels of PCB126 in rats in the MTX+PCB126 group and in the MTX+PCB126+genipin were 742.6 ± 31.2 and 576.5 ± 78.3 ng/g ($p=0.071$), respectively. Thus, it is possible that genipin could increase the excretion of PCB126 and might be useful as an antidote for such competitive inhibitors as PCB126 or other Mrp2 substrates. In MTX+PCB126+genipin group, liver MTX concentration levels were decreased significantly (Fig. 5.2). These results suggest that there may be an increase in Mrp2-mediated excretion of MTX, resulting from co-administration of PCB126 and genipin. Using the optimization process, the V_{max} values of Mrp2 to PCB126 and MTX were increased from 79,658.5 and 64.6 nmole/hr in the MTX+PCB126 group to 144,600.0 and 62.6 nmole/hr in the MTX+PCB126+genipin group, respectively. These findings also support our hypothesis that genipin and PCB126 could synergistically increase expression of Mrp2 at the canalicular membrane of the livers. To verify this hypothesis, additional pharmacokinetic studies with a larger sample size and a longer infusion period of genipin or higher administered dose of genipin will be necessary.

4.2. PBPK Modeling of MTX and PCB126 with Competitive Inhibitions at the Level of Hepatic Mrp2.

In this paper, for the first time, we presented a quantitative computational approach in predicting a drug-pollutant pharmacokinetic interaction. Using a PBPK model with competitive inhibition incorporated for hepatic Mrp2, our simulation results were closed to the liver concentration-time courses of MTX and PCB126 (Fig. 5.3B).

The present study illustrates that, a PBPK modeling approach which incorporates mechanistic information such as the Mrp2-mediated excretion process may quantitatively predict pharmacokinetic interactions between a therapeutic agent and any chemical sharing the same pharmacokinetic machinery in their absorption, distribution, excretion, and metabolism. This approach may be useful in predictions of therapeutic or possible adverse outcomes of drug-drug or drug-chemical interactions.

ACKNOWLEDGEMENT

This study is supported by the NIOSH/CDC grant 1 RO1 OH07556, NIEHS Training Grant 1 T32 ES 07321, and scholarships from U.S. Fulbright Foundation and Naresuan University, Thailand. We thank our colleagues in the Quantitative and Computational Toxicology Group for their excellent technical assistance.

REFERENCES

- Alkaysi, H. N., Gharaibeh, A. M., and Salem, M. A. (1990). High-performance liquid chromatographic determination of methotrexate in plasma. *Ther Drug Monit* **12**, 191-4.
- Beique, L., Giguere, P., la Porte, C., and Angel, J. (2007). Interactions between protease inhibitors and acid-reducing agents: a systematic review. *HIV Med* **8**, 335-45.
- Bischoff, K. B., Dedrick, R. L., Zaharko, D. S., and Longstreth, J. A. (1971). Methotrexate pharmacokinetics. *J Pharm Sci* **60**, 1128-33.
- Borst, P., Zelcer, N., and van de Wetering, K. (2006). MRP2 and 3 in health and disease. *Cancer Lett* **234**, 51-61.
- Brown, G. R. (1993). Cephalosporin-probenecid drug interactions. *Clin Pharmacokinet* **24**, 289-300.
- Clewell, H. J., 3rd, Lee, T. S., and Carpenter, R. L. (1994). Sensitivity of physiologically based pharmacokinetic models to variation in model parameters: methylene chloride. *Risk Anal* **14**, 521-31.
- Fujita, K. (2004). Food-drug interactions via human cytochrome P450 3A (CYP3A). *Drug Metabol Drug Interact* **20**, 195-217.
- Haddad, S., Beliveau, M., Tardif, R., and Krishnan, K. (2001). A PBPK modeling-based approach to account for interactions in the health risk assessment of chemical mixtures. *Toxicol Sci* **63**, 125-31.
- Han, Y. H., Kato, Y., Haramura, M., Ohta, M., Matsuoka, H., and Sugiyama, Y. (2001). Physicochemical parameters responsible for the affinity of methotrexate analogs for rat canalicular multispecific organic anion transporter (cMOAT/MRP2). *Pharm Res* **18**, 579-86.

- Hirono, S., Nakagome, I., Imai, R., Maeda, K., Kusuhara, H., and Sugiyama, Y. (2005). Estimation of the three-dimensional pharmacophore of ligands for rat multidrug-resistance-associated protein 2 using ligand-based drug design techniques. *Pharm Res* **22**, 260-9.
- Jedlitschky, G., Hoffmann, U., and Kroemer, H. K. (2006). Structure and function of the MRP2 (ABCC2) protein and its role in drug disposition. *Expert Opin Drug Metab Toxicol* **2**, 351-66.
- Juan, H., Terhaag, B., Cong, Z., Bi-Kui, Z., Rong-Hua, Z., Feng, W., Fen-Li, S., Juan, S., Jing, T., and Wen-Xing, P. (2007). Unexpected effect of concomitantly administered curcumin on the pharmacokinetics of talinolol in healthy Chinese volunteers. *Eur J Clin Pharmacol* **63**, 663-668.
- Lohitnavy, M., Lohitnavy, O., Thangkeattiyanon, O., and Srichai, W. (2005). Reduced oral itraconazole bioavailability by antacid suspension. *J Clin Pharm Ther* **30**, 201-6.
- Lohitnavy, M., Lu, Y., Lohitnavy, O., Chubb, L., Hirono, S., and Yang, R. S. H. (2007a). A Possible Role of Multidrug-Resistance-Associated Protein 2 (Mrp2) in Hepatic Excretion of PCB126, an Environmental Contaminant; PBPK/PD Modeling. *Toxicol Sci* (submitted).
- Lohitnavy, M., Lu, Y., Lohitnavy, O., Lyons, M. A., and Yang, R. S. H. (2007b). A Novel Physiologically-Based Pharmacokinetic Model of Methotrexate with an Incorporation of Hepatic Excretion via Multidrug-Resistance-Associated Protein 2 (Mrp2) in Mice, Rats, Dogs, and Humans. *J Pharm Sci* (submitted).
- Maher, J. M., Cheng, X., Slitt, A. L., Dieter, M. Z., and Klaassen, C. D. (2005). Induction of the multidrug resistance-associated protein family of transporters by chemical activators of receptor-mediated pathways in mouse liver. *Drug Metab Dispos* **33**, 956-62.
- Mallet, L., Spinewine, A., and Huang, A. (2007). The challenge of managing drug interactions in elderly people. *Lancet* **370**, 185-91.
- NTP (2006). NTP toxicology and carcinogenesis studies of 3,3',4,4',5-pentachlorobiphenyl (PCB 126) (CAS No. 57465-28-8) in female Harlan Sprague-Dawley rats (Gavage Studies). *Natl Toxicol Program Tech Rep Ser*, 4-246.
- Otagiri, M. (2005). A molecular functional study on the interactions of drugs with plasma proteins. *Drug Metab Pharmacokinet* **20**, 309-23.
- Petzinger, E., and Geyer, J. (2006). Drug transporters in pharmacokinetics. *Naunyn Schmiedebergs Arch Pharmacol* **372**, 465-75.

- Safe, S., Bandiera, S., Sawyer, T., Robertson, L., Safe, L., Parkinson, A., Thomas, P. E., Ryan, D. E., Reik, L. M., Levin, W., and et al. (1985). PCBs: structure-function relationships and mechanism of action. *Environ Health Perspect* **60**, 47-56.
- Safe, S. H. (1994). Polychlorinated biphenyls (PCBs): environmental impact, biochemical and toxic responses, and implications for risk assessment. *Crit Rev Toxicol* **24**, 87-149.
- Shitara, Y., Horie, T., and Sugiyama, Y. (2006). Transporters as a determinant of drug clearance and tissue distribution. *Eur J Pharm Sci* **27**, 425-46.
- Shoda, J., Miura, T., Utsunomiya, H., Oda, K., Yamamoto, M., Kano, M., Ikegami, T., Tanaka, N., Akita, H., Ito, K., Suzuki, H., and Sugiyama, Y. (2004). Genipin enhances Mrp2 (Abcc2)-mediated bile formation and organic anion transport in rat liver. *Hepatology* **39**, 167-78.
- Singh, B. N. (1999). Effects of food on clinical pharmacokinetics. *Clin Pharmacokinet* **37**, 213-55.
- Treon, S. P., and Chabner, B. A. (1996). Concepts in use of high-dose methotrexate therapy. *Clin Chem* **42**, 1322-9.
- Walker, S. E., and Ranatunga, S. K. (2006). Rheumatoid arthritis: A review. *Mo Med* **103**, 539-44.
- Walubo, A. (2007). The role of cytochrome P450 in antiretroviral drug interactions. *Expert Opin Drug Metab Toxicol* **3**, 583-98.
- Zhou, S. F., Zhou, Z. W., Li, C. G., Chen, X., Yu, X., Xue, C. C., and Herington, A. (2007). Identification of drugs that interact with herbs in drug development. *Drug Discov Today* **12**, 664-73.

CHAPTER 6

Overall Summary and Future Directions

Manupat Lohitnavy

1. DISSERTATION SUMMARY

Our Quantitative and Computational Toxicology Group has been developing a number of physiologically-based pharmacokinetic (PBPK) models of chemicals and chemical mixtures. These collective efforts have led to a deeper understanding of their pharmacokinetics and disposition (Belfiore *et al.* 2007; Dennison *et al.* 2004; Dennison *et al.* 2003; Dennison *et al.* 2005; Dobrev *et al.* 2001, 2002; Lee *et al.* 2007; Lee *et al.* 2002; Lu *et al.* 2006). In addition, our group has also been investigating carcinogenic potential of chemicals and chemical mixtures using our modified medium-term liver bioassay protocol (Dean *et al.* 2002; Gustafson *et al.* 1998; Gustafson *et al.* 2000; Lohitnavy *et al.* 2004; Lu *et al.* 2007; Ou *et al.* 2003; Ou *et al.* 2001). To predict liver foci development, we used the data from the liver foci bioassay studies, and successfully incorporated those into clonal growth models (Lu *et al.* 2007; Ou *et al.* 2003; Ou *et al.* 2001). More recently, our efforts have been continued in a project, Physiologically-based Pharmacokinetics and Clonal Growth Modeling: Predicting Cancer Potential of Chemical Mixtures. This project involves collecting tissue concentration-time course and liver glutathione-S-transferase placental form positive (GSTP⁺) foci data for 3,3',4,4',5-pentachlorobiphenyl (PCB126), hexachlorobenzene (HCB), arsenic, and their binary and ternary.

As part of the project, this dissertation research focused on: 1) PCB126 pharmacokinetics; 2) carcinogenic potential of PCB126 predicted by liver GSTP⁺ foci

development, and; 3) the role of multidrug-resistance-associated protein 2 (Mrp2), a versatile protein transporter, in PCB126 pharmacokinetics and disposition, and possible pharmacokinetic interactions between PCB126 and other Mrp2 substrates. These results are summarized as follows:

1.1. Pharmacokinetics of PCB126: A Possible Role of Mrp2

To study the pharmacokinetics of an environmental carcinogen like PCB126, experimental dose levels should mimic environmental concentrations. Few PCB126 pharmacokinetic studies have been published, thus, detailed information regarding absorption, distribution, metabolism and excretion of PCB126 was limited.

However, there were some tissue PCB126 concentration data available (Chu 1994; Dean *et al.* 2002; Fisher *et al.* 2006; Lohitnavy *et al.* 2004; NTP 2006). PCB126 was primarily found in liver (Chu 1994; Dean *et al.* 2002). In our own modified medium-term liver foci bioassay, preferential distribution of PCB126 in liver (110-400X higher than fat) was observed (Lohitnavy *et al.* 2004). In addition, despite high lipophilicity, fairly rapid achievement of a steady state was noted (Lohitnavy *et al.* 2004; NTP 2006). From these data, we suspected that not only is there binding between PCB126 and hepatic proteins, but there is also an efficient system responsible for PCB126 excretion.

The first PBPK model of PCB126 was recently reported (NTP 2006). A single-dose pharmacokinetic study and a 2-year repeated dose study were conducted and PCB126 concentration-time courses in tissues were shown. From these available tissue concentration-time course data, a PBPK model of PCB126 was developed (NTP 2006). The feature of the model was incorporation of liver protein binding between PCB126 and two hepatic proteins, aromatic hydrocarbon receptor (AhR) and cytochrome P450 1A2

(CYP1A2). However, the model could not accurately describe the experimental data (NTP 2006).

A three-dimensional quantitative structure-activity relationship (3D-QSAR) model of rat Mrp2 was also reported (Hirono *et al.* 2005). Through personal communications with the corresponding author, using the Hirono *et al.* 3D-QSAR model, PCB126 was predicted to be an Mrp2 substrate with a fairly high binding affinity (K_m) value compared to other Mrp2 substrates (Hirono *et al.* 2005; Lohitnavy *et al.* 2007b). With this novel information regarding the significant role of Mrp2 in PCB126 pharmacokinetics, we incorporated a Mrp2-mediated excretion process into our PBPK model of PCB126 (Lohitnavy *et al.* 2007b). The new PBPK model of PCB126 could successfully describe numerous tissue concentration-time courses including the NTP single-dose study (NTP 2006), the NTP 2-year repeated-dose study (NTP 2006), a single-dose study reported by Fisher *et al.* (Fisher *et al.* 2006) and our medium-term liver foci study (Lohitnavy *et al.* 2004). Our PBPK model, for the first time, revealed a major role of Mrp2 in PCB126 disposition.

In addition, we extended the utility of our PCB126 PBPK model to further predict an appropriate internal dose surrogate [i.e. area under the curve of PCB126 in liver (AUC_{Liver})] (Lohitnavy *et al.* 2007b). With this PBPK/PD model, correlation between the AUC_{Liver} and our liver GSTP⁺ foci development data was demonstrated.

1.2. Carcinogenic Potential of PCB126, HCB and Their Mixture

From several clonal growth models, it was hypothesized that there are at least two populations of preneoplastic cells (Conolly and Andersen 1997; Conolly and Kimbell 1994; Lu *et al.* 2007; Ou *et al.* 2003; Ou *et al.* 2001; Thomas *et al.* 2000). These hypothetical cells, namely A and B cells, have different growth characteristics where B cells eventually gain growth advantages and progressively transform to malignancy. To prove the existence of A and B cells among liver GSTP⁺ foci, we conducted an experiment by exposing F344 male rats to PCB126, HCB and their mixture for up to 6 months (Lohitnavy *et al.* 2007a). Liver GSTP⁺, transforming growth factor- α ⁺ (TGF α ⁺) and transforming growth factor- β Type 2 receptor⁻ (TGF β 2Rc⁻) foci development were investigated (Lohitnavy *et al.* 2007a). In rats treated with PCB126, time-dependent changes in all of these biomarkers for carcinogenicity were observed (Lohitnavy *et al.* 2007a). Interestingly, when the GSTP⁺ foci were categorized into four phenotypic groups based on their TGF α and TGF β 2Rc expression, GSTP⁺ foci with TGF α expression and absence of TGF β 2Rc expression (G⁺/ α ⁺/ β ⁻ phenotype) had significantly higher hepatocyte division rates than those of GSTP⁺ foci without TGF α expression and with TGF β 2Rc expression (G⁺/ α ⁻/ β ⁺ phenotype) (Lohitnavy *et al.* 2007a). These results provided the first experimental evidence suggesting that there are at least four different subpopulations among these liver GSTP⁺ foci.

1.3. Pharmacokinetic Interactions between PCB126 and Other Mrp2 Substrates

Since PCB126 is a Mrp2 substrate with a relatively high K_m value compared to other Mrp2 substrates (Hirono *et al.* 2005; Lohitnavy *et al.* 2007b), we hypothesized that when PCB126 and another Mrp2 substrate are concomitantly present in the body,

PCB126 can interact with the Mrp2 substrate resulting in changes in their concentration-time courses. To prove this hypothesis, we conducted an *in vivo* pharmacokinetic interaction study. We exposed F344 male rats to multiple oral doses of PCB126. Subsequently, the rats were exposed to a single oral dose of methotrexate (MTX), a known Mrp2 substrate. The rats were sacrificed at specified time points, and livers were harvested. Liver concentration levels of PCB126 and MTX were determined.

To quantitatively describe pharmacokinetic interactions between these two Mrp2 substrates, a modified version of MTX PBPK model incorporated with hepatic Mrp2-mediated excretion process was developed (Lohitnavy *et al.* 2007c). This PBPK model was modified from the original MTX PBPK model (Bischoff *et al.* 1971). In our reconstructed Bischoff *et al.* model, an empirical biliary MTX clearance was assumed. In our updated PBPK model of MTX, that biliary clearance was replaced by the Mrp2-mediated excretion process (Lohitnavy *et al.* 2007c). The binding affinity (K_m) value of MTX was a reported value from the Hirono *et al.* (2005) paper (Hirono *et al.* 2005; Lohitnavy *et al.* 2007b). Our new MTX PBPK model was able to describe a number of datasets obtained from several species in different experimental conditions.

We utilized this novel MTX PBPK model and our PCB126 PBPK/PD model (Lohitnavy *et al.* 2007b; Lohitnavy *et al.* 2007c). We hypothesized that competitive inhibition between PCB126 and MTX occurs at the hepatic Mrp2 (Lohitnavy *et al.* 2007d). Thus, the two existing PBPK models of PCB126 and MTX were integrated with two equations describing competitive inhibition processes between the two Mrp2 substrates in liver (Haddad *et al.* 2001; Lohitnavy *et al.* 2007b; Lohitnavy *et al.* 2007c).

Our experimental results demonstrated that the concomitant presence of hepatic PCB126 could increase liver MTX concentration levels (Lohitnavy *et al.* 2007d). Furthermore, computer simulation results from the extended PBPK model could describe our experimental data for both chemicals in liver samples (Lohitnavy *et al.* 2007d). These results not only supported the previous *in silico* predictions from the 3D-QSAR model that PCB126 is an Mrp2 substrate (Hirono *et al.* 2005; Lohitnavy *et al.* 2007b), but they also suggested that PCB126 can significantly affect pharmacokinetics and disposition of other Mrp2 substrates due to the relatively high affinity binding of PCB126 to the liver Mrp2 (Hirono *et al.* 2005; Lohitnavy *et al.* 2007b; Lohitnavy *et al.* 2007d).

In summary, these research works provided a better understanding of pharmacokinetics of PCB126 and its effects on liver foci formations. The prediction from the Hirono *et al.* 3D-QSAR model resulted in a successful development of the PCB126 PBPK model. The insight into pharmacokinetics of PCB126 and the roles of Mrp2 in PCB126 disposition led us to the development of the pharmacokinetic interaction model between PCB126 and MTX. The integrated PBPK model with the mathematical descriptions of the competitive inhibition processes provided us a computational tool in quantitative predictions of pharmacokinetic interactions between the two Mrp2 substrates. Pharmacodynamically, PCB126 could significantly increase in liver GSTP⁺, TGFα⁺ and TGFβIIIRc⁻ foci. Furthermore GSTP⁺ foci could be differentiated into four groups based on their surface protein expressions with different growth characteristics.

2. FUTURE DIRECTIONS

Some issues were not addressed in this dissertation yet deserve future study:

2.1. Merging between PBPK Modeling and Clonal Growth Modeling

From our PBPK/PD model of PCB126, using a selected internal dose metric (i.e. AUC_{Liver}), the model could successfully describe the liver foci data (Lohitnavy *et al.* 2007b). Thus, it is possible to incorporate this model into a clonal growth model to describe liver foci development data in rats treated with PCB126.

2.2. Incorporation of the Experimental Data Regarding the Different Growth Characteristics of A and B Cells into Clonal Growth Modeling

Recently a clonal growth model describing liver GSTP⁺ foci development in rats treated with PCB126, HCB and their mixture was reported (Lu *et al.* 2007). In this paper, the author used an optimization technique to estimate growth and death rate of the liver foci. Thus, it is possible to incorporate our novel experimental data regarding different growth characteristics in different types of the GSTP⁺ foci into this existing clonal growth model.

2.3. Isolation and Characterization of A and B Cells

From our findings, in rats treated with PCB126, liver GSTP⁺ foci could be classified into four different phenotypes (Lohitnavy *et al.* 2007a). These foci with different surface protein expressions had different growth characteristics. Selective isolation of hepatocytes (Berry and Friend 1969; Berry *et al.* 1992; Berry and Phillips 2000) from these specific GSTP⁺ foci may allow us to directly study their growth characteristics and their roles in chemical carcinogenesis. Since GSTP is an intracellular enzyme responsible for cellular protection against oxidative insults, some chemicals (e.g. ethacrynic acid) were used to selectively eliminate non-GSTP expressing cells (Stenius *et al.* 1994). In addition, since both TGF α and TGF β 2Rc are membrane-presenting proteins (Kumar *et al.* 1995; Shi and Massague 2003), specific isolations using antigen-coated

immunomagnetic cell isolation techniques may be useful in an isolation of the specific subsets of GSTP⁺ hepatocytes (Arza *et al.* 2001; Safarik and Safarikova 1999; Tai *et al.* 2000). Selective isolation may be useful for further characterizations of these cells and their roles in chemical carcinogenesis.

2.4. Pharmacokinetic Interactions among Mrp2 Substrates: A Possible Role of PBPK Modeling in Quantitative Predictions.

Pharmacokinetic interactions between drugs resulting in adverse effects and therapeutic failures are well-documented (Beique *et al.* 2007; Fujita 2004; Mallet *et al.* 2007; Singh 1999; Walubo 2007; Zhou *et al.* 2007). All four key pharmacokinetic processes including absorption, distribution, metabolism and excretion can play a major role in such changes (Beique *et al.* 2007; Brown 1993; Lohitnavy *et al.* 2005; Otagiri 2005; Walubo 2007). However, despite extensive evidences published in the literature, drug-drug/drug-chemical interactions can not be quantitatively predicted.

PBPK modeling is a computational tool with the ability to incorporate any mathematical description of a biological process into models. These also include the processes involving pharmacokinetic interactions (e.g. a competitive inhibition at a key metabolic enzyme) (Dobrev *et al.* 2001, 2002; Haddad *et al.* 2001). However, this particular technique has been used primarily in toxicological applications, not in pharmacological and therapeutic purposes.

Our integrated PBPK model between PCB126 and MTX (Lohitnavy *et al.* 2007d) is the first PBPK model that could quantitatively describe pharmacokinetic interactions between PCB126, an important persistent contaminant, and MTX, an antineoplastic drug widely used in many cancer treatments. In this PBPK model, the putative site of

pharmacokinetic interactions was at the hepatic Mrp2, a protein transporter responsible for disposition of numerous substrates (Hirono *et al.* 2005; Jedlitschky *et al.* 2006). The model included mathematical descriptions of competitive inhibition processes between the two chemicals at the liver Mrp2. This model demonstrates the ability to quantitatively predict pharmacokinetic interactions between two Mrp2 substrates. Thus, with the availability of 3D-QSAR of Mrp2 (Hirono *et al.* 2005) along with the versatility of PBPK modeling approach (Andersen 1995; Belfiore *et al.* 2007; Bischoff *et al.* 1971; Dennison *et al.* 2004; Dennison *et al.* 2005; Dobrev *et al.* 2002; Lee *et al.* 2007; Lee *et al.* 2002; Lohitnavy *et al.* 2007b; Lohitnavy *et al.* 2007c; Lohitnavy *et al.* 2007d; Ramsey and Andersen 1984; Sathirakul *et al.* 1993), it is possible to develop PBPK models to predict changes in pharmacokinetics and disposition of any Mrp2 substrates.

2.5. Genipin as a Possible Antidote for PCB126

Genipin, an intestinal metabolite of geniposide, is a Mrp2 translocation enhancer (Shoda *et al.* 2004). Genipin enhanced Mrp2 translocation from its intracellular storage pool to the canalicular membrane of hepatocytes. As a result, it increased bile flow and excretion of Mrp2 substrates (Shoda *et al.* 2004). Since PCB126 is also a Mrp2 substrate, we hypothesized that genipin can decrease PCB126 levels by enhancing Mrp2-mediated excretion of PCB126. Consequently, in our study, we exposed the rats with PCB126 and genipin infusion. In these rats, genipin slightly reduced hepatic PCB126 concentration levels throughout the entire time periods (Lohitnavy *et al.* 2007d). However, since the observed standard deviations were large, the experimental results were not statistically significant (Lohitnavy *et al.* 2007d). To confirm this hypothesis, an experiment with a

larger sample size at each time point and/or multiple levels of genipin infusion should be conducted.

2.6. Application of the PBPK Model of PCB126: Transplacental and Lactational Transfer Model

Recently, our group conducted a pharmacokinetic study of PCB126 in pregnant and lactating rats (Lee *et al.* 2004). In this study, four female Sprague-Dawley (SD) rats were orally administered with a single dose of ^{14}C -PCB126 (10 $\mu\text{g}/\text{kg}$ bw) on gestation day 9 (GD9). The rats were sacrificed on GD14 and postnatal day 2 (PND2). Maternal, fetal and pups' organs were collected and analyzed for PCB126 levels using a highly sensitive accelerated mass spectrometric (AMS) technique (Lee *et al.* 2004). Despite very low concentration levels of PCB126 in fetuses and pups, PCB126 concentration levels of fetal and pups' organs were successfully determined (Lee *et al.* 2004).

Thus, with our available PBPK model of PCB126, we could further modify the model with a description of changing physiological conditions in pregnant and lactating rats. Schematic diagrams of PBPK models of transplacental transfer and lactational transfer of PCB126 are demonstrated in Fig. 6.1 and Fig. 6.2, respectively.

In our preliminary transplacental model of PCB126, a placenta was incorporated into the original PBPK model of PCB126 as an additional organ. Placental transfer of PCB126 from the pregnant rat to its fetuses was assumed (Fig. 6.1). A first-order rate constant from placenta to fetuses (K_{Placenta}) transfers PCB126 from the dam to fetuses was utilized (Fig. 6.1). Other physiological parameters used in this model were adopted from the literature (Fisher *et al.* 1990; Lohitnavy *et al.* 2007b). Since PCB126 concentration levels in all examined organs were similar (Lee *et al.* 2004), thus, in this model, the

fetuses were considered as a one-compartment storage pool. Preliminary computer model simulation results in a pregnant and a non-pregnant rat (control) on GD14 were demonstrated in Fig. 6.3 and Fig. 6.4, respectively. Our preliminary model was able to successfully describe experimental data from a pregnant rat, a non-pregnant rat (control), and fetuses (Fig. 6.3 and 6.4).

In the preliminary lactation transfer model of PCB126, a first-order mammary excretion via milk was assumed (Fig. 6.2). A first-order rate constant of PCB126 excretion into milk ($K_{\text{Lactation}}$) was utilized. Subsequently, the pups were orally exposed to PCB126 via the lactation transfer process. In this model, the pups were considered as separate living organisms with their own physiological parameters (i.e. blood flows to organs) (Fig. 6.2). Computer model simulation results in a dam and its pups on PND2 were demonstrated in Fig. 6.5A and Fig. 6.5B, respectively. The preliminary computer simulation results were able to adequately describe our analytical results both in the dam (Fig. 6.5A) and in the pups (Fig. 6.5B).

From these preliminary computer simulation results, our original PCB126 PBPK model could be modified and applied in these different physiological conditions (i.e. pregnancy and lactation). However, there were only 4 rats in this experiment (2 non-pregnant and 2 pregnant/lactating rats): at each sacrificing time point (GD14 and PND2), there were 2 rats (one control and one pregnant/lactating rat). The sample size of this preliminary experiment was too small. Thus, it is warranted to repeat the experiment with a larger number of animals and/or having more sacrificing time points.

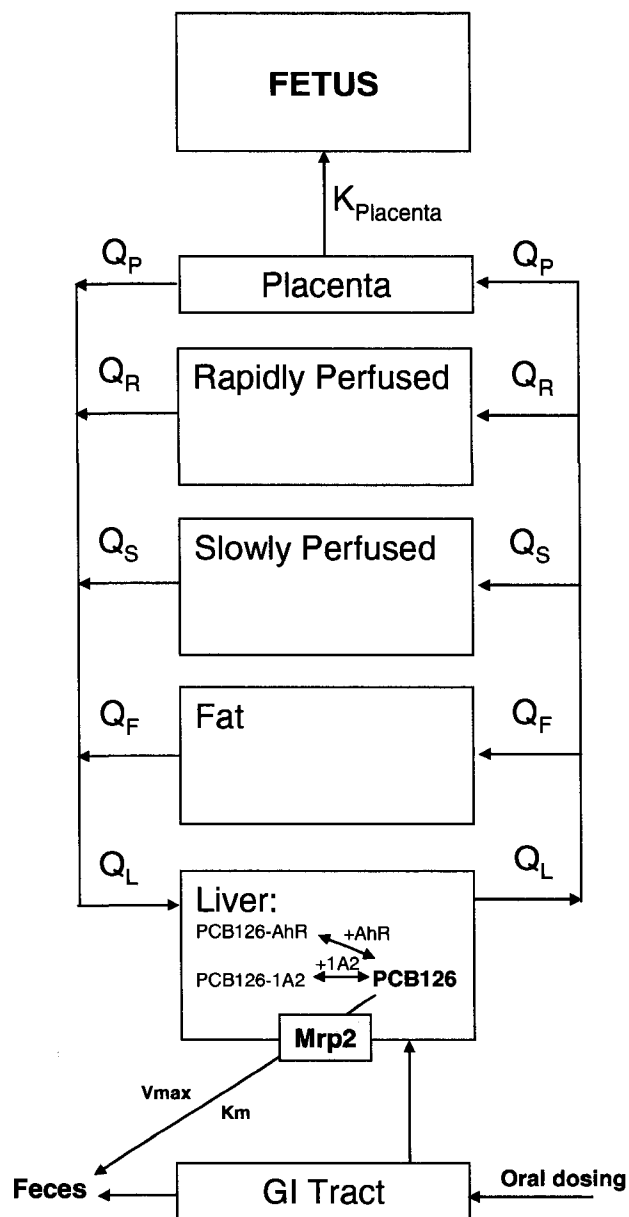


Fig. 6.1. A schematic diagram of the PBPK model of PCB126 with a description of PCB126 transplacental transfer from maternal placenta to fetuses.

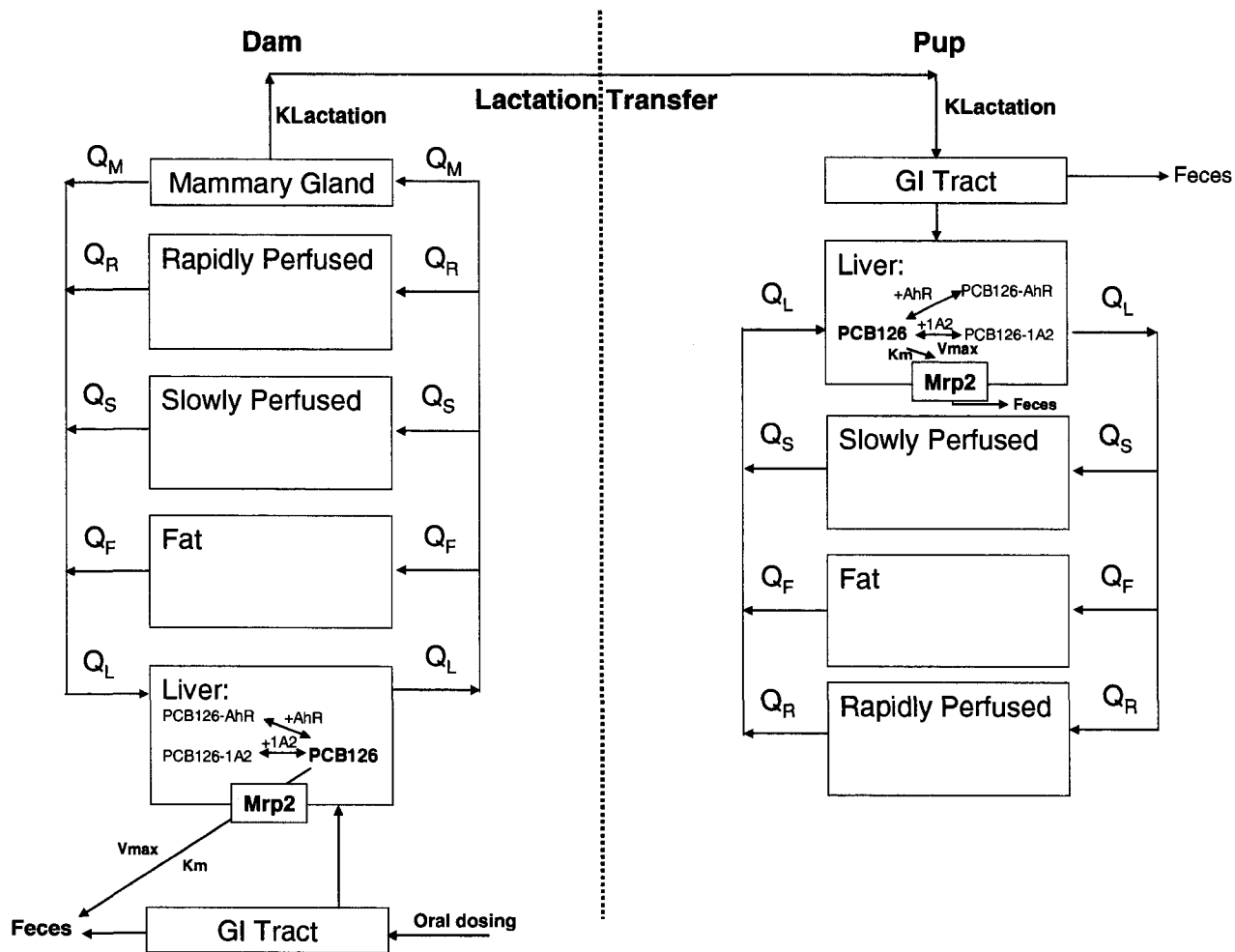


Fig. 6.2. A schematic diagram of the PBPK model of PCB126 with a description of PCB126 lactational transfer from a dam to its pups.

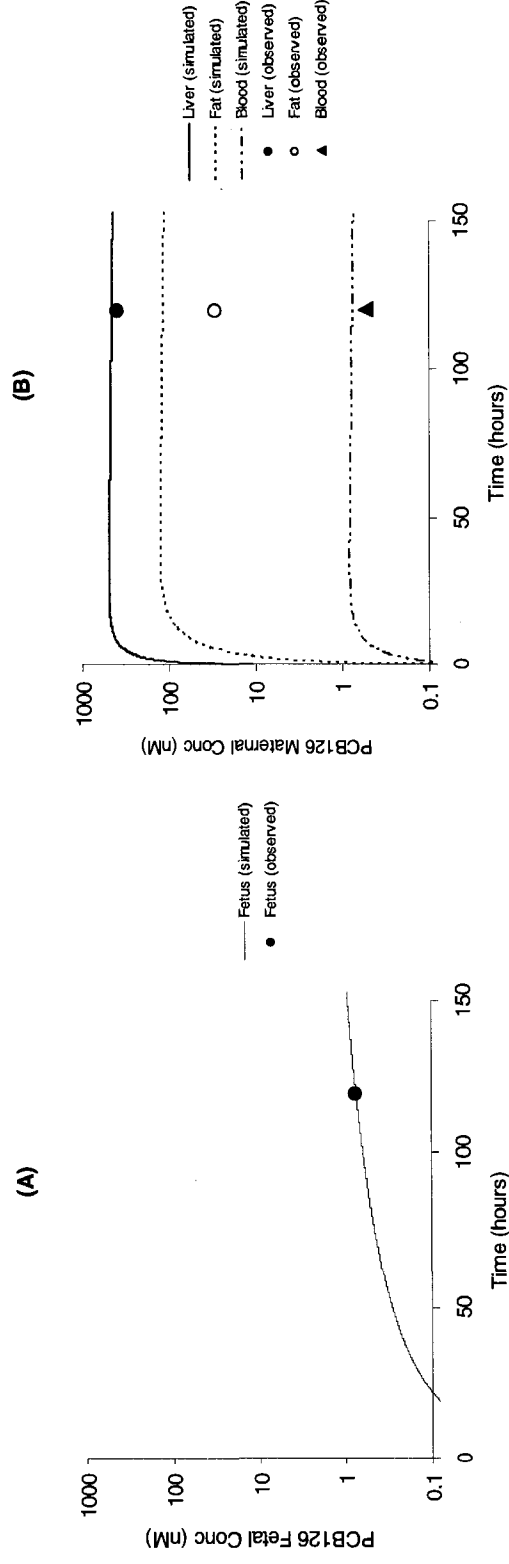


Fig. 6.3. Tissue concentration-time courses of PCB126 in fetuses (A) and a pregnant rat (B). A female SD rat was orally administered with ¹⁴C-PCB126 (10 μg/kg) on GD9 (time = zero). The pregnant rat was sacrificed on GD14 (time= 120 hours). Maternal tissues (i.e. liver, fat, kidney and blood) and fetuses were collected, and were analyzed for PCB126 levels using accelerated mass spectrometry techniques. Lines are model simulations and symbols represent experimental data obtained from Lee et al (2004).

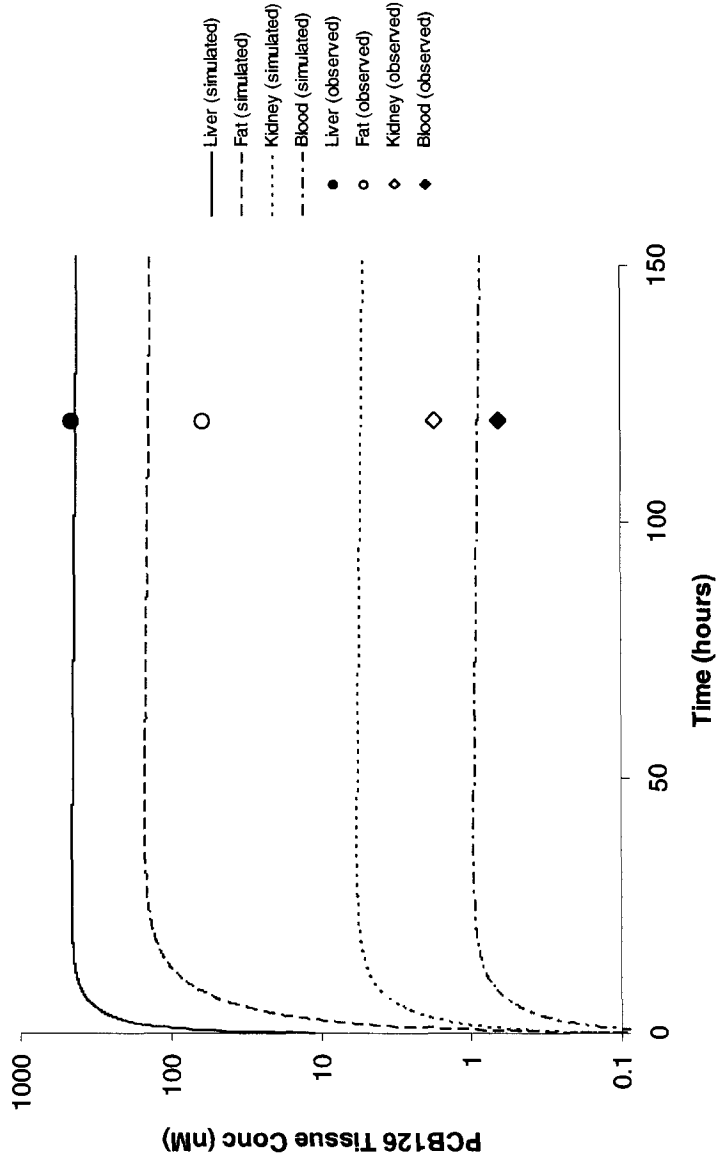


Fig. 6.4. Tissue concentration-time courses of PCB126 in a female non-pregnant rat (control). A female SD rat was orally administered with ¹⁴C-PCB126 (10 µg/kg) on GD9 (time = zero). The rat was sacrificed on GD14 (time= 120 hours). Tissues (i.e. liver, fat, kidney and blood) were collected, and were analyzed for PCB126 levels using accelerated mass spectrometry techniques. Lines are model simulations and symbols represent the experimental data obtain from Lee et al (2004).

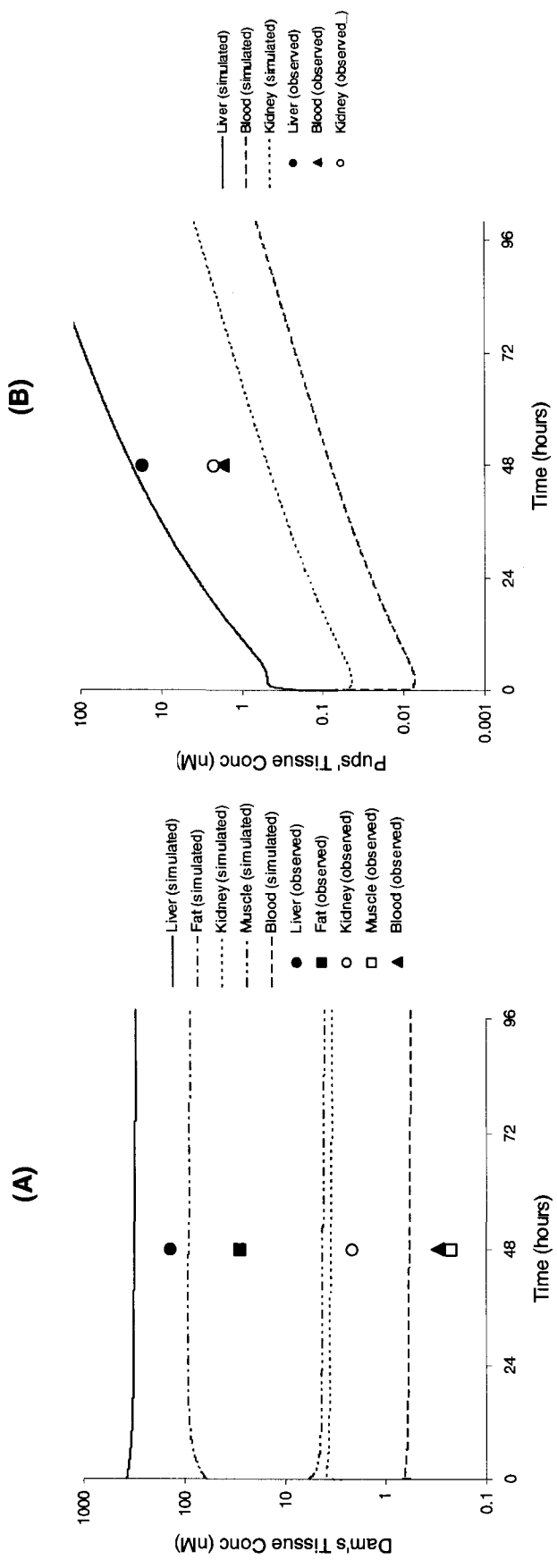


Fig. 6.5. Concentration-time courses of PCB126 in a dam (A) and pups (B). The dam was orally administered with ¹⁴C-PCB126 (10 μg/kg) on GD9 and was sacrificed on postnatal day 2 (PND2; time = 48 hours). Dam's tissues (i.e. liver, fat, kidney and blood) and pups' tissues (i.e. liver, blood and kidney) were collected, and were analyzed for PCB126 levels using accelerated mass spectrometry techniques. Lines are model simulations and symbols represent the experimental data obtain from Lee et al (2004).

REFERENCES

- Andersen, M. E. (1995). Development of physiologically based pharmacokinetic and physiologically based pharmacodynamic models for applications in toxicology and risk assessment. *Toxicol Lett* **79**, 35-44.
- Arza, E., Cubero, F. J., Garcia-Barrutia, M. S., Ortiz, A., Maganto, P., Mula, N., and Arahuetes, R. M. (2001). A compared study on the purification of fetal and adult rat hepatocyte suspensions by biomagnetic isolation techniques and flow cytometry analysis. *Cell Biol Int* **25**, 1285-9.
- Beique, L., Giguere, P., la Porte, C., and Angel, J. (2007). Interactions between protease inhibitors and acid-reducing agents: a systematic review. *HIV Med* **8**, 335-45.
- Belfiore, C. J., Yang, R. S., Chubb, L. S., Lohitnavy, M., Lohitnavy, O. S., and Andersen, M. E. (2007). Hepatic sequestration of chlordecone and hexafluoroacetone evaluated by pharmacokinetic modeling. *Toxicology* **234**, 59-72.
- Berry, M. N., and Friend, D. S. (1969). High-yield preparation of isolated rat liver parenchymal cells: a biochemical and fine structural study. *J Cell Biol* **43**, 506-20.
- Berry, M. N., Halls, H. J., and Grivell, M. B. (1992). Techniques for pharmacological and toxicological studies with isolated hepatocyte suspensions. *Life Sci* **51**, 1-16.
- Berry, M. N., and Phillips, J. W. (2000). The isolated hepatocyte preparation: 30 years on. *Biochem Soc Trans* **28**, 131-5.
- Bischoff, K. B., Dedrick, R. L., Zaharko, D. S., and Longstreth, J. A. (1971). Methotrexate pharmacokinetics. *J Pharm Sci* **60**, 1128-33.
- Brown, G. R. (1993). Cephalosporin-probenecid drug interactions. *Clin Pharmacokinet* **24**, 289-300.
- Chu, I., Villeneuve DC, Yagminas A, LeCavalier P, Poon R, Feeley M, Kennedy SW, Seegal RF, Hakansson H, Ahlborg UG, et al. (1994). Subchronic toxicity of 3,3',4,4',5-pentachlorobiphenyl in the rat. I. Clinical, biochemical, hematological, and histopathological changes. *Fundam Appl Toxicol.* **22**, 457-468.
- Conolly, R. B., and Andersen, M. E. (1997). Hepatic foci in rats after diethylnitrosamine initiation and 2,3,7,8-tetrachlorodibenzo-p-dioxin promotion: evaluation of a quantitative two-cell model and of CYP 1A1/1A2 as a dosimeter. *Toxicol Appl Pharmacol* **146**, 281-93.
- Conolly, R. B., and Kimbell, J. S. (1994). Computer simulation of cell growth governed by stochastic processes: application to clonal growth cancer models. *Toxicol Appl Pharmacol* **124**, 284-95.

- Dean, C. E., Jr., Benjamin, S. A., Chubb, L. S., Tessari, J. D., and Keefe, T. J. (2002). Nonadditive hepatic tumor promoting effects by a mixture of two structurally different polychlorinated biphenyls in female rat livers. *Toxicol Sci* **66**, 54-61.
- Dennison, J. E., Andersen, M. E., Clewell, H. J., and Yang, R. S. (2004). Development of a physiologically based pharmacokinetic model for volatile fractions of gasoline using chemical lumping analysis. *Environ Sci Technol* **38**, 5674-81.
- Dennison, J. E., Andersen, M. E., and Yang, R. S. (2003). Characterization of the pharmacokinetics of gasoline using PBPK modeling with a complex mixtures chemical lumping approach. *Inhal Toxicol* **15**, 961-86.
- Dennison, J. E., Bigelow, P. L., Mumtaz, M. M., Andersen, M. E., Dobrev, I. D., and Yang, R. S. (2005). Evaluation of potential toxicity from co-exposure to three CNS depressants (toluene, ethylbenzene, and xylene) under resting and working conditions using PBPK modeling. *J Occup Environ Hyg* **2**, 127-35.
- Dobrev, I. D., Andersen, M. E., and Yang, R. S. (2001). Assessing interaction thresholds for trichloroethylene in combination with tetrachloroethylene and 1,1,1-trichloroethane using gas uptake studies and PBPK modeling. *Arch Toxicol* **75**, 134-44.
- Dobrev, I. D., Andersen, M. E., and Yang, R. S. (2002). In silico toxicology: simulating interaction thresholds for human exposure to mixtures of trichloroethylene, tetrachloroethylene, and 1,1,1-trichloroethane. *Environ Health Perspect* **110**, 1031-9.
- Fisher, J. W., Campbell, J., Muralidhara, S., Bruckner, J. V., Ferguson, D., Mumtaz, M., Harmon, B., Hedge, J. M., Crofton, K. M., Kim, H., and Almekinder, T. L. (2006). Effect of PCB 126 on hepatic metabolism of thyroxine and perturbations in the hypothalamic-pituitary-thyroid axis in the rat. *Toxicol Sci* **90**, 87-95.
- Fisher, J. W., Whittaker, T. A., Taylor, D. H., Clewell, H. J., 3rd, and Andersen, M. E. (1990). Physiologically based pharmacokinetic modeling of the lactating rat and nursing pup: a multiroute exposure model for trichloroethylene and its metabolite, trichloroacetic acid. *Toxicol Appl Pharmacol* **102**, 497-513.
- Fujita, K. (2004). Food-drug interactions via human cytochrome P450 3A (CYP3A). *Drug Metabol Drug Interact* **20**, 195-217.
- Gustafson, D. L., Coulson, A. L., Feng, L., Pott, W. A., Thomas, R. S., Chubb, L. S., Saghir, S. A., Benjamin, S. A., and Yang, R. S. (1998). Use of a medium-term liver focus bioassay to assess the hepatocarcinogenicity of 1,2,4,5-tetrachlorobenzene and 1,4-dichlorobenzene. *Cancer Lett* **129**, 39-44.

- Gustafson, D. L., Long, M. E., Thomas, R. S., Benjamin, S. A., and Yang, R. S. (2000). Comparative hepatocarcinogenicity of hexachlorobenzene, pentachlorobenzene, 1,2,4,5-tetrachlorobenzene, and 1,4-dichlorobenzene: application of a medium-term liver focus bioassay and molecular and cellular indices. *Toxicol Sci* **53**, 245-52.
- Haddad, S., Beliveau, M., Tardif, R., and Krishnan, K. (2001). A PBPK modeling-based approach to account for interactions in the health risk assessment of chemical mixtures. *Toxicol Sci* **63**, 125-31.
- Hirono, S., Nakagome, I., Imai, R., Maeda, K., Kusuhara, H., and Sugiyama, Y. (2005). Estimation of the three-dimensional pharmacophore of ligands for rat multidrug-resistance-associated protein 2 using ligand-based drug design techniques. *Pharm Res* **22**, 260-9.
- Jedlitschky, G., Hoffmann, U., and Kroemer, H. K. (2006). Structure and function of the MRP2 (ABCC2) protein and its role in drug disposition. *Expert Opin Drug Metab Toxicol* **2**, 351-66.
- Kumar, V., Bustin, S. A., and McKay, I. A. (1995). Transforming growth factor alpha. *Cell Biol Int* **19**, 373-88.
- Lee, S. K., Buchholz, B., Reddy, M. B., Liao, K. H., Lohitnavy, M., Vogel, J., and R.S.H., Y. (2004). Biomedical Application of Accelerator Mass Spectrometry (AMS): Perinatal Pharmacokinetic and PBPK Modeling Study of PCB 126. *Toxicologist* **78**, 246.
- Lee, S. K., Ou, Y. C., Andersen, M. E., and Yang, R. S. (2007). A physiologically based pharmacokinetic model for lactational transfer of PCB 153 with or without PCB 126 in mice. *Arch Toxicol* **81**, 101-11.
- Lee, S. K., Ou, Y. C., and Yang, R. S. (2002). Comparison of pharmacokinetic interactions and physiologically based pharmacokinetic modeling of PCB 153 and PCB 126 in nonpregnant mice, lactating mice, and suckling pups. *Toxicol Sci* **65**, 26-34.
- Lohitnavy, M., Chubb, L. S., Lohitnavy, O., Yang, C. C., Homberg, J., Campaign, J. A., and Yang, R. S. (2004). Pharmacokinetic (PK)/Pharmacodynamic (PD) Relationship of PCB126 Under the Conditions of Modified Medium-Term Liver Bioassay. *Toxicologist* **78**, 271.
- Lohitnavy, M., Lohitnavy, O., Thangkeattiyanon, O., and Srichai, W. (2005). Reduced oral itraconazole bioavailability by antacid suspension. *J Clin Pharm Ther* **30**, 201-6.

- Lohitnavy, M., Benjamin S. A., Eickman E., Gerjevic L., Lohitnavy O., Lu Y., Yang R.S. H. (2007a). Hepatic Enzyme and Receptor Expression as Biomarkers for Carcinogenicity in Rats Exposed to PCB126, Hexachlorobenzene, and, Their Mixture. *Toxicol Sci* (submitted).
- Lohitnavy, M., Lu, Y., Lohitnavy, O., Chubb, L., Hirono, S., and Yang, R. S. H. (2007b). A Possible Role of Multidrug-Resistance-Associated Protein 2 (Mrp2) in Hepatic Excretion of PCB126, an Environmental Contaminant; PBPK/PD Modeling. *Toxicol Sci* (submitted).
- Lohitnavy, M., Lu, Y., Lohitnavy, O., Lyons, M. A., and Yang, R. S. H. (2007c). A Novel Physiologically-Based Pharmacokinetic Model of Methotrexate with an Incorporation of Hepatic Excretion via Multidrug-Resistance-Associated Protein 2 (Mrp2) in Mice, Rats, Dogs, and Humans. *J Pharm Sci* (submitted).
- Lohitnavy, M., Reisfeld, B., Lohitnavy, O., Lu, Y., Mayeno, A. N., and Yang, R. S. H. (2007d). A Physiologically-Based Pharmacokinetic Model of Pharmacokinetic Interactions Between Methotrexate, 3, 3', 4, 4', 5-Pentachlorobiphenyl (PCB126), and Genipin in Rats: A Competitive Inhibition at Multidrug-Resistance-Associated Protein 2 (Mrp2). *Toxicol Appl Pharmacol* (submitted).
- Lu, Y., Lohitnavy, M., Reddy, M., Lohitnavy, O., Eickman, E., Ashley, A., Gerjevic, L., Xu, Y., Conolly, R. B., and Yang, R. S. (2007). Quantitative analysis of liver GST-P foci promoted by a chemical mixture of hexachlorobenzene and PCB 126: implication of size-dependent cellular growth kinetics. *Arch Toxicol*. (in press)
- Lu, Y., Lohitnavy, M., Reddy, M. B., Lohitnavy, O., Ashley, A., and Yang, R. S. (2006). An updated physiologically based pharmacokinetic model for hexachlorobenzene: incorporation of pathophysiological states following partial hepatectomy and hexachlorobenzene treatment. *Toxicol Sci* **91**, 29-41.
- Mallet, L., Spinewine, A., and Huang, A. (2007). The challenge of managing drug interactions in elderly people. *Lancet* **370**, 185-91.
- NTP (2006). NTP toxicology and carcinogenesis studies of 3,3',4,4',5-pentachlorobiphenyl (PCB 126) (CAS No. 57465-28-8) in female Harlan Sprague-Dawley rats (Gavage Studies). *Natl Toxicol Program Tech Rep Ser*, 4-246.
- Otagiri, M. (2005). A molecular functional study on the interactions of drugs with plasma proteins. *Drug Metab Pharmacokinet* **20**, 309-23.
- Ou, Y. C., Conolly, R. B., Thomas, R. S., Gustafson, D. L., Long, M. E., Dobrev, I. D., Chubb, L. S., Xu, Y., Lapidot, S. A., Andersen, M. E., and Yang, R. S. (2003).

- Stochastic simulation of hepatic preneoplastic foci development for four chlorobenzene congeners in a medium-term bioassay. *Toxicol Sci* **73**, 301-14.
- Ou, Y. C., Conolly, R. B., Thomas, R. S., Xu, Y., Andersen, M. E., Chubb, L. S., Pitot, H. C., and Yang, R. S. (2001). A clonal growth model: time-course simulations of liver foci growth following penta- or hexachlorobenzene treatment in a medium-term bioassay. *Cancer Res* **61**, 1879-89.
- Ramsey, J. C., and Andersen, M. E. (1984). A physiologically based description of the inhalation pharmacokinetics of styrene in rats and humans. *Toxicol Appl Pharmacol* **73**, 159-75.
- Safarik, I., and Safarikova, M. (1999). Use of magnetic techniques for the isolation of cells. *J Chromatogr B Biomed Sci Appl* **722**, 33-53.
- Sathirakul, K., Suzuki, H., Yasuda, K., Hanano, M., Tagaya, O., Horie, T., and Sugiyama, Y. (1993). Kinetic analysis of hepatobiliary transport of organic anions in Eisai hyperbilirubinemic mutant rats. *J Pharmacol Exp Ther* **265**, 1301-12.
- Shi, Y., and Massague, J. (2003). Mechanisms of TGF-beta signaling from cell membrane to the nucleus. *Cell* **113**, 685-700.
- Shoda, J., Miura, T., Utsunomiya, H., Oda, K., Yamamoto, M., Kano, M., Ikegami, T., Tanaka, N., Akita, H., Ito, K., Suzuki, H., and Sugiyama, Y. (2004). Genipin enhances Mrp2 (Abcc2)-mediated bile formation and organic anion transport in rat liver. *Hepatology* **39**, 167-78.
- Singh, B. N. (1999). Effects of food on clinical pharmacokinetics. *Clin Pharmacokinet* **37**, 213-55.
- Stenius, U., Warholm, M., Martens, U., and Hogberg, J. (1994). Isolation of glutathione S-transferase P-positive hepatocytes from carcinogen treated rats by use of ethacrynic acid as selecting agent. *Carcinogenesis* **15**, 1561-6.
- Tai, Y. T., Teoh, G., Shima, Y., Chauhan, D., Treon, S. P., Raje, N., Hideshima, T., Davies, F. E., and Anderson, K. C. (2000). Isolation and characterization of human multiple myeloma cell enriched populations. *J Immunol Methods* **235**, 11-9.
- Thomas, R. S., Conolly, R. B., Gustafson, D. L., Long, M. E., Benjamin, S. A., and Yang, R. S. (2000). A physiologically based pharmacodynamic analysis of hepatic foci within a medium-term liver bioassay using pentachlorobenzene as a promoter and diethylnitrosamine as an initiator. *Toxicol Appl Pharmacol* **166**, 128-37.
- Walubo, A. (2007). The role of cytochrome P450 in antiretroviral drug interactions. *Expert Opin Drug Metab Toxicol* **3**, 583-98.

Zhou, S. F., Zhou, Z. W., Li, C. G., Chen, X., Yu, X., Xue, C. C., and Herington, A. (2007). Identification of drugs that interact with herbs in drug development. *Drug Discov Today* **12**, 664-73.

APPENDICES

Appendix I: Computer Code of the PBPK model for PCB126 (Single-dose NTP Study)

PROGRAM Single.csl

!Edited by M. Lohitnavy on Oct. 10th, 2007.

!PBPK modeling of PCB126.

!Developed by Lohitnavy M. and Lu Y.

!***** Experimental Conditions *****'

!Data obtained from the NTP PCB126 Study

!Female SD rats (aged 20-22 weeks) were orally administered

!with a single dose of PCB126 in corn oil.

!There were two dosing levels; 10 and 1000 ng PCB126/kg BW.

!***** End of the Conditions*****'

!***** Features of this PBPK model; *****'

!Binding between PCB126 and CYP1A2 in the liver,

!Binding between PCB126 and aromatic hydrocarbon receptor (AhR) in the liver,

!Excretion of PCB126 via hepatic Mrp2.

!***** End of the model features *****'

INITIAL

!Volume and blood flow parameters

!From tabulated data, at 20-22 weeks of age, a female SD rat weighs 280 g.

CONSTANT BW=0.28

!Body weight of a rat (kg)

CONSTANT VFC=0.05

!Fat volume fraction.

CONSTANT VLC=0.038

!Liver Volume Fraction

CONSTANT VRC=0.052

!Rapidly perfused volume fraction

CONSTANT VBC=0.062D0

!blood volume

CONSTANT QCC=14.1D0

!blood flow constant

CONSTANT QFC=0.07D0

CONSTANT QLC=0.18D0

CONSTANT QRC=0.58D0

QSC=1.0-QFC-QLC-QRC

!Scaled parameters

VF=BW*VFC

!total fat volume;

VL=BW*VLC

!total liver volume;

VB=BW*VBC+0.0012

!blood.Lee&Blaufox

VR=BW*VRC

!Rapidly perfused volume

VS=0.91*BW-VF-VL-VB-VR

!slowly perfused

QC=QCC*BW**0.75

!blood flow rate

QF=QC*QFC

QL=QC*QLC

QR=QC*QRC

QS=QC*QSC

```

!Chemical-specific paramters
!Partition coefficients
CONSTANT PF=155.                                !from the NTP model
CONSTANT PL=8.9D0                               !from the NTP model
CONSTANT PR=6.0D0                               !from the NTP model
CONSTANT PS=7.2D0                               !from the NTP model

!Elimination parameters
CONSTANT KGILV=0.1433                          !/hr,absorption rate, from GI to liver
CONSTANT KFEC=0.00                             !/hr,excretion in feces
CONSTANT KMET=0.00D0                           !/hr, metabolism rate
CONSTANT KLIV=0.0                              !/hr, first order elimination from the liver.

!PCB 126 Excretion via Mrp2 is mathematically described using
!the Michealis-Menten Equation; C=Vmax*C/(Km+C)
!***** PCB126 Section for Mrp2-mediated excretion from the liver*****
CONSTANT Vmax= 64.59                            !Maximal velocity of Mrp2
                                                !optimized value (unit, nmol/h).
CONSTANT Km=7.76e3                              !Binding affinity of Mrp2
                                                !calculated Km by Hirono S.(unit, nM)
!*****END of Mrp2-mediated excretion*****

!Simulation parameters
CONSTANT MW=326.4                               !molecular weight of PCB126
CONSTANT DoseRate=1000.                        !ng/kg
Dose = DoseRate*BW/MW                          !nmole
CONSTANT tstop=25.0                            !hr
cinterval CINT=0.1

!Constants related to protein binding
!PCB126 binding in the liver consists of binding to CYP1A2 and AhR.
!*****PCB126 SECTION FOR LIVER BINDING*****
CONSTANT BM1 = 0.004                            !PCB126 binding capacity to AhR
CONSTANT KB1 = 0.05637                         !PCB126 binding constant for AhR
                                                !Optimized value
CONSTANT BM2O = 10.                            !Binding protein: capacity (nmoles/liver)
CONSTANT BM2I = 101.25                         !Increase due to induction (nmoles/liver)
                                                !Optimized value
CONSTANT KB2 = 5.5437                          !Binding protein: affinity (nM)
                                                !Optimized value
CONSTANT N = 1.                                !Hill Coefficient
CONSTANT KD = 1.                               !Liganded receptor-DNA binding
!*****END of PCB126 Binding*****

END !END of Initial

```

DYNAMIC
ALGORITHM IALG=2

DERIVATIVE

!Mass balance in fat tissue

RAF=QF*(CA-CVF)

AF=INTEG(RAF,0.0)

CF=AF/VF

CVF=CF/PF

!Mass balance in liver

!Protein binding terms in the liver were added.

!An Mrp2 excretion term, $V_{max} * CVL / (K_m + CVL)$, is added.

RAL=QL*(CA-CVL)-KMET*CVL+KGILV*AGI -($V_{max} * CVL / (K_m + CVL)$)&
-KLIV*CVL

AL=INTEG(RAL,0.0) !Amount of PCB126 in the livers (nmole)

CL=AL/VL !Calculations of conc of PCB126 in the livers (nM).

AUCLIV=integ(CL,0.0) !Calculations of AUC of PCB126 in the livers (nM*hr)

PLiv=AL*100/Dose !% Retention of PCB126 in the livers
!compared to total administered dose(%)

!*****Calculations of Mrp2-mediated excretion*****'

RMrp2= $V_{max} * CVL / (K_m + CVL)$!Rate of excretion via mrp2 (nmole*h/L)

Mrp2=INTEG(RMrp2,0.0) !Amount of excretion via mrp2 (nmole)

PMrp2=Mrp2*100/(DOSE+1.0e-30) !Efficiency in Mrp2 excretion
!compared to total amount of PCB126
!in the liver(%)

Combine=PLIV+PMrp2 !Combination between liver retention&
!Mrp2 excretion compared to total dose (%)

Other=100-Combine !Mass deposited elsewhere (%)

!***** End of Mrp2-mediated excretion section*****'

Procedural

CVLt= $al / (vl * pl + bm1 / (kb1 + cvl) + bm2t / (kb2 + cvl))$

CVL = CVLt

END !End of Procedural

!*****Calculations of AhR-PCB126 Binding*****'

DB1 = $BM1 * Cv / (KB1 + Cv) / VL$!Conc. of AhR-PCB126 complex

BOUND = $(db1 ** n) / (db1 ** n + Kd ** n)$!Occupancy of DRE on DNA

PB1 = $Cv / (KB1 + Cv)$!AhR percent occupancy

BM2T = $BM2O + BM2I * BOUND$!Instantaneous level of protein induction

!*****End of AhR-PCB126 Binding section *****'

!Amount metabolized

RAM=KMET*CVL


```
!File single.cmd
!Command file for oral single dose study of PCB126.
!Edited by M. Lohitnavy on Oct. 10th, 2007.

set grdcpl=.f. !no grid on line plots
SET TITLE = 'PCB126 model- Female SD rat single oral dose'
prepare /all
```

```
procedure check
start
plot tmass, mb
print t,tmass,mb
end
```

```
PROCED plots1000
set doserate = 1000
s tstop=24
start
PLOT /DATA=NTP1000 CF /log /lo=0.1 /hi=50 /char=2 /xtag='hr' /tag='Fat
nmole/L'
PLOT /DATA=NTP1000 CL /log /lo=1.0 /hi=100 /char=1 /xtag='hr' /tag='Liver
nmole/L'
!PLOT /DATA=NTP1000 CR /lo=0 /char=5 /xtag='hr' /tag='Rapidly nmole/L'
!PLOT /DATA=NTP1000 CB /lo=0 /char=3 /xtag='hr' /tag='Blood nmole/L'
END
```

```
DATA NTP1000(T,CL,CF)
0.5 1.653991422 0.639038297
1 3.254591912 0.625879596
1.5 8.354979473 1.49971538
2 10.90011152 1.771324142
3 26.02457843 3.042550245
8 44.29501317 6.172579657
16 47.62674479 12.78591391
24 52.46209743 11.52261489
END
```

Appendix II: Computer Code of the PBPK model for PCB126 (Multiple dose 2-year NTP Study)

PROGRAM repeat.csl

!Edited by M. Lohitnavy on Oct. 10th, 2007.

!PBPK modeling of PCB126 (repeated dose studies)

!Developed by Lohitnavy M. and Lu Y.

!***** Experimental Conditions *****

!Data obtained from the NTP PCB126 Study

!There were 6 dosing levels;

!30, 100, 175, 300, 550 and 1000 ng PCB126/kg BW/day.

!The rats were orally administered with repeated doses of PCB126.

!Dosing was conducted 5 times per week up to 2 years.

!Body weight & liver weight data were available.

!***** End of the Conditions *****

!***** Features of this PBPK model, *****

!Binding between PCB126 and CYP1A2 in the liver,

!Binding between PCB126 and aromatic hydrocarbon receptor (AHR) in the liver,

!Excretion of PCB126 via hepatic Mrp2.

!***** End of the model features *****

INITIAL

!Volume and blood flow parameters

!BW data taken from the NTP 30-ng repeated-dose 2-yr study

Table BW30t, 1.36/168,336,504,672,840,1008,1176,1344,1512,1680,&

1848,2016,2184,2520,2856,3528,4200,4872,5544,6216,6888,7560,8232,&

8736,9576,10248,10920,11592,12264,12936,13608,14280,14952,15624,&

16296,16968,0.184,0.207,0.217,0.235,0.242,0.252,0.257,0.261,0.266,&

0.271,0.273,0.277,0.279,0.282,0.284,0.29,0.293,0.303,0.308,&

0.31,0.314,0.319,0.32,0.328,0.337,0.34,0.349,0.357,0.356,0.362,&

0.366,0.373,0.371,0.362,0.359/

!BW data taken from the NTP 100-ng repeated-dose 2-yr study

Table BW100t, 1.36/168,336,504,672,840,1008,1176,1344,1512,1680,&

1848,2016,2184,2520,2856,3528,4200,4872,5544,6216,6888,7560,8232,&

8736,9576,10248,10920,11592,12264,12936,13608,14280,14952,15624,&

16296,16968,0.185,0.206,0.22,0.236,0.241,0.25,0.254,0.259,0.261,&

0.267,0.272,0.275,0.278,0.283,0.284,0.295,0.3,0.307,0.312,&

0.313,0.319,0.322,0.325,0.33,0.338,0.344,0.352,0.359,0.369,0.369,&

0.375,0.383,0.379,0.381,0.388/

!BW data taken from the NTP 175-ng repeated-dose 2-yr study

Table BW175t, 1.36/168,336,504,672,840,1008,1176,1344,1512,1680,&

1848,2016,2184,2520,2856,3528,4200,4872,5544,6216,6888,7560,8232,&

8736,9576,10248,10920,11592,12264,12936,13608,14280,14952,15624,&
16296,16968,0.185,0.205,0.22,0.236,0.24,0.249,0.254,0.258,0.265,&
0.266,0.271,0.274,0.276,0.277,0.279,0.287,0.293,0.299,0.301,0.305,&
0.309,0.314,0.318,0.321,0.324,0.334,0.334,0.338,0.342,0.352,0.35,&
0.36,0.364,0.368,0.356,0.357/

!BW data taken from the NTP 300-ng repeated-dose 2-yr study
Table BW300t, 1,36/168,336,504,672,840,1008,1176,1344,1512,1680,&
1848,2016,2184,2520,2856,3528,4200,4872,5544,6216,6888,7560,8232,&
8736,9576,10248,10920,11592,12264,12936,13608,14280,14952,15624,&
16296,16968,0.185,0.206,0.22,0.237,0.243,0.248,0.253,0.257,0.263,&
0.268,0.271,0.274,0.276,0.278,0.281,0.278,0.289,0.299,0.303,0.306,&
0.308,0.313,0.317,0.318,0.322,0.333,0.337,0.341,0.348,0.354,0.35,&
0.354,0.348,0.354,0.344,0.346/

!BW data taken from the NTP 550-ng repeated-dose 2-yr study
Table BW550t, 1,36/168,336,504,672,840,1008,1176,1344,1512,1680,&
1848,2016,2184,2520,2856,3528,4200,4872,5544,6216,6888,7560,8232,&
8736,9576,10248,10920,11592,12264,12936,13608,14280,14952,15624,&
16296,16968,0.185,0.206,0.22,0.234,0.24,0.248,0.253,0.256,0.262,&
0.264,0.268,0.27,0.272,0.276,0.277,0.281,0.286,0.288,0.292,0.296,&
0.298,0.298,0.302,0.302,0.308,0.315,0.312,0.317,0.322,0.326,0.323,&
0.323,0.32,0.318,0.306,0.313/

!BW data taken from the NTP 1000-ng repeated-dose 2-yr study
Table BW1000t, 1,36/168,336,504,672,840,1008,1176,1344,1512,1680,&
1848,2016,2184,2520,2856,3528,4200,4872,5544,6216,6888,7560,8232,&
8736,9576,10248,10920,11592,12264,12936,13608,14280,14952,15624,&
16296,16968,0.184,0.203,0.218,0.232,0.239,0.246,0.249,0.253,0.257,&
0.26,0.263,0.266,0.266,0.269,0.27,0.276,0.279,0.282,0.284,0.285,&
0.286,0.285,0.288,0.285,0.286,0.287,0.289,0.29,0.292,0.29,0.287,&
0.282,0.279,0.278,0.275,0.279/

!Statement for changing BW data according to dosing groups.

```
If (doserate0.eq.30) then
  BW=BW30t(t)
  elseif (doserate0.eq.100) then
  BW=BW100t(t)
  elseif (doserate0.eq.175) then
  BW=BW175t(t)
  elseif (doserate0.eq.300) then
  BW=BW300t(t)
  elseif (doserate0.eq.550) then
  BW=BW550t(t)
  elseif (doserate0.eq.1000) then
  BW=BW1000t(t)
```

endif

!Liver weight data taken from the NTP 30-ng repeated-dose 2-yr study
Table VL30t, 1,5/0, 2352, 5208, 8904,16968, 0.007, .0101, .0096, .0103,.0103/

!Liver weight data taken from the NTP 100-ng repeated-dose 2-yr study
Table VL100t, 1,5/0, 2352, 5208, 8904,16968,0.007, 0.0089, .0093, .0111,.0111/

!Liver weight data taken from the NTP 175-ng repeated-dose 2-yr study
Table VL175t, 1,5/0, 2352, 5208, 8904,16968, 0.007, 0.0103,0.0109,0.0144,.0144/

!Liver weight data taken from the NTP 300-ng repeated-dose 2-yr study
Table VL300t, 1,5/0, 2352, 5208, 8904,16968, 0.007,0.0101,0.0100,0.0116,.0116/

!Liver weight data taken from the NTP 550-ng repeated-dose 2-yr study
Table VL550t, 1,5/0, 2352, 5208, 8904,16968, 0.007,0.0108,0.0107,0.0129, .0129/

!Liver weight data taken from the NTP 1000-ng repeated-dose 2-yr study
Table VL1000t, 1,5/0, 2352, 5208, 8904,16968, 0.007,0.0104,0.0103,0.0128, .0128/

!Statement for changing liver weight data according to dosing groups.

```
If (doserate0.eq.30) then
    VL=VL30t(t)
    elseif (doserate0.eq.100) then
    VL=VL100t(t)
    elseif (doserate0.eq.175) then
    VL=VL175t(t)
    elseif (doserate0.eq.300) then
    VL=VL300t(t)
    elseif (doserate0.eq.550) then
    VL=VL550t(t)
    elseif (doserate0.eq.1000) then
    VL=VL1000t(t)
```

endif

!Physiological Constants

```
CONSTANT VFC=0.05
CONSTANT VRC=0.052
CONSTANT VBC=0.062D0
CONSTANT QCC=14.1D0
CONSTANT QFC=0.07D0
CONSTANT QLC=0.18D0
CONSTANT QRC=0.58D0
    QSC=1.0-QFC-QLC-QRC
```

!Fat volume fraction.

!Rapidly perfused volume fraction

!blood volume

!blood flow constant

!Scaled parameters

```

VF=BW*VFC                                !total fat volume;
VB=BW*VBC+0.0012                          !blood.Lee&Blaufox
VR=BW*VRC                                  !Rapidly perfused volume
VS=0.91*BW-VF-VL-VB-VR                    !slowly perfused
    QC=QCC*BW**0.75                        !blood flow rate
    QF=QC*QFC
    QL=QC*QLC
    QR=QC*QRC
    QS=QC*QSC

!Chemical-specific paramters
!Partition coefficients
CONSTANT PF=155.                            !from the NTP model
CONSTANT PL=8.9D0                          !from the NTP model
CONSTANT PR=6.0D0                          !from the NTP model
CONSTANT PS=7.2D0                          !from the NTP model

!Elimination parameters
CONSTANT KGILV=0.1433                      !/hr,absorption rate, from GI to liver
                                           !Optimized value
CONSTANT KFEC=0.00                         !/hr,excretion in feces
CONSTANT KMET=0.00D0                       !/hr, PCB126 metabolism rate
CONSTANT KLIV=0.0                          !First order elimination from the liver.

!PCB 126 Excretion via Mrp2 is mathematically described using
!the Michealis-Menten Equation; C=Vmax*C/(Km+C)
!*****PCB126 Section for Mrp2-mediated excretion from the liver*****
CONSTANT Vmax= 64.59                       !Maximal velocity of Mrp2
                                           !Optimized value (unit, nmole/h).
CONSTANT Km=7.76e3                          !Binding affinity of Mrp2
                                           !calculated Km by Hirono S.(unit, nM)
!*****END of Mrp2-mediated excretion*****

!Constants related to protein binding
!PCB126 binding in the liver consists of binding to CYP1A2 and AhR.
!*****PCB126 SECTION FOR LIVER BINDING*****
CONSTANT BM1 = 0.004                       !PCB126 binding capacity to AhR (nmole/liver)
CONSTANT KB1 = 0.05637                     !PCB126 binding constant for AhR (nmole)
                                           !Optimized value
CONSTANT BM2O = 10.                        !Binding protein: capacity (nmoles/liver)
    BM2I0 = 85                             !Increase due to induction (nmoles/liver)
CONSTANT KB2 = 5.5437                     !Binding protein: affinity (nM)
                                           !Optimized value
CONSTANT N = 1.                            !Hill Coefficient
CONSTANT KD = 1.                           !Liganded receptor-DNA binding
CONSTANT slope=0.0066                     !Slope of the increase in capacity (nmol/hr)

```

!*****END of PCB126 Binding*****'

!Dosetime and frequency

DoseFrq=24.0 !hrs
k=0 !counter of doses
I=0

!Simulation parameters

CONSTANT MW=326.4 !molecular weight of PCB126
CONSTANT doserate0=30 !ng/kg
DoseRate=doserate0 !ng/kg
Dose = DoseRate*BW/MW !nmole
CONSTANT tstop=17500.0 !hr
cinterval CINT=24

!Initial value of total dose

TotalDose=0.0

END !of initial

!-----!-----!-----!-----!-----!-----!-----!-----!

DYNAMIC

ALGORITHM IALG=2

DERIVATIVE

If (doserate0.eq.30) then
 BW=BW30t(t)
 elseif (doserate0.eq.100) then
 BW=BW100t(t)
 elseif (doserate0.eq.175) then
 BW=BW175t(t)
 elseif (doserate0.eq.300) then
 BW=BW300t(t)
 elseif (doserate0.eq.550) then
 BW=BW550t(t)
 elseif (doserate0.eq.1000) then
 BW=BW1000t(t)
endif

If (doserate0.eq.30) then
 VL=VL30t(t)
 elseif (doserate0.eq.100) then
 VL=VL100t(t)
 elseif (doserate0.eq.175) then
 VL=VL175t(t)
 elseif (doserate0.eq.300) then

```

    VL=VL300t(t)
        elseif (doserate0.eq.550) then
    VL=VL550t(t)
        elseif (doserate0.eq.1000) then
    VL=VL1000t(t)
endif

!Setting exposure
IF(T.GE.(168*I).AND.T.LE.(96+168*I)) THEN
    DoseRate = doserate0
    Dose = DoseRate*BW/MW          !nmole
ENDIF

!Scaled parameters
VF=BW*VFC          !total fat volume;
VB=BW*VBC+0.0012  !blood.Lee&Blaufox
VR=BW*VRC          !Rapidly perfused volume
VS=0.91*BW-VF-VL-VB-VR !slowly perfused
    QC=QCC*BW**0.75 !blood flow rate
    QF=QC*QFC
    QL=QC*QLC
    QR=QC*QRC
    QS=QC*QSC

!Time-dependent increase in CYP1A2 expression
BM2I = BM2I0+slope*t

!Mass balance in fat tissue
RAF=QF*(CA-CVF)
AF=INTEG(RAF,0.0)
CF=AF/VF
CVF=CF/PF

!Mass balance in liver
!Protein binding terms in the liver were added.
!An Mrp2 excretion term,  $V_{max} * CVL / (K_m + CVL)$ , is added.
RAL=QL*(CA-CVL)-KMET*CVL+KGILV*AGI -&
(Vmax*CVL/(Km+CVL))-KLIV*CVL
AL=INTEG(RAL,0.0)          !Amount of PCB126 in the livers (nmole)
CL=AL/VL                  !Calculations of liver conc of PCB126 (nM)
AUCLIV=integ(CL,0.0)      !Calculations of hepatic AUC of PCB126 (nM*h/L)
PLiv=AL*100/(TOTALDOSE+1.0e-30) !% Retention of PCB126 in the livers
                                !compared to total administered dose(%)

!*****Calculations of Mrp2-mediated excretion*****'
RMrp2= Vmax*CVL/(Km+CVL)  !Rate of excretion via mrp2 (nmole*h/L)

```

```

Mrp2=INTEG(RMrp2,0.0)          !Amount of excretion via mrp2 (nmole)
PMrp2=Mrp2*100/(TOTALDOSE+1.0e-30) !Efficiency in Mrp2 excretion
                                   !compared to total amount of PCB126 in the liver(%)
Combine=PLIV+PMrp2             !Combination between liver retention and
                                   !Mrp2 excretion compared to total dose (%)
Other=100-Combine              !Mass deposited elsewhere (%)
!***** End of Mrp2-mediated excretion section*****'

```

Procedural

```

CVLt= al/(vl*pl+bm1/(kb1+cvl)+bm2t/(kb2+cvl))
CVL = CVLt
AhRBound= bm1*cvl/(kb1+cvl)      !Amount of PCB126 bound to AhR
CYPBound=bm2t*cvl/(kb2+cvl)     !Amount of PCB126 bound to CYP1A2
END                               !End of Procedural

```

```

!*****Calculations of AhR-PCB126 Binding*****'
DB1 = BM1*Cvl/(KB1+Cvl)/VL      !Conc. of AhR-PCB126 complex
BOUND = (db1**n)/(db1**n+Kd**n) !Occupancy of DRE on DNA
PB1 = Cvl/(KB1+Cvl)             !AhR percent occupancy
BM2T = BM2O+BM2I*BOUND         !Instantaneous level of protein induction
!*****End of AhR-PCB126 Binding section *****'

```

```

!Amount metabolized
RAM=KMET*CVL
AM=INTEG(RAM,0.0)

```

```

!Mass balance in rapidly perfused tissues
RAR=QR*(CA-CVR)
AR=INTEG(RAR,0.0)
CR=AR/VR
CVR=CR/PR

```

```

!Mass balance in slowly perfused tissues
RAS=QS*(CA-CVS)
AS=INTEG(RAS,0.0)
CS=AS/VS
CVS=CS/PS

```

```

!Mass balance in blood
RABlood=QF*CVF+QL*CVL+QR*CVR+QS*CVS-QC*CA
ABlood=INTEG(RABlood,0.0)
CA=ABlood/VB                    !Blood concentration

```

```

!GI lumen
RAGI=-KGILV*AGI-KFEC*AGI
AGI=INTEG(RAGI,0.0)+totalDOSE

```

```

!Excretion in feces
RAFEC=KFEC*AGI+(Vmax*CVL/(Km+CVL))+KLIV*CVL
AFEC=INTEG(RAFEC,0.0)
PFEC=AFEC*100/(TOTALDOSE+1.0e-30)

```

```

!Total mass
TMASS=AF+AL+AM+AR+AS+ABlood+AGI+AFEC
MB=(TOTALDose-TMASS)*100.0/(TOTALDose+11.0e-30)

```

```

!Setting the dosing scenarios to 5-days-per-week dosing
!Dosing is set to be off on day x*6 and day x*7

```

```

PROCEDURAL
  IF(T.GT.(96+168*I).AND.T.LT.(168+168*I)) THEN
    Doserate = 0
    Dose = DoseRate*BW/MW
    I=I+1
  ENDIF

```

```

!Addition of 1 more dose when the time meets the dosing time.

```

```

  dosetime=k*DoseFrq
  IF (t.ge.dosetime) THEN
    TotalDose=TotalDose+Dose
    k=k+1
  ENDIF

```

```

END ! END of Procedural

```

```

TERMT (T.GE.TSTOP)

```

```

END !END of Derivative

```

```

END !END of Dynamic

```

```

!-----!-----!-----!-----!-----!-----!-----!-

```

```

END !END of Program

```

!File repeat.cmd
!Command file for PBPK model of PCB126 (repeated dose studies)
!Edited by Lohitnavy M. on Oct. 10th, 2007.

set grdcpl=.f. !no grid on line plots
SET TITLE = 'PCB126 model-Female SD rat multiple oral dose'
prepare /all

procedure check
start
plot tmass, mb
print t,tmass,mb
end

PROCED repeat30
set doserate0=30
start
PLOT /DATA=repeat30 CF /log /lo=10 /hi=100 /char=2 /xtag='hr' /tag='Fat nmole/L'
PLOT /DATA=repeat30 CL /log /lo=1. /hi=1000. /char=1 /xtag='hr' /tag='Liver
nmole/L'
PLOT /DATA=repeat30 CA /lo=0. /hi=0.5 /char=3 /xtag='hr' /tag='Blood nmole/L'
END

PROCED repeat100
set doserate0 = 100
start
PLOT /DATA=repeat100 CF /lo=0 /hi= 120 /char=2 /xtag='hr' /tag='Fat nmole/L'
PLOT /DATA=repeat100 CL /log /lo=1. /hi=1000. /char=1 /xtag='hr' /tag='Liver
nmole/L'
PLOT /DATA=repeat100 CA /lo=0. /char=3 /xtag='hr' /tag='Blood nmole/L'
END

PROCED repeat175
set doserate0 = 175
start
PLOT /DATA=repeat175 CF /lo=0 /hi=125 /char=2 /xtag='hr' /tag='Fat nmole/L'
PLOT /DATA=repeat175 CL /log /lo=100. /hi=1000. /char=1 /xtag='hr' /tag='Liver
nmole/L'
PLOT /DATA=repeat175 CA /lo=0. /char=3 /xtag='hr' /tag='Blood nmole/L'
END

PROCED repeat300
set doserate0 = 300
start
PLOT /DATA=repeat300 CF /lo=0 /hi=250 /char=2 /xtag='hr' /tag='Fat nmole/L'

```
PLOT /DATA=repeat300 CL /log /lo=100. /hi=1000. /char=1 /xtag='hr' /tag='Liver
nmole/L'
PLOT /DATA=repeat300 CA /lo=0. /char=3 /xtag='hr' /tag='Blood nmole/L'
END
```

```
PROCED repeat550
set doserate0 = 550
start
PLOT /DATA=repeat550 CF /lo=0 /char=2 /xtag='hr' /tag='Fat nmole/L'
PLOT /DATA=repeat550 CL /log /lo=100. /hi=10000. /char=1 /xtag='hr' /tag='Liver
nmole/L'
PLOT /DATA=repeat550 CA /lo=0. /char=3 /xtag='hr' /tag='Blood nmole/L'
END
```

```
PROCED repeat1000
set doserate0 = 1000
start
PLOT /DATA=repeat1000 CF /lo=0 /char=2 /xtag='hr' /tag='Fat nmole/L'
PLOT /DATA=repeat1000 CL /log /lo=100. /hi=10000. /char=1 /xtag='hr'
/tag='Liver nmole/L'
PLOT /DATA=repeat1000 CA /lo=0. /char=3 /xtag='hr' /tag='Blood nmole/L'
END
```

```
DATA REPEAT30 (t, CA, CF, CL)
2184 0.3592 36.23 25.53
5040 0.0537 20.28 41.38
8736 0.1857 27.32 72.24
17472 0.1337 44.40 89.23
END
```

```
DATA REPEAT100 (t, CA, CF, CL)
2184 0.2784 59.95 104.64
5040 0.1594 47.46 171.90
8736 0.2171 63.39 239.06
17472 0.3014 105.86 279.68
END
```

```
DATA REPEAT175 (t, CA, CF, CL)
2184 0.2987 78.79 223.91
5040 0.2107 78.66 307.40
8736 0.2621 83.42 343.03
17472 0.5108 121.45 388.48
END
```

```
DATA REPEAT300 (t, CA, CF, CL)
2184 0.3874 112.38 364.36
```

5040 0.3720 111.41 434.77
8736 0.5021 136.17 742.07
17472 0.8419 222.43 675.65
END

DATA REPEAT550 (t, CA, CF, CL)
2184 1.3843 188.79 679.59
5040 0.5876 147.80 820.60
8736 0.7769 218.62 1200.73
17472 1.5751 298.40 1093.45
END

DATA REPEAT1000 (t, CA, CF, CL)
2184 1.7865 300.18 1240.06
5040 1.1940 339.25 1656.99
8736 1.6702 418.44 2510.02
17472 3.0544 396.12 1593.60
END

Appendix III: Computer Code of the PBPK model for PCB126 (multiple dose QCT Ito's Study)

PROGRAM ito.csl

!Edited by M. Lohitnavy on Oct. 10th, 2007.
!Developed by Lohitnavy M. and Lu Y.

```
***** Experimental Conditions *****
!Data obtained from CETT (PCB126 alone) Study
!Male F344 rats were used.
!The rats were intraperitoneally administered with DEN on day0.
!PCB126 in corn oil was orally administered daily starting on day14 until sacrifices.
!There were 2 dosing levels; 3.3 (Low Dose) and 9.8 (High Dose) ug/kg BW/day.
!On day21, 2/3rd partial hepatectomy (PH) surgery was conducted.
!PCB126 dosing was stopped between day21-23.
!Then dosing was resumed until sacrifices.
!Body weight & liver weight data were available.
***** End of the Conditions *****

***** Features of this PBPK model; *****
!Binding between PCB126 and CYP1A2 in the liver,
!Binding between PCB126 and aromatic hydrocarbon receptor (AhR) in the liver,
!Excretion of PCB126 via hepatic Mrp2,
!Physiological changes due to PH.
***** End of the model features *****
```

INITIAL

```
!Volume and blood flow parameters
!Body Wt data were taken from CETT PCB126 alone study.
!Table Function of Body Weight Data from the High Dose Group (9.8 ug/kg/day)
!Table BWHight, 1,6/336,480,576,672,1128,1344,&
.2, .21, .206, .213, .268, .286/
!Table Function of Body Weight Data from the Low Dose Group (3.3 ug/kg/day)
!Table BLOWt, 1,6/336,480,576,672,1128,1344,&
.2, .216, .21, .21, .259, .292/
```

!Statement for changing BW data according to dosing groups.

```
If (doserate0.eq,9800) then
```

```
BW=BWhight(t)
```

```
elseif (doserate0.eq,3300) then
```

```
BW=BWlowt(t)
```

```
endif
```

!Liver weight data were taken from CETT PCB126 alone study.

```
!Liver weight data from the High Dose Group (9.8 ug PCB126/kg/day)
!Table VLhight, 1,7/336, 503.9, 504,576,672,1128,1344,&
```

0.0074,.0078,.0024, .0058, .0070, .0097, 0.0103/

!Liver weight data from the Low Dose Group (3.3 ug PCB126/kg/day)
Table VLlowt, 1,7/336, 503.9, 504,576,672,1128,1344,&
0.0074,.0078, 0.0024, 0.0059, 0.0071, 0.0098, 0.0099/

!Statement for changing liver weight according to dosing groups.

```
  If (doserate0.eq.9800) then
    VL=VLhight(t)
  elseif (doserate0.eq.3300) then
    VL=VLlowt(t)
  Endif
```

!Physiological Constants

```
CONSTANT VFC=0.05           !Fat volume fraction.
CONSTANT VRC=0.052         !Rapidly perfused volume fraction
CONSTANT VBC=0.062D0      !blood volume
CONSTANT QCC=14.1D0       !blood flow constant
CONSTANT QFC=0.07D0
CONSTANT QLC=0.18D0
CONSTANT QRC=0.58D0
      QSC=1.0-QFC-QLC-QRC
```

!Scaled parameters

```
VF=BW*VFC                 !total fat volume;
!VL=BW*VLC                !total liver volume;
VB=BW*VBC+0.0012         !blood.Lee&Blafox
VR=BW*VRC                 !Rapidly perfused volume
VS=0.91*BW-VF-VL-VB-VR  !slowly perfused
      QC=QCC*BW**0.75    !blood flow rate
      QF=QC*QFC
      QL=QC*QLC
      QR=QC*QRC
      QS=QC*QSC
```

!Chemical-specific paramters

```
!Partition coefficients
CONSTANT PF=155.         !from the NTP model
CONSTANT PL=8.9D0       !from the NTP model
CONSTANT PR=6.0D0       !from the NTP model
CONSTANT PS=7.2D0       !from the NTP model
```

!Elimination parameters

```
CONSTANT KGILV=0.1433   !/hr,absorption rate, from GI to liver
CONSTANT KFEC=0.00      !/hr,excretion in feces
CONSTANT KMET=0.00D0    !/hr, PCB126 metabolism rate
```

```

CONSTANT KLIV=0.0                !First order elimination from the liver.

!PCB 126 Excretion via Mrp2 is mathematically described using
!the Michealis-Menten Equation; C=Vmax*C/(Km+C)
!***** PCB126 Section for Mrp2-mediated excretion from the liver*****
      Vmax= 64.59                !Maximal velocity of Mrp2
                                   !optimized value
CONSTANT Km=7.76e3              !Binding affinity of Mrp2
                                   !calculated Km by Hirono S.(unit, nM)
!*****END of Mrp2-mediated excretion*****

!Constants related to protein binding
!PCB126 binding in the liver consists of binding to CYP1A2 and AhR.
!*****PCB126 SECTION FOR LIVER BINDING*****
CONSTANT  BM1 = 0.004           !PCB126 binding capacity to Ah
CONSTANT  KB1 = .05637         !PCB126 binding constant for Ah
      BM2O = 10.                !Binding protein: capacity (nmoles/liver)
CONSTANT BM2IO = 101.25       !Increase due to induction (nmoles/liver)
CONSTANT  KB2 = 5.5437        !Binding protein: affinity (nM)
CONSTANT   N = 1.              !Hill Coefficient
CONSTANT  KD = 1.              !Liganded receptor-DNA binding
CONSTANT slope=0.0066         !Slope of the increase in capacity (nmol/hr)
                                   !Optimized value
!*****END of PCB126 Binding*****

!Dosetime and frequency
DoseFrq=24.0                    !hrs
k=0                              !counter of doses

!Simulation parameters
CONSTANT MW=326.4              !molecular weight of PCB126
CONSTANT doserate0=30          !ng/kg
      DoseRate=doserate0       !ng/kg
      Dose = DoseRate*BW/MW    !nmole
CONSTANT tstop=1500.0         !hr
cinterval CINT=0.1

!Initial value of total dose
TotalDose=0.0

END                              !END of Initial

DYNAMIC
ALGORITHM IALG=2

!On Day21, a partial hepatectomy (PH) surgery was conducted.

```

```

!2/3rd of the liver was surgically removed.
!Amount removed with 2/3rd liver
IF (T.eq.503.9) THEN
  AL=AL*0.3
  ARemove=AL*0.7
ELSE
  AL=AL
ENDIF
!These lines must be in this part;otherwise it is wrong.

```

```

!Setting an increase in Mrp2-mediated excretion after 2/3rd PH surgery
If (t.ge.504 .and. t.le.576) then
  vmax = 2000.
  BM2O = .3*10.      !30% remaining of CYP1A2 due to 2/3rd PH
else
  vmax=64.59
  BM2O = 10.
endif

```

```

DERIVATIVE
If (doserate0.eq.9800) then
  BW=BWhight(t)
  elseif (doserate0.eq.3300) then
  BW=BWlowt(t)
endif
If (doserate0.eq.9800) then
  VL=VLhight(t)
  elseif (doserate0.eq.3300) then
  VL=VLlowt(t)
endif

```

```

!Scaled parameters
VF=BW*VFC          !total fat volume;
VB=BW*VBC+0.0012  !blood.Lee&Blafox
VR=BW*VRC          !Rapidly perfused volume
VS=0.91*BW-VF-VL-VB-VR !slowly perfused
QC=QCC*BW**0.75   !blood flow rate
QF=QC*QFC
QL=QC*QLC
QR=QC*QRC
QS=QC*QSC

```

```

!Time-dependent increase in CYP1A2 expression
BM2I = BM2I0+slope*t

```

```

!Mass balance in fat tissue
RAF=QF*(CA-CVF)

```

AF=INTEG(RAF,0.0)
 CF=AF/VF
 CVF=CF/PF

!Mass balance in liver

!Protein binding terms in the liver were added.

!An Mrp2 excretion term, $V_{max} * CVL / (K_m + CVL)$, is added.

$RAL = QL * (CA - CVL) - KMET * CVL + KGILV * AGI - (V_{max} * CVL / (K_m + CVL)) - KLIV * CVL$

AL=INTEG(RAL,0.0) !Amount of PCB126 in the livers (nmole)
 CL=AL/VL !Calculations of liver conc of PCB126 (nM)
 AUCLIV=integ(CL,0.0) !Calculations of AUC of liver PCB126 (nM*h)
 PLiv=AL*100/(TOTALDOSE+1.0e-30) !% Retention of PCB126 in the livers
 !compared to total administered dose(%)

!*****Calculations of Mrp2-mediated excretion*****

RMrp2= $V_{max} * CVL / (K_m + CVL)$!Rate of excretion via mrp2 (nM*h)
 Mrp2=INTEG(RMrp2,0.0) !Amount of excretion via mrp2 (nmole)
 PMrp2=Mrp2*100/(TOTALDOSE+1.0e-30) !Efficiency in Mrp2 excretion
 !compared to total amount of liver PCB126 (%)
 Combine=PLIV+PMrp2 !Combination between liver retention and
 !Mrp2 excretion compared to total dose (%)
 Other=100-Combine !Mass deposited elsewhere (%)

!***** End of Mrp2-mediated excretion section*****

Procedural

$CVL_t = al / (vl * pl + bm1 / (kb1 + cvl) + bm2t / (kb2 + cvl))$
 CVL = CVL_t
 AhRBound= $bm1 * cvl / (kb1 + cvl)$!Amount of PCB126 bound to AhR
 CYPBound= $bm2t * cvl / (kb2 + cvl)$!Amount of PCB126 bound to CYP1A2
 END !End of Procedural

!*****Calculations of AhR-PCB126 Binding*****

DB1 = $BM1 * Cv1 / (KB1 + Cv1) / VL$!Conc. of AhR-PCB126 complex
 BOUND = $(db1 ** n) / (db1 ** n + Kd ** n)$!Occupancy of DRE on DNA
 PB1 = $Cv1 / (KB1 + Cv1)$!AhR percent occupancy
 BM2T = $BM2O + BM2I * BOUND$!Instantaneous level of protein induction
 !*****End of AhR-PCB126 Binding section*****

!Amount metabolized

RAM=KMET*CVL
 AM=INTEG(RAM,0.0)

!Mass balance in rapidly perfused tissues

RAR=QR*(CA-CVR)
 AR=INTEG(RAR,0.0)

CR=AR/VR
CVR=CR/PR

!Mass balance in slowly perfused tissues
RAS=QS*(CA-CVS)
AS=INTEG(RAS,0.0)
CS=AS/VS
CVS=CS/PS

!Mass balance in blood
RABlood=QF*CVF+QL*CVL+QR*CVR+QS*CVS-QC*CA
ABlood=INTEG(RABlood,0.0)
CA=ABlood/VB !Blood concentration

!GI lumen
RAGI=-KGILV*AGI-KFEC*AGI
AGI=INTEG(RAGI,0.0)+totalDOSE

!Excretion in feces
RAFEC=KFEC*AGI+(Vmax*CVL/(Km+CVL))+KLIV*CVL
AFEC=INTEG(RAFEC,0.0)
PFEC=AFEC*100/(TOTALDOSE+1.0e-30) !% Fecal excretion compared
!to total administered dose (%)

!Total mass
TMASS=AF+AL+AM+AR+AS+ABlood+AGI+AFEC
MB=(TOTALDose-TMASS)*100.0/(TOTALDose+11.0e-30)

!Since dosing was stopped on day21 (PH), 22 and 23
!Statement to stop PCB126 dosing for 3 days
Procedural

```
IF (t.lt.336.0) THEN
    Doserate=0.0D0 !ng PCB126/kg/day
    Dose=0.0
ELSE IF (t.gt.480.0 .and. t.lt.600) THEN
    Doserate=0.0
    Dose=0.0
ELSE
    Doserate=Doserate0 !ng PCB126/kg/day
    Dose=BW*Doserate/MW
ENDIF
```

!Addition of 1 more dose when the time meets the dosing time.
dosetime=k*DoseFrq
IF (t.ge.dosetime) THEN
TotalDose=TotalDose+Dose

```
                k=k+1
                ENDIF
END                ! END of Procedural

TERMT (T.GE.TSTOP)

END                !END of Derivative
END                !END of Dynamic
!-----!-----!-----!-----!-----!-----!-
END                !END of Program
```

```
!File ito.cmd
!Command file for PBPK model of PCB126 (Ito's study)
!Edited by Lohitnavy M on Oct. 10th, 2007.
```

```
set grdcpl=.f. !no grid on line plots
SET TITLE = 'PCB126 model-Male F344 rat multiple oral dose'
prepare /all
```

```
procedure check
start
plot tmass, mb
print t,tmass,mb
end
```

```
start
```

```
PROCED low
set doserate0 = 3300
start
PLOT /DATA=Low CF /lo=0 /char=2 /xtag='hr' /tag='Fat nmole/L'
PLOT /DATA=Low CL /log /lo=10. /hi=10000. /char=1 /xtag='hr' /tag='Liver
nmole/L'
PLOT /DATA=Low CA /lo=0 /char=3 /xtag='hr' /tag='Blood nmole/L'
PLOT /DATA=Low CR /lo=0 /char=3 /xtag='hr' /tag='Rapidly Perfused nmole/L'
PLOT /DATA=Low CS /lo=0 /char=3 /xtag='hr' /tag='Slowly Perfused nmole/L'
END
```

```
PROCED high
set doserate0 = 9800
start
PLOT /DATA=high CF /lo=0 /char=2 /xtag='hr' /tag='Fat nmole/L'
PLOT /DATA=high CL /log /lo=100. /hi=10000 /char=1 /xtag='hr' /tag='Liver
nmole/L'
PLOT /DATA=high CA /lo=0 /char=3 /xtag='hr' /tag='Blood nmole/L'
PLOT /DATA=high CR /lo=0 /char=3 /xtag='hr' /tag='Rapidly Perfused nmole/L'
PLOT /DATA=high CS /lo=0 /char=3 /xtag='hr' /tag='Slowly Perfused nmole/L'
END
```

```
Data low (t, CL, CF, CA, CR, CS)
480 368.87 0.00 1.09 0.00 0.45
576 0.01 0.00 0.52 0.00 1.47
672 940.87 0.00 0.50 2.34 1.36
1128 1106.92 17.31 1.72 9.51 0.82
1344 1278.49 11.61 4.37 5.08 1.00
END
```

Data high (t, CL, CF, CA, CR, CS)

480	1526.04		0.00	0.57	0.00	0.45
576	0.01	0.00	1.16	0.81	1.80	
672	3946.69		23.84	0.68	1.26	1.88
1128	5355.70		37.41	2.00	5.21	2.29
1344	4847.43		11.70	4.53	1.76	1.85

END

Appendix IV: Computer Code of the PBPK model for PCB126 (Fisher's single dose Study)

PROGRAM Fisher.csl

!Edited by M. Lohitnavy on Oct. 10th, 2007.

!PBPK modeling of PCB126.

!The program was modified to simulate data from Fisher et al (2006).

!Developed by Lohitnavy M.

!***** Experimental Conditions *****'

!Female SD rats (aged 20-22 weeks) were orally administered

!with a single dose of PCB126 in corn oil.

!There were three dosing levels; 7.5, 75 and 275 ug PCB126/kg BW.

!***** End of the Conditions*****'

!***** Features of this PBPK model; *****'

!Binding between PCB126 and CYP1A2 in the liver,

!Binding between PCB126 and aromatic hydrocarbon receptor (AhR) in the liver,

!Excretion of PCB126 via hepatic Mrp2.

!***** End of the model features *****'

INITIAL

!Volume and blood flow parameters

!BW data taken from Fisher et al (2006) study

Table BW7t, 1,5/0,120,216,360,528,&

0.163,0.212,0.243,0.272,0.307/

Table BW75t, 1,5/0,120,216,360,528,&

0.163,0.208,0.227,0.261,0.293/

Table BW275t, 1,5/0,120,216,360,528,&

0.163,0.214,0.228,0.253,0.287/

!Statement for changing BW data according to dosing groups.

If (doserate.eq.7500) then

 BW=BW7t(t)

 elseif (doserate.eq.75000) then

 BW=BW75t(t)

 elseif (doserate.eq.275000) then

 BW=BW275t(t)

endif

CONSTANT VFC=0.05

!Fat volume fraction.

CONSTANT VLC=0.038

!Liver Volume Fraction

CONSTANT VRC=0.052

!Rapidly perfused volume fraction

CONSTANT VBC=0.062D0

!blood volume

CONSTANT QCC=14.1D0

!blood flow constant

CONSTANT QFC=0.07D0
 CONSTANT QLC=0.18D0
 CONSTANT QRC=0.58D0
 QSC=1.0-QFC-QLC-QRC

!Scaled parameters

VF=BW*VFC !total fat volume;
 VL=BW*VLC !total liver volume;
 VB=BW*VBC+0.0012 !blood.Lee&Blafox
 VR=BW*VRC !Rapidly perfused volume
 VS=0.91*BW-VF-VL-VB-VR !slowly perfused
 QC=QCC*BW**0.75 !blood flow rate
 QF=QC*QFC
 QL=QC*QLC
 QR=QC*QRC
 QS=QC*QSC

!Chemical-specific paramters

!Partition coefficients

CONSTANT PF=155. !from the NTP model
 CONSTANT PL=8.9D0 !from the NTP model
 CONSTANT PR=6.0D0 !from the NTP model
 CONSTANT PS=7.2D0 !from the NTP model

!Elimination parameters

CONSTANT KGILV=0.1433 !/hr,absorption rate, from GI to liver
 CONSTANT KFEC=0.00 !/hr,excretion in feces
 CONSTANT KMET=0.00D0 !/hr, metabolism rate
 CONSTANT KLIV=0.0 !/hr, first order elimination from the liver.

!PCB 126 Excretion via Mrp2 is mathematically described using

!the Michealis-Menten Equation; $C=V_{max} * C / (K_m + C)$

!***** PCB126 Section for Mrp2-mediated excretion from the liver*****'

CONSTANT Vmax= 64.59 !Maximal velocity of Mrp2
 !optimized value
 CONSTANT Km=7.76e3 !Binding affinity of Mrp2
 !calculated Km by Hirono S.(unit, nM)

!*****END of Mrp2-mediated excretion*****'

!Simulation parameters

CONSTANT MW=326.4 !molecular weight of PCB126
 CONSTANT DoseRate=1000. !ng/kg
 Dose = DoseRate*BW/MW !nmole
 CONSTANT tstop=25.0 !hr
 cinterval CINT=0.1

```

! Protein Binding
!PCB126 binding in the liver consists of binding to CYP1A2 and AhR.
!*****PCB126 SECTION FOR LIVER BINDING*****
CONSTANT BM1 = 0.004      !PCB126 binding capacity to AhR
CONSTANT KB1 = 0.05637   !PCB126 binding constant for AhR
                           !Optimized value
CONSTANT BM2O = 10.      !Binding protein: capacity (nmoles/liver)
CONSTANT BM2I = 101.25   !Increase due to induction (nmoles/liver)
                           !Optimized value
CONSTANT KB2 = 5.5437    !Binding protein: affinity (nM)
                           !Optimized value
CONSTANT N = 1.          !Hill Coefficient
CONSTANT KD = 1.         !Liganded receptor-DNA binding
!*****END of PCB126 Binding*****

```

```

END !END of Initial
!-----!-----!-----!-----!-----!-----!-

```

```

DYNAMIC
ALGORITHM IALG=2

```

```

DERIVATIVE
!Statement for changing BW data according to dosing groups.
If (doserate.eq.7500) then
    BW=BW7t(t)
    elseif (doserate.eq.75000) then
    BW=BW75t(t)
    elseif (doserate.eq.275000) then
    BW=BW275t(t)
endif

```

```

!Mass balance in fat tissue
RAF=QF*(CA-CVF)
AF=INTEG(RAF,0.0)
CF=AF/VF
CVF=CF/PF

```

```

!Mass balance in liver
!Protein binding terms in the liver were added.
!An Mrp2 excretion term,  $V_{max} \cdot CVL / (K_m + CVL)$ , is added.
RAL=QL*(CA-CVL)-KMET*CVL+KGILV*AGI &
-( $V_{max} \cdot CVL / (K_m + CVL)$ )-KLIV*CVL
AL=INTEG(RAL,0.0)      !Amount of PCB126 in the livers (nmole)
CL=AL/VL              !Calculations of conc of PCB126 in the livers (nM).
AUCLIV=integ(CL,0.0)  !Calculations of AUC of PCB126 in the livers (nM*h).
PLiv=AL*100/Dose      !% Retention of PCB126 in the livers

```

!compared to total administered dose(%)

```
!*****Calculations of Mrp2-mediated excretion*****  
RMrp2= Vmax*CVL/(Km+CVL)      !Rate of excretion via mrp2 (nM*h)  
Mrp2=INTEG(RMrp2,0.0)        !Amount of excretion via mrp2 (nmole)  
PMrp2=Mrp2*100/(DOSE+1.0e-30) !Efficiency in Mrp2 excretion  
                                !compared to total amount of PCB126 in the liver(%)  
Combine=PLIV+PMrp2           !Combination between liver retention and  
                                !Mrp2 excretion compared to total dose (%)  
Other=100-Combine           !Mass deposited elsewhere (%)  
!***** End of Mrp2-mediated excretion section*****
```

Procedural

CVLt= al/(v1*pl+bm1/(kb1+cv1)+bm2t/(kb2+cv1))

CVL = CVLt

END

!End of Procedural

```
!*****Calculations of AhR-PCB126 Binding*****  
DB1 = BM1*Cv1/(KB1+Cv1)/VL    !Conc. of AhR-PCB126 complex  
BOUND = (db1**n)/(db1**n+Kd**n) !Occupancy of DRE on DNA  
PB1 = Cv1/(KB1+Cv1)           !AhR percent occupancy  
BM2T = BM2O+BM2I*BOUND        !Instantaneous level of protein induction  
!*****End of AhR-PCB126 Binding section *****
```

!Amount metabolized

RAM=KMET*CVL

AM=INTEG(RAM,0.0)

!Mass balance in rapidly perfused tissues

RAR=QR*(CA-CVR)

AR=INTEG(RAR,0.0)

CR=AR/VR

CVR=CR/PR

!Mass balance in slowly perfused tissues

RAS=QS*(CA-CVS)

AS=INTEG(RAS,0.0)

CS=AS/VS

CVS=CS/PS

!Mass balance in blood

RABlood=QF*CVF+QL*CVL+QR*CVR+QS*CVS-QC*CA

ABlood=INTEG(RABlood,0.0)

CA=ABlood/VB !Blood concentration

```

!GI lumen
RAGI=-KGILV*AGI-KFEC*AGI
AGI=INTEG(RAGI,Dose)

!Excretion in feces
RAFEC=KFEC*AGI+(Vmax*CVL/(Km+CVL))
AFEC=INTEG(RAFEC,0.0)
PFEC=AFEC*100/Dose      !% Fecal excretion compared to total dose (%)

!Total mass
TMASS=AF+AL+AM+AR+AS+ABlood+AGI+AFEC
MB=(Dose-TMASS)*100.0/Dose

TERMT (T.GE.TSTOP)

END  !END of Derivative
END  !END of Dynamic
!-----!-----!-----!-----!-----!-----!-----!-
END  !END of Program

```

```
!File Fisher.cmd
!Command file for oral single dose study of PCB126.
!To simulate data taken from Fisher et al (2006).
!Edited by M. Lohitnavy on Oct. 10th, 2007.

set grdcpl=.f. !no grid on line plots
SET TITLE = 'PCB126 model- Female SD rat single oral dose'
prepare /all
```

```
procedure check
start
plot tmass, mb
print t,tmass,mb
end
```

```
!To simulate the data from Fisher et al (2006)
!Dosing level is 7.5 ug/kg
Proced fisher7.5
set doserate=7500
set tstop=528
start
PLOT /DATA=Fisher7.5 CL /log /lo=1.0 /hi=1000 /char=1 /xtag='hr' /tag='Liver
nmole/L'
END
```

```
!To simulate the data from Fisher et al (2006)
!Dosing level is 75 ug/kg
Proced fisher75
set doserate=75000
set tstop=528
start
PLOT /DATA=Fisher75 CL /log /lo=1.0 /hi=10000 /char=1 /xtag='hr' /tag='Liver
nmole/L'
END
```

```
!To simulate the data from Fisher et al (2006)
!Dosing level is 275 ug/kg
Proced fisher275
set doserate=275000
set tstop=528
start
PLOT /DATA=Fisher275 CL /log /lo=1.0 /hi=10000 /char=1 /xtag='hr' /tag='Liver
nmole/L'
END
```

DATA Fisher7.5 (T,CL)

24	276.2
72	206.0
120	213.7
216	148.1
360	102.7
528	97.2

END

DATA Fisher75 (T,CL)

24	2399.7
72	2882.2
120	1997.9
216	2149.8
360	1545.9
528	1335.1

END

DATA Fisher275 (T,CL)

24	6222.2
72	5782.5
120	5998.3
216	4994.0
360	4234.8
528	3337.2

END

**Appendix V: Computer Code of the PBPK model for methotrexate in mice
(Bischoff's model)**

PROGRAM mice.csl

!Edited by M. Lohitnavy on Oct. 10th, 2007.

!Developed by Lohitnavy M. and Lu Y.

!Reconstruction of MTX PBPK model

!Original model by Bischoff (1971).

!Single dose of MTX was orally administered to mice.

!There were 2 dosing levels; 3 and 300 mg/kg bw.

!In original model, the PBPK model consists of blood, liver, GI, kidney,

!and muscle subcompartment.

!MTX is excreted into the bile to GI tract and, then, reabsorbed.

!Enterohepatic re-circulation is responsible for prolonged half-life of MTX.

INITIAL

!Volume and blood flow parameters

!All parameters were taken from the paper

!Units are transformed to forms of which compatible with ACSL.

CONSTANT BW=0.022 !Body weight of a mouse (kg)

CONSTANT VP=0.001 !Volume of plasma (L)

CONSTANT VM=0.010 !Volume of muscle (L)

CONSTANT VK=0.00034 !Volume of kidney (L)

CONSTANT VL=0.0013 !Volume of liver (L)

CONSTANT VGT=0.0015 !Volume of GI tract (L)

CONSTANT VGL=0.0015 !Volume of gut lumen (L)

CONSTANT QM=.03 !Blood flow to muscle (L/h)

CONSTANT QK=.048 !Blood flow to kidney (L/h)

CONSTANT QL=.066 !Blood flow to liver (L/h)

CONSTANT QGT=.054 !Blood flow to GI tract (L/h)

CONSTANT PM=.15 !Partition coefficient of muscle

CONSTANT PK=3.0 !Partition coefficient of kidney

CONSTANT PL=10.0 !Partition coefficient of liver

CONSTANT PGT=1.0 !Partition coefficient of GI tract

CONSTANT BMaxM=0.0 !Maximal binding capacity in muscle (mg/L)

CONSTANT BMaxK=0.27 !Maximal binding capacity in kidney (mg/L)

CONSTANT BMaxL=0.28 !Maximal binding capacity in liver (mg/L)

CONSTANT BMaxGT=0.147 !Maximal binding capacity in GI tract (mg/L)

CONSTANT KmBind=1e-5 !Protein binding parameter (mg/L)

CONSTANT KKidney=0.012 !kidney clearance rate constant (L/h)

CONSTANT KBile= 0.024 !Biliary clearance rate constant (L/h)

```

CONSTANT TGI=1.67          !GI transit time (h)
CONSTANT KF=.60           !Rate of MTX mass-tranferred down
                          !through the smallintestine (/h)
!*****!
!In this model, Absorption of MTX from GI is described by a first order rate constant
!and a saturable process. In this process, Michelis-Menten equation is employed.
!VmaxGI is similar to Vmax and KG is similar to Km in M-M equation.
!Kabs is a first order GI absorption rate constant.
CONSTANT VmaxGT=.012      !M-M absorption maximum rate into GI (mg/h)
CONSTANT KmGT=6.0        !M-M absorption paramter into GI tissue (mg/L)
CONSTANT Kabs=0.00006    !First order GI absorption rate constant(L/h)
!*****!
!Simulation parameters
CONSTANT MW=454.44       !molecular weight of MTX
CONSTANT DoseRate=3.0    !mg/kg
Dose = DoseRate*BW       !mg
CONSTANT tstop=6.0      !hr
cinterval CINT=0.01

END                        !END of Initial
!-----!-----!-----!-----!-----!-----!-----!-

DYNAMIC
ALGORITHM IALG=2

DERIVATIVE
!Mass balance in liver
RAL=(QL-QGT)*(CA-CVL)+QGT*(CVGT-CVL)-KBile*CVL
AL=INTEG(RAL,0.0)        !Amount of MTX (mg)
CL=AL/VL                !Calculations of conc of MTX (mg/L).
AUCLIV=integ(CL,0.0)    !Calculations of AUC of MTX (mg*h/L).
Procedural
      CVLt=AL/(VL*PL+BMaxL*VL/KmBind+CVL)
      CVL=CVLt
END                        !End of Procedural

!Biliary Excretion
RABile= KBile*CVL
ABile=integ(RABile, 0.0)

!Tranfer of MTX in bile into 3 segments; r1, r2 and r3.
r=Kbile*CVL
Rr1=(r-r1)*30.
r1=integ(Rr1, 0.0)
Ar1=integ(r1,0.0)

```


$RAGL3 = kf \cdot VGL \cdot CGL2 - .25 \cdot (VmaxGT \cdot CGL3 / (KmGT + CGL3) + Kabs \cdot CGL3) - kf \cdot VGL \cdot CGL3$
 $AGL3 = \text{integ}(RAGL3, 0.0)$
 $CGL3 = AGL3 / .25 / VGL$

$RAGL4 = kf \cdot VGL \cdot CGL3 - .25 \cdot (VmaxGT \cdot CGL4 / (KmGT + CGL4) + Kabs \cdot CGL4) - kf \cdot VGL \cdot CGL4$
 $AGL4 = \text{integ}(RAGL4, 0.0)$
 $CGL4 = AGL4 / .25 / VGL$

$RAGL = RAGL1 + RAGL2 + RAGL3 + RAGL4$
 $AGL = \text{integ}(RAGL, 0.)$
 $CGL = AGL / VGL$

!Fecal Excretion of MTX from GI Lumen
 $RAFeces = kf \cdot VGL \cdot CGL4$
 $AFEC = \text{integ}(RAFeces, 0.0)$

!GUT Tissue
 $RAGT = QGT \cdot (CA - CVGT) + .25 \cdot (VmaxGT \cdot CGL1 / (KmGT + CGL1) + Kabs \cdot CGL1) + .25 \cdot (VmaxGT \cdot CGL2 / (KmGT + CGL2) + Kabs \cdot CGL2) + .25 \cdot (VmaxGT \cdot CGL3 / (KmGT + CGL3) + Kabs \cdot CGL3) + .25 \cdot (VmaxGT \cdot CGL4 / (KmGT + CGL4) + Kabs \cdot CGL4)$
 $AGT = \text{integ}(RAGT, 0.)$
 $CGT = AGT / VGT$
 Procedural
 $CVGTt = AGT / (VGT \cdot PGT + BMaxGT \cdot VGT / KmBind + CVGT)$
 $CVGT = CVGTt$

END !End of Procedural

!Total mass
 $TMASS = AGT + AGL + APls + AM + AK + AL + AFEC + AUrine$
 $MB = (Dose - TMASS) \cdot 100.0 / Dose$

TERMT (T.GE.TSTOP)

END !END of Derivative
 END !END of Dynamic
 !-----!-----!-----!-----!-----!-----!-----!
 END !END of Program

!File mice.cmd
!Edited by M. Lohitnavy on Oct. 10th, 2007.

set grdcpl=.f. !no grid on line plots
SET TITLE = 'MTX model- Mice'
prepare /all

start
procedure check
start
plot tmass, mb
print t,tmass,mb
end

proced all
s DoseRate=3.0
start
PLOT /DATA=iv CA /log /lo=0.01 /hi=50.0 cl /log /lo=0.01 /hi=50.0 &
ck /log /lo=0.01 /hi=50.0 cm /log /lo=0.01 /hi=50.0&
cgl /log /lo=0.01 /hi=50.0 /xhi=4.1 /xtag='hr' /tag='Tissue conc mg/L'
END

proced mousehigh
s doserate=300.
start
PLOT /DATA=mousehigh CA /log /lo=0.03 /hi=3000.0 &
cgl /log /lo=0.03 /hi=3000.0 /xhi=4.1 /xtag='hr' /tag='Tissue conc mg/L'
END

DATA iv (T,CA,CL, CK, CM, CGL)
0.02 5.40 19.12 12.73 0.41 1.05
0.05 4.28 28.31 9.11 0.50 3.70
0.17 2.04 17.02 ? 0.27 5.25
0.25 1.59 14.09 3.81 0.30 8.23
0.50 0.99 8.72 2.57 0.15 10.39
0.75 ? 6.62 1.74 0.25 17.78
1.00 0.30 4.16 1.00 ? 17.02
1.50 0.39 4.67 1.12 0.12 21.17
2.00 0.17 2.16 0.76 0.03 5.89
3.00 0.07 2.01 ? 0.03 8.85
4.00 0.13 2.01 0.71 0.02 2.89
END

DATA mousehigh (t, CA, CGL)
0.4 100.5 1304.7
0.8 24.8 1814.9

1.2	18.2	1961.5
1.3	10.2	2161.5
2.4	2.1	2203.9
3.0	1.4	439.8
3.3	4.2	265.4

END

Appendix VI: Computer Code of the PBPK model for methotrexate in rats (Bischoff's model)

PROGRAM rat.csl

!Edited by M. Lohitnavy on Oct. 10th, 2007.

!Developed by Lohitnavy M. and Lu Y.

!Reconstruction of MTX PBPK model

!Original model by Bischoff (1971).

!Single dose of MTX was intraperitoneally administered to rats.

!There were dosing 3 dosing levels; 0.5, 6, and 25 mg/kg.

!In the original model, the PBPK model consists of blood, liver, GI, gut lumen,

!kidney, and muscle subcompartment.

!MTX is excreted into the bile to GI tract and, then, reabsorbed.

!Enterohepatic re-circulation is responsible for prolonged half-life of MTX.

INITIAL

!Volume and blood flow parameters

!All parameters were taken from the paper

!Units are transformed to forms of which compatible with ACSL.

CONSTANT BW=0.2 !Body weight of a rat(kg)

CONSTANT VP=.009 !Volume of plasma (L)

CONSTANT VM=0.1 !Volume of muscle (L)

CONSTANT VK=0.0019 !Volume of kidney (L)

CONSTANT VL=0.0083 !Volume of liver (L)

CONSTANT VGT=0.011 !Volume of GI tract (L)

CONSTANT VGL=0.011 !Volume of gut lumen (L)

CONSTANT QM=.18 !Blood flow to muscle (L/h)

CONSTANT QK=.3 !Blood flow to kidney (L/h)

CONSTANT QL=.39 !Blood flow to liver (L/h)

CONSTANT QGT=.318 !Blood flow to GI tract (L/h)

CONSTANT PM=.15 !Partition coefficient of muscle

CONSTANT PK=3.0 !Partition coefficient of kidney

CONSTANT PL=3.0 !Partition coefficient of liver

CONSTANT PGT=1.0 !Partition coefficient of GI tract

CONSTANT BMaxM=0.0 !Maximal binding capacity in muscle (mg/L)

CONSTANT BMaxK=0.3 !Maximal binding capacity in kidney (mg/L)

CONSTANT BMaxL=0.5 !Maximal binding capacity in liver (mg/L)

CONSTANT BMaxGT=0.1 !Maximal binding capacity in GI tract (mg/L)

CONSTANT KmBind=1e-5 !Protein binding parameter (mg/L)

CONSTANT KKidney=0.066 !kidney clearance rate (L/h)

CONSTANT KBile= 0.18 !Biliary clearance rate (L/h)

CONSTANT TGI=1.67 !GI transit time (h)

```

!*****!
!In this model, Absorption of MTX from GI is described
!by a first order rate constant and a saturable process.
!In this process, Michelis-Menten equation is employed.
!VmaxGI is similar to Vmax
!and KG is similar to Km in M-M equation.
!Kabs is a first order GI absorption rate constant.
CONSTANT VmaxGT=1.2      !M-M absorption maximum rate into GI (mg/h)
CONSTANT KmGT=200.      !M-M absorption paramter into GI (mg/L)
CONSTANT Kabs=0.00006   !First order GI absorption rate constant (L/h)
!*****!
CONSTANT KF=.60         !Rate of MTX mass-tranferred down through
                        ! the small intestine (/h)

!Simulation parameters
CONSTANT MW=454.44      !molecular weight of MTX
CONSTANT DoseRate=6.0   !mg/kg
Dose = DoseRate*BW      !mg
CONSTANT tstop=6.0     !hr
cinterval CINT=0.01

END !END of Initial
!-----!-----!-----!-----!-----!-----!-----!-

DYNAMIC
ALGORITHM IALG=2

DERIVATIVE
!Mass balance in liver
RAL=(QL-QGT)*(CA-CVL)+QGT*(CVGT-CVL)-KBile*CVL
AL=INTEG(RAL,0.0)      !Amount of MTX (mg)
CL=AL/VL              !Calculations of conc of MTX (mg/L).
AUCLIV=integ(CL,0.0)  !Calculations of AUC of MTX (mg*h/L).
CVL=CL/PL

!Biliary Excretion
RABile= KBile*CVL
ABile=integ(RABile, 0.0)

!Tranfer of MTX in bile into 3 segments; r1, r2 and r3.
r=KBile*CVL
Rr1=(r-r1)*30.
r1=integ(Rr1, 0.0)
Ar1=integ(r1,0.0)

```

Rr2=(r1-r2)*30
r2=integ(Rr2, 0.0)
Ar2=integ(r2,0.0)

Rr3=(r2-r3)*30
r3=integ(Rr3, 0.0)
Ar3=integ(r3,0.0)

!Mass balance in kidney
RAK=QK*(CA-CVK)-KKidney*CVK
AK=INTEG(RAK,0.0)
CK=AK/VK
CVK=CK/PK

!Amount excreted in urine
RAUrine=KKidney*CVK
AUrine=integ(RAUrine, 0.0)

!Mass balance in muscle
RAM=QM*(CA-CVM)
AM=INTEG(RAM,0.0)
CM=AM/VM
CVM=CM/PM

!Mass balance in plasma
RAPls=QL*CVL+QK*CVK+QM*CVM-(QL+QK+QM)*CA
APls=integ(RAPls,0.)
CA=APls/VP

!Plasma concentration

!Gut lumen
RAGL1=KBile*CVL-.25*(VmaxGT*CGL1/(KmGT+CGL1)+Kabs*CGL1)&
-kf*VGL*CGL1
AGL1=integ(RAGL1,0.)
CGL1=AGL1/.25/VGL

RAGL2=kf*VGL*CGL1-.25*(VmaxGT*CGL2/(KmGT+CGL2)+Kabs*CGL2)&
-kf*VGL*CGL2
AGL2=integ(RAGL2,0.0)
CGL2=AGL2/.25/VGL

RAGL3=kf*VGL*CGL2-.25*(VmaxGT*CGL3/(KmGT+CGL3)+Kabs*CGL3)&
-kf*VGL*CGL3
AGL3=integ(RAGL3,0.0)
CGL3=AGL3/.25/VGL

RAGL4=kf*VGL*CGL3-.25*(VmaxGT*CGL4/(KmGT+CGL4)+Kabs*CGL4)&

```

- $kf \cdot VGL \cdot CGL4$ 
AGL4=integ(RAGL4,0.0)
CGL4=AGL4/.25/VGL

RAGL=RAGL1+RAGL2+RAGL3+RAGL4
AGL=integ(RAGL,0.)
CGL=AGL/VGL

!Fecal Excretion of MTX from GI Lumen
RAFeces= $kf \cdot VGL \cdot CGL4$ 
AFEC=integ(RAFeces, 0.0)

!GUT Tissue
RAGT=QGT*(CA-
CVGT)+.25*(VmaxGT*CGL1/(KmGT+CGL1)+Kabs*CGL1)+&
.25*(VmaxGT*CGL2/(KmGT+CGL2)+Kabs*CGL2)+&
.25*(VmaxGT*CGL3/(KmGT+CGL3)+Kabs*CGL3)+&
.25*(VmaxGT*CGL4/(KmGT+CGL4)+Kabs*CGL4)
AGT=integ(RAGT, dose)
CGT=AGT/VGT
CVGT=CGT/PGT

!Total mass
TMASS=AGT+AGL+APIs+AM+AK+AL+AFEC+AUrine
MB=(Dose-TMASS)*100.0/Dose

TERMT (T.GE.TSTOP)

END !END of Derivative
END !END of Dynamic
!-----!-----!-----!-----!-----!-----!-----!-
END !END of Program

```

!File rat.cmd
!Edited by M. Lohitnavy on Oct. 10th, 2007.

```
set grdcpl=.f. !no grid on line plots  
SET TITLE = 'MTX model- Rat'  
prepare /all
```

```
start  
procedure check  
start  
plot tmass, mb  
print t,tmass,mb  
end
```

```
proced rat  
s doserate=6.0  
start  
PLOT /DATA=rat CA /log /lo=0.01 /hi=100.0 cl /log /lo=0.01 /hi=100.0 &  
ck /log /lo=0.01 /hi=100.0 cm /log /lo=0.01 /hi=100.0&  
cgl /log /lo=0.01 /hi=100.0 /xhi=4.1 /xtag='hr' /tag='Tissue conc mg/L'  
END
```

```
proced rat0.5  
s doserate=0.5  
start  
PLOT /DATA=rat0.5 CA /log /lo=0.01 /hi=400.0 &  
cgl /log /lo=0.01 /hi=400.0 /xhi=4.1 /xtag='hr' /tag='Tissue conc mg/L'  
END
```

```
proced rat25  
s doserate=25.  
start  
PLOT /DATA=rat25 CA /log /lo=0.01 /hi=400.0 &  
cgl /log /lo=0.01 /hi=400.0 /xhi=4.1 /xtag='hr' /tag='Tissue conc mg/L'  
END
```

```
DATA RAT (T, CA,CL,CK, CM, CGL)  
0.25  5.22  17.28  14.35  0.69  13.77  
0.50  3.91  13.22  4.42  0.56  34.88  
0.92  1.45  6.03   3.52  0.20  59.67  
1.47  1.26  4.33   2.59  0.12  40.31  
2.00  0.70  3.24   1.06  0.09  59.67  
3.00  0.22  1.82   1.42  0.03  34.17  
4.00  0.33  1.36   ?      0.05  6.03  
END
```

DATA Rat0.5 (t, CA, CGL)

0.17	?	0.53
0.33	0.43	1.26
0.92	0.36	1.26
1.50	0.20	1.32
2.00	0.07	5.11
3.00	0.02	1.38
4.00	0.01	0.05

END

DATA Rat25 (t, CA, CGL)

0.17	26.44	42.56
0.33	25.82	60.82
0.92	10.20	161.43
1.50	5.24	177.56
2.00	1.84	121.31
3.00	0.86	82.89
4.00	0.57	21.85

END

Appendix VII: Computer Code of the PBPK model for methotrexate in dogs (Bischoff's model)

PROGRAM dog.csl

!Edited by M. Lohitnavy on Jan. 3rd, 2007.

!Developed by Lohitnavy M. and Lu Y.

!Reconstruction of MTX PBPK model

!Original model by Bischoff (1971).

!Single dose of MTX was intravenously administered to dogs.

!There was dosing 1 dosing level; 3 mg/kg.

!In the original model, the PBPK model consists of blood, liver, GI, gut lumen,

!kidney, and muscle subcompartment.

!MTX is excreted into the bile to GI tract and, then, reabsorbed.

!Enterohepatic re-circulation is responsible for prolonged half-life of MTX.

!There were two dogs in the experiment.

!Each dog was considered separately in this model.

!All other parameters in this model were identical to those in Bischoff et al. (1971).

INITIAL

!Volume and blood flow parameters

!All parameters were taken from the paper

!Units are transformed to forms of which compatible with ACSL.

CONSTANT BW=17.0 !Body weight of a dog(kg)

CONSTANT VP=.65 !Volume of plasma (L)

CONSTANT VM=7.5 !Volume of muscle (L)

CONSTANT VK=0.076 !Volume of kidney (L)

CONSTANT VL=0.360 !Volume of liver (L)

CONSTANT VGT=0.640 !Volume of GI tract (L)

CONSTANT VGL=0.640 !Volume of gut lumen (L)

CONSTANT QM=8.4 !Blood flow to muscle (L/h)

CONSTANT QK=11.4 !Blood flow to kidney (L/h)

CONSTANT QL=13.2 !Blood flow to liver (L/h)

CONSTANT QGT=11.4 !Blood flow to GI tract (L/h)

CONSTANT PM=.15 !Partition coefficient of muscle

CONSTANT PK=14.0 !Partition coefficient of kidney

CONSTANT PL=2.0 !Partition coefficient of liver

CONSTANT PGT=1.0 !Partition coefficient of GI tract

CONSTANT BMaxM=0.0 !Maximal binding capacity in muscle (mg/L)

CONSTANT BMaxK=0.3 !Maximal binding capacity in kidney (mg/L)

CONSTANT BMaxL=0.4 !Maximal binding capacity in liver (mg/L)

CONSTANT BMaxGT=0.1 !Maximal binding capacity in GI tract (mg/L)

CONSTANT KmBind=1e-5 !Protein binding parameter (mg/L)

```

CONSTANT KKidney=3.36      !kidney clearance rate s (L/h)
CONSTANT KBile= 0.48      !Biliary clearance rate (L/h)
CONSTANT TGI=1.67         !GI transit time (h)

!*****!
!In this model, Absorption of MTX from GI is described by a first order rate constant.
!and a saturable process. In this process, Michelis-Menten equation is employed.
!VmaxGI is similar to Vmax and KG is similar to Km in M-M equation.
!Kabs is a first order GI absorption rate constant.
CONSTANT VmaxGT=90.       !M-M absorption maximum rate into GI (mg/h)
CONSTANT KmGT=200.       !M-M absorption paramter into GI (mg/L)
CONSTANT Kabs=0.00006    !First order GI absorption rate constant (L/h)
!*****!
CONSTANT KF=.09          !Rate of MTX mass-transferred down through
                        !the small intestine (/h)

!Simulation parameters
CONSTANT MW=454.44       !molecular weight of MTX
CONSTANT DoseRate=3.0    !mg/kg
Dose = DoseRate*BW       !mg
CONSTANT tstop=6.0      !hr
cinterval CINT=0.01

END                      !END of Initial
!-----!-----!-----!-----!-----!-----!-----!-

DYNAMIC
ALGORITHM IALG=2

DERIVATIVE
!Mass balance in liver
RAL=(QL-QGT)*(CA-CL/PL)+QGT*(CGT/PGT-CL/PL)-KBile*CL/PL
AL=INTEG(RAL,0.0)       !Amount of MTX (mg)
CL=AL/VL                !Calculations of conc of MTX (mg/L).
AUCLIV=integ(CL,0.0)   !Calculations of AUC of MTX (mg*h/L).
CVL=CL/PL

!Biliary Excretion
RABile= KBile*CL/PL
ABile=integ(RABile, 0.0)

!Tranfer of MTX in bile into 3 segments; r1, r2 and r3.
r=kbile*CL/PL
Rr1=(r-r1)*30.
r1=integ(Rr1, 0.0)
Ar1=integ(r1,0.0)

```

Rr2=(r1-r2)*30
r2=integ(Rr2, 0.0)
Ar2=integ(r2,0.0)

Rr3=(r2-r3)*30
r3=integ(Rr3, 0.0)
Ar3=integ(r3,0.0)

!Mass balance in kidney
RAK=QK*(CA-CK/PK)-KKidney*CK/PK
AK=INTEG(RAK,0.0)
CK=AK/VK
CVK=CK/PK

!Amount excreted in urine
RAUrine=KKidney*CK/PK
AUrine=integ(RAUrine, 0.0)

!Mass balance in muscle
RAM=QM*(CA-CM/PM)
AM=INTEG(RAM,0.0)
CM=AM/VM
CVM=CM/PM

!Mass balance in plasma
RAPls=QL*CL/PL+QK*CK/PK+QM*CM/PM-(QL+QK+QM)*CA
APls=integ(RAPls,dose)
CA=APls/VP

!Plasma concentration

!Gut lumen
RAGL1=KBile*CL/PL&
-.25*(VmaxGT*CGL1/(KmGT+CGL1)+Kabs*CGL1)&
-kf*VGL*CGL1
AGL1=integ(RAGL1,0.0)
CGL1=AGL1/.25/VGL

RAGL2=kf*VGL*CGL1-.25*(VmaxGT*CGL2/(KmGT+CGL2)+Kabs*CGL2)&
-kf*VGL*CGL2
AGL2=integ(RAGL2,0.0)
CGL2=AGL2/.25/VGL

RAGL3=kf*VGL*CGL2-.25*(VmaxGT*CGL3/(KmGT+CGL3)+Kabs*CGL3)&
-kf*VGL*CGL3
AGL3=integ(RAGL3,0.0)
CGL3=AGL3/.25/VGL

```

RAGL4=kf*VGL*CGL3-.25*(VmaxGT*CGL4/(KmGT+CGL4)+Kabs*CGL4)&
-kf*VGL*CGL4
AGL4=integ(RAGL4,0.0)
CGL4=AGL4/.25/VGL

```

```

RAGL=RAGL1+RAGL2+RAGL3+RAGL4
AGL=integ(RAGL,0.)
CGL=AGL/VGL

```

```

!Fecal Excretion of MTX from GI Lumen
RAFeces=kf*VGL*CGL4
AFEC=integ(RAFeces, 0.0)

```

```

!GUT Tissue
RAGT=QGT*(CA-CGT/PGT)+&
.25*(VmaxGT*CGL1/(KmGT+CGL1)+Kabs*CGL1)+&
.25*(VmaxGT*CGL2/(KmGT+CGL2)+Kabs*CGL2)+&
.25*(VmaxGT*CGL3/(KmGT+CGL3)+Kabs*CGL3)+&
.25*(VmaxGT*CGL4/(KmGT+CGL4)+Kabs*CGL4)
AGT=integ(RAGT, 0.)
CGT=AGT/VGT
CVG=CGT/PGT

```

```

!Total mass
TMASS=AGT+AGL+APls+AM+AK+AL+AFEC+AUrine
MB=(Dose-TMASS)*100.0/Dose

```

```

TERMT (T.GE.TSTOP)

```

```

END !END of Derivative
END !END of Dynamic
!-----!-----!-----!-----!-----!-----!-----!-----!-
END !END of Program

```

```

!File dog.cmd
!Edited by M. Lohitnavy on Oct. 10th, 2007.
set grdcpl=.f. !no grid on line plots
SET TITLE = 'MTX model- Dogs'
prepare /all

start
procedure check
start
plot tmass, mb
print t,tmass,mb
end

proced dog1
start
PLOT /DATA=dog1 CA /log /lo=0.01 /hi=100.0 /char=1 cl /log /lo=0.01 /hi=100.0 &
/char=2 cm /log /lo=0.01 /hi=100.0 /char=3 cgl /log /lo=0.01 /hi=1000.0&
/xhi=4.1 /xtag='hr' /tag='Tissue MTX Conc (mg/L)'
END

proced dog2
start
PLOT /DATA=dog2 CA /log /lo=0.01 /hi=100.0 /char=1 cl /log /lo=0.01 /hi=100.0 &
/char=2 ck /log /lo=0.01 /hi=100.0 /char=3&
/xhi=4.1 /xtag='hr' /tag='Tissue MTX Conc (mg/L)'
END
DATA dog1 (T, CA,CL,CM, CGL)
0.05  19.54  ?    ?    ?
0.25  8.72  ?    ?    ?
0.5   6.74  ?    ?    ?
0.67  ?    14.85  ?    ?
1     3.76  ?    ?    ?
1.5   2.53  ?    ?    ?
2     2.17  ?    ?    ?
2.5   2.28  ?    ?    ?
3     1.92  3.95  0.53  7.60
END
DATA dog2 (t, CA, CL, CK)
0.25  8.14  ?    ?
0.5   5.48  ?    ?
1     3.16  ?    ?
1.5   2.36  ?    ?
2     1.79  ?    ?
2.5   1.48  ?    ?
3     1.46  2.57  19.88
END

```

Appendix VIII: Computer Code of the PBPK model for methotrexate in humans (Bischoff's model)

PROGRAM human.csl
!Edited by M. Lohitnavy on Oct. 10th, 2007.
!Developed by Lohitnavy M. and Lu Y.
!Reconstruction of MTX PBPK model
!Original model by Bischoff (1970).
!Single dose of MTX was intravenously administered to humans.
!There was dosing 1 dosing level; 1 mg/kg.
!In the original model, the PBPK model consists of blood, liver, GI, gut lumen,
!kidney, and muscle subcompartment.
!MTX is excreted into the bile to GI tract and, then, reabsorbed.
!Enterohepatic re-circulation is responsible for prolonged half-life of MTX.
!There were two humans in the experiment.
!Each subject was considered separately in this model.
!All other parameters in this model were identical to those in Bischoff et al. (1971).

INITIAL

!Volume and blood flow parameters
!All parameters were taken from the paper
!Units are transformed to forms of which compatible with ACSL.

CONSTANT BW=70.0	!Body weight of a rat(kg)
CONSTANT VP=3.0	!Volume of plasma (L)
CONSTANT VM=35.0	!Volume of muscle (L)
CONSTANT VK=0.28	!Volume of kidney (L)
CONSTANT VL=1.35	!Volume of liver (L)
CONSTANT VGT=2.1	!Volume of GI tract (L)
CONSTANT VGL=2.1	!Volume of gut lumen (L)
CONSTANT QM=25.2	!Blood flow to muscle (L/h)
CONSTANT QK=42.	!Blood flow to kidney (L/h)
CONSTANT QL=48.	!Blood flow to liver (L/h)
CONSTANT QGT=42.	!Blood flow to GI tract (L/h)
CONSTANT PM=.15	!Partition coefficient of muscle
CONSTANT PK=3.0	!Partition coefficient of kidney
CONSTANT PL=3.0	!Partition coefficient of liver
CONSTANT PGT=1.0	!Partition coefficient of GI tract
CONSTANT BMaxM=0.0	!Maximal binding capacity in muscle (mg/L)
CONSTANT BMaxK=0.3	!Maximal binding capacity in kidney (mg/L)
CONSTANT BMaxL=0.5	!Maximal binding capacity in liver (mg/L)
CONSTANT BMaxGT=0.1	!Maximal binding capacity in GI tract (mg/L)
CONSTANT KmBind=1e-5	!Protein binding parameter (mg/L)

CONSTANT KKidney=11.4 !kidney clearance rate s (L/h)
 CONSTANT KBile= 12. !Biliary clearance rate s (kL/KL, L/h)
 CONSTANT TGI=1.67 !GI transit time (h)

!*****!
 !In this model, Absorption of MTX from GI is described by a first order rate constant.
 !and a saturable process. In this process, Michelis-Menten equation is employed.
 !VmaxGI is similar to Vmax and KG is similar to Km in M-M equation.
 !b is a first order GI absorption rate constant.

CONSTANT VmaxGT=114. !M-M absorption maximum rate into GI (mg/h)
 CONSTANT KmGT=200. !M-M absorption paramter into GI (mg/L)
 CONSTANT Kabs=0.00006 !First order GI absorption rate constant(L/h)

!*****!
 CONSTANT KF=.06 !Rate of MTX mass-tranferred down through
 !the small intestine (/h)

!Simulation parameters
 CONSTANT MW=454.44 !molecular weight of MTX
 CONSTANT DoseRate=1.0 !mg/kg
 Dose = DoseRate*BW !mg
 CONSTANT tstop=6.0 !hr
 cinterval CINT=0.01

END !END of Initial
 !-----!-----!-----!-----!-----!-----!-----!-

DYNAMIC
 ALGORITHM IALG=2

DERIVATIVE
 !Mass balance in liver
 RAL=(QL-QGT)*(CA-CL/PL)+QGT*(CGT/PGT-CL/PL)-KBile*CL/PL
 AL=INTEG(RAL,0.0) !Amount of MTX (mg)
 CL=AL/VL !Calculations of conc of MTX (mg/L).
 AUCLIV=integ(CL,0.0) !Calculations of AUC of MTX (mg*h/L).
 CVL=CL/PL

!Biliary Excretion
 RABile= KBile*CL/PL
 ABile=integ(RABile, 0.0)

!Tranfer of MTX in bile into 3 segments; r1, r2 and r3.
 r=KBile*CL/PL
 Rr1=(r-r1)*30.
 r1=integ(Rr1, 0.0)
 Ar1=integ(r1,0.0)

Rr2=(r1-r2)*30
r2=integ(Rr2, 0.0)
Ar2=integ(r2,0.0)

Rr3=(r2-r3)*30
r3=integ(Rr3, 0.0)
Ar3=integ(r3,0.0)

!Mass balance in kidney
RAK=QK*(CA-CK/PK)-KKidney*CK/PK
AK=INTEG(RAK,0.0)
CK=AK/VK
CVK=CK/PK

!Amount excreted in urine
RAUrine=KKidney*CK/PK
AUrine=integ(RAUrine, 0.0)

!Mass balance in muscle
RAM=QM*(CA-CM/PM)
AM=INTEG(RAM,0.0)
CM=AM/VM
CVM=CM/PM

!Mass balance in plasma
RAPls=QL*CL/PL+QK*CK/PK+QM*CM/PM-(QL+QK+QM)*CA
APls=integ(RAPls, dose)
CA=APls/VP

!Plasma concentration

!Gut lumen
RAGL1=KBile*CL/PL&
-.25*(VmaxGT*CGL1/(KmGT+CGL1)+Kabs*CGL1)&
-kf*VGL*CGL1
AGL1=integ(RAGL1,0.0)
CGL1=AGL1/.25/VGL

RAGL2=kf*VGL*CGL1-.25*(VmaxGT*CGL2/(KmGT+CGL2)+Kabs*CGL2)&
-kf*VGL*CGL2
AGL2=integ(RAGL2,0.0)
CGL2=AGL2/.25/VGL

RAGL3=kf*VGL*CGL2-.25*(VmaxGT*CGL3/(KmGT+CGL3)+Kabs*CGL3)&
-kf*VGL*CGL3
AGL3=integ(RAGL3,0.0)
CGL3=AGL3/.25/VGL

```

RAGL4=kf*VGL*CGL3-.25*(VmaxGT*CGL4/(KmGT+CGL4)+Kabs*CGL4)&
-kf*VGL*CGL4
AGL4=integ(RAGL4,0.0)
CGL4=AGL4/.25/VGL

```

```

RAGL=RAGL1+RAGL2+RAGL3+RAGL4
AGL=integ(RAGL,0.)
CGL=AGL/VGL

```

```

!Fecal Excretion of MTX from GI Lumen
RAFeces=kf*VGL*CGL4
AFEC=integ(RAFeces, 0.0)

```

```

!GUT Tissue
RAGT=QGT*(CA-
CGT/PGT)+.25*(VmaxGT*CGL1/(KmGT+CGL1)+Kabs*CGL1)+&
.25*(VmaxGT*CGL2/(KmGT+CGL2)+Kabs*CGL2)+&
.25*(VmaxGT*CGL3/(KmGT+CGL3)+Kabs*CGL3)+&
.25*(VmaxGT*CGL4/(KmGT+CGL4)+Kabs*CGL4)
AGT=integ(RAGT, 0.)
CGT=AGT/VGT
CVG=CGT/PGT

```

```

!Total mass
TMASS=AGT+AGL+APls+AM+AK+AL+AFEC+AUrine
MB=(Dose-TMASS)*100.0/Dose

```

```

TERMT (T.GE.TSTOP)

```

```

END !END of Derivative
END !END of Dynamic
!-----!-----!-----!-----!-----!-----!-
END !END of Program

```

```
!File human.cmd
!Edited by M. Lohitnavy on Oct. 10th, 2007.
```

```
set grdcpl=.f. !no grid on line plots
SET TITLE = 'MTX model- Human'
prepare /all
```

```
start
procedure check
start
plot tmass, mb
print t,tmass,mb
end
```

```
proced human1
start
PLOT /DATA=human1 CA /log /lo=0.1 /hi=10. /char=1 /xhi=6.1 /xtag='hr' &
/tag='Blood conc mg/L'
END
```

```
proced human2
start
PLOT /DATA=human2 CA /log /lo=0.1 /hi=10. /char=1 /xhi=6.1 /xtag='hr' &
/tag='Blood conc mg/L'
END
```

```
DATA human1 (t,ca)
0.25  1.0744
0.75  0.7826
1      0.6808
2      0.4596
4      0.2912
6      0.2042
END
```

```
DATA human2 (t,ca)
0.25  1.85
0.75  1.30
1.00  1.02
2.42  0.54
5.00  0.23
END
```

Appendix IX: Computer Code of the PBPK model for methotrexate in mice (PBPK model with Mrp2)

PROGRAM miceKm.csl

!Edited by M. Lohitnavy on Oct. 10th, 2007.

!Original model by Bischoff (1971).

!Single dose of MTX was intravenously administered to mice.

!There were two dosing levels; 3 and 300 mg/kg.

!In the original model, the PBPK model consists of blood, liver, GI, gut lumen,

!kidney, and muscle subcompartment.

!MTX is excreted into the bile to GI tract and, then, reabsorbed.

!Enterohepatic re-circulation is responsible for prolonged half-life of MTX.

!The biliary excretion was replaced by Mrp2-mediated excretion.

!Value of Km of Mrp2 and Vmax of mrp2 were optimized.

!All other parameters in this model were identical to those in Bischoff et al. (1971).

INITIAL

!Volume and blood flow parameters

!All parameters were taken from the paper

!Units are transformed to forms of which compatible with ACSL.

CONSTANT BW=0.022 !Body weight of a mouse (kg)

CONSTANT VP=0.001 !Volume of plasma (L)

CONSTANT VM=0.010 !Volume of muscle (L)

CONSTANT VK=0.00034 !Volume of kidney (L)

CONSTANT VL=0.0013 !Volume of liver (L)

CONSTANT VGT=0.0015 !Volume of GI tract (L)

CONSTANT VGL=0.0015 !Volume of gut lumen (L)

CONSTANT QM=.03 !Blood flow to muscle (L/h)

CONSTANT QK=.048 !Blood flow to kidney (L/h)

CONSTANT QL=.066 !Blood flow to liver (L/h)

CONSTANT QGT=.054 !Blood flow to GI tract (L/h)

CONSTANT PM=.15 !Partition coefficient of muscle

CONSTANT PK=3.0 !Partition coefficient of kidney

CONSTANT PL=10.0 !Partition coefficient of liver

CONSTANT PGT=1.0 !Partition coefficient of GI tract

CONSTANT BMaxM=0.0 !Maximal binding capacity in muscle (mg/L)

CONSTANT BMaxK=0.27 !Maximal binding capacity in kidney (mg/L)

CONSTANT BMaxL=0.28 !Maximal binding capacity in liver (mg/L)

CONSTANT BMaxGT=0.147 !Maximal binding capacity in GI tract (mg/L)

CONSTANT KmBind=1e-5 !Protein binding parameter (mg/L)

CONSTANT KKidney=0.012 !kidney clearance rate constant (L/h)

CONSTANT KBile= 0.0 !Biliary clearance rate constant (L/h)

```

CONSTANT KmMrp2=154.03      !Km of Mrp2 (opimized value, mg/L)
CONSTANT VmaxMrp2=5.7038   !Vmax of Mrp2 (optimized value, mg/h)
CONSTANT TGI=1.67          !GI transit time (h)
CONSTANT KF=.60            !Rate of MTX mass-tranferred down through
                           !the small intestine (/h)

!*****!
!In this model, Absorption of MTX from GI is described by a first order rate constant.
!and a saturable process. In this process, Michelis-Menten equation is employed.
!VmaxGI is similar to Vmax and KG is similar to Km in M-M equation.
!Kabs is a first order GI absorption rate constant.
CONSTANT VmaxGT=.012       !M-M absorption maximum rate into GI (mg/h)
CONSTANT KmGT=6.0          !M-M absorption paramter into GI (mg/L)
CONSTANT Kabs=0.00006     !First order GI absorption rate constant (L/h)
!*****!

!Simulation parameters
CONSTANT MW=454.44        !molecular weight of MTX
CONSTANT DoseRate=3.0     !mg/kg
Dose = DoseRate*BW        !mg
CONSTANT tstop=6.0        !hr
cinterval CINT=0.01

END                          !END of Initial

DYNAMIC
ALGORITHM IALG=2

DERIVATIVE
!Mass balance in liver
RAL=(QL-QGT)*(CA-CL/PL)+QGT*(CGT/PGT-CL/PL)&
-KBile*CL/PL-(vmaxmrp2*cvl/(kmmrp2+cvl))
AL=INTEG(RAL,0.0)         !Amount of MTX (mg)
CL=AL/VL                  !Calculations of conc of MTX (mg/L).
AUCLIV=integ(CL,0.0)     !Calculations of AUC of MTX (mg*h/L).
CVL=CL/PL
Procedural
      CVLt=AL/(VL*PL+BMaxL*VL/KmBind+CVL)
      CVL=CVLt
END                          !End of Procedural

!Biliary Excretion
RABile= KBile*CL/PL+vmaxmrp2*cvl/(kmmrp2+cvl)
ABile=integ(RABile, 0.0)

!Tranfer of MTX in bile into 3 segments; r1, r2 and r3.
r=Kbile*CL/PL+vmaxmrp2*cvl/(kmmrp2+cvl)
Rr1=(r-r1)*30.

```



```

- $kf \cdot VGL \cdot CGL2$ 
AGL2=integ(RAGL2,0.0)
CGL2=AGL2/.25/VGL

RAGL3= $kf \cdot VGL \cdot CGL2 - .25 \cdot (VmaxGT \cdot CGL3 / (KmGT + CGL3) + Kabs \cdot CGL3)$ &
- $kf \cdot VGL \cdot CGL3$ 
AGL3=integ(RAGL3,0.0)
CGL3=AGL3/.25/VGL

RAGL4= $kf \cdot VGL \cdot CGL3 - .25 \cdot (VmaxGT \cdot CGL4 / (KmGT + CGL4) + Kabs \cdot CGL4)$ &
- $kf \cdot VGL \cdot CGL4$ 
AGL4=integ(RAGL4,0.0)
CGL4=AGL4/.25/VGL

RAGL=RAGL1+RAGL2+RAGL3+RAGL4
AGL=integ(RAGL,0.)
CGL=AGL/VGL

!Fecal Excretion of MTX from GI Lumen
RAFeces= $kf \cdot VGL \cdot CGL4$ 
AFEC=integ(RAFeces, 0.0)

!GUT Tissue
RAGT=QGT*(CA-CGT/PGT)+&
.25*(VmaxGT*CGL1/(KmGT+CGL1)+Kabs*CGL1)+&
.25*(VmaxGT*CGL2/(KmGT+CGL2)+Kabs*CGL2)+&
.25*(VmaxGT*CGL3/(KmGT+CGL3)+Kabs*CGL3)+&
.25*(VmaxGT*CGL4/(KmGT+CGL4)+Kabs*CGL4)
AGT=integ(RAGT, 0.0)
CVG=CGT/PGT
CGT=AGT/VGT
Procedural
      CVGTt=AGT/(VGT*PGT+BmaxGT*VGT/KMBind+CVGT)
      CVGT=CVGTt
END                                !End of Procedural

!Total mass
TMASS=AGT+AGL+APls+AM+AK+AL+AFEC+AUrine
MB=(Dose-TMASS)*100.0/Dose

TERMT (T.GE.TSTOP)

END  !END of Derivative
END  !END of Dynamic
!-----!-----!-----!-----!-----!-----!-----!-
END  !END of Program

```

!File miceKm.cmd
!Edited by M. Lohitnavy on Oct. 10th, 2007.

set grdcpl=.f. !no grid on line plots
SET TITLE = 'MTX model- Mice'
prepare /all

start
procedure check
start
plot tmass, mb
print t,tmass,mb
end

proced all
s DoseRate=3.0
start
PLOT /DATA=iv CA /log /lo=0.01 /hi=50.0 cl /log /lo=0.01 /hi=50.0 &
ck /log /lo=0.01 /hi=50.0 cm /log /lo=0.01 /hi=50.0&
cgl /log /lo=0.01 /hi=50.0 /xhi=4.1 /xtag='hr' /tag='Tissue conc mg/L'
END

proced mousehigh
s doserate=300.
start
PLOT /DATA=mousehigh CA /log /lo=0.03 /hi=3000.0 &
cgl /log /lo=0.03 /hi=3000.0 /xhi=4.1 /xtag='hr' /tag='Tissue conc mg/L'
END

DATA iv (T,CA,CL, CK, CM, CGL)
0.02 5.40 19.12 12.73 0.41 1.05
0.05 4.28 28.31 9.11 0.50 3.70
0.17 2.04 17.02 ? 0.27 5.25
0.25 1.59 14.09 3.81 0.30 8.23
0.50 0.99 8.72 2.57 0.15 10.39
0.75 ? 6.62 1.74 0.25 17.78
1.00 0.30 4.16 1.00 ? 17.02
1.50 0.39 4.67 1.12 0.12 21.17
2.00 0.17 2.16 0.76 0.03 5.89
3.00 0.07 2.01 ? 0.03 8.85
4.00 0.13 2.01 0.71 0.02 2.89
END

DATA mousehigh (t, CA, CGL)
0.4 100.5 1304.7
0.8 24.8 1814.9

1.2	18.2	1961.5
1.3	10.2	2161.5
2.4	2.1	2203.9
3.0	1.4	439.8
3.3	4.2	265.4

END

**Appendix X: Computer Code of the PBPK model for methotrexate in rats
(PBPK model with Mrp2)**

PROGRAM ratKm.csl
!Edited by M. Lohitnavy on Oct. 10th, 2007.
!Developed by Lohitnavy M. and Lu Y.
!Reconstruction of MTX PBPK model
!Original model by Bischoff (1970).
!Single dose of MTX was intraperitoneally administered to rats.
!There were dosing 3 dosing levels; 0.5, 6, and 25 mg/kg.
!In the original model, the PBPK model consists of blood, liver, GI, gut lumen,
!kidney, and muscle subcompartment.
!MTX is excreted into the bile to GI tract and, then, reabsorbed.
!Enterohepatic re-circulation is responsible for prolonged half-life of MTX.
!The zero-order biliary secretion was replaced by Mrp2-mediated excretion.
!Km of Mrp2 was taken from Hirono S. (2005)
!Value of Vmax of mrp2 was optimized.
!All other parameters in this model were identical to those in Bischoff et al. (1971).

INITIAL

!Volume and blood flow parameters
!All parameters were taken from the paper
!Units are transformed to forms of which compatible with ACSL.
CONSTANT BW=0.2 !Body weight of a rat(kg)
CONSTANT VP=.009 !Volume of plasma (L)
CONSTANT VM=0.1 !Volume of muscle (L)
CONSTANT VK=0.0019 !Volume of kidney (L)
CONSTANT VL=0.0083 !Volume of liver (L)
CONSTANT VGT=0.011 !Volume of GI tract (L)
CONSTANT VGL=0.011 !Volume of gut lumen (L)

CONSTANT QM=.18 !Blood flow to muscle (L/h)
CONSTANT QK=.3 !Blood flow to kidney (L/h)
CONSTANT QL=.39 !Blood flow to liver (L/h)
CONSTANT QGT=.318 !Blood flow to GI tract (L/h)

CONSTANT PM=.15 !Partition coefficient of muscle
CONSTANT PK=3.0 !Partition coefficient of kidney
CONSTANT PL=3.0 !Partition coefficient of liver
CONSTANT PGT=1.0 !Partition coefficient of GI tract

CONSTANT BMaxM=0.0 !Maximal binding capacity in muscle (mg/L)
CONSTANT BMaxK=0.3 !Maximal binding capacity in kidney (mg/L)
CONSTANT BMaxL=0.5 !Maximal binding capacity in liver (mg/L)
CONSTANT BMaxGT=0.1 !Maximal binding capacity in GI tract (mg/L)
CONSTANT KmBind=1e-5 !Protein binding parameter (mg/L)

```

CONSTANT KKidney=0.066      !kidney clearance rate (L/h)
CONSTANT KBile= 0.         !Biliary clearance rate (L/h)
CONSTANT kmmrp2= 153.984   !Km of mrp2 from Hirono S. (2005)
CONSTANT vmaxmrp2=36.20   !Vmax of mrp2 (mg/h)
                           !Optimized value
CONSTANT TGI=1.67         !GI transit time (h)

```

```

!*****!
!In this model, Absorption of MTX from GI is described by a first order rate constant.
!and a saturable process. In this process, Michelis-Menten equation is employed.
!VmaxGI is similar to Vmax and KG is similar to Km in M-M equation.
!b is a first order GI absorption rate constant.

```

```

CONSTANT VmaxGT=1.2        !M-M absorption maximum rate into GI (mg/h)
CONSTANT KmGT=200.        !M-M absorption paramter into GI (mg/L)
CONSTANT Kabs=0.00006     !First order GI absorption rate constant (L/h)
!*****!
CONSTANT KF=.60           !Rate of MTX mass-transferred down through
                           !the small intestine (/h)

```

```

!Simulation parameters
CONSTANT MW=454.44        !molecular weight of MTX
CONSTANT DoseRate=6.0     !mg/kg
Dose = DoseRate*BW        !mg
CONSTANT tstop=6.0       !hr
cinterval CINT=0.01

```

```

END !END of Initial
!-----!-----!-----!-----!-----!-----!-----!

```

```

DYNAMIC
ALGORITHM IALG=2

```

```

DERIVATIVE
!Mass balance in liver
RAL=(QL-QGT)*(CA-CL/PL)+QGT*(CGT/PGT-CL/PL)-&
(vmaxmrp2*CVL/(kmmrp2+cvl))-KBile*CL/PL
AL=INTEG(RAL,0.0)        !Amount of MTX (mg)
CL=AL/VL                 !Calculations of conc of MTX (mg/L).
AUCLIV=integ(CL,0.0)     !Calculations of AUC of MTX (mg*h/L).
CVL=CL/PL

```

```

!Biliary Excretion
RABile= vmaxmrp2*CVL/(kmmrp2+cvl)+KBile*CL/PL
ABile=integ(RABile, 0.0)

```

!Transfer of MTX in bile into 3 segments; r1, r2 and r3.

$r = v_{maxmrp2} * CL / PL / k_{mmp2}$

$Rr1 = (r - r1) * 30$

$r1 = \text{integ}(Rr1, 0.0)$

$Ar1 = \text{integ}(r1, 0.0)$

$Rr2 = (r1 - r2) * 30$

$r2 = \text{integ}(Rr2, 0.0)$

$Ar2 = \text{integ}(r2, 0.0)$

$Rr3 = (r2 - r3) * 30$

$r3 = \text{integ}(Rr3, 0.0)$

$Ar3 = \text{integ}(r3, 0.0)$

!Mass balance in kidney

$RAK = QK * (CA - CK / PK) - K_{Kidney} * CK / PK$

$AK = \text{INTEG}(RAK, 0.0)$

$CK = AK / VK$

$CVK = CK / PK$

!Amount excreted in urine

$RAUrine = K_{Kidney} * CK / PK$

$AUrine = \text{integ}(RAUrine, 0.0)$

!Mass balance in muscle

$RAM = QM * (CA - CM / PM)$

$AM = \text{INTEG}(RAM, 0.0)$

$CM = AM / VM$

$CVM = CM / PM$

!Mass balance in plasma

$RAPls = QL * CL / PL + QK * CK / PK + QM * CM / PM - (QL + QK + QM) * CA$

$APls = \text{integ}(RAPls, 0.)$

$CA = APls / VP$!Plasma concentration

!Gut lumen

$RAGL1 = (v_{maxmrp2} * cv1 / (k_{mmp2} + cv1)) + K_{Bile} * CL / PL &$

$-.25 * (V_{maxGT} * CGL1 / (K_{mGT} + CGL1) + K_{abs} * CGL1) &$

$-kf * VGL * CGL1$

$AGL1 = \text{integ}(RAGL1, 0.0)$

$CGL1 = AGL1 / .25 / VGL$

$RAGL2 = kf * VGL * CGL1 - .25 * (V_{maxGT} * CGL2 / (K_{mGT} + CGL2) + K_{abs} * CGL2) &$

$-kf * VGL * CGL2$

$AGL2 = \text{integ}(RAGL2, 0.0)$

$CGL2 = AGL2 / .25 / VGL$

```

RAGL3=kf*VGL*CGL2-.25*(VmaxGT*CGL3/(KmGT+CGL3)+Kabs*CGL3)&
-kf*VGL*CGL3
AGL3=integ(RAGL3,0.0)
CGL3=AGL3/.25/VGL

```

```

RAGL4=kf*VGL*CGL3-.25*(VmaxGT*CGL4/(KmGT+CGL4)+Kabs*CGL4)&
-kf*VGL*CGL4
AGL4=integ(RAGL4,0.0)
CGL4=AGL4/.25/VGL

```

```

RAGL=RAGL1+RAGL2+RAGL3+RAGL4
AGL=integ(RAGL,0.)
CGL=AGL/VGL

```

```

!Fecal Excretion of MTX from GI Lumen
RAFeces=kf*VGL*CGL4
AFEC=integ(RAFeces, 0.0)

```

```

!GUT Tissue
RAGT=QGT*(CA-
CGT/PGT)+.25*(VmaxGT*CGL1/(KmGT+CGL1)+Kabs*CGL1)+&
.25*(VmaxGT*CGL2/(KmGT+CGL2)+Kabs*CGL2)+&
.25*(VmaxGT*CGL3/(KmGT+CGL3)+Kabs*CGL3)+&
.25*(VmaxGT*CGL4/(KmGT+CGL4)+Kabs*CGL4)
AGT=integ(RAGT, dose)
CGT=AGT/VGT
CVG=CGT/PGT

```

```

!Total mass
TMASS=AGT+AGL+APls+AM+AK+AL+AFEC+AUrine
MB=(Dose-TMASS)*100.0/Dose

```

```

TERMT (T.GE.TSTOP)

```

```

END !END of Derivative
END !END of Dynamic
!-----!-----!-----!-----!-----!-----!-----!-
END !END of Program

```

!File ratKm.cmd
!Edited by M. Lohitnavy on Oct. 10th, 2007.

set grdcpl=.f. !no grid on line plots
SET TITLE = 'MTX model with Mrp2 excretion- Rat'
prepare /all

start
procedure check
start
plot tmass, mb
print t,tmass,mb
end

proced rat
s doserate=6.0
start
PLOT /DATA=rat CA /log /lo=0.01 /hi=1000.0 /char=1 cl /log /lo=0.01 /hi=100.0 &
/char=2 ck /log /lo=0.01 /hi=1000.0 /char=3 cm /log /lo=0.01 /hi=1000.0&
/char=4 cgl /log /lo=0.01 /hi=1000.0 /char=5 /xhi=4.1 /xtag='hr' &
/tag='Tissue conc mg/L'
END

proced rat0.5
s doserate=0.5
start
PLOT /DATA=rat0.5 CA /log /lo=0.01 /hi=400.0 &
cgl /log /lo=0.01 /hi=400.0 /xhi=4.1 /xtag='hr' /tag='Tissue conc mg/L'
END

proced rat25
s doserate=25.
start
PLOT /DATA=rat25 CA /log /lo=0.01 /hi=400.0 &
cgl /log /lo=0.01 /hi=400.0 /xhi=4.1 /xtag='hr' /tag='Tissue conc mg/L'
END

DATA RAT (T, CA,CL,CK, CM, CGL)
0.25 5.22 17.28 14.35 0.69 13.77
0.50 3.91 13.22 4.42 0.56 34.88
0.92 1.45 6.03 3.52 0.20 59.67
1.47 1.26 4.33 2.59 0.12 40.31
2.00 0.70 3.24 1.06 0.09 59.67
3.00 0.22 1.82 1.42 0.03 34.17
4.00 0.33 1.36 ? 0.05 6.03
END

DATA Rat0.5 (t, CA, CGL)

0.17	?	0.53
0.33	0.43	1.26
0.92	0.36	1.26
1.50	0.20	1.32
2.00	0.07	5.11
3.00	0.02	1.38
4.00	0.01	0.05

END

DATA Rat25 (t, CA, CGL)

0.17	26.44	42.56
0.33	25.82	60.82
0.92	10.20	161.43
1.50	5.24	177.56
2.00	1.84	121.31
3.00	0.86	82.89
4.00	0.57	21.85

END

Appendix XI: Computer Code of the PBPK model for methotrexate in dogs (PBPK model with Mrp2)

PROGRAM dogKm.csl

!Edited by M. Lohitnavy on Oct. 10th, 2007.

!Developed by Lohitnavy M. and Lu Y.

!Reconstruction of MTX PBPK model

!Original model by Bischoff (1970).

!Single dose of MTX was intravenously administered to dogs.

!There was dosing 1 dosing level; 3 mg/kg.

!In the original model, the PBPK model consists of blood, liver, GI, gut lumen,

!kidney, and muscle subcompartment.

!MTX is excreted into the bile to GI tract and, then, reabsorbed.

!Enterohepatic re-circulation is responsible for prolonged half-life of MTX.

!The zero-order biliary secretion was replaced by Mrp2-mediated excretion.

!There were two dogs in the experiment.

!Each dog was considered separately in this model.

!Value of Km of Mrp2 and Vmax of mrp2 were optimized individually.

!All other parameters in this model were identical to those in Bischoff et al. (1971).

INITIAL

!Volume and blood flow parameters

!All parameters were taken from the paper

!Units are transformed to forms of which compatible with ACSL.

CONSTANT BW=17.0

!Body weight of a dog(kg)

CONSTANT VP=.65

!Volume of plasma (L)

CONSTANT VM=7.5

!Volume of muscle (L)

CONSTANT VK=0.076

!Volume of kidney (L)

CONSTANT VL=0.360

!Volume of liver (L)

CONSTANT VGT=0.640

!Volume of GI tract (L)

CONSTANT VGL=0.640

!Volume of gut lumen (L)

CONSTANT QM=8.4

!Blood flow to muscle (L/h)

CONSTANT QK=11.4

!Blood flow to kidney (L/h)

CONSTANT QL=13.2

!Blood flow to liver (L/h)

CONSTANT QGT=11.4

!Blood flow to GI tract (L/h)

CONSTANT PM=.15

!Partition coefficient of muscle

CONSTANT PK=14.0

!Partition coefficient of kidney

CONSTANT PL=2.0

!Partition coefficient of liver

CONSTANT PGT=1.0

!Partition coefficient of GI tract

CONSTANT BMaxM=0.0

!Maximal binding capacity in muscle (mg/L)

CONSTANT BMaxK=0.3

!Maximal binding capacity in kidney (mg/L)

CONSTANT BMaxL=0.5

!Maximal binding capacity in liver (mg/L)

CONSTANT BMaxGT=0.1 !Maximal binding capacity in GI tract (mg/L)
 CONSTANT KmBind=1e-5 !Protein binding parameter (mg/L)

CONSTANT KKidney=3.36 !kidney clearance rate (L/h)
 CONSTANT KBile= 0. !Biliary clearance rate (L/h)
 CONSTANT kmmrp2= 153.984 !Km of mrp2 (optimized value, mg/L)
 CONSTANT vmaxmrp2=160.11 !Vmax of mrp2 (optimized value, mg/h)
 CONSTANT TGI=1.67 !GI transit time (h)

!*****!
 !In this model, Absorption of MTX from GI is described by a first order rate constant.
 !and a saturable process. In this process, Michelis-Menten equation is employed.
 !VmaxGI is similar to Vmax and KG is similar to Km in M-M equation.

!b is a first order GI absorption rate constant
 CONSTANT VmaxGT=90. !M-M absorption maximum rate into GI (mg/h)
 CONSTANT KmGT=200. !M-M absorption paramter into GI tissue (mg/L)
 CONSTANT Kabs=0.00006 !First order GI absorption rate constant(L/h)
 !*****!

CONSTANT KF=.09 !Rate of MTX mass-tranferred down through
 !the small intestine (/h)

!Simulation parameters
 CONSTANT MW=454.44 !molecular weight of MTX
 CONSTANT DoseRate=3.0 !mg/kg
 Dose = DoseRate*BW !mg
 CONSTANT tstop=6.0 !hr
 cinterval CINT=0.01

END !END of Initial
 !-----!-----!-----!-----!-----!-----!-----!

DYNAMIC
 ALGORITHM IALG=2

DERIVATIVE
 !Mass balance in liver
 RAL=(QL-QGT)*(CA-CL/PL)+QGT*(CGT/PGT-CL/PL)-&
 (vmaxmrp2*CVL/(kmmrp2+cvl))-KBile*CL/PL
 AL=INTEG(RAL,0.0) !Amount of MTX (mg)
 CL=AL/VL !Calculations of conc of MTX (mg/L).
 AUCLIV=integ(CL,0.0) !Calculations of AUC of MTX (mg*h/L).
 CVL=CL/PL

!Biliary Excretion
 RABile= vmaxmrp2*CVL/(kmmrp2+cvl)+KBile*CL/PL
 ABile=integ(RABile, 0.0)

!Transfer of MTX in bile into 3 segments; r1, r2 and r3.

$r = v_{max}mrp2 * CL / PL / k_{m}mrp2$

$Rr1 = (r - r1) * 30$

$r1 = \text{integ}(Rr1, 0.0)$

$Ar1 = \text{integ}(r1, 0.0)$

$Rr2 = (r1 - r2) * 30$

$r2 = \text{integ}(Rr2, 0.0)$

$Ar2 = \text{integ}(r2, 0.0)$

$Rr3 = (r2 - r3) * 30$

$r3 = \text{integ}(Rr3, 0.0)$

$Ar3 = \text{integ}(r3, 0.0)$

!Mass balance in kidney

$RAK = QK * (CA - CK / PK) - K_{Kidney} * CK / PK$

$AK = \text{INTEG}(RAK, 0.0)$

$CK = AK / VK$

$CVK = CK / PK$

!Amount excreted in urine

$RAUrine = K_{Kidney} * CK / PK$

$AUrine = \text{integ}(RAUrine, 0.0)$

!Mass balance in muscle

$RAM = QM * (CA - CM / PM)$

$AM = \text{INTEG}(RAM, 0.0)$

$CM = AM / VM$

$CVM = CM / PM$

!Mass balance in plasma

$RAPls = QL * CL / PL + QK * CK / PK + QM * CM / PM - (QL + QK + QM) * CA$

$APls = \text{integ}(RAPls, \text{dose})$

$CA = APls / VP$

!Plasma concentration

!Gut lumen

$RAGL1 = (v_{max}mrp2 * cvl / (k_{m}mrp2 + cvl)) + K_{Bile} * CL / PL &$

$-.25 * (V_{maxGT} * CGL1 / (K_{mGT} + CGL1) + K_{abs} * CGL1) &$

$-kf * VGL * CGL1$

$AGL1 = \text{integ}(RAGL1, 0.0)$

$CGL1 = AGL1 / .25 / VGL$

$RAGL2 = kf * VGL * CGL1 - .25 * (V_{maxGT} * CGL2 / (K_{mGT} + CGL2) + K_{abs} * CGL2) &$

$-kf * VGL * CGL2$

$AGL2 = \text{integ}(RAGL2, 0.0)$

CGL2=AGL2/.25/VGL

RAGL3=kf*VGL*CGL2-.25*(VmaxGT*CGL3/(KmGT+CGL3)+Kabs*CGL3)&
-kf*VGL*CGL3

AGL3=integ(RAGL3,0.0)

CGL3=AGL3/.25/VGL

RAGL4=kf*VGL*CGL3-.25*(VmaxGT*CGL4/(KmGT+CGL4)+Kabs*CGL4)&
-kf*VGL*CGL4

AGL4=integ(RAGL4,0.0)

CGL4=AGL4/.25/VGL

RAGL=RAGL1+RAGL2+RAGL3+RAGL4

AGL=integ(RAGL,0.)

CGL=AGL/VGL

!Fecal Excretion of MTX from GI Lumen

RAFeces=kf*VGL*CGL4

AFEC=integ(RAFeces, 0.0)

!GUT Tissue

RAGT=QGT*(CA-

CGT/PGT)+.25*(VmaxGT*CGL1/(KmGT+CGL1)+Kabs*CGL1)+&
.25*(VmaxGT*CGL2/(KmGT+CGL2)+Kabs*CGL2)+&
.25*(VmaxGT*CGL3/(KmGT+CGL3)+Kabs*CGL3)+&
.25*(VmaxGT*CGL4/(KmGT+CGL4)+Kabs*CGL4)

AGT=integ(RAGT, 0.)

CGT=AGT/VGT

CVG=CGT/PGT

!Total mass

TMASS=AGT+AGL+APls+AM+AK+AL+AFEC+AUrine

MB=(Dose-TMASS)*100.0/Dose

TERMT (T.GE.TSTOP)

END !END of Derivative

END !END of Dynamic

!-----!-----!-----!-----!-----!-----!-----!-----!

END !END of Program

```
!File dogKm.cmd
!Edited by M. Lohitnavy on Oct. 10th, 2007.
set grdcpl=.f. !no grid on line plots
SET TITLE = 'MTX model with Mrp2 excretion- Dogs'
prepare /all
```

```
start
procedure check
start
plot tmass, mb
print t,tmass,mb
end
```

```
PROCED dog1
s vmaxmrp2=160.11
s kmmrp2=153.98
start
PLOT /DATA=dog1 CA /log /lo=0.01 /hi=100.0 /char=1 cl /log /lo=0.01 /hi=100.0 &
/char=2 cm /log /lo=0.01 /hi=100.0 /char=3 cgl /log /lo=0.01 /hi=1000.0&
/xhi=4.1 /xtag='hr' /tag='Tissue conc mg/L'
END
```

```
PROCED dog2
s vmaxmrp2=706.55
s kmmrp2=154.18
start
PLOT /DATA=dog2 CA /log /lo=0.01 /hi=100.0 /char=1 cl /log /lo=0.01 /hi=100.0 &
/char=2 ck /log /lo=0.01 /hi=100.0 /char=3&
/xhi=4.1 /xtag='hr' /tag='Tissue conc mg/L'
END
```

```
DATA dog1 (T, CA,CL,CM, CGL)
0.05  19.54  ?    ?    ?
0.25  8.72   ?    ?    ?
0.5   6.74   ?    ?    ?
0.67  ?     14.85 ?    ?
1     3.76   ?    ?    ?
1.5   2.53   ?    ?    ?
2     2.17   ?    ?    ?
2.5   2.28   ?    ?    ?
3     1.92   3.95  0.53  7.60
END
```

```
DATA dog2 (t, CA, CL, CK)
0.25  8.14  ?    ?
0.5   5.48  ?    ?
```

1	3.16	?	?
1.5	2.36	?	?
2	1.79	?	?
2.5	1.48	?	?
3	1.46	2.57	19.88

END

Appendix XII: Computer Code of the PBPK model for methotrexate in humans (PBPK model with Mrp2)

PROGRAM humanKm.csl
!Edited by M. Lohitnavy on Oct. 10th, 2007.
!Developed by Lohitnavy M. and Lu Y.
!Reconstruction of MTX PBPK model
!Original model by Bischoff (1970).
!Single dose of MTX was intravenously administered to humans.
!There was dosing 1 dosing level; 1 mg/kg.
!In the original model, the PBPK model consists of blood, liver, GI, gut lumen,
!kidney, and muscle subcompartment.
!MTX is excreted into the bile to GI tract and, then, reabsorbed.
!Enterohepatic re-circulation is responsible for prolonged half-life of MTX.
!The zero-order biliary secretion was replaced by Mrp2-mediated excretion.
!There were two humans in the experiment.
!Each subject was considered separately in this model.
!Value of Km and Vmax of mrp2 were optimized individually.
!All other parameters in this model were identical to those in Bischoff et al. (1971).

INITIAL

!Volume and blood flow parameters
!All parameters were taken from the paper
!Units are transformed to forms of which compatible with ACSL.

CONSTANT BW=70.0	!Body weight of a rat(kg)
CONSTANT VP=3.0	!Volume of plasma (L)
CONSTANT VM=35.0	!Volume of muscle (L)
CONSTANT VK=0.28	!Volume of kidney (L)
CONSTANT VL=1.35	!Volume of liver (L)
CONSTANT VGT=2.1	!Volume of GI tract (L)
CONSTANT VGL=2.1	!Volume of gut lumen (L)
CONSTANT QM=25.2	!Blood flow to muscle (L/h)
CONSTANT QK=42.	!Blood flow to kidney (L/h)
CONSTANT QL=48.	!Blood flow to liver (L/h)
CONSTANT QGT=42.	!Blood flow to GI tract (L/h)
CONSTANT PM=.15	!Partition coefficient of muscle
CONSTANT PK=3.0	!Partition coefficient of kidney
CONSTANT PL=3.0	!Partition coefficient of liver
CONSTANT PGT=1.0	!Partition coefficient of GI tract
CONSTANT BMaxM=0.0	!Maximal binding capacity in muscle (mg/L)
CONSTANT BMaxK=0.3	!Maximal binding capacity in kidney (mg/L)
CONSTANT BMaxL=0.5	!Maximal binding capacity in liver (mg/L)
CONSTANT BMaxGT=0.1	!Maximal binding capacity in GI tract (mg/L)

```

CONSTANT KmBind=1e-5      !Protein binding parameter (mg/L)

CONSTANT KKidney=11.4    !kidney clearance rate (L/h)
CONSTANT KBile= 0.       !Biliary clearance rate (L/h)
CONSTANT kmmrp2= 150.15  !Km of mrp2 (optimized value, mg/L)
CONSTANT vmaxmrp2=3888.9 !Vmax of mrp2 (optimized value, mg/h)
CONSTANT TGI=1.67       !GI transit time (h)

!*****!
!In this model, Absorption of MTX from GI is described by a first order rate constant.
!and a saturable process. In this process, Michelis-Menten equation is employed.
!VmaxGI is similar to Vmax and KG is similar to Km in M-M equation.
!b is a first order GI absorption rate constant.
CONSTANT VmaxGT=114.     !M-M absorption maximum rate into GI (mg/h)
CONSTANT KmGT=200.       !M-M absorption paramter into GI (mg/L)
CONSTANT Kabs=0.00006    !First order GI absorption rate constant (L/h)
!*****!
CONSTANT KF=.06          !Rate of MTX mass-tranferred down through
                        !the small intestine (/h)

!Simulation parameters
CONSTANT MW=454.44      !molecular weight of MTX
CONSTANT DoseRate=1.0   !mg/kg
Dose = DoseRate*BW      !mg
CONSTANT tstop=6.0     !hr
cinterval CINT=0.01

END !END of Initial
!-----!-----!-----!-----!-----!-----!-

DYNAMIC
ALGORITHM IALG=2

DERIVATIVE
!Mass balance in liver
RAL=(QL-QGT)*(CA-CL/PL)+QGT*(CGT/PGT-CL/PL)&
-(vmaxmrp2*CVL/(kmmrp2+cvl))-KBile*CL/PL
AL=INTEG(RAL,0.0)      !Amount of MTX (mg)
CL=AL/VL               !Calculations of conc of MTX (mg/L).
AUCLIV=integ(CL,0.0)   !Calculations of AUC of MTX (mg*h/L).
CVL=CL/PL

!Biliary Excretion
RABile= vmaxmrp2*CVL/(kmmrp2+cvl)+KBile*CL/PL
ABile=integ(RABile, 0.0)

```

!Tranfer of MTX in bile into 3 segments; r1, r2 and r3.

$r = v_{\max mrp2} * CL / PL / k_{mmp2}$

$Rr1 = (r - r1) * 30$

$r1 = \text{integ}(Rr1, 0.0)$

$Ar1 = \text{integ}(r1, 0.0)$

$Rr2 = (r1 - r2) * 30$

$r2 = \text{integ}(Rr2, 0.0)$

$Ar2 = \text{integ}(r2, 0.0)$

$Rr3 = (r2 - r3) * 30$

$r3 = \text{integ}(Rr3, 0.0)$

$Ar3 = \text{integ}(r3, 0.0)$

!Mass balance in kidney

$RAK = QK * (CA - CK / PK) - K_{Kidney} * CK / PK$

$AK = \text{INTEG}(RAK, 0.0)$

$CK = AK / VK$

$CVK = CK / PK$

!Amount excreted in urine

$RAUrine = K_{Kidney} * CK / PK$

$AUrine = \text{integ}(RAUrine, 0.0)$

!Mass balance in muscle

$RAM = QM * (CA - CM / PM)$

$AM = \text{INTEG}(RAM, 0.0)$

$CM = AM / VM$

$CVM = CM / PM$

!Mass balance in plasma

$RAPls = QL * CL / PL + QK * CK / PK + QM * CM / PM - (QL + QK + QM) * CA$

$APls = \text{integ}(RAPls, \text{dose})$

$CA = APls / VP$

!Plasma concentration

!Gut lumen

$RAGL1 = (v_{\max mrp2} * cv1 / (k_{mmp2} + cv1)) + K_{Bile} * CL / PL \&$

$-.25 * (V_{\max GT} * CGL1 / (K_{mGT} + CGL1) + K_{abs} * CGL1) \&$

$-kf * VGL * CGL1$

$AGL1 = \text{integ}(RAGL1, 0.0)$

$CGL1 = AGL1 / .25 / VGL$

$RAGL2 = kf * VGL * CGL1 - .25 * (V_{\max GT} * CGL2 / (K_{mGT} + CGL2) + K_{abs} * CGL2) \&$

$-kf * VGL * CGL2$

$AGL2 = \text{integ}(RAGL2, 0.0)$

$CGL2 = AGL2 / .25 / VGL$

$RAGL3 = kf * VGL * CGL2 - .25 * (VmaxGT * CGL3 / (KmGT + CGL3) + Kabs * CGL3) &$
 $- kf * VGL * CGL3$
 $AGL3 = \text{integ}(RAGL3, 0.0)$
 $CGL3 = AGL3 / .25 / VGL$

$RAGL4 = kf * VGL * CGL3 - .25 * (VmaxGT * CGL4 / (KmGT + CGL4) + Kabs * CGL4) &$
 $- kf * VGL * CGL4$
 $AGL4 = \text{integ}(RAGL4, 0.0)$
 $CGL4 = AGL4 / .25 / VGL$

$RAGL = RAGL1 + RAGL2 + RAGL3 + RAGL4$
 $AGL = \text{integ}(RAGL, 0.)$
 $CGL = AGL / VGL$

!Fecal Excretion of MTX from GI Lumen
 $RAFeces = kf * VGL * CGL4$
 $AFEC = \text{integ}(RAFeces, 0.0)$

!GUT Tissue
 $RAGT = QGT * (CA -$
 $CGT / PGT) + .25 * (VmaxGT * CGL1 / (KmGT + CGL1) + Kabs * CGL1) + &$
 $.25 * (VmaxGT * CGL2 / (KmGT + CGL2) + Kabs * CGL2) + &$
 $.25 * (VmaxGT * CGL3 / (KmGT + CGL3) + Kabs * CGL3) + &$
 $.25 * (VmaxGT * CGL4 / (KmGT + CGL4) + Kabs * CGL4)$
 $AGT = \text{integ}(RAGT, 0.)$
 $CGT = AGT / VGT$
 $CVG = CGT / PGT$

!Total mass
 $TMASS = AGT + AGL + AP1s + AM + AK + AL + AFEC + AUrine$
 $MB = (Dose - TMASS) * 100.0 / Dose$

TERMT (T.GE.TSTOP)

END !END of Derivative
 END !END of Dynamic
 !-----!-----!-----!-----!-----!-----!-----!
 END !END of Program

```
!File humanKm.cmd
!Edited by M. Lohitnavy on Oct. 10th, 2007.
set grdcpl=.f. !no grid on line plots
SET TITLE = 'MTX model with Mrp2 excretion- Human'
prepare /all
```

```
start
procedure check
start
plot tmass, mb
print t,tmass,mb
end
```

```
PROCED human1
s vmaxmrp2=3888.9
start
PLOT /DATA=human1 CA /log /lo=0.1 /hi=10. /char=1 /xhi=6.1 /xtag='hr' &
/tag='Tissue conc mg/L'
END
```

```
PROCED human2
s vmaxmrp2=2188.8
start
PLOT /DATA=human2 CA /log /lo=0.1 /hi=10. /char=1 /xhi=6.1 /xtag='hr' &
/tag='Tissue conc mg/L'
END
```

```
DATA human1 (t,ca)
0.25  1.0744
0.75  0.7826
1      0.6808
2      0.4596
4      0.2912
6      0.2042
END
```

```
DATA human2 (t,ca)
0.25  1.85
0.75  1.30
1.00  1.02
2.42  0.54
5.00  0.23
END
```

Appendix XIII: Computer Code of the PBPK model for methotrexate in mutant rats (Bile duct cannulation; PBPK model with Mrp2)

PROGRAM mutantIV.csl

!Edited by M. Lohitnavy on Oct. 10th, 2007.

!Developed by Lohitnavy M. and Lu Y.

!Reconstruction of MTX PBPK model

!Infusion of MTX

!There were dosing 1 levels; 60 ug/min.

!In original model, the PBPK model consists of blood, liver, GI, kidney,

!and muscle subcompartment.

!Since, in the experimental conditions, bile duct was cannulated.

!Thus there was no entero-hepatic recirculation in this model.

INITIAL

!Volume and blood flow parameters

!All parameters were taken from the paper

!Units are transformed to forms of which compatible with ACSL.

CONSTANT BW=0.468 !Body weight of a rat(kg)

CONSTANT VP=.009 !Volume of plasma (L)

CONSTANT VM=0.1 !Volume of muscle (L)

CONSTANT VK=0.0019 !Volume of kidney (L)

CONSTANT VL=0.0083 !Volume of liver (L)

CONSTANT VGT=0.011 !Volume of GI tract (L)

CONSTANT VGL=0.011 !Volume of gut lumen (L)

CONSTANT QM=.18 !Blood flow to muscle (L/h)

CONSTANT QK=.3 !Blood flow to kidney (L/h)

CONSTANT QL=.39 !Blood flow to liver (L/h)

CONSTANT QGT=.318 !Blood flow to GI tract (L/h)

CONSTANT PM=.15 !Partition coefficient of muscle

CONSTANT PK=3.0 !Partition coefficient of kidney

CONSTANT PL=3.0 !Partition coefficient of liver

CONSTANT PGT=1.0 !Partition coefficient of GI tract

CONSTANT BMaxM=0.0 !Maximal binding capacity in muscle (mg/L)

CONSTANT BMaxK=0.3 !Maximal binding capacity in kidney (mg/L)

CONSTANT BMaxL=0.5 !Maximal binding capacity in liver (mg/L)

CONSTANT BMaxGT=0.1 !Maximal binding capacity in GI tract (mg/L)

CONSTANT KmBind=1e-5 !Protein binding parameter (mg/L)

CONSTANT KKidney=0.066 !kidney clearance rate (L/h)

CONSTANT KBile= 0. !Biliary clearance rate (L/h)

CONSTANT kmmrp2= 153.984 !Km of mrp2 from Hirono S. (2005)

CONSTANT vmaxmrp2=36.20 !Vmax of mrp2 from PCB126 (mg/h)

```

CONSTANT kmov=0.418
CONSTANT kgilv=0.05
CONSTANT TGI=1.67          !GI transit time (h)

!*****!
!In this model, Absorption of MTX from GI is described by a first order rate constant.
!and a saturable process. In this process, Michelis-Menten equation is employed.
!VmaxGI is similar to Vmax and KG is similar to Km in M-M equation.
!b is a first order GI absorption rate constant.
CONSTANT VmaxGT=1.2        !M-M absorption maximum rate into GI (mg/h)
CONSTANT KmGT=200.         !M-M absorption paramter into GI (mg/L)
CONSTANT Kabs=0.00006     !First order GI absorption rate constant (L/h)
!*****!
CONSTANT KF=.60           !Rate of MTX mass-tranferred down through
                          !the small intestine (/h)

!Simulation parameters
CONSTANT MW=454.44        !molecular weight of MTX
CONSTANT tstart=0.0
CONSTANT tstop=8.0
CONSTANT tinf=2.0         !duration of iv infusion (h)
CONSTANT ivdose=7.2      !total administered dose of MTX (mg)
CONSTANT tchnng=2.0

rdose=ivdose/tinf        !dosing rate (mg/h)

END !END of Initial
!-----!-----!-----!-----!-----!-----!-----!-

DYNAMIC
ALGORITHM IALG=2

DERIVATIVE
!GI lumen
RAGI=-KGILV*AGI-Kmov*AGI
AGI=INTEG(RAGI,0.)

!Mass balance in liver
RAL=(QL-QGT)*(CA-CL/PL)+QGT*(CGT/PGT-CL/PL)&
-(vmaxmrp2*CVL/(kmmrp2+cvl))-KBile*CL/PL+KGILV*AGI
AL=INTEG(RAL,0.0)        !Amount of MTX (mg)
CL=AL/VL                 !Calculations of conc of MTX (mg/L).
AUCLIV=integ(CL,0.0)     !Calculations of AUC of MTX (mg*h/L).
CVL=CL/PL

```

!Biliary Excretion

$RABile = v_{max}mrp2 * CVL / (k_{m}mrp2 + cvl) + KBile * CL / PL$

$ABile = \text{integ}(RABile, 0.0)$

$PBile = ABile * 100 / \text{ivdose}$

!Mass balance in kidney

$RAK = QK * (CA - CK / PK) - K_{Kidney} * CK / PK$

$AK = \text{INTEG}(RAK, 0.0)$

$CK = AK / VK$

$AUCk = \text{integ}(CK, 0.0)$

$CVK = CK / PK$

!Amount excreted in urine

$RAUrine = K_{Kidney} * CK / PK$

$AUrine = \text{integ}(RAUrine, 0.0)$

$PUrine = AUrine * 100 / \text{ivdose}$

$PCombine = (ABile + AUrine) * 100 / \text{ivdose}$

!Mass balance in muscle

$RAM = QM * (CA - CM / PM)$

$AM = \text{INTEG}(RAM, 0.0)$

$CM = AM / VM$

$AUCM = \text{integ}(CM, 0.0)$

$CVM = CM / PM$

!Mass balance in plasma

$RAPls = QL * CL / PL + QK * CK / PK + QM * CM / PM - (QL + QK + QM) * CA + riv$

$APls = \text{integ}(RAPls, 0.)$

$CA = APls / VP$

!Plasma concentration

$AUCP = \text{integ}(CA, 0.0)$

!Calculations of AUC of MTX in plasma(mg*h/L)

$RAGL1 = -kf * VGL * CGL1 + K_{mov} * AGI$

$AGL1 = \text{integ}(RAGL1, 0.)$

$CGL1 = AGL1 / .25 / VGL$

$RAGL2 = kf * VGL * CGL1 - kf * VGL * CGL2$

$AGL2 = \text{integ}(RAGL2, 0.0)$

$CGL2 = AGL2 / .25 / VGL$

$RAGL3 = kf * VGL * CGL2 - kf * VGL * CGL3$

$AGL3 = \text{integ}(RAGL3, 0.0)$

$CGL3 = AGL3 / .25 / VGL$

$RAGL4 = kf * VGL * CGL3 - kf * VGL * CGL4$

$AGL4 = \text{integ}(RAGL4, 0.0)$

$CGL4 = AGL4 / .25 / VGL$

```

RAGL=RAGL1+RAGL2+RAGL3+RAGL4
AGL=integ(RAGL,0.)
CGL=AGL/VGL

!Fecal Excretion of MTX from GI Lumen
RAFeces=kf*VGL*CGL4
AFEC=integ(RAFeces, 0.0)

!GUT Tissue
RAGT=QGT*(CA-CGT/PGT)+KGILV*AGI
AGT=integ(RAGT, 0.)
CGT=AGT/VGT
CVG=CGT/PGT

!Termination of IV infusion at t=2.0 h
if (t.le.tinf) then
    riv=rdose
else
    riv=0.0
endif

!Total mass
TMASS=AGT+AGL+APIs+AM+AK+AL+AFEC+AUrine+AGI+Abile
MB=(ivdose-TMASS)*100.0/ivdose

TERMT (T.GE.TSTOP)

END  !END of Derivative
END  !END of Dynamic
!-----!-----!-----!-----!-----!-----!-----!-
END  !END of Program

```

!File mutantIV.cmd
!Edited by M. Lohitnavy on Oct. 10th, 2007.

set grdcpl=.f. !no grid on line plots
SET TITLE = 'MTX model- Rat'
prepare /all

start
procedure check
start
plot tmass, mb
print t,tmass,mb
end

PROCED PBILE

start
PLOT /DATA=BILE PBILE /lo=0. /hi=100. /xhi=4. /xtag='hr' /tag='%Cumulative in
Bile'
END

DATA BILE (t, PBILE)

0.17	1.42
0.33	2.83
0.50	6.73
0.67	10.97
1.00	24.07
1.33	34.69
2.00	57.35

END

Appendix XIV: Computer Code of the PBPK model for methotrexate in mutant rats (oral administration ; PBPK model with Mrp2)

PROGRAM mutant.csl

!Edited by M. Lohitnavy on Oct. 10th, 2007.

!Developed by Lohitnavy M. and Lu Y.

!Single dose of MTX was orally administered to SD and Eisai rats.

!Eaisi rats are mutant rats with mrp2 deficiency.

!There were dosing 2 levels; 0.2 and 0.6 mg/kg bw.

!In original model, the PBPK model consists of blood, liver, GI, kidney,
!and muscle subcompartment.

!All parameters including Vmax and Km of mrp2 were identical to
!those of the rat model, ratKm.csl .

!Since this experiment was oral administration,

!a site of absorption in the GI tract was added.

!There were two rates in this subcompartment;

! 1) KGILV, an absorption rate CONSTANT from the site to liver, and,

! 2)Kmove, a movement of MTX mass from the site to other areas of the GI tract.

!MTX is excreted into the bile to GI tract and, then, reabsorbed.

!Enterohepatic re-circulation is responsible for prolonged half-life of MTX.

INITIAL

!Volume and blood flow parameters

!All parameters were taken from the paper

!Units are transformed to forms of which compatible with ACSL.

CONSTANT BW=0.2 !Body weight of a rat(kg)

CONSTANT VP=.009 !Volume of plasma (L)

CONSTANT VM=0.1 !Volume of muscle (L)

CONSTANT VK=0.0019 !Volume of kidney (L)

CONSTANT VL=0.0083 !Volume of liver (L)

CONSTANT VGT=0.011 !Volume of GI tract (L)

CONSTANT VGL=0.011 !Volume of gut lumen (L)

CONSTANT QM=.18 !Blood flow to muscle (L/h)

CONSTANT QK=.3 !Blood flow to kidney (L/h)

CONSTANT QL=.39 !Blood flow to liver (L/h)

CONSTANT QGT=.318 !Blood flow to GI tract (L/h)

CONSTANT PM=.15 !Partition coefficient of muscle

CONSTANT PK=3.0 !Partition coefficient of kidney

CONSTANT PL=3.0 !Partition coefficient of liver

CONSTANT PGT=1.0 !Partition coefficient of GI tract

CONSTANT BMaxM=0.0 !Maximal binding capacity in muscle (mg/L)

CONSTANT BMaxK=0.3 !Maximal binding capacity in kidney (mg/L)

CONSTANT BMaxL=0.5 !Maximal binding capacity in liver (mg/L)

```

CONSTANT BMaxGT=0.1          !Maximal binding capacity in GI tract (mg/L)
CONSTANT KmBind=1e-5        !Protein binding parameter (mg/L)

CONSTANT KKidney=0.066      !kidney clearance rate s (L/h)
CONSTANT KBile= 0.          !Biliary clearance rate s (kL/KL, L/h)
CONSTANT kmmrp2= 153.984    !Km of mrp2 from Hirono S. (2005)
CONSTANT vmaxmrp2=36.20    !Vmax of mrp2 from PCB126 (mg/h)
CONSTANT kmov=0.418        !Optimized value (/h)
CONSTANT kgilv=0.05        !Optimized value (/h)
CONSTANT TGI=1.67          !GI transit time (h)

!*****!
!In this model, Absorption of MTX from GI is described by a first order rate constant.
!and a saturable process. In this process, Michelis-Menten equation is employed.
!VmaxGI is similar to Vmax and KG is similar to Km in M-M equation.
!b is a first order GI absorption rate constant.
CONSTANT VmaxGT=1.2        !M-M absorption maximum rate into GI (mg/h)
CONSTANT KmGT=200.        !M-M absorption paramter into GI (mg/L)
CONSTANT Kabs=0.00006     !First order GI absorption rate constant (L/h)
!*****!
CONSTANT KF=.60           !Rate of MTX mass-transferred down through
                          ! the small intestine (/h)

!Simulation parameters
CONSTANT MW=454.44        !molecular weight of MTX
CONSTANT DoseRate=0.2     !mg/kg
Dose = DoseRate*BW        !mg
CONSTANT tstop=12.0       !hr
cinterval CINT=0.01

END                        !END of Initial

DYNAMIC
ALGORITHM IALG=2

DERIVATIVE
!GI lumen
RAGI=-KGILV*AGI-Kmov*AGI
AGI=INTEG(RAGI,Dose)

!Mass balance in liver
RAL=(QL-QGT)*(CA-CL/PL)+QGT*(CGT/PGT-CL/PL)&
-(vmaxmrp2*CVL/(kmmrp2+cvl))-KBile*CL/PL
AL=INTEG(RAL,0.0)        !Amount of MTX (mg)
CL=AL/VL                 !Calculations of conc of MTX (mg/L).
AUCLIV=integ(CL,0.0)     !Calculations of AUC of MTX (mg*h/L).
CVL=CL/PL

```

!Biliary Excretion

$RABile = v_{maxmrp2} * CVL / (k_{mmp2} + cvl) + KBile * CL / PL$

$ABile = \text{integ}(RABile, 0.0)$

!Transfer of MTX in bile into 3 segments; r1, r2 and r3.

$r = v_{maxmrp2} * CL / PL / k_{mmp2}$

$Rr1 = (r - r1) * 30$

$r1 = \text{integ}(Rr1, 0.0)$

$Ar1 = \text{integ}(r1, 0.0)$

$Rr2 = (r1 - r2) * 30$

$r2 = \text{integ}(Rr2, 0.0)$

$Ar2 = \text{integ}(r2, 0.0)$

$Rr3 = (r2 - r3) * 30$

$r3 = \text{integ}(Rr3, 0.0)$

$Ar3 = \text{integ}(r3, 0.0)$

!Mass balance in kidney

$RAK = QK * (CA - CK / PK) - K_{Kidney} * CK / PK$

$AK = \text{INTEG}(RAK, 0.0)$

$CK = AK / VK$

$AUCk = \text{integ}(CK, 0.0)$

$CVK = CK / PK$

!Amount excreted in urine

$RAUrine = K_{Kidney} * CK / PK$

$AUrine = \text{integ}(RAUrine, 0.0)$

!Mass balance in muscle

$RAM = QM * (CA - CM / PM)$

$AM = \text{INTEG}(RAM, 0.0)$

$CM = AM / VM$

$AUCM = \text{integ}(CM, 0.0)$

$CVM = CM / PM$

!Mass balance in plasma

$RAPls = QL * CL / PL + QK * CK / PK + QM * CM / PM - (QL + QK + QM) * CA$

$APls = \text{integ}(RAPls, 0.)$

$CA = APls / VP$

!Plasma concentration

$AUCP = \text{integ}(CA, 0.0)$

!Calculations of AUC of MTX in plasma(mg*h/L).

!Gut lumen

$RAGL1 = (v_{maxmrp2} * cvl / (k_{mmp2} + cvl) + KBile * CL / PL &$

$- .25 * (V_{maxGT} * CGL1 / (K_{mGT} + CGL1) + K_{abs} * CGL1) &$

$- kf * VGL * CGL1 + K_{mov} * AGI$

```

AGL1=integ(RAGL1,0.)
CGL1=AGL1/.25/VGL

RAGL2=kf*VGL*CGL1-.25*(VmaxGT*CGL2/(KmGT+CGL2)+Kabs*CGL2)&
-kf*VGL*CGL2
AGL2=integ(RAGL2,0.0)
CGL2=AGL2/.25/VGL

RAGL3=kf*VGL*CGL2-.25*(VmaxGT*CGL3/(KmGT+CGL3)+Kabs*CGL3)&
-kf*VGL*CGL3
AGL3=integ(RAGL3,0.0)
CGL3=AGL3/.25/VGL

RAGL4=kf*VGL*CGL3-.25*(VmaxGT*CGL4/(KmGT+CGL4)+Kabs*CGL4)&
-kf*VGL*CGL4
AGL4=integ(RAGL4,0.0)
CGL4=AGL4/.25/VGL

RAGL=RAGL1+RAGL2+RAGL3+RAGL4
AGL=integ(RAGL,0.)
CGL=AGL/VGL

!Fecal Excretion of MTX from GI Lumen
RAFeces=kf*VGL*CGL4
AFEC=integ(RAFeces, 0.0)

!GUT Tissue
RAGT=QGT*(CA-CGT/PGT)+&
.25*(VmaxGT*CGL1/(KmGT+CGL1)+Kabs*CGL1)+&
.25*(VmaxGT*CGL2/(KmGT+CGL2)+Kabs*CGL2)+&
.25*(VmaxGT*CGL3/(KmGT+CGL3)+Kabs*CGL3)+&
.25*(VmaxGT*CGL4/(KmGT+CGL4)+Kabs*CGL4)+KGILV*AGI
AGT=integ(RAGT, 0.)
CGT=AGT/VGT
CVG=CGT/PGT

!Total mass
TMASS=AGT+AGL+APls+AM+AK+AL+AFEC+AUrine +AGI
MB=(Dose-TMASS)*100.0/Dose

TERMT (T.GE.TSTOP)

END !END of Derivative
END !END of Dynamic
!-----!-----!-----!-----!-----!-----!-----!-
END !END of Program

```

```
!File mutant.cmd
!Edited by M. Lohitnavy on Oct. 10th, 2007.
!Data were taken from Naba et al (2003).
```

```
set grdcpl=.f. !no grid on line plots
SET TITLE = 'MTX model- SD and mutant Rats'
prepare /all
```

```
start
procedure check
start
plot tmass, mb
print t,tmass,mb
end
```

```
PROCED normal0.2
s doserate=0.2
s vmaxmrp2=36.2
start
PLOT /DATA=normal0.2 CA /log /lo=.0001 /hi=.2 /xhi=12. /xtag='hr' /tag='Blood
conc mg/L'
END
```

```
PROCED normal0.6
s doserate=0.6
s vmaxmrp2=36.2
start
PLOT /DATA=normal0.6 CA /log /lo=.0001 /hi=.2/xhi=12. /xtag='hr' /tag='Blood
conc mg/L'
END
```

```
PROCED mutant0.2
s doserate=0.2
s vmaxmrp2=0.
start
PLOT /DATA=mutant0.2 CA /log /lo=.0001 /hi=.2/xhi=12. /xtag='hr' /tag='Blood
conc mg/L'
END
```

```
PROCED mutant0.6
s doserate=0.6
s vmaxmrp2=0.
start
PLOT /DATA=mutant0.6 CA /log /lo=.0001 /hi=.5/xhi=13. /xtag='hr' /tag='Blood
conc mg/L'
END
```

DATA normal0.2 (t, CA)

0.10 0.0045

0.25 0.0155

0.5 0.0207

1.0 0.0335

2.0 0.0305

4.0 0.0167

8.0 0.0042

END

DATA mutant0.2 (t, CA)

0.10 0.0063

0.25 0.0193

0.50 0.0257

1.0 0.0305

2.0 0.0257

4.0 0.0116

8.0 0.0065

END

DATA normal0.6 (t, CA)

0.01 0.0141

0.25 0.0437

0.50 0.0674

1.0 0.0858

2.0 0.0643

4.0 0.0297

8.0 0.0122

END

DATA mutant0.6 (t,CA)

0.10 0.0197

0.25 0.0658

0.50 0.1146

1.0 0.1423

2.0 0.0992

4.0 0.0378

8.0 0.0251

12.0 0.0077

END

Appendix XV: Computer Code of the PBPK model with a description of competitive inhibition between MTX and PCB126 in rats

PROGRAM discrete.csl

!Edited by M. Lohitnavy on Oct. 10th, 2007.

!This code is modified using PCB126 repeated dose model in rats and
!single oral dose MTX model in rats.

!Developed by Lohitnavy M. and Lu Y.

!Since, the previous model could not successfully produce reasonable outputs.

!We suspected that coding (if-then-else statements) might cause the problems.

!Thus we are trying to use another approach to solve the problems by replacing

!The if-then-else statements in dosing regimens of MTX to discrete blocks.

!Discrete blocks will be added in the Dynamic section of the program.

!This code will give one oral dosing of MTX at time 96 hours.

!Features of this model.

!Since both PCB126 and MTX were excreted by mrp2, this hybrid model consisted of

!a PBPK of PCB126 and a PBPK of MTX. The models ran separately,

!however the two chemicals shared the same mrp2 in the liver.

!Competitive inhibition between the two chemicals at mrp2 in the liver was

!mathematically described.

!Equations describing competitive inhibition of proteins/enzymes/transporters

!were taken from Haddad S. (Toxicol. Sci., 2001).

!***** Experimental Conditions *****'

!PCB126 in corn oil (9.8 ug/kg) was orally

!administered to the rats 4 doses before MTX dosing.

!In the following dat, MTX (3 mg/kg) was orally administered.

!Body weight & liver weight data were available.

!***** End of the Conditions *****'

!***** Features of this PCB126 model; *****'

!Binding between PCB126 and CYP1A2 in the liver,

!Binding between PCB126 and aromatic hydrocarbon receptor

!(AhR) in the liver and excretion of PCB126 via hepatic Mrp2.

!***** End of the PCB126 model features *****'

!***** Features of this MTX model; *****'

!In the original model, the PBPK model consists of blood, liver,

!GI, gut lumen, kidney, and muscle subcompartment.

!MTX is excreted into the bile to GI tract and, then,

!reabsorbed. Enterohepatic re-circulation is responsible for

!prolonged half-life of MTX in the body.

!The biliary excretion was replaced by Mrp2-mediated excretion.

!Km of Mrp2 was taken from Hirono S. (2005)

!Value of Vmax of mrp2 was optimized.
 !All other parameters in this model were identical to those in Bischoff et al. (1971).
 !***** End of the MTX model features *****'

INITIAL

!-----INITIAL SECTION for PCB126-----

!Volume and blood flow parameters

CONSTANT BW=0.277 !Body weight of a rat (kg)
 CONSTANT VFC=0.05 !Fat volume fraction.
 CONSTANT VLC=0.038 !Liver Volume Fraction
 CONSTANT VRC=0.052 !Rapidly perfused volume fraction
 CONSTANT VBC=0.062D0 !blood volume
 CONSTANT QCC=14.1D0 !blood flow constant
 CONSTANT QFC=0.07D0
 CONSTANT QLC=0.18D0
 CONSTANT QRC=0.58D0
 QSC=1.0-QFC-QLC-QRC

!Chemical-specific paramters (Partition coefficients)

CONSTANT PFP=155. !from the NTP model
 CONSTANT PLP=8.9D0 !from the NTP model
 CONSTANT PRP=6.0D0 !from the NTP model
 CONSTANT PSP=7.2D0 !from the NTP model

!Elimination parameters

CONSTANT KGILVP=0.1433 !/hr,absorption rate, from GI to liver
 !Optimized value
 CONSTANT KFECVP=0.00 !/hr,excretion in feces
 CONSTANT KMETP=0.00D0 !/hr, PCB126 metabolism rate
 CONSTANT KLIVP=0.0 !First order elimination from the liver.

!PCB 126 Excretion via Mrp2 is mathematically described using

!the Michealis-Menten Equation; Rate=Vmax*C/(Km+C)

!*****PCB126 Section for Mrp2-mediated excretion from the liver*****'

CONSTANT VmaxP= 64.59 !Maximal velocity of Mrp2
 !Optimized value (unit, nmole/h).
 CONSTANT KmP=7.76e3 !Binding affinity of Mrp2
 !calculated Km by Hirono S.(unit, nM)

!*****END of Mrp2-mediated excretion*****'

!Constants related to protein binding

!PCB126 binding in the liver consists of binding to CYP1A2 and AhR.

!*****PCB126 SECTION FOR LIVER BINDING*****'

CONSTANT BM1 = 0.004 !PCB126 binding capacity to AhR (nmole/liver)
 CONSTANT KB1 = 0.05637 !PCB126 binding constant for AhR (nmole)
 !Optimized value

CONSTANT BM2O = 10. !Binding protein: capacity (nmoles/liver)
 BM2IO = 85 !Increase due to induction (nmoles/liver)
 CONSTANT KB2 = 5.5437 !Binding protein: affinity (nM)
 !Optimized value
 CONSTANT N = 1. !Hill Coefficient
 CONSTANT KD = 1. !Liganded receptor-DNA binding
 CONSTANT slope=0.0066 !Slope of the increase in capacity (nmole/hr)
 !optimized value
 !*****END of PCB126 Binding*****'

!Dosetime and frequency
 DoseFrq=24.0 !hrs
 k=0 !counter of PCB126 doses

!Simulation parameters
 CONSTANT MWP=326.4 !molecular weight of PCB126
 CONSTANT doserate0P=9800 !ng/kg
 DoseRateP=doserate0P !ng/kg
 DoseP = DoseRateP*BW/MWP !nmole

!Initial value of total dose
 TotalDoseP=0.0

!-----END of INITIAL SECTION OF PCB126-----

!-----INITIAL SECTION of MTX-----

!Volume and blood flow paramenters
 !All parameters were taken from Bischoff et al (1971)
 !Units are transformed to forms of which compatible with ACSL.
 CONSTANT VPM=.009 !Volume of plasma (L)
 CONSTANT VMM=0.1 !Volume of muscle (L)
 CONSTANT VKM=0.0019 !Volume of kidney (L)
 CONSTANT VLM=0.0083 !Volume of liver (L)
 CONSTANT VGTM=0.011 !Volume of GI tract (L)
 CONSTANT VGLM=0.011 !Volume of gut lumen (L)

 CONSTANT QMM=.18 !Blood flow to muscle (L/h)
 CONSTANT QKM=.3 !Blood flow to kidney (L/h)
 CONSTANT QLM=.39 !Blood flow to liver (L/h)
 CONSTANT QGTM=.318 !Blood flow to GI tract (L/h)

 CONSTANT PMM=.15 !Partition coefficient of muscle
 CONSTANT PKM=3.0 !Partition coefficient of kidney
 CONSTANT PLM=3.0 !Partition coefficient of liver
 CONSTANT PGTM=1.0 !Partition coefficient of GI tract

CONSTANT BMaxM=0.0 !Max. binding capacity in muscle (nM)
 CONSTANT BMaxK=6601.5 !Max. binding capacity in kidney (nM)
 CONSTANT BMaxL=1100.3 !Max. binding capacity in liver (nM)
 CONSTANT BMaxGT=220.1 !Max. binding capacity in GI tract (nM)
 CONSTANT KmBind=0.022 !Protein binding parameter (nM)

CONSTANT KKidney=0.066 !kidney clearance rate (L/h)
 CONSTANT KBile= 0. !Biliary clearance rate (L/h)
 CONSTANT kmmrp2= 338834.6 !Km of mrp2 from Hirono S. (nM)
 CONSTANT vmaxmrp2=79658.5 !Vmax of mrp2 (nmole/h)
 !Optimized value

CONSTANT TGI=1.67 !GI transit time (h)
 CONSTANT kmov=0.418 !Optimized value (/h)
 CONSTANT KGILVM=0.05 !Optimized value (/h)
 CONSTANT FM=0.15 !Bioavailability of MTX

!*****!

!In this model, Absorption of MTX from GI is described by
 !a first order rate CONSTANT and a saturable process.
 !In this process, Michelis-Menten equation is employed.
 !VmaxGI is similar to Vmax and KG is similar to Km in M-M equation.
 !KabsM is a first order GI absorption rate constant.

CONSTANT VmaxGTM=2640.6 !M-M absorption max. rate into GI (nmole/h)
 CONSTANT KmGTM=440102.1 !M-M absorption paramter into GI (nmole/L)
 CONSTANT KabsM=0.00006 !First order GI absorption rate constant (L/h)

!*****!

CONSTANT KF=.60 !Rate of MTX mass-tranferred down through
 !the small intestine (/h)

!Simulation parameters

CONSTANT MWM=454.44 !molecular weight of MTX
 CONSTANT DoseRate0M=3.0 !mg/kg
 DoseRateM=DoseRate0M
 DoseM = DoseRateM*BW !mg
 DoseMnano=DoseM*1e6/MWM !administered dose of MTX (nmole)

CONSTANT TCHNG=120.0 !End of dosing exposure (hrs)
 CONSTANT TMAX=120.0 !Maximum length of multiple exposure

!-----END of INTITAL SECTION OF MTX-----

!Settings for stopping the experiments and calculating interval

CONSTANT tstop=120.0 !hr
 cinterval CINT=0.01

!Equations describing competitive inhibition of proteins were taken from
 !Haddad S. (Toxicol. Sci., 2001).

!Competitive inhibition parameters
!These following parameters were newly introduced into the hybrid model.
!Originally, they were unknown.
!Thus, optimizations to determine values of these parameters were conducted.
CONSTANT KIM= 12.07 !competitive inhibition of MTX towards PCB126
!(nM; Optimized value).
CONSTANT KIP= 3926.3 !competitive inhibition of PCB126 towards MTX
!(nM; Optimized value).

END !End of initial
!-----!-----!-----!-----!-----!-----!-----!-----!-

DYNAMIC
ALGORITHM IALG=2
!Setting oral dosing for PCB126
IF(T.eq.24*k) THEN
DoseRateP = doserateOP
DoseP = DoseRateP*BW/MWP !nmole
ENDIF
IF (k.gt.3) THEN
doseP=0
ENDIF

!Setting oral dosing for MTX
Discrete DoseMOn
Interval DoseMInt=24.0
Schedule DoseMOff .AT. T + TChng
If (k.eq.5) then
DoseRateM=DoseRate0M
DoseM = DoseRateM*BW !mg
DoseMnano=DoseM*1e6/MWM
else
DoseRateM=0.0
DoseM = DoseRateM*BW !mg
DoseMnano=DoseM*1e6/MWM
Endif
End
Discrete DoseMOff
DoseRateM=0.0
End

DERIVATIVE
!-----DERIVATIVE SECTION FOR PCB126-----
!Scaled parameters
VFP=BW*VFC !total fat volume;
VBP=BW*VBC+0.0012 !blood.Lee&Blafox
VRP=BW*VRC !Rapidly perfused volume

VLP=BW*VLC
 VSP=0.91*BW-VFP-VLP-VBP-VRP !slowly perfused
 QC=QCC*BW**0.75 !blood flow rate
 QF=QC*QFC
 QL=QC*QLC
 QR=QC*QRC
 QS=QC*QSC

!Time-dependent increase in CYP1A2 expression
 BM2I = BM2I0+slope*t

!Mass balance of PCB126 in fat tissue
 RAFP=QF*(CAP-CVFP)
 AFP=INTEG(RAFP,0.0)
 CFP=AFP/VFP
 CVFP=CFP/PFP

!Equations describing competitive inhibition of proteins were taken from
 !Haddad S. (Toxicol. Sci., 2001).
 !Mass balance of PCB126 in liver
 RALP=QL*(CAP-CVLP)-KMETP*CVLP+KGILVP*AGIP-&
 VmaxP*CVLP/(KmP*(1+CVLM/(KIP+1e-30))+CVLP)-KLIVP*CVLP
 ALP=INTEG(RALP,0.0) !Amount of PCB126 in the livers (nmole)
 CLP=ALP/VLP !Calculations of conc of PCB126 in the livers
 !(nM).
 AUCLIVP=integ(CLP,0.0) !Calculations of AUC of PCB126 in the livers
 !(nM*h).
 PLivP=ALP*100/(TOTALDOSEP+1.0e-30)
 !% Retention of PCB126 in the livers
 !compared to total administered dose(%)

!*****Calculations of Mrp2-mediated excretion*****
 RMrp2P= VmaxP*CVLP/(KmP+CVLP) !Rate of excretion via mrp2
 !(nmole*h/L)
 Mrp2P=INTEG(RMrp2P,0.0) !Amount of excretion via mrp2
 !(nmole)
 PMrp2P=Mrp2P*100/(TOTALDOSEP+1.0e-30) !Efficiency in Mrp2 excretion
 !compared to total amount of
 !PCB126 in the liver(%)
 CombineP=PLIVP+PMrp2P !Combination between liver
 !retention and Mrp2 excretion
 !compared to total dose (%)
 OtherP=100-CombineP !!Mass deposited elsewhere (%)
 !***** End of Mrp2-mediated excretion section*****

Procedural

```

CVLtP= ALP/(VLP*PLP+bm1/(kb1+CVLP)+bm2t/(kb2+CVLP))
CVLP = CVLtP
AhRBound= bm1*CVLP/(kb1+CVLP)    !Amount of PCB126 bound to AhR
CYPBound=bm2t*CVLP/(kb2+CVLP)    !Amount of PCB126 bound to CYP1A2
END                                !End of Procedural

!*****Calculations of AhR-PCB126 Binding*****'
DB1 = BM1*CVLP/(KB1+CVLP)/VLP    !Conc. of AhR-PCB126 complex
BOUND = (db1**n)/(db1**n+Kd**n)  !Occupancy of DRE on DNA
PB1 = CVLP/(KB1+CVLP)           !AhR percent occupancy
BM2T = BM2O+BM2I*BOUND          !Instantaneous level of protein induction
!*****End of AhR-PCB126 Binding section *****'

!Amount of PCB126 metabolized
RAMP=KMETP*CVLP
AMP=INTEG(RAMP,0.0)

!Mass balance of PCB126 in rapidly perfused tissues
RARP=QR*(CAP-CVRP)
ARP=INTEG(RARP,0.0)
CRP=ARP/VRP
CVRP=CRP/PRP

!Mass balance of PCB126 in slowly perfused tissues
RASP=QS*(CAP-CVSP)
ASP=INTEG(RASP,0.0)
CSP=ASP/VSP
CVSP=CSP/PSP

!Mass balance of PCB126 in blood
RABloodP=QF*CVFP+QL*CVLP+QR*CVRP+QS*CVSP-QC*CAP
ABloodP=INTEG(RABloodP,0.0)
CAP=ABloodP/VBP

!PCB126 in GI lumen
RAGIP=-KGILVP*AGIP-KFECP*AGIP
AGIP=INTEG(RAGIP,0.0)+TotalDoseP

!Excretion of PCB126 in feces
RAFECF=KFECP*AGIP+&
VmaxP*CVLP/((KmP*(1+CVLM/(KIP+1e-30))+CVLP))+KLIVP*CVLP
AFECF=INTEG(RAFECF,0.0)
PFECF=AFECF*100/(TOTALDOSEP+1.0e-30)
                                !%Fecal excretion compared to total dose(%)

!Total mass of PCB126

```

$TMASSP=AFP+ALP+AMP+ARP+ASP+ABloodP+AGIP+AFCEP$
 $MBP=(TOTALDoseP-TMASSP)*100.0/(TOTALDoseP+11.0e-30)$

!Setting the dosing scenarios 4 doses at intervals of 24 hrs
 !Addition of 1 more dose when the time meets the dosing time.

Procedural

dosetime=k*DoseFrq

IF (t.ge.dosetime) THEN

 TotalDoseP=TotalDoseP+DoseP

 k=k+1

ENDIF

End

!End of Procedural

!-----END of DERIVATIVE SECTION FOR PCB126-----

!-----DERIVATIVE SECTION FOR MTX-----

!Amount of MTX in GI lumen

$RAGIM=-KGILVM*AGIM-Kmov*AGIM$

$AGIM=INTEG(RAGIM,0.0)+DoseMnano*FM$

!Equations describing competitive inhibition of proteins were taken from

!Haddad S. (Toxicol. Sci., 2001).

!Mass balance of MTX in liver

$RALM=(QLM-QGTM)*(CAM-CLM/PLM)\&$

$+QGTM*(CGTM/PGTM-CLM/PLM)-KBile*CLM/PLM\&$

$-VmaxMrp2*CVLM/(KmMrp2*(1+CVLP/(KIM+1e-30))+CVLM)$

$ALM=INTEG(RALM,0.0)$!Amount of MTX (nmole)

$CLM=ALM/VLM$!Calculations of conc of MTX (nM).

$AUCLIVM=integ(CL,0.0)$!Calculations of AUC of MTX (nM*h).

$CVLM=CLM/PLM$

!Biliary Excretion of MTX

$RABileM=KBile*CLM/PLM\&$

$+VmaxMrp2*CVLM/(KmMrp2*(1+CVLP/(KIM+1e-30))+CVLM)$

$ABileM=integ(RABileM,0.0)$

!Transfer of MTX in bile into 3 segments; r1, r2 and r3.

$r=Kbile*CLM/PLM+\&$

$VmaxMrp2*CVLM/(KmMrp2*(1+CVLP/(KIM+1e-30))+CVLM)$

$Rr1=(r-r1)*30.$

$r1=integ(Rr1,0.0)$

$Ar1=integ(r1,0.0)$

$Rr2=(r1-r2)*30$

$r2=integ(Rr2,0.0)$

$Ar2=integ(r2,0.0)$

Rr3=(r2-r3)*30
r3=integ(Rr3, 0.0)
Ar3=integ(r3,0.0)

!Mass balance in kidney
RAKM=QKM*(CAM-CKM/PKM)-KKidney*CKM/PKM
AKM=INTEG(RAKM,0.0)
CKM=AKM/VKM
CVKM=CKM/PKM

!Amount of MTX excreted in urine
RAUrineM=KKidney*CKM/PKM
AUrineM=integ(RAUrineM, 0.0)

!Mass balance of MTX in muscle
RAMM=QMM*(CAM-CMM/PMM)
AMM=INTEG(RAMM,0.0)
CMM=AMM/VMM
CVMM=CMM/PMM

!Mass balance of MTX in plasma
RAPlsM=QLM*CLM/PLM+QKM*CKM/PKM+QMM*CMM/PMM-&
(QLM+QKM+QMM)*CAM
APlsM=integ(RAPlsM,0.)
CAM=APlsM/VPM

!Mass balance of MTX in gut lumen
RAGL1M=VmaxMrp2*CVLM/(KmMrp2*(1+CVLP/(KIM+1e-30))+CVLM)&
+KBile*CLM/PLM-.25*(VmaxGTM*CGL1M/(KmGTM+CGL1M)+&
KabsM*CGL1M)-kf*VGLM*CGL1M+Kmov*AGIM
AGL1M=integ(RAGL1M,0.0)
CGL1M=AGL1M/.25/VGLM

RAGL2M=kf*VGLM*CGL1M-&
.25*(VmaxGTM*CGL2M/(KmGTM+CGL2M)+KabsM*CGL2M)&
-kf*VGLM*CGL2M
AGL2M=integ(RAGL2M,0.0)
CGL2M=AGL2M/.25/VGLM

RAGL3M=kf*VGLM*CGL2M-&
.25*(VmaxGTM*CGL3M/(KmGTM+CGL3M)+KabsM*CGL3M)&
-kf*VGLM*CGL3M
AGL3M=integ(RAGL3M,0.0)
CGL3M=AGL3M/.25/VGLM

$RAGL4M = kf * VGLM * CGL3M - .25 * (VmaxGTM * CGL4M / (KmGTM + CGL4M) + KabsM * CGL4M) - kf * VGLM * CGL4M$
 $AGL4M = \text{integ}(RAGL4M, 0.0)$
 $CGL4M = AGL4M / .25 / VGLM$

$RAGLM = RAGL1M + RAGL2M + RAGL3M + RAGL4M$
 $AGLM = \text{integ}(RAGLM, 0.)$
 $CGLM = AGLM / VGLM$

!Fecal Excretion of MTX from GI Lumen
 $RAFecesM = kf * VGLM * CGL4M$
 $AFECM = \text{integ}(RAFecesM, 0.0)$

!Mass balance of MTX in gUT tissue
 $RAGTM = QGTM * (CAM - CGTM / PGTM) + .25 * (VmaxGTM * CGL1M / (KmGTM + CGL1M) + KabsM * CGL1M) +$
 $.25 * (VmaxGTM * CGL2M / (KmGTM + CGL2M) + KabsM * CGL2M) +$
 $.25 * (VmaxGTM * CGL3M / (KmGTM + CGL3M) + KabsM * CGL3M) +$
 $.25 * (VmaxGTM * CGL4M / (KmGTM + CGL4M) + KabsM * CGL4M) +$
 $KGILVM * AGIM$
 $AGTM = \text{integ}(RAGTM, 0.0)$
 $CVGM = CGTM / PGTM$
 $CGTM = AGTM / VGTM$
 $CVGTM = CGTM / PGTM$

!Total mass of MTX
 $TMASSM = AGTM + AGLM + APISM + AMM + AKM + ALM + AFECM + AUrineM$
 $MBM = (DoseMnano - TMASSM) * 100.0 / (DoseMnano + 1e-30)$
 !-----END OF DERIVATIVE SECTION FOR MTX-----

TERMT (T.GE.TSTOP)

END !END of Derivative
 END !END of Dynamic
 !-----!-----!-----!-----!-----!-----!-----!
 END !END of Program

```

!File discrete.cmd
!Command file for PBPK model of a hybrid model between PCB126 and MTX
!Edited by M. Lohitnavy on Oct. 10th, 2007.

set grdcpl=.f. !no grid on line plots
SET TITLE = 'PCB126-MTX interaction model-Rats'
prepare /all

procedure check
start
plot tmassp, mbp
print t,tmassp,mbp
end

!For MTX alone experiment
PROCED MAlone
set BW=0.298
set DoseRate0M=3.0
set doserate0P=0.
start
PLOT /DATA=MAlone CLM /lo=0. /hi=800. /char=1 /xtag='hr' /tag='[Liver MTX
(nmole/L)]'
END

!For MTX+PCB126 experiment
PROCED MPCB
set BW=0.277
set DoseRate0M=3.0
set doserate0P=9800.
start
PLOT /DATA=PPCB CLP /log /lo=100. /hi=10000. /char=1 /xtag='hr' /tag='[Liver
PCB126 (nmole/L)]'
PLOT /DATA=MPCB CLM /lo=0. /hi=1200. /char=1 /xtag='hr' /tag='[Liver MTX
(nmole/L)]'
END

!For MTX+Genipin experiment
PROCED MGenipin
set BW=0.278
set DoseRate0M=3.0
set doserate0P=0.
start
PLOT /DATA=MGenipin CLM /lo=0. /hi=800. /char=1 /xtag='hr' /tag='[Liver MTX
(nmole/L)]'
END

```

```

!For MTX+PCB126+Genipin experiment
PROCED MMixture
set BW=0.274
set DoseRate0M=3.0
set doserate0P=9800.
set vmaxmrp2=144600.
set vmaxp=62.616
start
PLOT /DATA=PMixture CLP /log /lo=100. /hi=10000. /char=1 /xtag='hr'
/tag='[Liver PCB126 (nmole/L)]'
PLOT /DATA=MMixture CLM /lo=0. /hi=800. /char=1 /xtag='hr' /tag='[Liver MTX
(nmole/L)]'
END

```

```

!Conc-time course of PCB126 in MTX+PCB126 Study.
DATA PPCB (t, CLP)
96.5  1542.8
97    1743.8
99    2275.1
102   1886.7
108   2287.4
END

```

```

!Conc-time course of PCB126 in MTX+PCB126+Genipin Study.
DATA PMixture (t, CLP)
96.5  1854.8
97    2215.0
99    1766.1
102   1700.6
108   2124.1
END

```

```

!Conc-time course of MTX in MTX Alone Study.
DATA MAlone (t, CLM)
96.5  394.3
97    461.7
99    193.9
102   479.1
108   447.1
END

```

```

!Conc-time course of MTX in MTX+PCB126 Study.
DATA MPCB (t, CLM)
96.5  225.1
97    719.1
99    659.5

```

102 387.1
108 594.8
END

!Conc-time course of MTX in MTX+Genipin Study.

DATA MGenipin (t, CLM)

96.5 248.2

97 184.0

99 349.7

102 518.4

108 230.0

END

!Conc-time course of MTX in MTX+PCB126+Genipin Study.

DATA MMixture (t, CLM)

96.5 208.4

97 180.9

99 370.3

102 170.5

108 159.3

END